University of Notre Dame

2022-2023

Notre Dame Rocketry Team
Preliminary Design Review

NASA Student Launch 2023

360° Rotating Optical Imager and Apogee Control System

Submitted October 26, 2022

365 Fitzpatrick Hall of Engineering
Notre Dame, IN 46556

Contents

List of Tables

List of Figures

Table 1: Commonly-Used Acronyms

Acronym	Meaning
ACS	Apogee Control System
AGL	Above Ground Level
APRS	(Automated Packet Reporting System
CDR	Critical Design Review
CFD	Computational Fluid Dynamics
CG	Center of Gravity
CP	Center of Pressure
CPU	Central Processing Unit
FMEA	Failure Modes and Effects Analysis
FPS	Frames Per Second
FRR	Flight Readiness Review
IMU	Inertial Measurement Unit
INS	Inertial Navigation System
LED	Light Emitting Diode
LiPo	Lithium Polymer
NAR	National Association of Rocketry
NDRT	Notre Dame Rocketry Team
PCB	Printed Circuit Board
PID	Proportional-Integral-Derivative
PDR	Preliminary Design Review
PLA	Polylactic Acid
PRM	Primary Recovery Module
PWM	Pulse-Width Modulation
RF	Radio Frequency
SOP	Standard Operating Procedure
SRM	Secondary Recovery Module
TRA	Tripoli Rocketry Association
TROI	360º Rotating Optical Imager
UAS	Unmanned Aerial System
UAV	Unmanned Aerial Vehicle
WNV	Weighted Normal Value

1 Summary of Report

1.1 Team Summary

Team Info:	Notre Dame Rocketry Team (NDRT) University of Notre Dame 365 Fitzpatrick Hall of Eng. Notre Dame, IN 46556	**Facebook:**	Notre Dame Rocketry Team
		Instagram:	@ndrocketryteam
		LinkedIn:	Notre Dame Rocketry Team
		Twitter:	@NDRocketry
Mentor:	Dave Brunsting Level 3 – NAR #85879, TRA #12369 e: dacsmema@gmail.com p: (269) 838-4275	**Website:**	ndrocketry.weebly.com
NAR/TRA Sec:	TRA #12340, Michiana Rocketry		
PDR Hours:	1153		

1.2 Launch Vehicle Summary

Table 2 gives an overview of the launch vehicle design. The vehicle recovery system consists of the Fin Can Energetic Device (FED), Payload Energetic Device (PED), and Nose Cone Energetic Device (NED). The FED deploys a 2 ft diameter, 1.6 C_d Rocketman elliptical drogue parachute at apogee. The PED deploys a 9 ft diameter, 2.2 C_d Rocketman high performance main parachute at 600 ft AGL. The NED ejects the nose cone at 800 ft AGL to allow payload deployment. The nose cone remains tethered to the vehicle.

Table 2: Launch Vehicle Summary

Feature	Value				
Target Apogee (ft.)	4600				
Selected Motor	Aerotech L2200G-P				
Outer Diameter (in.)	6.17				
Rail Size	12 ft, 1515				
Feature	**Nose Cone**	**Payload Bay**	**ACS Tube**	**Fin Can**	**Total**
Length (in.)	24	27	35	35	**121**
Mass (oz)	87.2	206	276	298	**867**

1.3 Payload Summary

The **3**60º **R**otating **O**ptical **I**mager (**TROI**) receives radio signal commands to rotate and capture images. The TROI uses a lead screw to maneuver a camera out of the payload bay after landing, employs a spring to deploy the camera vertically above the payload bay, utilizes a stepper motor to rotate and orient the camera (NASA Reqs. 4.2.1.1., 4.2.1.2., 4.2.4., 4.3.1.), processes the images as commanded, and stores images on a PCB (NASA Req. 4.2.2.).

2 Changes Made Since Proposal

2.1 Vehicle Criteria

The overall layout and specifications of the launch vehicle have changed since proposal. A separation point was added directly aft of the nose cone allowing an exit point for the payload. The ACS and Recovery Body Tubes have combined into a singular body tube to compensate for this additional fore separation point, while retaining the aftmost separation point between the Fin Can and the ACS Body Tube. Additionally, the launch vehicle grew 3 inches in overall length and the static stability has increased.

2.2 Recovery Criteria

Since proposal, a third recovery module has been added to the recovery system to allow for the ejection of the nose cone to allow the updated payload design to function properly. Additionally, the main parachute deployment altitude was decreased by 100 ft to reduce the descent time and drift of the vehicle while still abiding by NASA Req. 3.1.1. The full vehicle will now descend tethered together so only one GPS will be required. This change was made since the kinetic energy requirement outlined in NASA Req. 3.3. can still be fulfilled with all of the sections tethered and it greatly reduces complexity. Further details of these notable changes and other recovery details can be viewed in Section 4.

2.3 Payload Criteria

The overall design of the payload has been updated since Proposal submission. The payload is still a lead screw system that emerges from the payload body tube. The location of the payload is still within the payload bay aft of the nose cone, and the payload still uses a stepper motor for the 360º rotation of the camera. The deployment and movement of the camera assembly to clear the payload body tube has been slightly altered since proposal. The payload now uses one lead screw for motion along the axis of the payload tube and a spring in order to move the camera to visually clear the payload body tube. The amount of allowable mass has also changed from 60 oz. to 90 oz. to leave room for redundancy in the design (NDRT Req. TROI.11). In addition, the subsystems of the payload are now more specified and outlined in Table 89. All changes made since the proposal submission reduce the complexity of the system to create a more fluid and reliable design.

2.4 Project Plan

Project progress is on course regarding both schedule and budget as described in Proposal. Section 9.3 details the purchases made thus far for subscale construction and preliminary component testing. The only change to the budget is a $500 increase to the experimental payload budget. This addition reflects the funds allocated by the Department of Electrical Engineering to senior electrical engineers working on the experimental payload as a capstone project. Overall, the team has sufficient funds to complete the project due to carry-over funds from last year, donations from corporate sponsors, and various fundraising events. Section 9.4 shows Gantt charts for the team and each squad. The team is on track to complete the next milestone, a subscale flight, on November 6. Backup subscale flight dates are planned for November 12 and December 3.

3 Technical Design: Launch Vehicle

3.1 Mission Statement

The main responsibility of the launch vehicle is to complete the mission goals of the 2023 launch competition safely and reliably. To accomplish this goal, the vehicle design is driven by NASA-specified and team-derived requirements deemed necessary for mission success. The main NASA requirements driving the vehicle design are: an apogee between 4,000 and 6,000 feet above ground level (NASA Req. 2.1.), a maximum motor impulse of 5,120 Newton-seconds (NASA Req. 2.12.), a minimum velocity of 52 feet per second upon rail exit (NASA Req. 2.17.); a static stability margin of at least 2.0 at launch rail exit (NASA Req. 2.14.); and a minimum thrust to weight ratio of 5:1 (NASA Req. 2.15.).

The scoring payload requires that the launch vehicle safely enables the system to take unobstructed 360° images. The non-scoring payload, the apogee control system (ACS), requires the launch vehicle to reach an altitude that exceeds target apogee for the device to actively control the final vehicle apogee by increasing form drag around the launch vehicle. Additionally, all vehicle components must be designed to withstand forces experienced throughout all portions of the mission.

3.1.1 Mission Success Criteria

The following criteria will be used to determine the success of the launch vehicle:

- The launch vehicle shall achieve the desired stability in flight.

- The launch vehicle shall achieve the desired exit-rail velocity.
- The trajectory of the launch vehicle shall be above the target apogee.
- The vehicle sections shall separate during recovery events.
- The vehicle shall land undamaged.

3.2 System Alternative Designs

While many configurations of the launch vehicle were evaluated, the configurations that were compatible with the mission shrunk as the payload design was refined. Once the payload design was fully understood, three distinct configurations were evaluated. Sections 3.2.1, 3.2.2, and 3.2.2 list the three evaluated configurations. **It is highly recommended that one reads Payload Section 6.7 before reading the configurations, for an understanding of what payload plans on executing will explain the configuration choices.**

3.2.1 Traditional Layout

Figure 1 was the first considered configuration, named the "Traditional Layout," given that this configuration was used by the team last year.

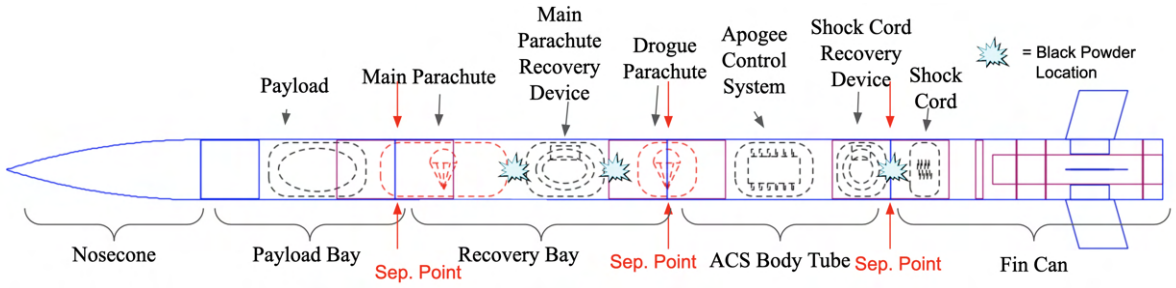

Figure 1: Possible Configuration 1: Traditional Layout

For this configuration, there are three separation points, giving the launch vehicle four separate sections. Table 3 lists a summarized explanation of the "Traditional Layout."

Table 3: Traditional Layout Summary

Section	Internal Components
Nosecone and Payload Bay	Payload
Recovery Bay	2-Sided Recovery Device, Main Parachute, Drogue Parachute
ACS Body Tube	ACS, 1-Sided Recovery Device
Fin Can	Shock Cord, Motor, Motor Mount, Fins

The first section includes the nosecone and payload bay. Housed inside the payload bay is the payload, with the aft of the payload housing a bulkhead and eyebolt to connect this section to the Recovery Bay with the main parachute's tethers.

The second section is the Recovery Bay, where the main parachute, drogue parachute, and a recovery device are located inside. Connected to both sides of the recovery device are bulkheads with eyebolts on them, allowing the parachutes to be secured and connect multiple launch vehicle sections together. As well, the recovery device would eject black powder in both direction, with each direction occurring at different stages for different parachute deployments.

The third section is the ACS Body Tube, where the ACS and another recovery module are located inside. The recovery device would eject black powder in the aft direction, separating the ACS Body Tube and the Fin Can, but keeping these two sections tethered together with the use of a shock cord.

The final section is the Fin Can, which includes the motor, motor mount, and fins.

The main benefit of this design is the team's familiarity with how the configuration operates on launch day construction and integration compared to the other two configurations. Another benefit of this design is the use of only two recovery modules. Although one of the recovery modules ejects black powder in both axial directions, one less recovery module will ease launch day integration, as well as reduce the number of parts within the launch vehicle.

The major concerns with this design are the fact that the payload may interfere with the main parachute, given that the main parachute and payload deploy out of the same point. Deployment interference includes both the main parachute being unable to deploy out of the launch vehicle due to being stuck within the payload bay and the main parachute restricting the payload from deploying out of the launch vehicle upon impact. Additionally, the potential for the black powder ejection to cover the payload camera/mechanics with black powder is cause for concern.

3.2.2 Through-Bulkhead Layout

Figure 2 was the second considered configuration, named the "Through-Bulkhead Layout," given that this configuration would require the payload to move "through" the recovery device's bulkheads to perform its duties.

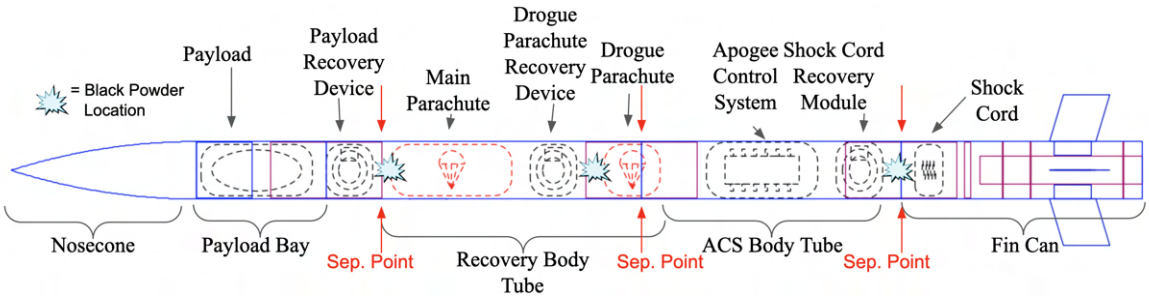

Figure 2: Possible Configuration 2: Through-Bulkhead Layout

For this configuration, there are three separation points, giving the launch vehicle four separate sections. Table 4 lists a summarized explanation of the "Through-Bulkhead Layout."

Table 4: Through-Bulkhead Layout Summary

Section	Internal Components
Nosecone and Payload Bay	Payload, 1-Sided Recovery Device
Recovery Bay	1-Sided Recovery Device, Main Parachute, Drogue Parachute
ACS Body Tube	ACS, 1-Sided Recovery Device
Fin Can	Shock Cord, Motor, Motor Mount, Fins

The first section includes the nosecone and payload bay. Housed inside the payload bay is the payload and a recovery device. The recovery device would eject aft, with the use of black powder, and it would include eyebolts to secure the Payload Bay to the Recovery Body Tube. The key to this recovery device's design would be a method of separating the body tubes with black powder pressurisation without the need to pressurize the entire tube; this allow the recovery device's bulkheads to be "ring shaped," which would give the payload room to move out of the payload bay by going through the recovery device.

The second section is the Recovery Bay, where the main parachute, drogue parachute, and a recovery device are located inside. Connected to both sides of the recovery device are bulkheads with eyebolts on them, allowing the parachutes to be secured and connect multiple launch vehicle sections together. The recovery device would eject black powder in only the aft direction to separate the Recovery Body Tube and the ACS Body Tube.

The third section is the ACS Body Tube, where the ACS and another recovery module are located inside. The recovery device would eject black powder in the aft direction, separating the ACS Body Tube and the Fin Can, while keeping these two sections tethered together with the use of a shock cord.

The final section is the Fin Can, which includes the motor, motor mount, and fins.

The main benefit of this design is the opportunity to separate the Payload Bay and the Recovery Body tube without the need of pressurizing the entire body tube. This mitigates the black powder contamination problem from the "Traditional Layout" configuration.

The major concerns with this design is the ability of the payload recovery device to successfully separate the body tubes without any damage, due to high pressurization in a small, centralized location. Additionally, another major concern is that the payload may have issues with deployment interference from the main parachute, given that the main parachute and payload are deploying out of the same point. Deployment interference includes both the main parachute being unable to deploy out of the launch vehicle due to being stuck within the payload bay and the main parachute restricting the payload from deploying out of the launch vehicle upon impact.

3.2.3 Nosecone Ejection Layout

Figure 3 was the third considered configuration, named the "Nosecone Ejection Layout," given that this configuration will eject the Nosecone.

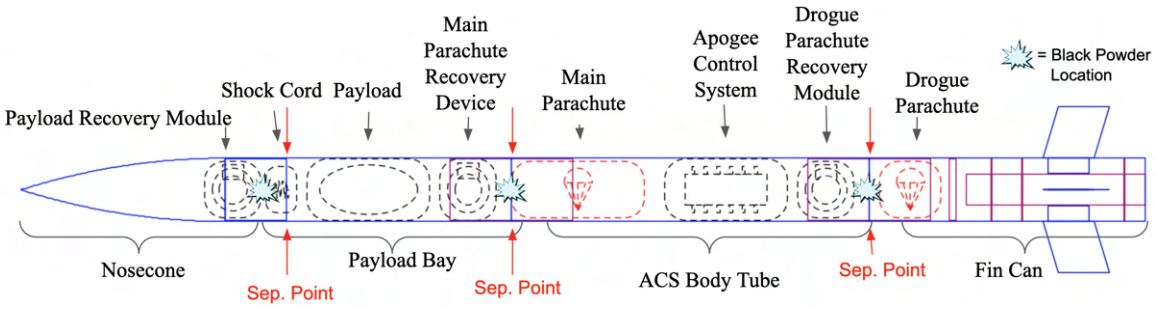

Figure 3: Possible Configuration 3: Nosecone Ejection Layout

For this configuration, there are three separation points, giving the launch vehicle four separate sections. Table 5 lists a summarized explanation of the "Through-Bulkhead Layout."

Table 5: Nose Cone Ejection Layout Summary

Section	Internal Components
Nose cone	1-Sided Recovery Device, Shock Cord
Payload Bay	Payload, 1-Sided Recovery Device
ACS Body Tube	Main Parachute, ACS, 1-Sided Recovery Device
Fin Can	Drogue Parachute, Motor, Motor Mount, Fins

The first section includes the nose cone and a recovery device. The recovery device is secured

within the nose cone, and is ejected aft using black powder. Secured to the recovery device is an eyebolt, and the shock cord attached to it secures the nose cone to the Payload Bay.

The second section is the Payload Bay, where the payload and a recovery device are located inside. Connected to aft side of the recovery device is an eyebolt, allowing the main parachute to tether the ACS Body Tube and the Payload Bay together. The payload would deploy fore of the body tube.

The third section is the ACS Body Tube, where the ACS, main parachute, and another recovery module are located inside. The recovery device would eject black powder in the aft direction, separating the ACS Body Tube and the Fin Can, but keeping these two sections tethered together with the use of the drogue parachute.

The final section is the Fin Can, which includes the motor, motor mount, and fins.

The main benefit of this design is its simplicity. The three recovery devices can potentially be the same model, which will simplify the construction process. As well, the main concern of deployment interference of the other configurations is avoided with the use of a shock cord on the side of payload deployment; the shock cord is less likely to interfere and is less critical to the recovery's success.

The main concern with this design is the mass distribution. Every section is heavier than the other configurations' sections. This issue can be mitigated with ideal parachute and motor selections, but both selections will also contribute to the mass and cost of the launch vehicle.

3.2.4 Chosen System Configuration

Given the three configurations presented, the team chose the third option (Section 3.2.3), referred to as the "Nosecone Ejection Layout," due to its simplicity and the fact that it was able to solve the major concerns of the other configurations. It should be noted that its main concern can be avoided if the right selections are made.

Given a team confirmed configuration, the launch vehicle squad performed trade studies to determine the optimal materials and shapes of the launch vehicle components. Section 3.3 lists the trade studies and their results, and Section 3.5 lists the Preliminary Design overall vehicle design.

3.3 Component Level Design

3.3.1 Airframe Material Selection

The team performed a trade study in order to determine the optimal airframe material for the launch vehicle. The following materials were analyzed: carbon fiber, fiberglass, blue tube, and phenolic. These four materials were compared based on the following criteria: Yield strength, mass, ease of construction, and material cost. Table 6 lists the results of the trade study.

Table 6: Airframe Material Trade Study

		Carbon Fiber		Fiberglass		Blue Tube		Phenolic	
Criteria	**Weight**	**Value**	**WNV**	**Value**	**WNV**	**Value**	**WNV**	**Value**	**WNV**
Yield Strength (psi)	0.4	360000	0.351	30000	0.029	5000	0.005	15000	0.015
Mass (ft/oz)	0.1	.068	0.022	0.042	0.013	0.096	0.031	0.108	0.035
Ease of Construction (1-5)	0.1	1	0.009	3	0.027	4	0.036	3	0.027
Durability (1-5)	0.35	5	0.135	4	0.108	2	0.054	2	0.054
Material Cost ($ft/\$$)	0.05	0.009	0.0005	0.019	0.001	0.052	0.003	0.847	0.046
Total WNV		**0.517**		**0.179**		**0.129**		**0.176**	

Yield strength was measured based on the units of psi, and it was given a weight of 40% because of the importance of the material's strength. The next criteria is mass, and which is measured based on the units of ft/oz. While this is not the traditional units for mass, it is an optimal method of measuring the mass for body tubes. With the units of ft/oz, any change in the length of the body tube can easily be measured. Mass was given a weight of 10% due to the body tubes contributing to a majority of the launch vehicle's overall mass. Ease of construction was given a weight of 10%; it's important to consider the team's ability to work with the materials selected. The durability was given a weight of 35% due to the fact that the body tubes are reused for multiple launches, and the material needs to withstand cyclical loads. This weight is valued highly because if body tubes are unable to withstand repeated loads, repurchasing body tubes will increase overall cost greatly. The material's cost, measured based on the units ft/$) was given a weight of 5%. The body tubes are typically the major contributor to the vehicle squad's budget, so it is critical to consider the cost of them. The units of ft/$ were used in order to determine the distance purchasable with $1, with a cheaper material allowing for more to be purchased.

From the results of the trade study, carbon fiber is the optimal material for the launch vehicle airframe, due to its strength and mass. However, it should be noted that carbon fiber is a non-transmissible material, and the payload needs to be able to send and receive radio signals. Thus, the best transmissible airframe material, fiberglass, was chosen for the payload bay body tube.

With the airframe body tube materials selected, the body tubes were created in CAD to visualize the design. Figure 4 displays the Payload Bay, made out of G12 Fiberglass; Table 7 lists the dimensions of the Payload Bay body tube. Figure 5 displays the Recovery/ACS Bay, made out of Carbon Fiber; Table 8 lists the dimensions of the Recovery/ACS Bay body tube. Figure 6 displays the Fin Can body tube, made out of Carbon Fiber; Table 9 lists the dimensions of the Fin Can body tube.

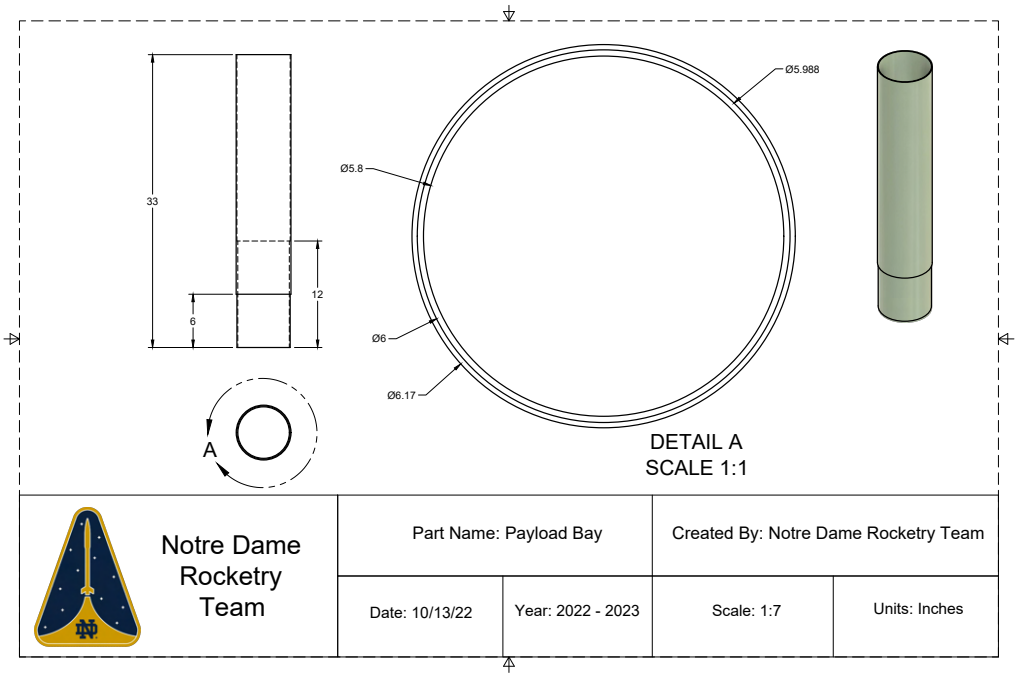

Figure 4: Payload Bay CAD Drawing

Table 7: Payload Bay Dimensions

Dimension	Value
Length	27.0 in
Outer Diameter	6.17 in
Inner Diameter	6.00 in
Coupler Outer Diameter	5.988 in
Coupler Inner Diameter	5.8 in
Material	G12 Fiberglass

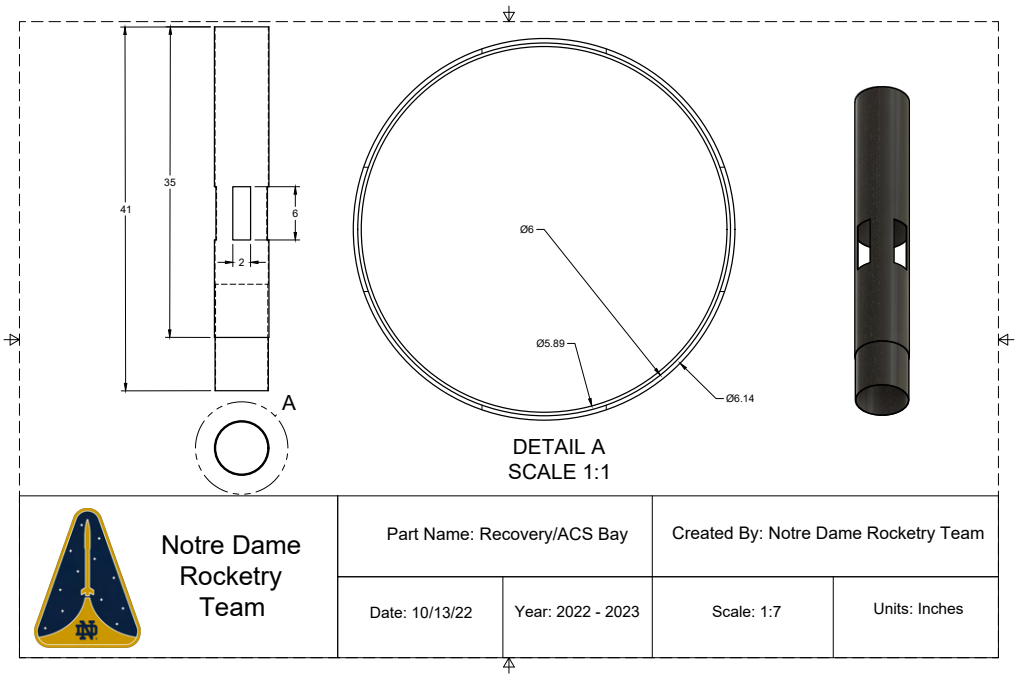

Figure 5: Recovery/ACS Bay CAD Drawing

Table 8: Recovery/ACS Bay Dimensions

Dimension	Value
Length	35.0 in
Outer Diameter	6.114 in
Inner Diameter	6.00 in
ACS Flap Cutout Length	6.00 in
ACS Flap Cutout Width	2.00 in
Coupler Outer Diameter	6.00 in
Coupler Inner Diameter	5.888 in
Material	Carbon Fiber

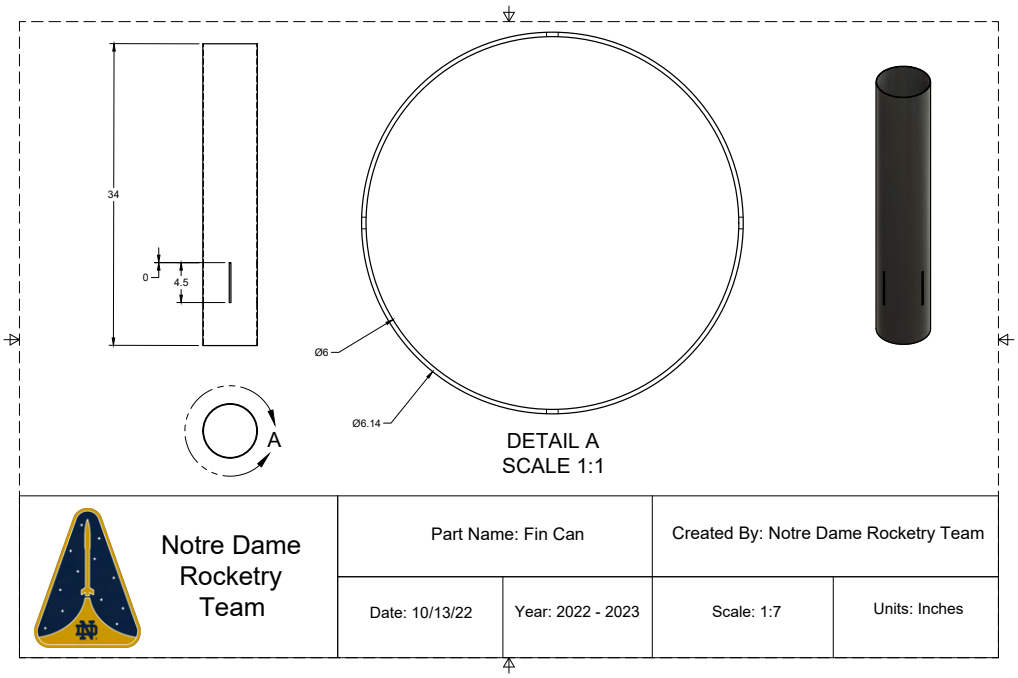

Figure 6: Fin Can CAD Drawing

Table 9: Fin Can Dimensions

Dimension	Value
Length	34.0 in
Outer Diameter	6.114 in
Inner Diameter	6.00 in
Fin Slit Length	4.50 in
Fin Slit Width	0.187 in
Material	Carbon Fiber

3.3.2 Motor Mount Material

The purpose of the motor mount is to constrain the motor within the launch vehicle. The material selected for this part has to be able to withstand the forces transferred to the motor tube by the motor and waste heat from the motor. Therefore, the team determined that the motor tube material must have sufficient temperature resistance, measured by the maximum operating temperature in degrees Celsius, and yield strength, measured in pounds per square inch (psi), to withstand these forces. In addition to withstanding these load forces, the material utilized in the motor tube should add as little mass and cost to the rocket as possible. As such, categories for mass, measured in ounces per foot of material, and cost, measured in

dollars per foot of material, were added to the trade study. These values were inverted in the trade study to indicate in the calculations that smaller values are better. Once these criteria were established, values for the weighted calculations were determined based on the importance of each trait. Temperature resistance was defined as the most important and assigned a value of 0.35 because it is a critical design requirement unique to the motor tube. Mass was assigned the second highest weighting at 0.30 due the overall importance of keeping the launch vehicle mass as low as possible. Yield strength was defined as the third most important because the material must be able to withstand the forces imparted on it by the motor and was assigned a weighting of 0.25 accordingly. Cost was assigned the smallest weighting, with a value of 0.10, as there is a sufficient amount of the budget set aside for the motor tube to cover the cost of most ordinary materials.

After defining the criteria of the materials trade study, the following materials were selected: carbon fiber, fiberglass, blue tube, and phenolic resin. After researching each material and evaluating the values produced by the trade study, carbon fiber was determined to be the best material for the motor tube. With a total weighted value of 0.414, carbon fiber significantly outclassed the other materials in the areas of yield strength and temperature resistance while being competitive in terms of mass. Phenolic resin, with a total weighted value of 0.241, was determined to be the next best material due to its higher temperature resistance and competitive values in the categories of mass, yield strength, and cost when compared to blue tube and fiberglass. Blue tube, with a total weighted value of 0.174, was determined to be the second worst material because of its low yield strength and low temperature resistance. Fiberglass was the worst material of those investigated, albeit by a small amount with a total weighted value of 0.171, because of its low temperature resistance and high mass. In conclusion, carbon fiber is the best material for the motor tube when reviewed under the specified criteria.

Table 10: Motor Mount Material Trade Study

		Blue Tube		Carbon Fiber		Fiberglass		Phenolic	
Criteria	**Weight**	**Value**	**WNV**	**Value**	**WNV**	**Value**	**WNV**	**Value**	**WNV**
Yield Strength (psi)	0.25	5000	0.003	360000	0.220	30000	0.018	15000	0.009
Mass (ft/oz)	0.3	0.199	0.077	0.192	0.075	0.132	0.051	0.248	0.097
Temperature Resistance (Maximum Operating Temperature °C)	0.35	110	0.055	230	0.115	167	0.084	190	0.095
Cost	0.1	0.115	0.038	0.014	0.005	0.052	0.017	0.112	0.040
Total WNV		**0.174**		**0.414**		**0.171**		**0.241**	

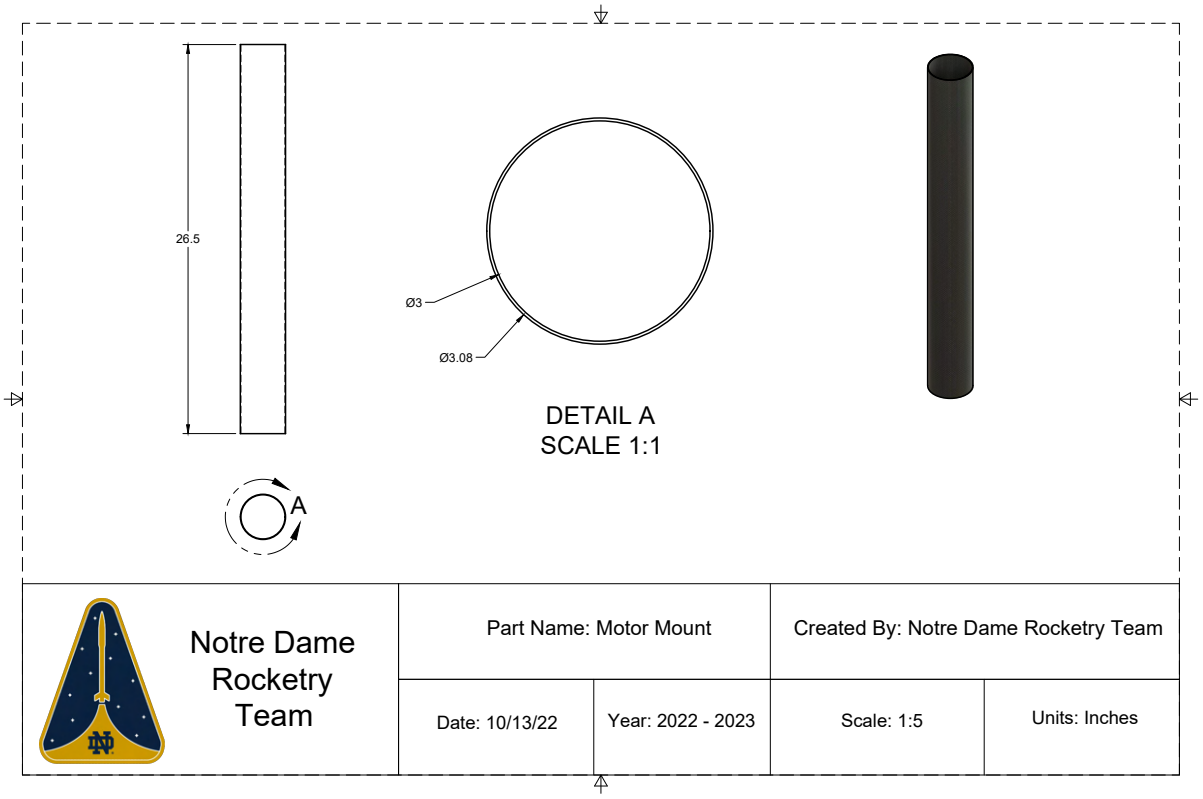

Figure 7: Carbon Fiber Motor Mount Tube, Modeled on Fusion360

Table 11: Motor Mount Tube Dimensions

Dimension	Value
Length	26.5 in
Outer Diameter	3.08 in
Inner Diameter	3.00 in
Material	Carbon Fiber

3.3.3 Nosecone Selection

The optimal nose cone selection is essential to minimize drag and achieve our desired apogee. NASA Req. 2.42. requires the nose cone shoulder to be at least half of the body diameter in length. The diameter of the nose cone as well as the shoulder will be 6 inches for maximum mounting stability. The team evaluated six nose cones that suited the requirements with varying materials and shapes as seen in Table 12 and Table 13. For materials, the team investigated fiberglass and 3D printed ABS, and for shapes, the team investigated Parabolic, Ogive, Von Karman, and Conical designs.

The following criteria were used to select the nosecone: manufacturing ease, specific volume, durability, aerodynamics/apogee produced, and cost. Durability and specific volume were determined to be the most important qualities due to the forces and kinetic energy associated with landing. Ease of manufacturing, aerodynamics, and cost are all minor criteria, since the team has access to 3D printers and sufficient budget to purchase a nose cone. Since maximum apogee is not a component of this competition, aerodynamics is not the most important consideration. All of the nosecones were modeled and simulated in OpenRocket to determine the maximum apogee they could reasonably achieve.

Table 12: Nosecone Trade Study Part 1: 3D Printed Shapes

3D Printed							
		Parabolic		Ogive		Von Karman	
Criteria	**Weight**	**Value**	**WNV**	**Value**	**WNV**	**Value**	**WNV**
Manufacturing Ease (1-5)	0.05	4	0.007	4	0.007	4	0.007
Specific Volume (in^3/oz)	0.25	0.031	0.038	0.036	0.044	0.028	0.034
Durability (Yield Strength-psi)	0.3	7000	0.019	7000	0.019	7000	0.019
Aerodynamics/Apogee	0.2	5560	0.033	5555	0.033	5562	0.033
Cost (1/$)	0.2	0.013	0.043	0.013	0.043	0.013	0.043
Total WNV		**0.141**		**0.146**		**0.136**	

Table 13: Nosecone Trade Study Part 2: Fiberglass Shapes

Fiberglass							
		Ogive		Von Karman		Conical	
Criteria	**Weight**	**Value**	**WNV**	**Value**	**WNV**	**Value**	**WNV**
Manufacturing Ease (1-5)	0.05	5	0.009	5	0.009	5	0.009
Specific Volume (in^3/oz)	0.25	0.044	0.054	0.028	0.034	0.038	0.047
Durability (Yield Strength-psi)	0.3	30000	0.081	30000	0.081	30000	0.081
Aerodynamics/Apogee	0.2	5555	0.033	5582	0.033	5540	0.033
Cost (1/$)	0.2	0.008	0.028	0.007	0.023	0.007	0.023
Total WNV		**0.204**		**0.180**		**0.193**	

Through the trade study, the team determined that the Fiberglass Ogive nose cone is the best option. This design iteration offers the team a highly-efficient aerodynamic profile, as tested in OpenRocket, with the advantage of having minimal manufacturing process at a cost lower than that of an in-house 3D printed nose cone. Fiberglass is also advantageous because of its high durability when compared to ABS This further supports the decision to select the Fiberglass Ogive nose cone.

With the nose cone material and shape determined, the nose cone was created in CAD in order to visualise the design. Figure 8 shows the nose cone CAD drawing, and Table 14 lists the dimensions of the nose cone design.

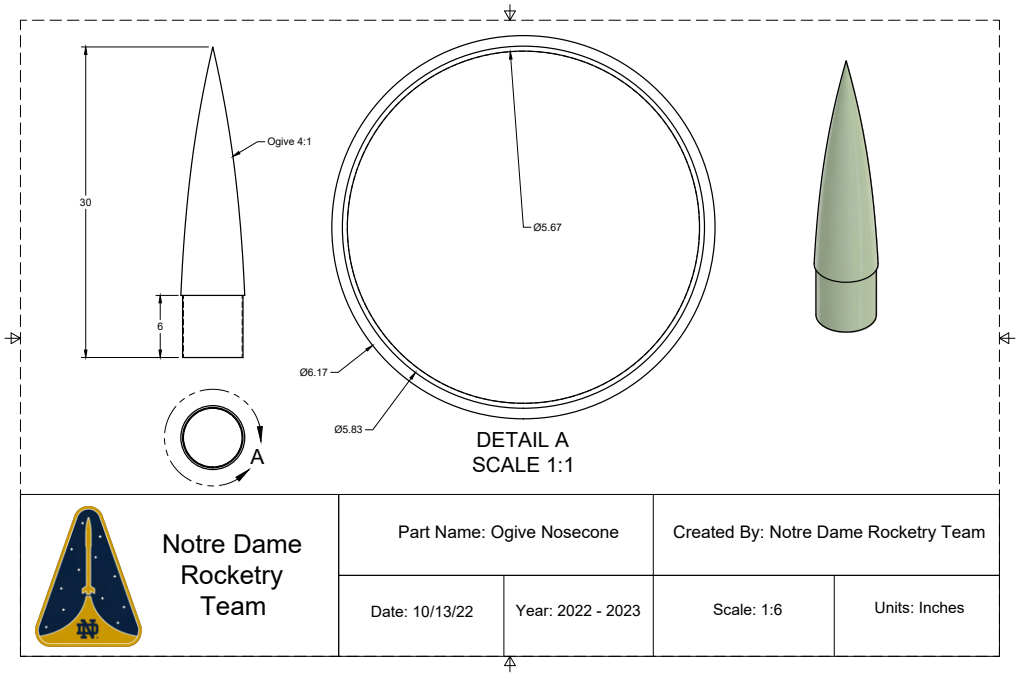

Figure 8: Nose cone CAD Drawing

Table 14: Nose Cone Dimensions

Dimension	Value
Nose Cone Length	24.0 in
Nose Cone Base Diameter	6.17 in
Shoulder Length	6.0 in.
Shoulder Outer Diameter	6.00 in.
Total Length	30 in.
Shape	Ogive
Nose Cone Ratio	4:1
Material	Fiberglass

3.3.4 Fin Material Selection

The trade study in Table 15 examines the three materials considered for the fins. These materials include Fiberglass, Carbon Fiber, and Wood.

Table 15: Fin Material Trade Study

		Fiberglass		Carbon Fiber		Wood	
Criteria	**Weight**	**Value**	**WNV**	**Value**	**WNV**	**Value**	**WNV**
Flexural Strength (psi)	0.15	52500	0.042	131500	0.106	2700	0.002
Specific Volume (in^3/oz)	0.10	0.865	0.044	0.906	0.046	0.198	0.010
Durability (1-5)	0.2	4	0.080	5	0.100	1	0.020
Cost ($\$/in^3$)	0.25	0.917	0.044	0.228	0.011	4.016	0.195
Manufacturability (1-5)	0.3	5	0.150	3	0.090	2	0.060
Total WNV		**0.361**		**0.353**		**0.287**	

The criteria used to evaluate these alternatives were flexural strength, specific volume, durability, cost, and manufacturability. Flexural strength was considered because the fins must withstand bending forces due to drag and lift forces. This criteria had the second lowest importance of the five materials with only 15% of the total weight. This was deemed less important due to the fact that the fins do not experience a great deal of perpendicular force as they have a thin profile, and don't experience severe lift forces due to the subsonic velocity of the launch vehicle. The next criteria considered was specific volume. This was given a relative weight of 10% due to the fact that specific volume determines the weight of a material. While reducing mass is important, this criteria was not weighted higher because the fins are not a large contributor to the overall mass of the launch vehicle, and due to the importance of other criteria. The next metric was durability with a relative weight of 20%. This is because the fins must withstand the forces of the fin can impacting the ground while retaining their

functionality. The next metric was cost. This was assigned a weight of 25% in order for the fins to fit within the project budget. A small increase in performance is not worth a drastic increase in cost. The last metric was manufacturability, which has a weight of 30%. This was due to the fact that the fin shape is very important to achieving the desired function and, in order to achieve the fin shape, the material must be manipulated and formed with the available manufacturing resources. The trade study indicates that fiberglass is the best material due to its respectable performance characteristics, relatively lower cost when compared to carbon fiber, and superior ease of manufacturing.

3.3.5 Fin Shape Analysis

The fin shape of a launch vehicle greatly influences the center of pressure, which produces a calculated stability. With access to CNC Techno Routers in the workshop, multiple options were considered regardless of their ease of manufacture. Rectangular, trapezoidal, swept, tapered swept, and elliptical fins were all considered. To compare the shapes, the team an OpenRocket flight simulation, changing the fin type for each simulation while keeping the rest of the launch vehicle the same. This ensured that the mass of the vehicle, fins not included, was kept constant. Then, the height and root chord lengths of the fins were held constant at 6 in. and 7 in. respectively. These simulations informed a trade study to determine the best design for the fin shape.

Table 16: Fin Shape Trade Study Dimensions

	Rectangular	Swept	Elliptical	Tapered Swept	Trapezoidal
Root Chord (in.)	6	6	6	6	6
Tip Chord (in.)	6	6	N/A	4	4
Height (in.)	7	7	7	7	7
Swept Angle (°)	0	25	0	25	8.1
Airfoil Thickness	0.125	0.125	0.125	0.125	0.125
Mass (oz)	21.2	21.2	17.1	18.0	18.0

Three calculated values were chosen as the criteria of the trade study: the apogee, center of pressure, and stability. Both centers of pressure and stability were given the largest weight as they provide stability to the launch vehicle, the main function of the fins. The stability (cal/oz) is a function of the center of pressure calculated by OpenRocket simulations. Because the profile drag of the fins creates minimal impact on the apogee of the vehicle, the apogee was weighted lower than the other categories. Apogee produced was the simplest method of determining the drag produced by each fin type. The same material density was used for all fin shapes. Thus, the values from the center of pressure and stability were divided by the mass of

their respective fin shape in order for the values to reflect the true aerodynamic effect of each fin on the launch vehicle. This eliminates the possibility that results are impacted by an external factor of the shape's area, which is directly proportional to the mass of the fin.

Table 17: Fin Shape Trade Study

		Rectangular		Trapezoidal		Swept		Tapered Swept		Elliptical	
Criteria	**Weight**	**Value**	**WNV**	**Value**	**WNV**	**Value**	**WNV**	**Value**	**WNV**	**Value**	**WNV**
Apogee (ft)	0.2	5103	0.040	5155	0.04	5215	0.040	5159	0.040	5197	0.040
Center of Pressure (1/oz)	0.4	0.126	0.072	0.144	0.082	0.133	0.076	0.15	0.085	0.149	0.085
Stability (cal/oz)	0.4	0.122	0.071	0.143	0.083	0.122	0.071	0.151	0.088	0.151	0.088
Total WNV		**0.182**		**0.205**		**0.187**		**0.213**		**0.213**	

Through this trade study, there were similar results between the tapered swept and elliptical fin shapes. The elliptical fin was chosen because an elliptical fin was made in recent years, allowing for historical reliance and concrete results of the design compared to the lack of experience with the tapered swept fin. The CAD drawings of the fins are included in Figure 9. All fin dimensions can be found in Table 18.

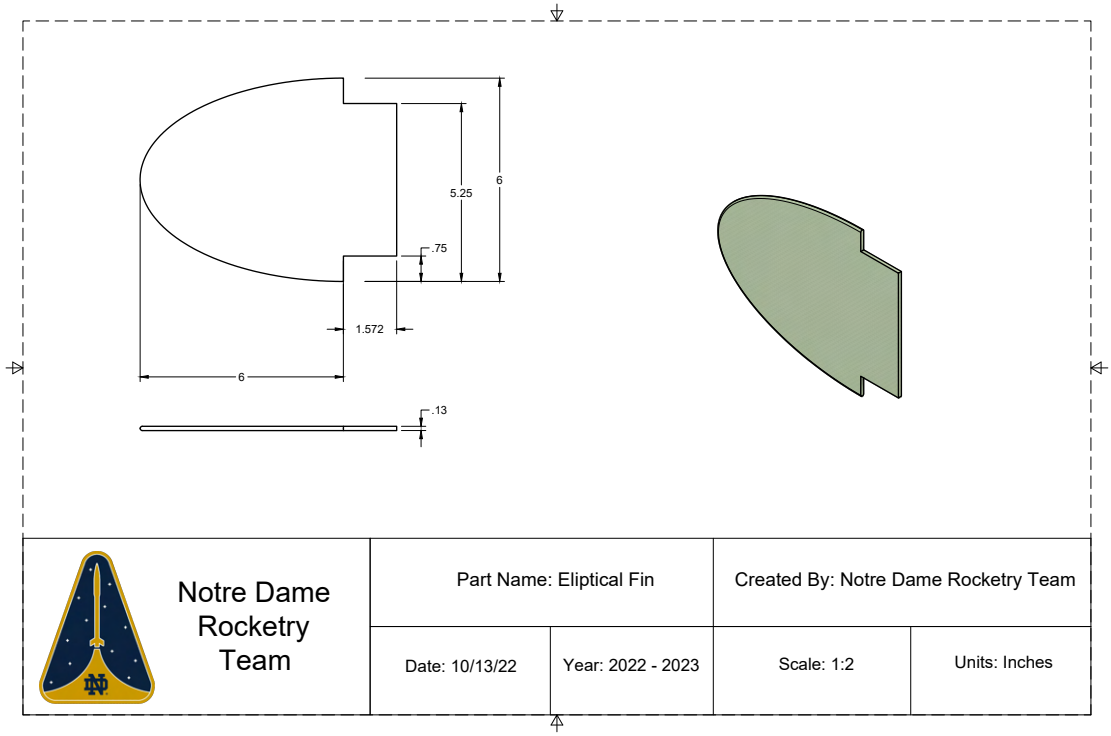

Figure 9: Fin CAD Drawing

Table 18: Fin Dimensions

Dimension	Value
Root Chord	6.00 in.
Height	6.00 in.
Tab Length	4.50 in.
Tab Height	1.572 in.
Shape	Elliptical
Material	Fiberglass

3.3.6 Aft Design

The purpose of a boattail or tailcone is to potentially reduce aerodynamic drag at the rear of the launch vehicle. The team considered three options for the aft design of the launch vehicle. Purchasing a premanufactured boattail is not an option due to a lack of commercial availability of 6 in. diameter boattails. Fabricating a boattail is not an option due to the complexity and inaccurate nature of in-house layups. Instead, purchasing a fiberglass ogive nosecone and removing the tip is the team's only viable option for a boattail. The team considered two other options: a 3D printed tailcone and using no tailcone or boattail, leaving a flat surface at the aft of the launch vehicle. The results of this trade study can be seen in Table 19.

Table 19: Aft Design Trade Study

		3D Printed Tailcone		Cut Ogive Nosecone (Boat-tail)		No Tailcone	
Criteria	**Weight**	**Value**	**WNV**	**Value**	**WNV**	**Value**	**WNV**
Apogee (ft)	0.15	5555	0.049	5764	0.051	5574	0.049
Heat Resistance (C)	0.15	100	0.008	845	0.071	845	0.071
Inverse Mass (1/oz)	0.3	0.092	0.076	0.051	0.042	0.217	0.181
Centering Ring Compatibility	0.4	4	0.145	2	0.073	5	0.182
Total WNV		**0.280**		**0.237**		**0.483**	

Four criteria determined the aft design selection. Centering ring compatibility has the most weight at 40%. The centering rings distribute the thrust force of the motor into the airframe.

Due to the nature of a variable diameter aft design, the aft design of the launch vehicle impacts the ability to mount centering rings along the length of the motor mount tube, and could compromise the structural integrity of the motor mounting system. The mass criteria has a weight of 30%, due to the effect that the added mass would have on the overall mass of the fin can. Added mass on the fin can could easily affect the kinetic energy requirements for this section of the launch vehicle because of the additional mass of the motor mount tube, fins, and spent motor casing in this specific section. Heat resistance has a weight of 15% due to the proximity to the motor during flight. However, the aft design serves no major structural purpose, so heat resistance is not essential to its function. Finally, the apogee produced has a weight of 15%. While aerodynamic performance is important to the functionality of the launch vehicle, maximum apogee is not a factor of this competition. The contribution of the aft design to the apogee is not major when compared to the other factors, such as the nose cone, body tubes, and components' mass. The team used OpenRocket to simulate the three options and recorded the apogee produced by each design, keeping every other aspect of the design constant between versions. With the aft design completed, a CAD model of the fin can was constructed. Figure 10 shows the fully constructed fin can, and it can be observed that the aft design is not a tail cone nor a boattail.

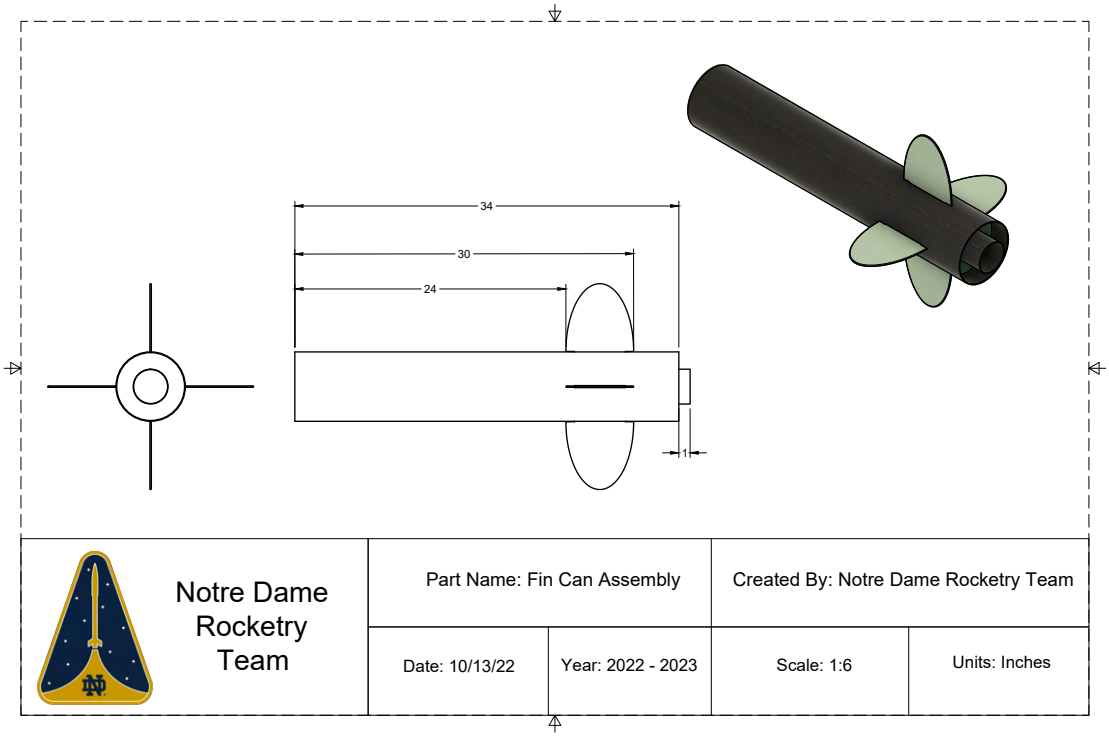

Figure 10: Fin Can Assembly CAD Drawing

3.4 Propulsion System Design

3.4.1 Motor Selection

A trade study was performed in order to determine the optimal motor for the launch vehicle. The four motors compared in the trade study were the L2200, L2375, L1395, and L1115. Table 31 lists the motor trade study results.

Table 20: Motor Trade Study

		L2200		L2375		L1395		L1115	
Criteria	**Weight**	**Value**	**WNV**	**Value**	**WNV**	**Value**	**WNV**	**Value**	**WNV**
Max Apogee (ft)	0.25	5611	0.067	5274	0.063	5067	0.061	4957	0.059
Min Apogee (ft)	0.25	5050	0.069	4736	0.065	4318	0.059	4116	0.056
Cost (1/$)	0.2	0.0029	0.045	0.0029	0.045	0.0033	0.051	0.0038	0.059
Availability	0.3	5	0.125	2	0.167	1	0.025	4	0.100
Total WNV		**0.307**		**0.223**		**0.196**		**0.275**	

The criteria used to compare the motors were the maximum apogee, minimum apogee, cost, and availability. Maximum and minimum apogee were given a weight of 25 % each, due to the fact that the motor is one of the main influences on the launch vehicle's apogee, and the selected motor needs to reach our target apogee for all launch scenarios. For the maximum apogee, the launch vehicle was launched at a five degree launch rail angle with zero mph winds. This is the most extreme, best case scenario within the restrictions of the competition (NASA Req.1.12.). For the minimum apogee, the launch vehicle was launched at a ten degree launch rail angle with 20 mph winds. This is the most extreme, worst case scenario within the restrictions of the competition (NASA Req.1.12.). The cost of the motors was taken off of Chris's Rocketry Supplies; all information on each motor can be found by clicking the hyperlink, found on the names of the motors above Table 31. The cost of the motors was given a weight of 20% due to the high expense of motors. The availability criteria was given a weight of 30% due to the fact that this must be purchased from a vendor, and if the selected motor becomes unavailable the team is unable to launch.

From the trade study results, the L2200 motor is the optimal motor for the competition. The L2200 gave the best range of apogees for all launch scenarios, was the most available, and the costs of this motor was on par with the other options. Another benefit of the L2200 is the team's familiarity with the motor, as it was used during the 2021-2022 season. The thrust curve of the L2200 motor can be found in Figure 11 below, and the overall specifications of the L2200 motor can be found in Table 21. The thrust-to-weight ratio of the full-scale motor, with the

L2200 motor inside, is 9.34:1.

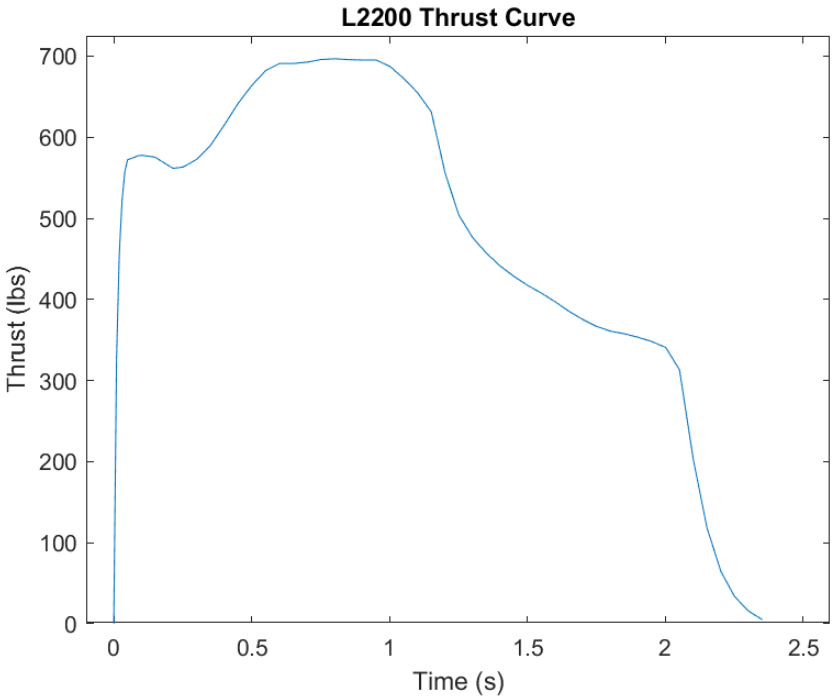

Figure 11: L2200 Thrust Curve, Taken from OpenRocket Data

Table 21: L2200 Motor Specifications, Taken from OpenRocket

L2200	
Dimension	**Value**
Diameter	2.95 in.
Length	26.2 in.
Loaded Weight	168 oz
Propellant Weight	89.2 oz
Burnout Weight	78.8 oz
Total Impulse	1147 lb-sec
Average Thrust	504 lb
Maximum Thrust	677 lb
Burn Time	2.27 sec
Cost	$341.99
Thrust-to-Weight	9.34:1

3.4.2 Motor Retention

The motor retention system houses the motor and is assembled from the motor mount, centering rings, and fins. Three centering rings will connect the motor mount and fin can. This keeps the motor centered in the vehicle and transfers the thrust load to the airframe of the vehicle. The inner and outer diameter of the centering rings were determined by the diameters of the motor mount and the fin can, respectively. The tab height of the fins was determined by the outer diameters of the motor mount and fin can. The fins will be epoxied to to the motor mount using JB Weld, for maximum heat resistance. The CAD drawings of the centering rings and motor retention assembly are shown below in Figures 12 and 13.

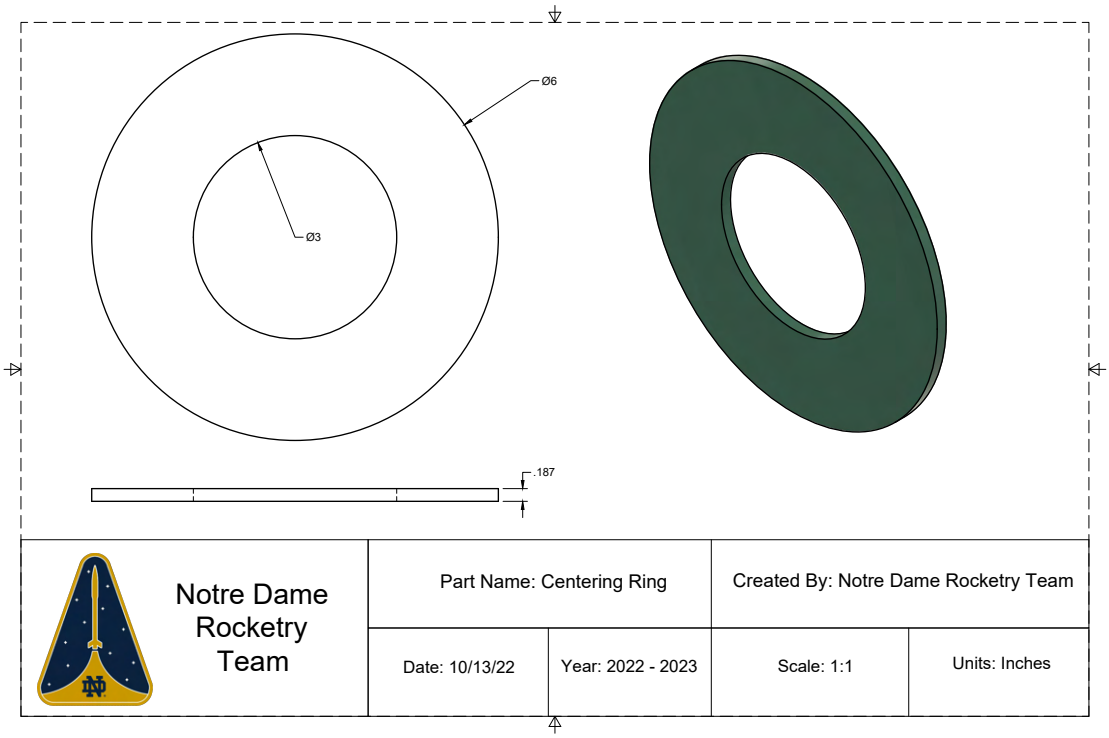

Figure 12: Centering Ring CAD Drawing

Table 22: Centering Ring Dimensions

Dimension	Value
Thickness	0.187 in.
Outer Diameter	6.00 in.
Inner Diameter	3.00 in.
Material	Fiberglass

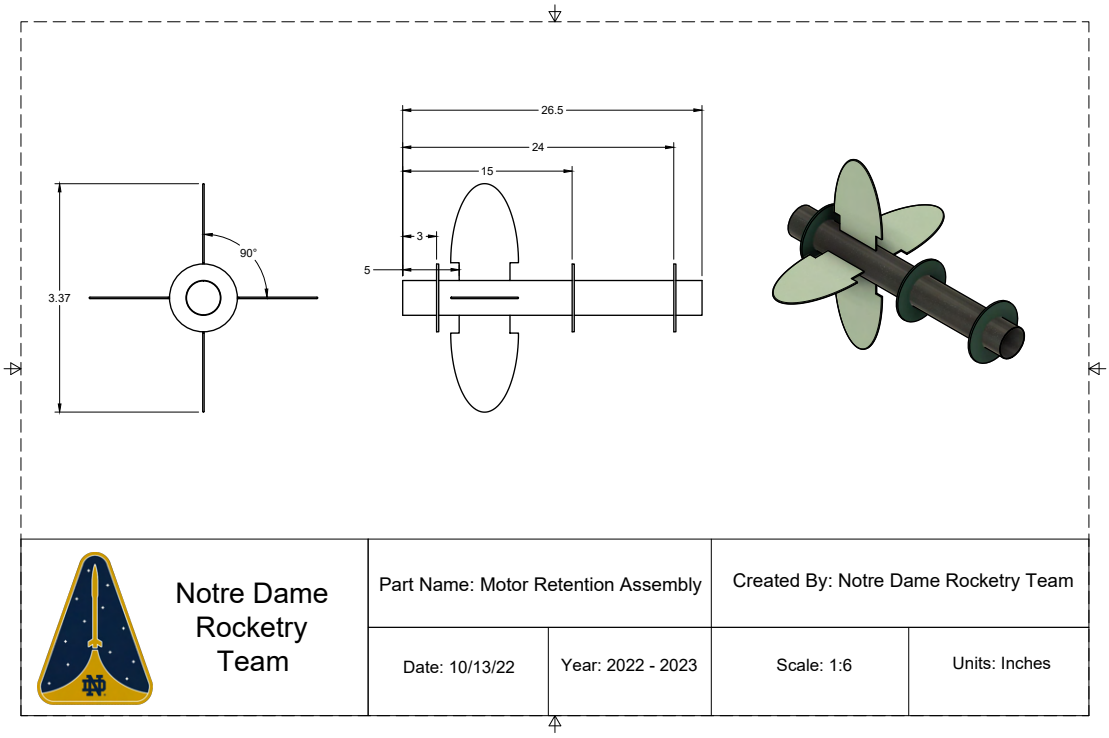

Figure 13: Motor Retention Assembly CAD Drawing

3.5 Vehicle Design Summary

The launch vehicle is 121 inches long, with the most outer diameter of 6.17 in. The target apogee is set to 4600 ft; to achieve this apogee, the launch vehicle will be designed to overshoot the value, and the ACS will induce drag to slow the launch vehicle down to the target apogee value. There are three separation points, resulting in four independent sections. All independent sections are tethered together during flight and descent. The vehicle thrust-to-weight ratio is 9.34:1. Figure 14 displays all launch vehicle sections,internal components, and CG and CP locations. Figure 15 lists all coupler/shoudler locations and additional fin can components. Figure 16 is the CAD model of the launch vehicle.

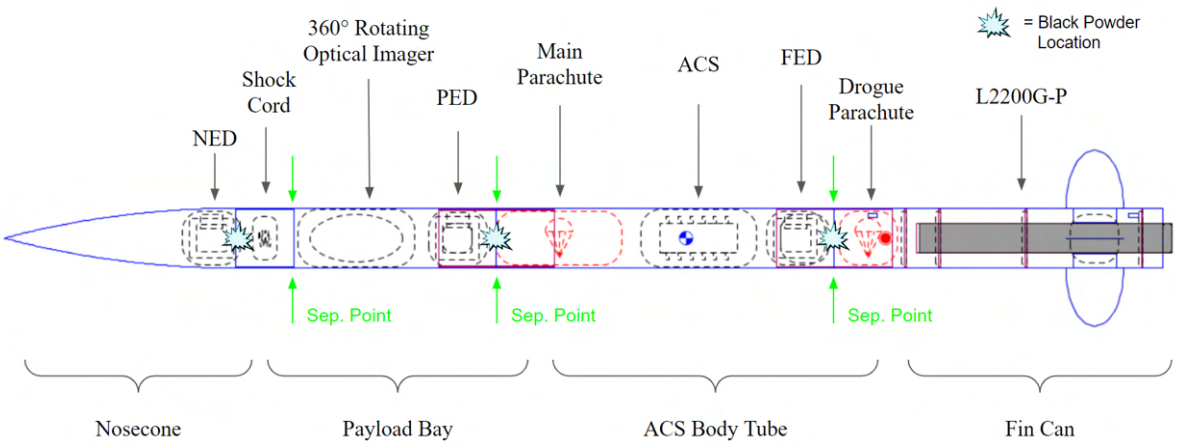

Figure 14: Launch Vehicle Internal Components Part II, Displayed Using OpenRocket

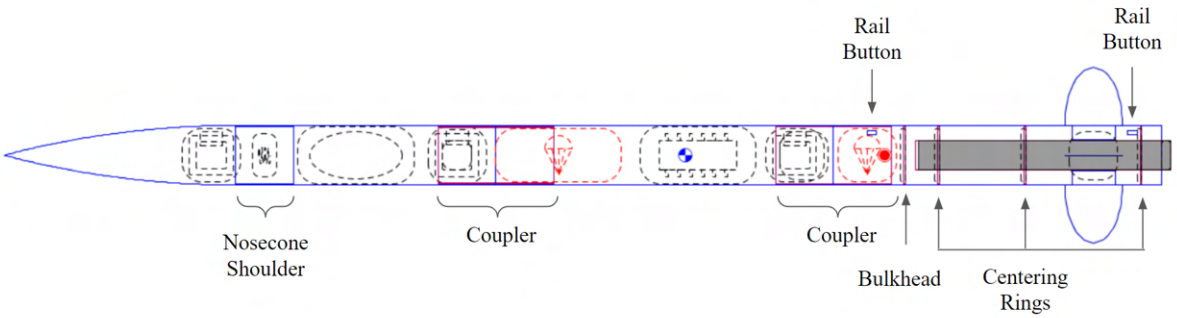

Figure 15: Launch Vehicle Internal Components Part II, Displayed Using OpenRocket

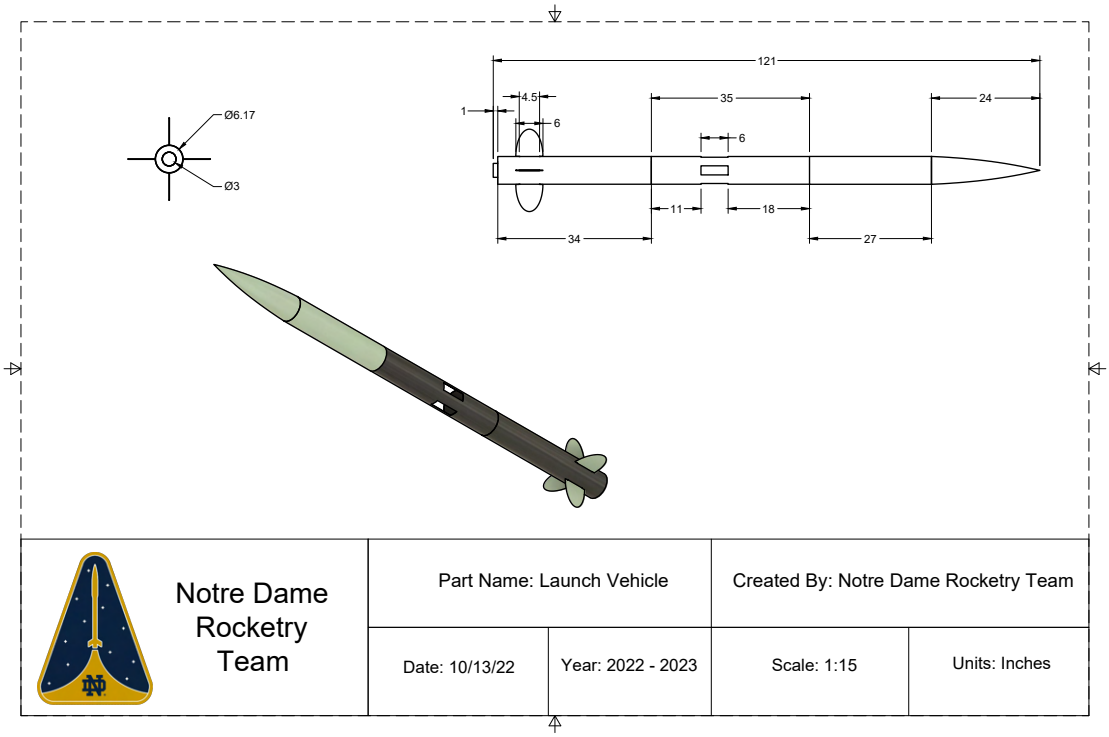

Figure 16: Launch Vehicle CAD Drawing

Table 23 lists all the components found inside each section of the launch vehicle, and the section's length and weight.

Table 23: Launch Vehicle Section Dimensions

Section	Length	Components	Weight
Nosecone	24.0 in.	NED, Shock Cord	87.181 oz
Payload Bay	27.0 in.	360^o Rotating Optical Imager, PED	206.412 oz
ACS Body Tube	35.0 in.	Main Parachute, ACS, FED, Drogue Parachute	275.920 oz
Fin Can	35.0 in. (34.0 in. body tube + motor mount extends out 1.00 in. aft body tube)	Motor, Motor Mount, Centering Rings, Fins, Bulkhead	297.964 oz
Total Length	121.0 in	**Total Weight**	867.477 oz

Table 24 lists the key parameters associated with the launch vehicle's stability and the

thrust-to-weight ratio value. See Section 5.2.4 to understand how the Static Stability Margin is calculated. The thrust-to-weight ratio is taken from the OpenRocket simulation software.

Table 24: Stability and Thrust Dimensions

Dimension	Value
Total Length	121.0 in.
CG Location*	71.593 in.
CP Location*	91.335 in.
Outer Diameter	6.17 in.
Static Stabiltiy Margin	3.20 cal
Thrust-to-Weight Ratio	9.34:1

* Taken from tip of nosecone

Table 25 lists the materials for all the main launch vehicle components.

Table 25: Component Materials

Dimension	Value
Nose Cone	Fiberglass
Paylaod Bay	Fiberglass
ACS Body Tube	Carbon Fiber
Fin Can Body Tube	Carbon Fiber
Fins	Fiberglass
Motor Mount Tube	Carbon Fiber
Centering Rings	Fiberglass
Bulkheads	Fiberglass

3.5.1 Updated Mass Estimate

Table 26 lists the basic, predicted, and allowable mass. The basic mass is the current design's mass. The predicted mass utilizes the ASNI S-120A-201X American National Standard for mass growth allowance; some of the growth percentages were modified to reflect the expected mass growth on the component. For more information on the theory behind the predicted mass, see this link. It should be noted that the Launch vehicle section masses no not include the internal components (recovery electronics, parachutes, ACS, payload). Table 27 lists the mass breakdown for each independent section of the launch vehicle, including all internal components during ascent and descent.

Table 26: Launch Vehicle Mass Breakdown

Component	Basic Mass Estimate (oz)	Predicted Mass (oz)		Allowable Mass (oz)	Margin (%)
Launch Vehicle	554.050	580.990		585.000	0.685
Recovery Device (PED)	42.411	43.631	127.969	134.854	0.108
Recovery Device (FED)	42.411	43.631			
Recovery Device (NED)	43.147	43.593			
ACS	70.328	75.564		80.000	5.545
Payload	69.966	76.069		90.000	15.479
Total	822.312	867.477		890.000	2.531

Table 27: Launch Vehicle Independent Section Mass Breakdown

Section	Basic Ascent Mass Estimate (oz)	Predicted Ascent Mass (oz)	Basic Descent Mass Estimate* (oz)	Predicted Descent Mass* (oz)
Nose cone	82.847	87.181	72.847	76.481
Payload Bay	194.038	206.412	194.038	206.412
ACS Bay	258.777	275.920	178.777	190.320
Fin Can	286.650	297.964	197.450	206.980
Total	822.312	867.477	643.112	680.193

* Main Parachute, Drogue Parachute, Shock Cord, and Motor Propellant are not Included in Section Mass

3.6 Launch Vehicle Preliminary Testing Plan

Table 28 lists the preliminary testing plan for the launch vehicle airframe. This list is subject to expand in the future.

Table 28: Launch Vehicle Preliminary Testing Plan

Test Name	Description	Success Criteria
Shake Test	The airframe and integrated components will be subjected to vibrations to test structural security and connection strength	All components and systems maintain attached after vibration
Drop Test (Airframe Strength Test)	The airframe will be dropped from a height that simulates the predicted kinetic energy and forces experienced during launch vehicle landing	The airframe does not exhibit cracks or additional damage after testing
Wind Tunnel Testing (Camera Shroud & Nose Cone)	The camera shroud and nose cone will be subjected to aerodynamic forces equivalent to those predicted during flight	Components do not have major contributions to the air flow
Bulkhead Static Strength Test	Bulkheads will be subjected to a constant load representing 1.5 times the maximum thrust experienced during flight	Bulkheads do not exhibit damage or failure during or after loading
Bulkhead Impact Strength Test	Bulkheads will be subjected to an impulse representing 1.5 times the impulse caused by in-flight separation events	Bulkheads do not exhibit damage or failure during or after impulse
Motor Mount Strength Test	The motor mount will be subjected to 1.5 times the expected load caused by upwards motor forces	The motor mount does not exhibit damage or failure during or after loading

Table 28: Launch Vehicle Preliminary Testing Plan (continued)

Test Name	Description	Success Criteria
Subscale Demonstration Flight	A subscale version of the launch vehicle will be launched and recovered to evaluate stability and configuration of the design	The subscale launch vehicle is successfully launched and recovered
Full-scale Demonstration Flight	The full-scale launch vehicle with integrated recovery, payload, and ACS systems or substitutions of equal mass will be launched	The full-scale launch vehicle is launched and recovered successfully with relevant performance data and does not sustain significant damage from launch, landing, or recovery
Full-scale Payload Demonstration Flight	The full-scale launch vehicle with the integrated payload system and additional systems or substitutions of equal mass will be launched, and the payload will be deployed	The payload system successfully deploys upon landing of the full-scale launch vehicle and is not significantly damaged

3.7 Subscale

The subscale launch is important to confirm the success of flight profile of the launch vehicle design. The Notre Dame Rocketry Team has tailored the design of the subscale model, including sizings and motor selection, to simulate the full-scale model as realistically as possible, while allowing every other squad the opportunity to collect data that may be of use during during the CDR stage.

3.7.1 Subscale Sizing

The team determined that a 50% scaled version of the full scale launch vehicle will provide an accurate prediction of the full scale launch vehicle's performance. The subscale launch vehicle and the full scale launch vehicle will have comparable thrust-to-weight ratios and stabilities. A scale of 50% provides enough internal volume for the test payloads while also minimizing the cost of materials.

It should be noted that the individual sections of the full-scale launch vehicle will not be reflected in the subscale model. Instead, there will be two individual sections, connected together with a parachute. Figure 17 shows the OpenRocket model of the subscale launch vehicle. The individual sections of the full-scale model are not reflected in the subscale model due to the motor ejecting black powder after burnout (and a delay), and there are no other recovery modules inside the subscale vehicle to induce separation. Most importantly, the purpose of a subscale launch is to perform as accurately as possible to the full-scale launch vehicle (NASA Req. 2.18.1); this can be accomplished as long as the total length, nosecone dimensions, stability, and thrust-to-weight ratio of the launch vehicle are as accurate as possible.

The OpenRocket model of the subscale launch vehicle can be found in Figure 17, where the inner components are clearly seen and all parts are labeled. Table 29 lists the specifications of the subscale launch vehicle. A comparison between the dimensions and specifications for the full scale and subscale launch vehicles can be seen in Table 30. The CAD model of the subscale launch vehicle can be found in Figure 18.

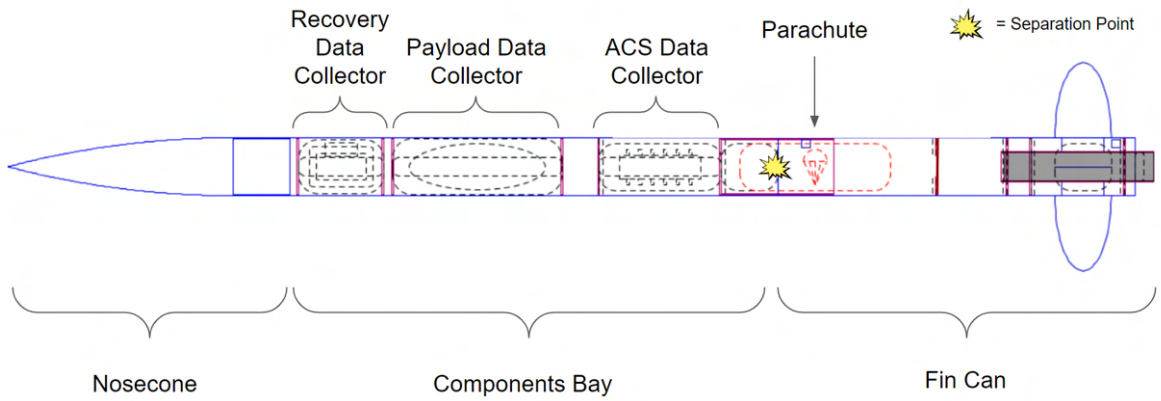

Figure 17: Subscale Launch Vehicle Inner Configuration

If should be noted that for the subscale model, the individual sections are separated with black powder ignition, occurring after the burnout of the I357 motor.

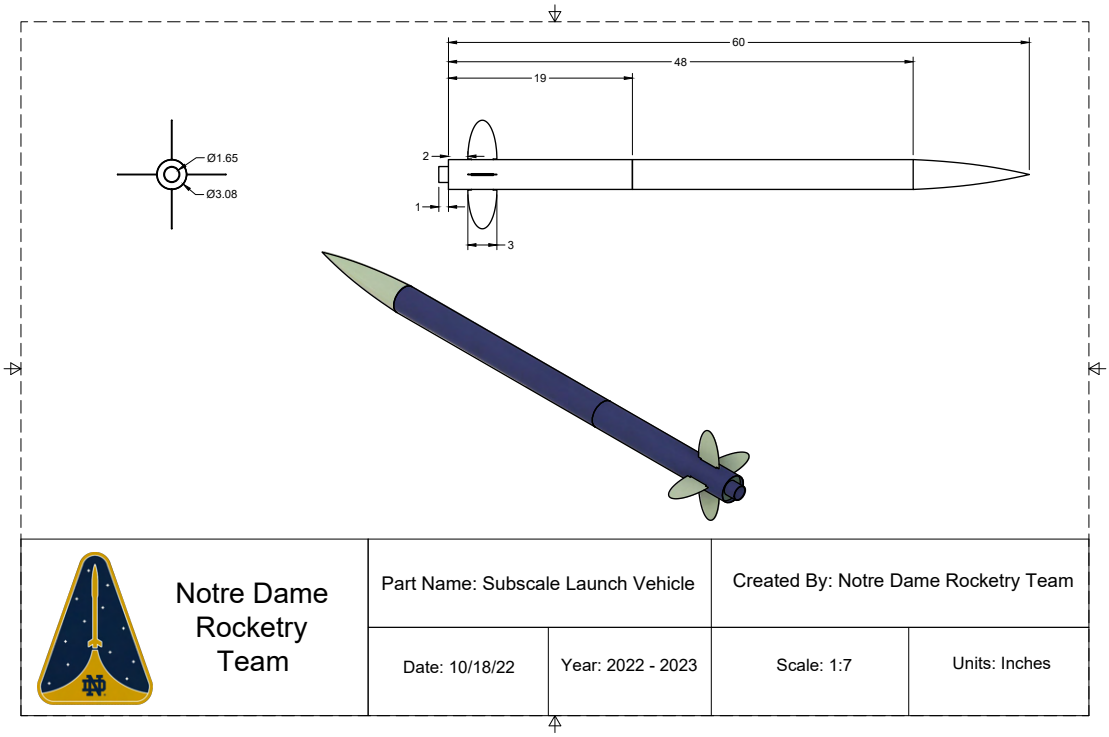

Figure 18: Subscale Launch Vehicle CAD Drawing

Table 29: Subscale Launch Vehicle Dimensions

Section	Length	Components	Weight
Nosecone & Components Bay	41.0 in.	Main Parachute, ACS, FED, Drogue Parachute	58.87 oz
Fin Can	20.0 in. (19.0 in. body tube + motor mount extends out 1.00 in. aft body tube)	Motor, Motor Mount, Centering Rings, Fins, Baffle	70.41 oz
Total Length	61.0 in	**Total Weight**	129.28 oz

Table 30: Preliminary Subscale Sizing, Including Dimensions and Materials

Component	Full-scale Material	Subscale Material	Full-scale Dimensions	Ideal Subscale Dimensions	Official Subscale Dimension	Percent Difference (Ideal vs Official)
Nose cone	Fiberglass	ABS Plastic (3D Printed)	L = 24.0 in D = 6.17 in Ogive	L = 12.0 in D = 3.085 in Ogive	L = 12.0 in D = 3.08 in Ogive	L = 0.00% D = 0.162%
Body Tubes	**Payload Bay:** G12 Fiberglass	G12 Fiberglass	L = 96 in D_{outer} = 6.17 in D_{inner} = 6.00 in	L = 48 in D_{outer} = 3.085 in D_{inner} = 3.00 in	L = 48 in D_{outer} = 3.08 in D_{inner} = 3.00 in	L = 0.00% D_{outer} = 0.162% D_{inner} = 0.00%
	Rest: Carbon Fiber	G12 Fiberglass				
Motor Mount	Carbon Fiber	G12 Fiberglass	L = 26.5 in D_{outer} = 3.08 in D_{inner} = 3.00 in	L = 13.25 in D_{outer} = 1.54 in D_{inner} = 1.50 in	L = 8.1 in D_{outer} = 1.65 in D_{inner} = 1.50 in	L = 38.9% D_{outer} = 7.14% D_{inner} = 0.00%
Total Length	N/A	N/A	L = 120 in	L = 60 in	L = 61 in	L = 1.67 %
Fins	G10 Fiberglass	G10 Fiberglass	Root = 6.00 in Height = 6.00 in Tab Length = 4.50 in Tab Height = 1.50 in	Root = 3.00 in Height = 3.00 in Tab Length = 2.25 in Tab Height = 0.75 in	Root = 3.00 in Height = 4.00 in Tab Length = 2.25 in Tab Height = 0.75 in	Root = 0.00% Height = 33.3% Tab Length = 0.00% Tab Height = 0.00%
Stability	N/A	N/A	CG = 71.593 CP = 91.335 D_{outer} = 6.17 in Stability = 3.20	Stability = 3.20	CG = 39.676 CP = 49.252 D_{outer} = 3.08 in Stability = 3.11	Stability = 2.81%
Thrust-to-Weight (T2W)	N/A	N/A	T2W = 9.34:1	T2W = 9.34:1	T2W = 9.10:1	T2W = 2.57%

3.7.2 Subscale Motor Selection

A trade study was performed in order to determine the optimal motor for the subscale launch vehicle. The three motors compared in the trade study were the I161, I225, and I357. Table 31 lists the motor trade study results.

Table 31: Motor Trade Study

		I161		L225		I357	
Criteria	**Weight**	**Value**	**WNV**	**Value**	**WNV**	**Value**	**WNV**
Max Apogee (ft)	0.25	1027	0.076	1114	0.082	1253	0.092
Min Apogee (ft)	0.25	860	0.073	965	0.082	1105	0.094
Cost (1/$)	0.2	0.018	0.070	0.015	0.060	0.018	0.070
Availability (Number on Chris's Rocket Supplies)	0.3	11	0.114	8	0.083	10	0.103
Total WNV		**0.333**		**0.307**		**0360**	

The criteria used to compare the motors were the maximum apogee, minimum apogee, cost, and availability. Maximum and minimum apogee were given a weight of 25% each, due to the fact that the motor is one of the main influences on the launch vehicle's apogee, and the selected motor needs to reach an optimal apogee for all launch scenarios. For the maximum apogee, the launch vehicle was launched at a five degree launch rail angle with zero mph winds. This is the most extreme, best case scenario within the restrictions of the competition (NASA Req. NASA Req.1.12.. For the minimum apogee, the launch vehicle was launched at a ten degree launch rail angle with 20 mph winds. This is the most extreme, worst case scenario within the restrictions of the competition (NASA Req. NASA Req.1.12.). The cost of the motors was taken off of Chris's Rocketry Supplies; all information on each motor can be found by clicking the hyperlink, found on the names of the motors above Table 31. The cost of the motors was given a weight of 20% due to the high cost of motors. The availability criteria was given a weight of 30% due to the fact that this must be purchased from a vendor, and if the selected motor becomes unavailable the team is unable to launch.

From the trade study results, the I357 motor is the optimal motor for the competition. The I357 motor gave the best range of apogees for all launch scenarios, was very available, and the costs of this motor was on par with the other options. The thrust curve of the I357 motor can be found in Figure 19 below, and the overall specifications of the I357 motor can be found in Table 32.

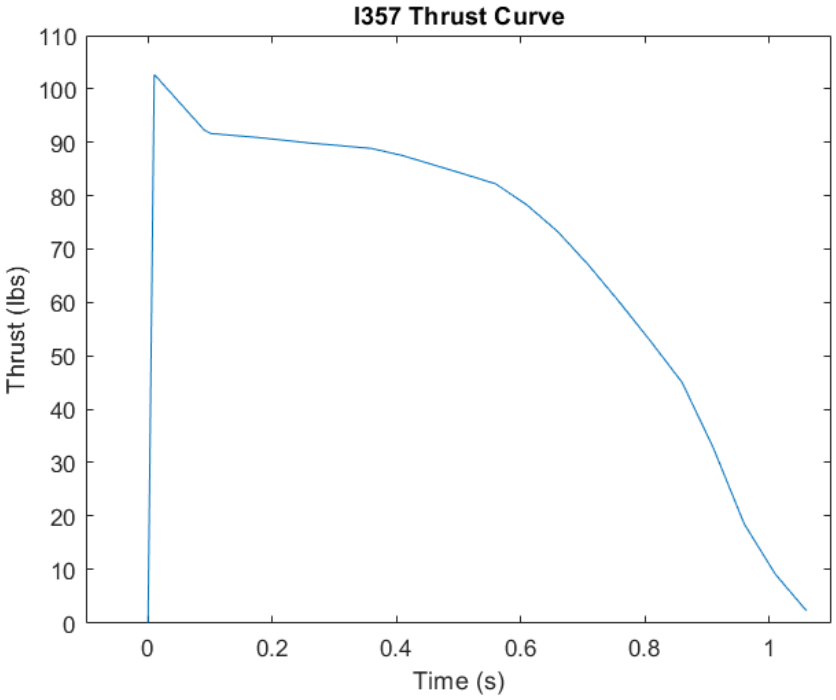

Figure 19: I357 Thrust Curve, Taken from OpenRocket Data

Table 32: I357 Motor Specifications, Taken from OpenRocket

I357	
Dimension	**Value**
Diameter (in.)	1.5
Length (in.)	7.95
Loaded Weight (oz)	12.8
Propellant Weight (oz)	5.84
Burnout Weight (oz)	6.96
Total Impulse (lb-sec)	76.7
Average Thrust (lb)	72.2
Maximum Thrust (lb)	104.8
Burn Time (sec)	1.06
Cost ($)	55.99
Thrust-to-Weight	9.10:1

3.8 Subscale Flight Simulations

The same methods for simulating the full-scale launch vehicle were applied to the subscale launch vehicle. Section 3.8.1 outlines the methods used to simulate the flight of the launch vehicle.

As long as recovery protects the subscale vehicle from damage during descent, there are no specific recovery requirements for the subscale launch. Therefore, only the flight ascent simulations were performed; the descent drift radius, kinetic energy, and descent time analysis simulations were not performed.

3.8.1 Simulation Methods

Multiple simulation methods were used for the same type of mission performance analysis as a method of redundancy; the team wanted to ensure the data found was precise. The team has used the following simualtion methods in past years and have found them to be both accurate and precise, given the proper inputs. Table 33 lists the type of mission performance analysis, what its respective simulation methods are, methods for simulating the mission performance, and what stage the mission performance will be evaluated at.

Table 33: Mission Performance Method Overview

Mission Performance Method	Description	Methods of Analysis
Simulated Flight Profiles	Analysis on launch vehicle altitude, velocity, acceleration, and thrust as a function of time	OpenRocket, RockSim
Launch Target Apogee	after an analysis of the launch vehicle predicted apogee, the team sets a target apogee during PDR	OpenRocket, RockSim
Stability	Analysis on launch vehicle CP, CG , and Stability margin, both for the static (on-rail stability) stability margin and the dynamic (during flight) stability margin	OpenRocket, RockSim

3.8.2 Flight Altitude

The team simulated various flight conditions to understand the projected altitude of the sub-scale launch vehicle as a function of time. Per NASA's USLI PDR requirements, the simulated flight conditions included varying launch rail angles and wind speeds. The simulations used launch rail angles of 5, 7, and 10 degrees, and for each launch rail angle, wind speeds of 0, 5 10, 15, and 20 miles per hour were used. All other launch conditions were held constant between iterations. The team simulated flights using both OpenRocket and RockSim. Section 3.8.2.1 lists the altitude results for the OpenRocket simulations and Section 3.8.2.2 lists the altitude results for the RockSim simulations.

3.8.2.1 OpenRocket Simulations Figures 20, 21, and 21 list the OpenRocket simulations for the launch vehicle altitude for various launch rail angles and wind speeds.

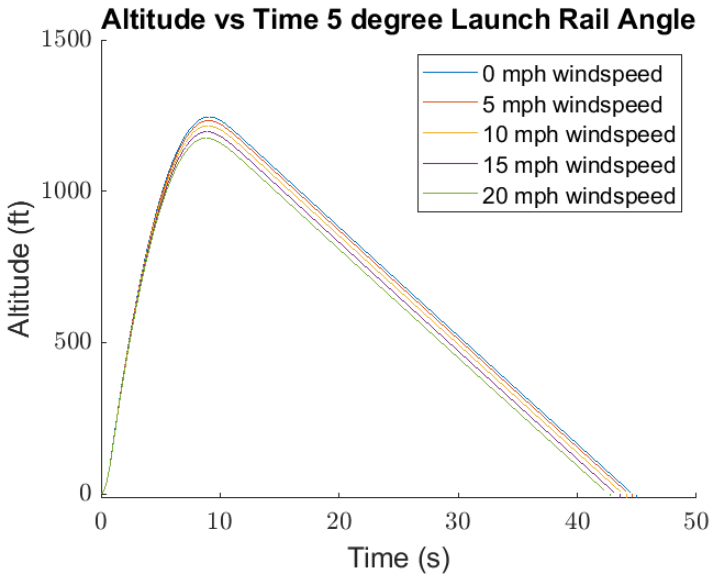

Figure 20: OpenRocket: Simulated Altitude vs Time for Various Wind Speeds, 5° Rail Angle

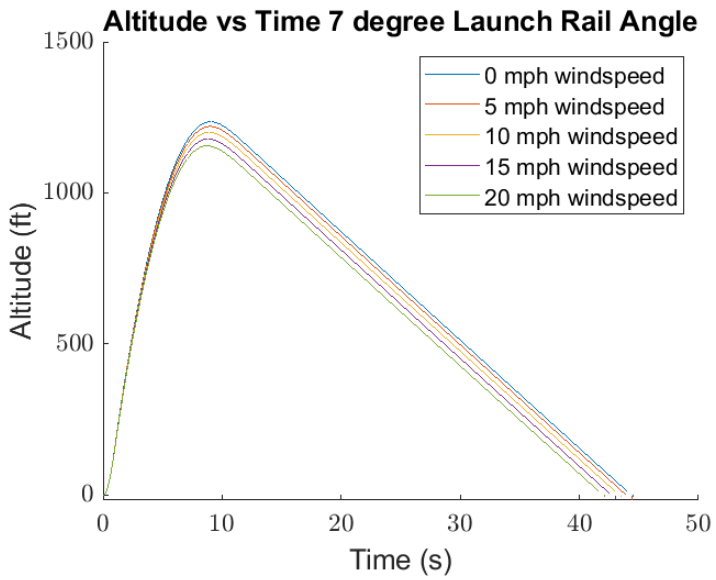

Figure 21: OpenRocket: Simulated Altitude vs Time for Various Wind Speeds, 7° Rail Angle

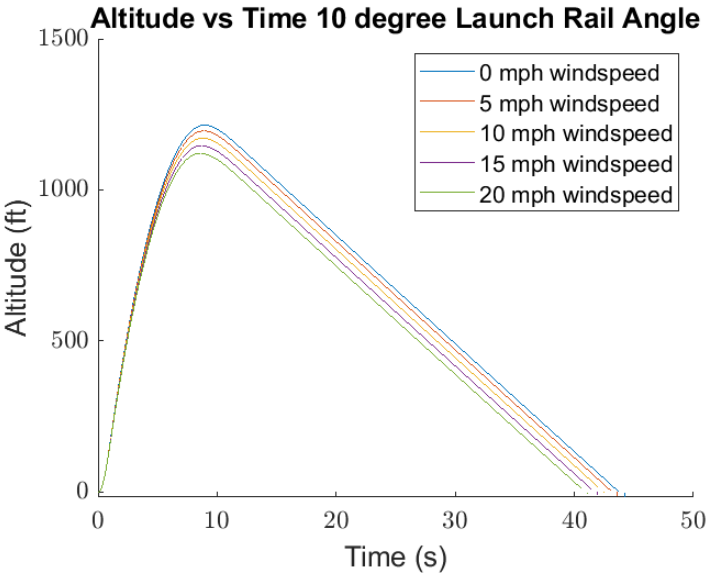

]

Figure 22: OpenRocket: Simulated Altitude vs Time for Various Wind Speeds, 10° Rail Angle

Table 34 summarizes the results of the OpenRocket altitude simulations. From the table, the highest predicted apogee is 1245.8 ft, and the lowest predicted apogee is 1121.2 ft.

Table 34: OpenRocket Altitude Simulations

	Launch Rail 5° (ft)	Launch Rail 7° (ft)	Launch Rail 10° (ft)
0 MPH Wind	1245.8	1235.6	1214.6
5 MPH Wind	1233.5	1220.4	1195.4
10 MPH Wind	1216.5	1200.8	1171.6
15 MPH Wind	1196.4	1178.4	1146.4
20 MPH Wind	1175.6	1155.7	1121.2

3.8.2.2 RockSim Simulations

Figures 23, 24, and 25 lists the RockSim simulations for the subscale launch vehicle altitude for various launch rail angles and wind speeds.

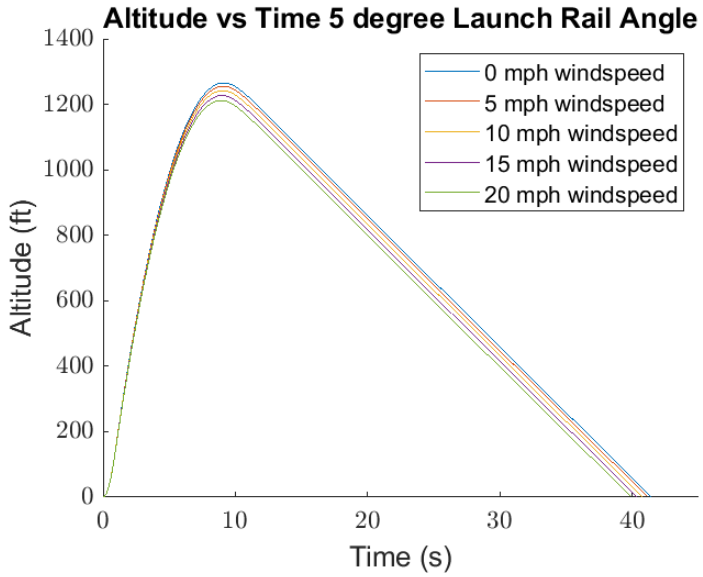

Figure 23: RockSim: Simulated Altitude vs Time for Various Wind Speeds, 5° Rail Angle

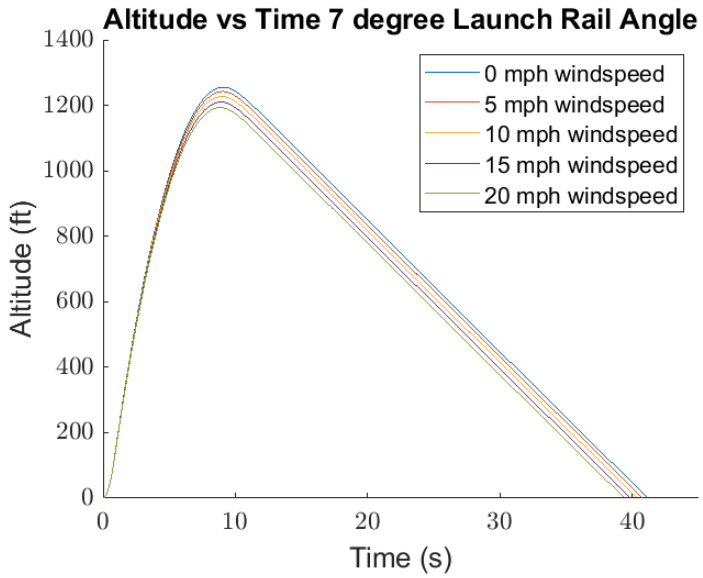

Figure 24: RockSim: Simulated Altitude vs Time for Various Wind Speeds, 7° Rail Angle

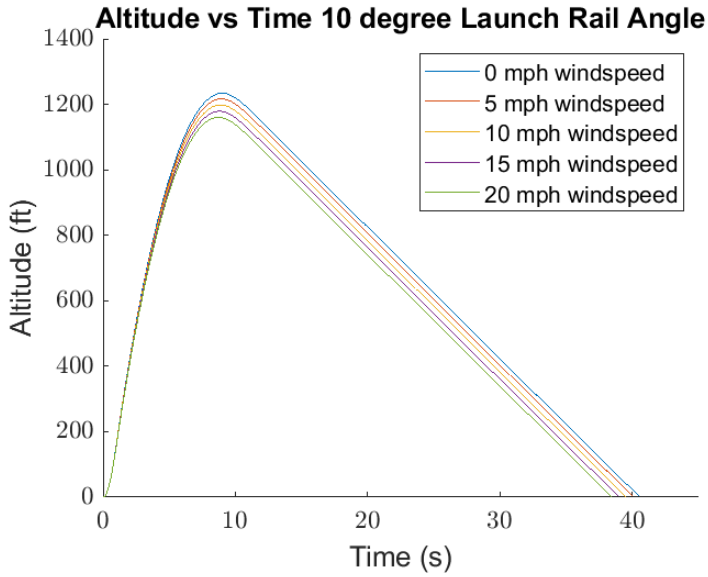

Figure 25: RockSim: Simulated Altitude vs Time for Various Wind Speeds, 10° Rail Angle

Table 35 summarizes the results of the RockSim altitude simulations. From the table, the highest predicted apogee is 1265.6 ft, and the lowest predicted apogee is 1160.2 ft.

Table 35: RockSim Altitude Simulations

	Launch Rail 5° (ft)	Launch Rail 7° (ft)	Launch Rail 10° (ft)
0 MPH Wind	1265.6	1255.4	1233.9
5 MPH Wind	1255.3	1242.3	1216.9
10 MPH Wind	1242.0	1226.7	1198.1
15 MPH Wind	1227.0	1209.9	1178.9
20 MPH Wind	1211.5	1193.1	1160.2

3.8.2.2.1 OpenRocket vs RockSim Values & the Average Apogee Table 36 lists the average predicted apogee of the two simulation softwares for all flight conditions. The average between the two softwares provides the best method to determine the predicted apogee because the models demonstrate equal accuracy based on previous years.

Table 36: Average Apogee Between OpenRocket and RockSim Simulations

	Launch Rail 5° (ft)	Launch Rail 7° (ft)	Launch Rail 10° (ft)
0 MPH Wind	1255.7	1245.5	1224.3
5 MPH Wind	1244.4	1231.4	1206.2
10 MPH Wind	1229.3	1223.8	1184.9
15 MPH Wind	1211.7	1194.2	1162.7
20 MPH Wind	1193.6	1174.4	1140.7

3.8.3 Flight Velocity Simulations and Off-Rail Velocity Values

The team ran simulations for various flight conditions to understand the projected flight velocity and off-rail velocity of the launch vehicle as a function of time. Per NASA's USLI PDR requirements, the varied flight conditions included launch rail angles and wind speeds. The launch rail was angled at 5, 7, and 10 degrees, and for each launch rail angle, the wind speeds were placed at 0, 5 10, 15, and 20 miles per hour; all other launch conditions were held constant between iterations. The team ran launch simulations using both OpenRocket and RockSim. Section 3.8.3.1 outlines the velocity results for the OpenRocket simulations and Section 3.8.3.2 outlines the velocity results for the RockSim simulations.

3.8.3.1 OpenRocket Simulations Figures 26, 27, and 28 lists the OpenRocket simulations for the launch vehicle velocity for various launch rail angles and wind speeds.

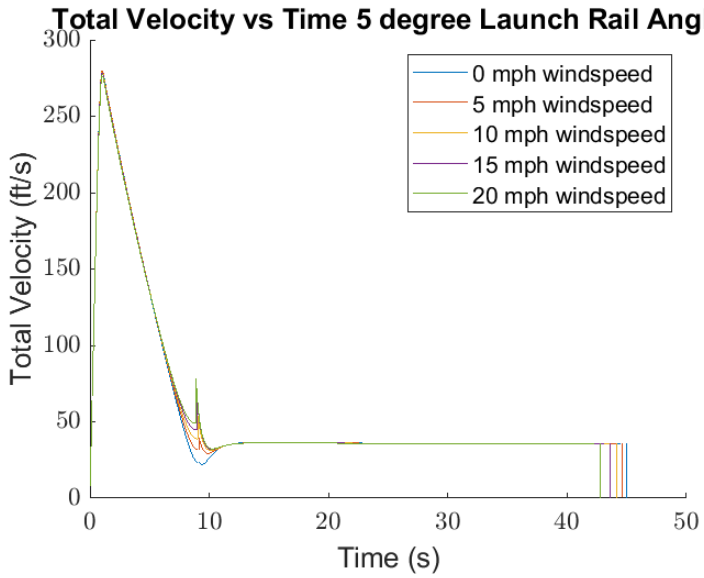

Figure 26: OpenRocket: Simulated Velocity vs Time for Various Wind Speeds, 5° Rail Angle

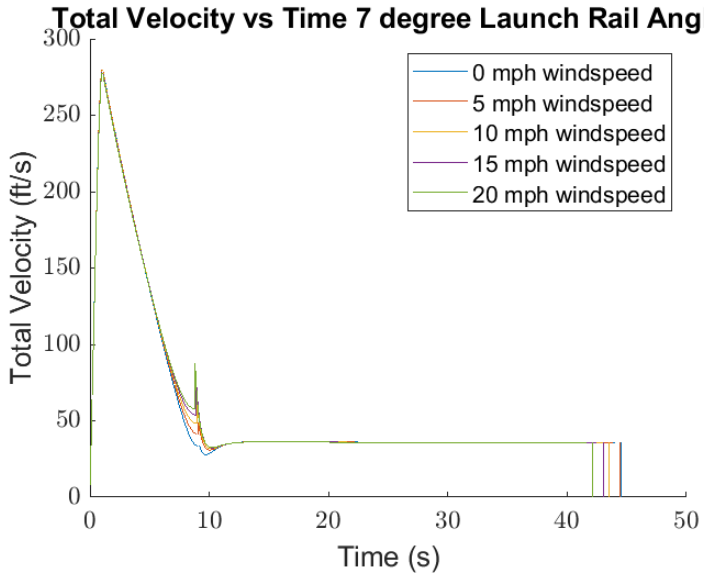

Figure 27: OpenRocket: Simulated Velocity vs Time for Various Wind Speeds, 7° Rail Angle

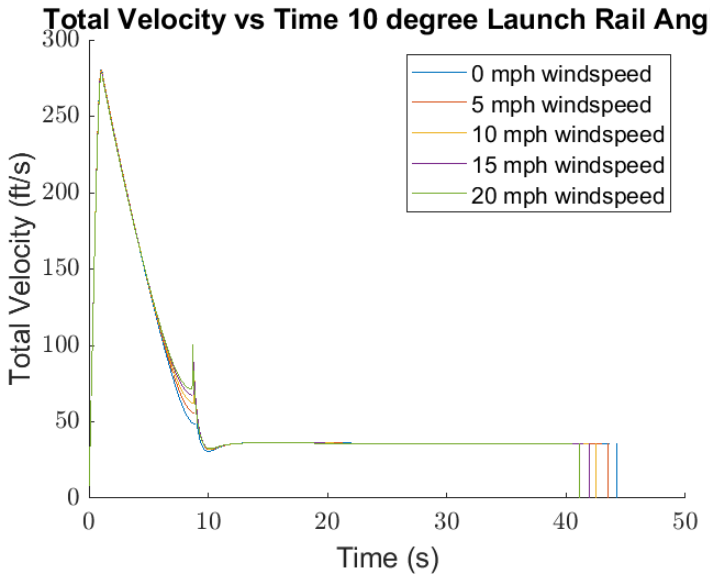

Figure 28: OpenRocket: Simulated Velocity vs Time for Various Wind Speeds, 10° Rail Angle

Table 37 lists the off-rail velocity for the launch vehicle for all OpenRocket simulations. OpenRocket calculates that off-rail occurs at 0.189 seconds.

Table 37: OpenRocket Simulations' Off-Rail Velocity of Launch Vehicle

	Launch Rail 5° (fps)	Launch Rail 7° (fps)	Launch Rail 10° (fps)
0 MPH Wind	64.0160	64.036	64.079
5 MPH Wind	64.010	64.029	64.071
10 MPH Wind	64.002	64.021	64.062
15 MPH Wind	64.000	64.018	64.058
20 MPH Wind	63.999	64.017	64.056

3.8.3.2 RockSim Simulations Figures 29, 30, and 31 lists the RockSim simulations for the launch vehicle velocity for various launch rail angles and wind speeds.

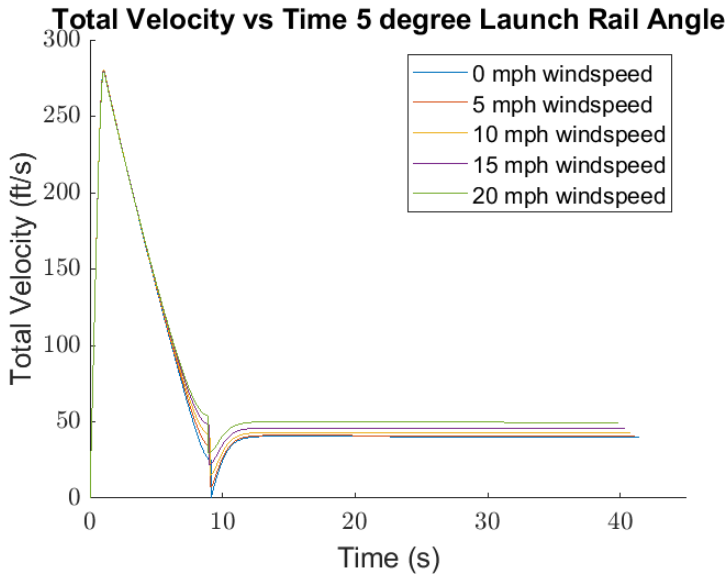

Figure 29: RockSim: Simulated Velocity vs Time for Various Wind Speeds, 5° Rail Angle

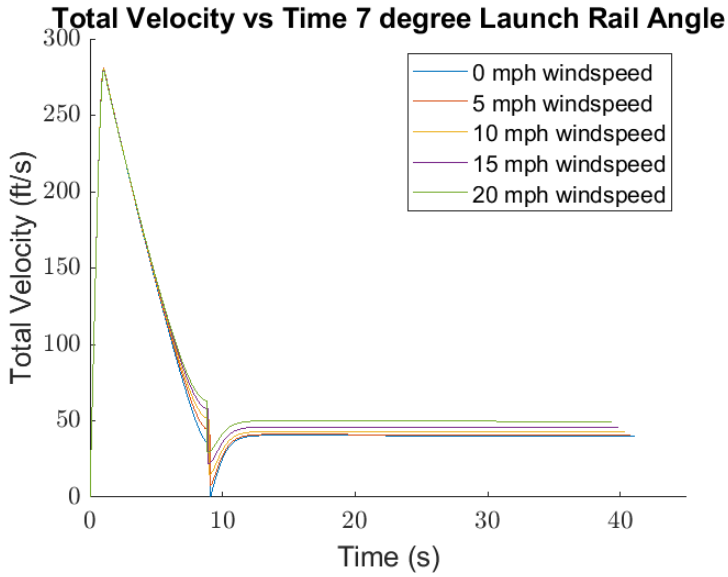

Figure 30: RockSim: Simulated Velocity vs Time for Various Wind Speeds, 7° Rail Angle

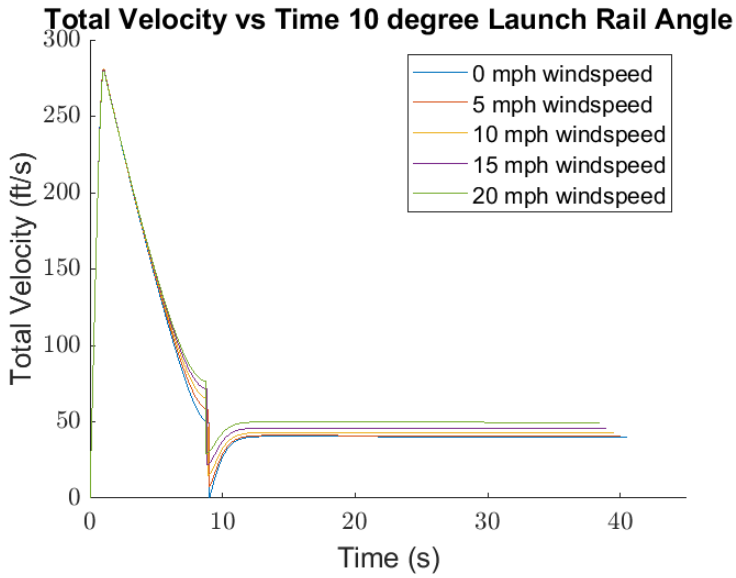

Figure 31: RockSim: Simulated Velocity vs Time for Various Wind Speeds, 10° Rail Angle

For all RockSim simulations the launch vehicle exited the rail at 0.182 seconds. Table 38 lists the off-rail velocity for the launch vehicle for all RockSim simulations.

Table 38: RockSim Simulations' Off-Rail Velocity of Launch Vehicle

	Launch Rail 5° (fps)	Launch Rail 7° (fps)	Launch Rail 10° (fps)
0 MPH Wind	60.667	60.667	60.667
5 MPH Wind	60.667	60.667	60.667
10 MPH Wind	60.667	60.667	57.258
15 MPH Wind	60.667	57.258	57.258
20 MPH Wind	57.258	57.258	57.258

3.8.3.2.1 OpenRocket vs RockSim Values & the Average Velocity The off-rail velocities between both flight simulation softwares is comparable, with a difference of around 2 fps. The reasonable precision allows the team to compare the two versions.

Table 42 lists the average value of the two simulation softwares for all flight conditions. The average between the two softwares provides the best method to determine the predicted apogee because the models demonstrate equal accuracy based on previous years.

Table 39: Average Off-Rail Velocity Between OpenRocket and RockSim Simulations

	Launch Rail 5° (fps)	Launch Rail 7° (fps)	Launch Rail 10° (fps)
0 MPH Wind	62.342	62.352	62.373
5 MPH Wind	60.839	62.348	62.639
10 MPH Wind	62.335	62.344	60.660
15 MPH Wind	62.334	60.638	60.658
20 MPH Wind	60.629	60.638	60.657

3.8.4 Flight Acceleration

The team ran simulations for various flight conditions to understand the projected acceleration of the launch vehicle as a function of time. Per NASA's USLI PDR requirements, the varied flight conditions included launch rail angles and wind speeds. The launch rail was angled at 5, 7, and 10 degrees, and for each launch rail angle, the wind speeds were placed at 0, 5 10, 15, and 20 miles per hour; all other launch conditions were held constant between iterations. The team ran launch simulations ran for both OpenRocket and RockSim. Section 3.8.4.1 lists the acceleration results for the OpenRocket simulations and Section 3.8.4.2 lists the acceleration results for the RockSim simulations. The team determined acceptable precision between the softwares based on the similarity between the two software's data.

3.8.4.1 OpenRocket Simulations Figures 32, 33, and 63 lists the OpenRocket simulations for the subscale launch vehicle acceleration for various launch rail angles and wind speeds.

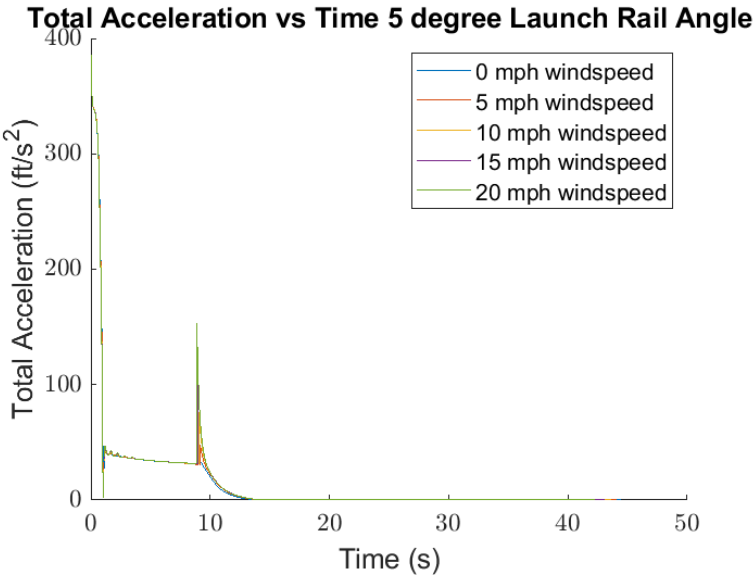

Figure 32: OpenRocket: Simulated Acceleration vs Time for Various Wind Speeds, 5° Rail Angle

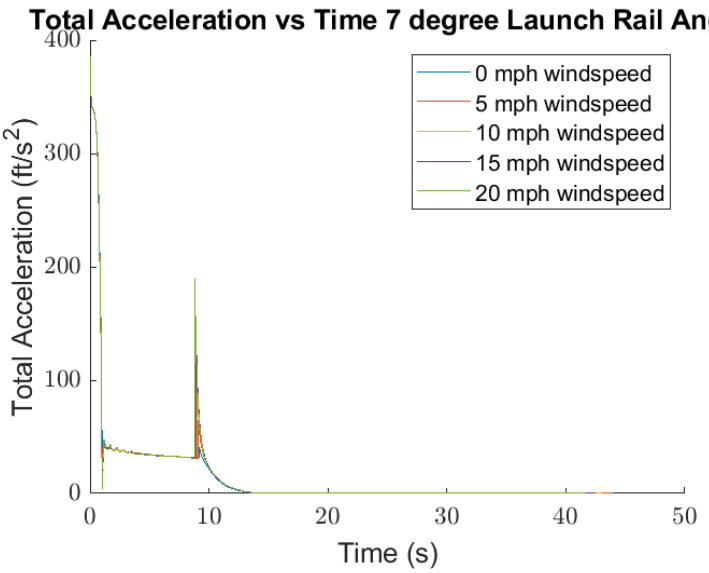

Figure 33: OpenRocket: Simulated Acceleration vs Time for Various Wind Speeds, 7° Rail Angle

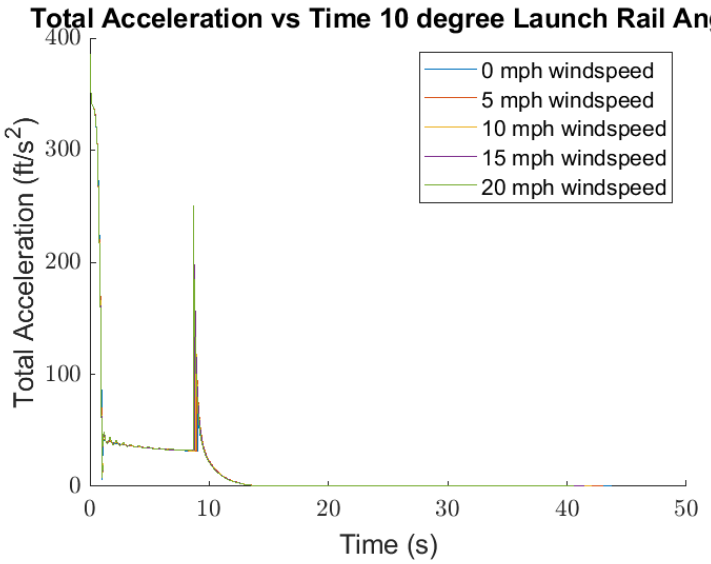

Figure 34: OpenRocket: Simulated Acceleration vs Time for Various Wind Speeds, 10° Rail Angle

3.8.4.2 RockSim Simulations

Figures 35, 36, and 37 lists the RockSim simulations for the subscale launch vehicle acceleration for various launch rail angles and wind speeds.

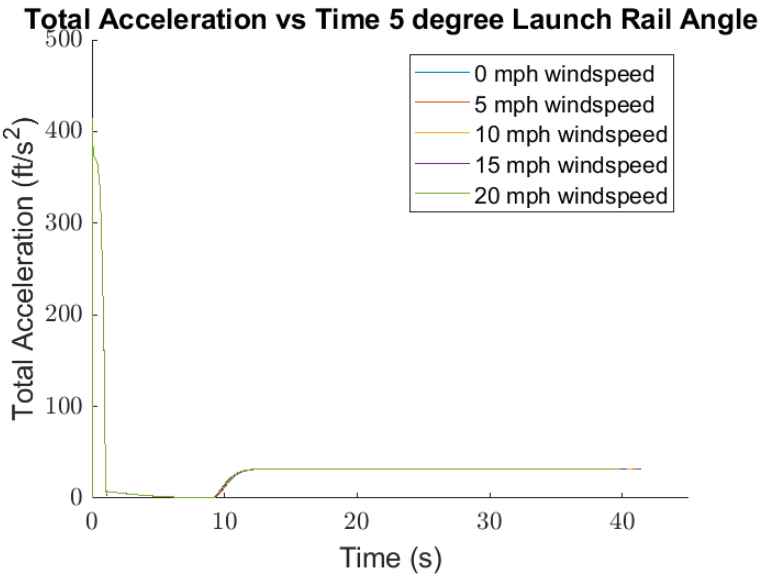

Figure 35: RockSim: Simulated Acceleration vs Time for Various Wind Speeds, 5° Rail Angle

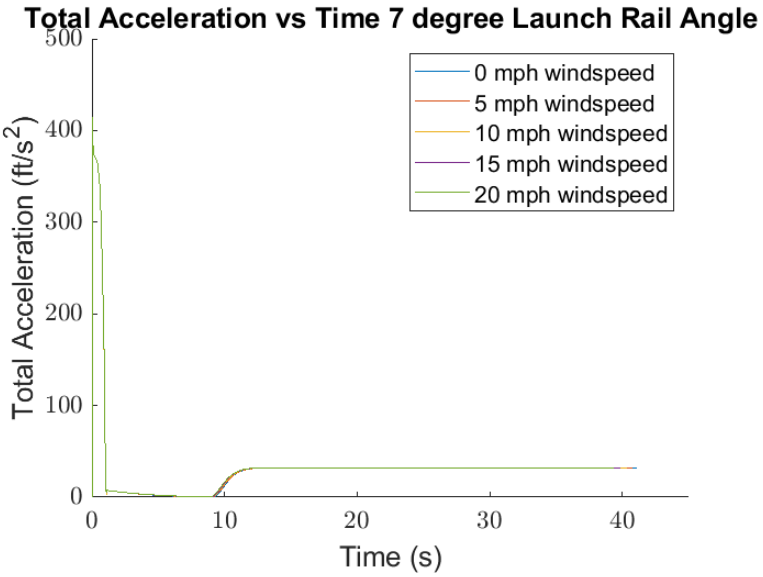

Figure 36: RockSim: Simulated Acceleration vs Time for Various Wind Speeds, 5° Rail Angle

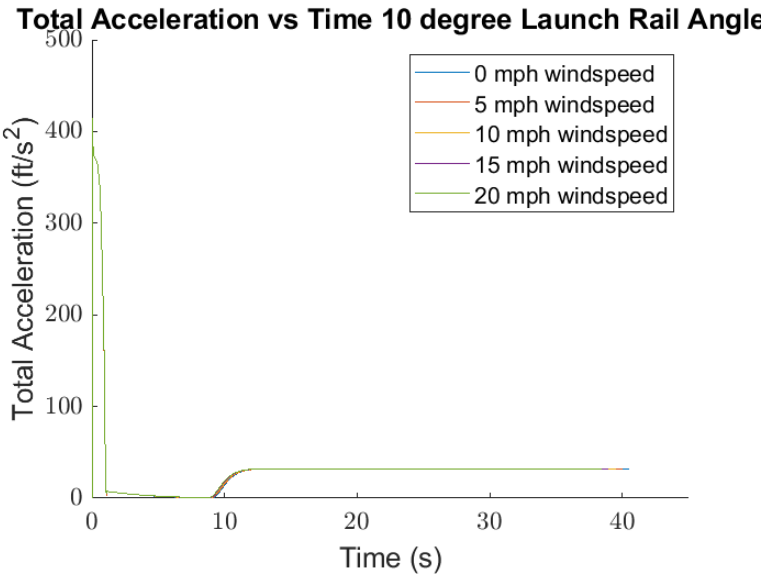

Figure 37: RockSim: Simulated Acceleration vs Time for Various Wind Speeds, 5° Rail Angle

3.8.5 Stability

3.8.5.1 Static Stability The following equation is used to find the static stability of the launch vehicle:

$$\text{Stability} = \frac{CP - CG}{d_{outer}} \tag{1}$$

where CP is the location of the center of pressure (in), CG is the location of the center of gravity (in), and d_{outer} is the outer diameter of the body tubes (in). Note: the CG and CP origin is the nose cone tip.

3.8.5.1.1 OpenRocket Static Stability Margin The notable values of CP, CG, and the outer diameter from the OpenRocket model are:

- CG = 39.676 in
- CP = 49.252in
- Outer Diameter 3.08 in

One can now plug the values into the equation:

$$\text{Stability} = \frac{CP - CG}{d_{outer}} = \frac{49.252 - 39.676}{3.08} = 3.11 cal \tag{2}$$

A large static stability margin may cause concern for weather-cocking, but the team would need a significantly larger static stability margin for weather-cocking to become a major issue, based on current calculations from RockSim (See the next section).

3.8.5.1.2 RockSim Static Stability Margin The notable values of CP, CG, and the outer diameter from the RockSim model are:

- CG = 39.120 in
- CP = 49.112 in
- Outer Diameter 3.08 in

One can now plug the values into the equation:

$$\text{Stability} = \frac{CP - CG}{d_{outer}} = \frac{49.112 - 39.120}{3.08} = 3.24cal \tag{3}$$

A large static stability margin may cause concern for weather-cocking, but the current RockSim design says different. The software says that, for weathercocking, "with current settings, the rocket stays inside the 40 degree weathercocking cone before apogee which is considered safe."

3.8.5.1.3 OpenRocket versus RockSim Values There is around a 4% difference between the two different static stability values. This difference comes from the CP value, which is calculated slightly differently for the two softwares. The small difference between the stability values allows the team to determine acceptable precision for the two softwares. As noted before, the software's accuracy cannot be confidently determined until a demonstration flight occurs during CDR.

3.8.5.2 Dynamic Stability Simulations and Off-Rail Stability Values Dynamic stability comes from analyzing changing forces on the launch vehicle. While this is not a specific NASA requirement, the team plans on having the dynamic stability margin as close to 2.00 cal as possible. The same equation, Equation 2, is used to calculate the dynamic stability, but with CP and CG values that change during flight.

The team ran simulations for various flight conditions to understand the projected dynamic stability of the launch vehicle as a function of time. Per NASA's USLI PDR requirements, the varied flight conditions included launch rail angles and wind speeds. The launch rail was

angled at 5, 7, and 10 degrees, and for each launch rail angle, the wind speeds were placed at 0, 5 10, 15, and 20 miles per hour; all other launch conditions were held constant between iterations. Launch simulations were ran for both OpenRocket and RockSim. Section 3.8.5.2.1 lists the stability results for the OpenRocket simulations and Section 3.8.5.2.2 lists the altitude results for the RockSim simulations.

3.8.5.2.1 OpenRocket Simulations Figures 38, 39, and 40 lists the OpenRocket simulations for the launch vehicle stability for various launch rail angles and wind speeds.

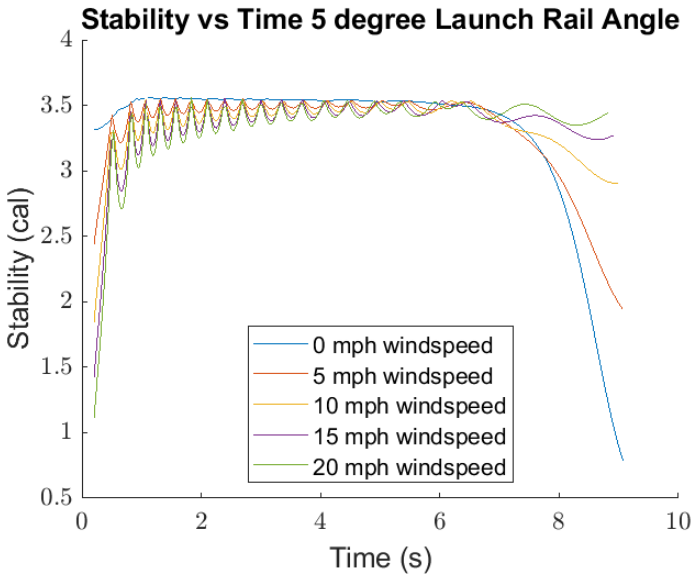

Figure 38: OpenRocket: Simulated Stability vs Time for Various Wind Speeds, 5° Rail Angle

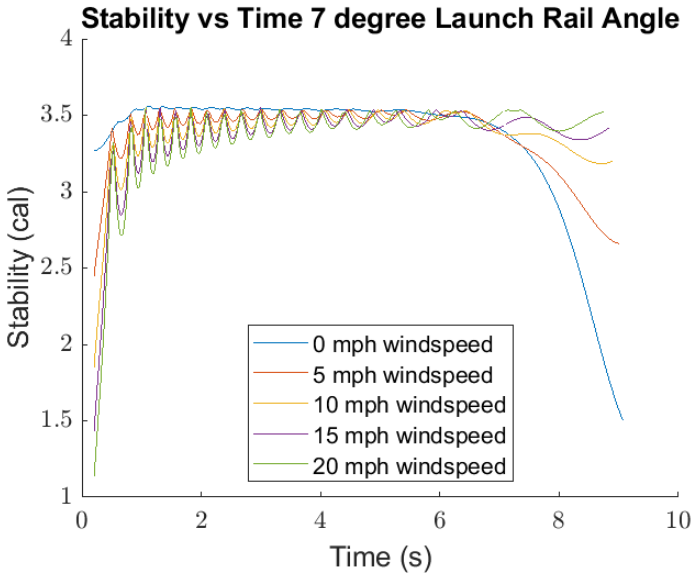

Figure 39: OpenRocket: Simulated Stability vs Time for Various Wind Speeds, 7° Rail Angle

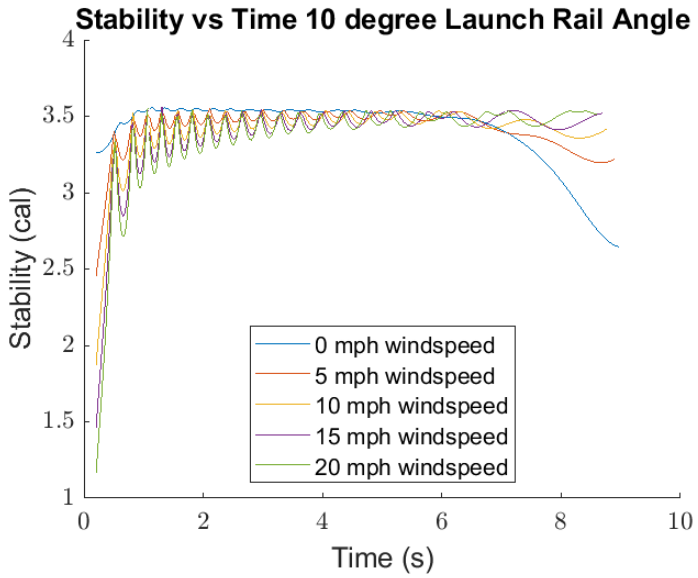

Figure 40: OpenRocket: Simulated Stability vs Time for Various Wind Speeds, 10° Rail Angle

As expected, the stability increases during flight as the CP shifts aftward (due to an increased velocity) and the CG shifts forward (due to motor burnout removing weight). For all OpenRocket simulations the launch vehicle went off-rail at 0.189 seconds. Table 40 lists the off-rail stabilities for the launch vehicle for all OpenRocket simulations.

From the table, the launch vehicle abides by this NDRT requirement for winds 10MPH or less. A brief re-design during CDR may allow the launch vehicle to abide under all wind conditions, but there may be limitations due to the max velocity of the motor by burnout; CP is affected by the launch vehicle's velocity. As well, a smaller launch vehicle does not require as much stability to have a safe launch, so the stability should still be okay as long as the static value is greater than 2.0 (which it is).

Table 40: OpenRocket Simulations' Off-Rail Dynamic Stability of Launch Vehicle

	Launch Rail 5°(cal)	Launch Rail 7°(cal)	Launch Rail 10°(cal)
0 MPH Wind	3.314	3.266	3.263
5 MPH Wind	2.443	3.447	2.454
10 MPH Wind	1.843	1.853	1.870
15 MPH Wind	1.420	1.435	1.460
20 MPH Wind	1.116	1.134	1.164

3.8.5.2.2 RockSim Simulations Figures 41, 42, and 43 lists the RockSim simulations for the launch vehicle altitude for various launch rail angles and wind speeds.

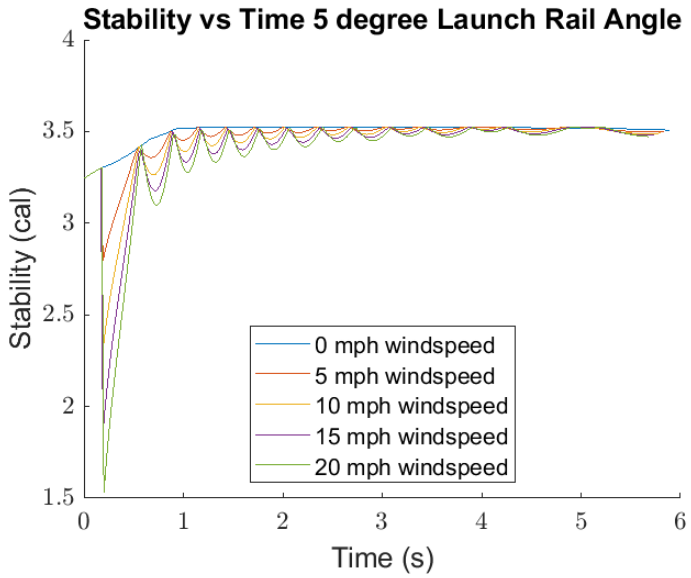

Figure 41: RockSim: Simulated Stability vs Time for Various Wind Speeds, 5° Rail Angle

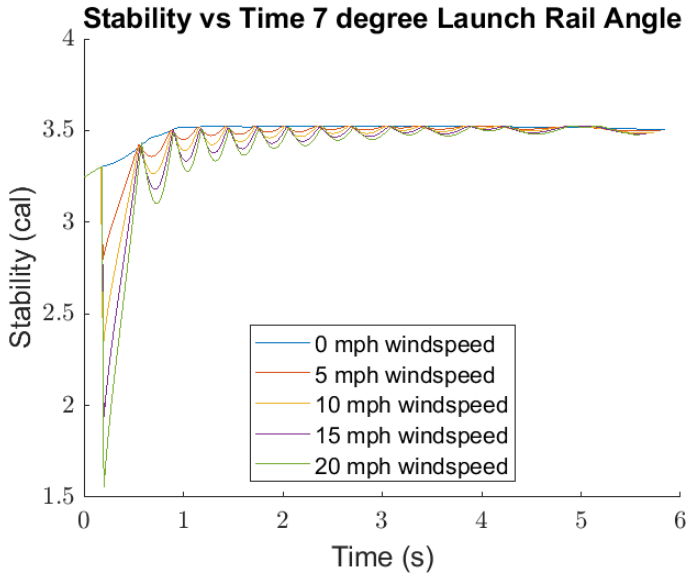

Figure 42: RockSim: Simulated Stability vs Time for Various Wind Speeds, 7° Rail Angle

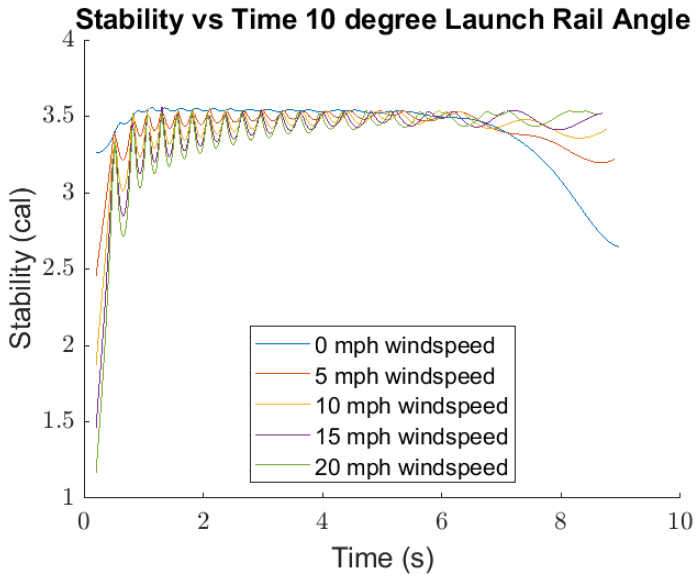

Figure 43: RockSim: Simulated Stability vs Time for Various Wind Speeds, 10° Rail Angle

As expected, the stability increases during flight as the CP increases (due to an increased velocity) and the CG decreases (due to motor burnout removing weight). The software also says that, for weathercocking, "with current settings, the rocket stays inside the 40 degree weathercocking cone before apogee which is considered safe."

Table 41 lists the off-rail stabilities for the launch vehicle for all RockSim simulations. All RockSim simulations went off-rail at 0.182 seconds, and the value in Table 41 is the stability at that time point. From the table, the RockSim model for calculating the stability does not differ as the launch angle or wind changes. For all situations, the CG would change the same. The CP should change but the altering flight conditions have no logical influence on the CP value. Therefore, it makes sense as to why the values appear the same. Given that all values are above the desired 2.00 cal, the launch vehicle is at a stable level of stability.

Table 41: RockSim Simulations' Off-Rail Dynamic Stability of Launch Vehicle

	Launch Rail 5°(cal)	Launch Rail 7°(cal)	Launch Rail 10°(cal)
0 MPH Wind	3.3014	3.3014	3.3014
5 MPH Wind	3.3014	3.3014	3.3014
10 MPH Wind	3.3014	3.3014	3.298
15 MPH Wind	3.3014	3.298	3.298
20 MPH Wind	3.298	3.298	3.298

3.8.5.2.3 OpenRocket versus RockSim Values and the Average Off-Rail Stability Between Versions The difference between the predicted stability margin of the simulation methods is

noticeable. Table 42 lists the average value of the two simulation softwares for all flight conditions. The average between the two softwares provides the best method to determine the predicted apogee because both models have demonstrated accuracy in the past.

Table 42: Average Off-Rail Stability Between OpenRocket and RockSim Simulations

	Launch Rail 5°(cal)	Launch Rail 7°(cal)	Launch Rail 10°(cal)
0 MPH Wind	3.31	3.28	3.28
5 MPH Wind	2.87	3.37	2.88
10 MPH Wind	2.57	2.58	2.58
15 MPH Wind	2.36	2.37	2.38
20 MPH Wind	2.21	2.22	2.23

4 Technical Design: Vehicle Recovery System

4.1 System Overview

The success of the recovery system will be judged on its ability to adequately reduce the kinetic energy of the launch vehicle while also ensuring the descent time and drift abide by competition requirements (NASA Reqs. 3.3., 3.10., 3.11.). The recovery system will be composed of three independent modules: the FED, NED, and PED. The first recovery event will be when the FED deploys the drogue parachute at apogee. Subsequently, the NED will eject the nose cone from the payload body tube at 800 ft AGL. The sole purpose of this recovery event is to allow the payload to deploy from its respective body tube upon landing. Therefore, this event will not deploy a parachute but will keep the nose cone tethered to the payload bay to keep the entire vehicle connected. The shock cord will be attached to the payload body tube along the edges of the tube such that there is an opening for the payload to deploy. To protect the payload from the ejection gases created by the NED's charges, a removable fiberglass wall and Nomex blanket will be placed in between the payload and the NED. These components will be connected to the bulkhead of the NED and will be pulled out of the payload body tube after the nose cone is ejected. The PED and the main parachute will be housed in the payload body tube aft of the payload module. The PED will deploy the main parachute at an altitude of 600 ft AGL. Black powder charges will be used to trigger all separation events. The main and drogue parachutes will be attached to the launch vehicle with shock cords, quicklinks, and eye-bolts. The main parachute will be protected from ejection gases by a deployment bag and the drogue will be wrapped in a Nomex blanket. Each energetic device will house three redundant altimeters, which are separate from any altimeters used by the ACS or payload systems (for a total of 9 altimeters). The GPS used to track the

vehicle will be located in the nose cone above the NED.

4.1.1 Mission Success Criteria

The following criteria will be used to determine the success of the recovery system for any given launch:

- All components of the launch vehicle shall land with a maximum kinetic energy of 65 ft-lbf.
- The launch vehicle shall stay within 2500 feet of the location where apogee is reached.
- The launch vehicle shall land within 80 seconds of reaching apogee.
- The GPS system shall transmit the location of the launch vehicle after landing so that the vehicle and the payload media can be recovered.
- The altimeters, located in all of the recovery modules, shall record altitude data for proof of flight and the altitude score.
- No flight critical damage shall occur to the vehicle that would prevent another launch on the same day without emergency repairs.

4.2 Separation and Deployment

Each major phase of the recovery process requires a separation event where black powder charges detonate and separate two sections that remain tethered together. Two of these events also coincide with the deployment of a parachute while the third event only separates the sections. The various components and methods of separation are considered in this section.

4.2.1 Separation Method

Black powder ejection charges will continue to be used as the separation method for the sections of the vehicle. Other methods considered include compressed carbon dioxide, phosphorous-based charges, and pyrodex. Separation methods were evaluated based on cost, ease of integration, safety, efficiency, and deployment temperature. Black powder was deemed the most effective method in the evaluation largely due to its ease of integration, low cost, and high degree of safety in part due to the NAR mentor's frequent experience handling the substance.

Table 43: Separation Method Trade Study

		Black Powder		Compressed CO_2		Phosphorus		Pyrodex	
Criteria	**Weight**	**Value**	**WNV**	**Value**	**WNV**	**Value**	**WNV**	**Value**	**WNV**
Cost (1/$)	0.15	0.03	0.06	0.01	0.02	0.01	0.01	0.03	0.06
Ease of Integration (Scale of 1-5)	0.2	5	0.08	1	0.02	2	0.03	4	0.07
Safety (Scale of 1-5)	0.3	4	0.08	5	0.09	3	0.06	4	0.08
Efficiency (Scale of 1-5)	0.25	5	0.09	1	0.02	3	0.06	4	0.08
Temperature at Ejection (1/F°)	0.1	0.002	0.02	0.005	0.05	0.002	0.02	0.002	0.02
Total WNV		**0.32**		**0.20**		**0.17**		**0.31**	

4.2.2 Ejection Charge Sizing

Preliminary estimates for the black powder ejection charges were calculated by hand and by using the Huntsville Area Rocketry Association's (HARA's) charge size estimator. Nine charges will be needed, three at each separation point which can be viewed in Figure 44, below.

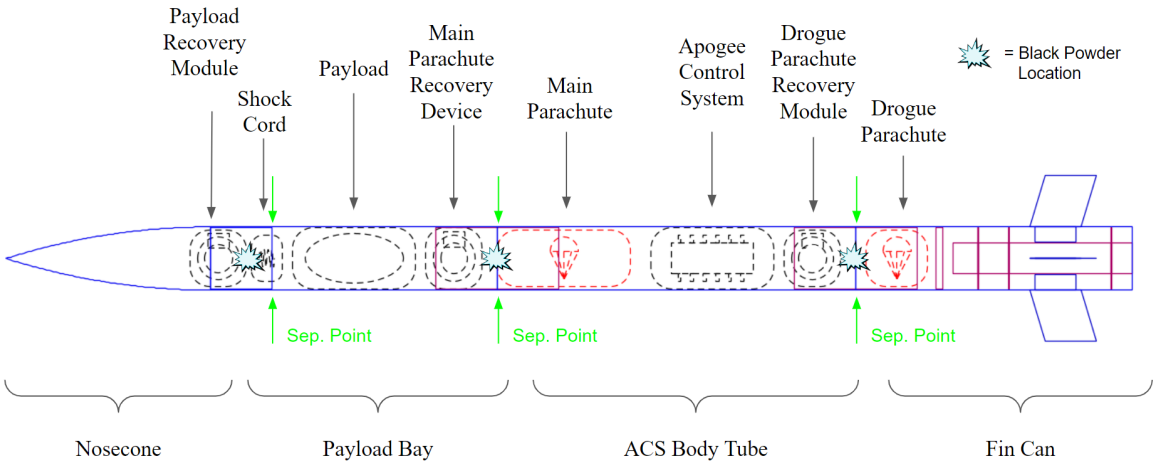

Figure 44: Full Vehicle Layout with Separation Points

First, the dimensions of the areas to be pressurized must be determined. The pressurized sections, listed in order of most forward separation point to furthest aft separation point, are

listed in Table 1, below.

Table 44: Pressurized Section Dimensions

Section	Length (in)	Diameter (in)	Volume (in^3)
NED (Fore)	7.5	6.00	212.06
PED (Middle)	15.5	6.00	438.25
FED (Aft)	6.5	6.00	183.78

As a preliminary estimate for PDR, the team estimates that five 4-40 nylon shear pins will be used to connect the sections of the vehicle based on prior vehicle requirements. This will be verified and altered as needed during CDR based on the anticipated max drag force produced by ACS. However, for the sake of this initial estimate, the equation

$$P_{shear} = \frac{\tau_{max} A_{pin} N_{pins}}{\frac{\pi}{4} D^2} \tag{4}$$

was used to calculate P_{shear}, the pressure needed to shear the pins, where τ_{max} is the shear strength of nylon (6500 psi), A_{pin} is the cross-sectional area of one pin at the point of shear (0.0099 in^2), N_{pins} is the number of pins (5) and D is the diameter of the bulkhead to which force will be applied (listed in Table 44). Using hand calculations, P_{shear} was calculated to be 11.32 psi by hand which was confirmed by the HARA calculator. Finally, the HARA calculator was used to estimate black powder amounts for this phase of the recovery design process. For CDR, these quantities will be confirmed by manual stoichiometric calculations for black powder. However, for brevity's sake in this report, the HARA black powder quantities with a factor of safety of 1.5 are listed below in Table 45. The factor of safety is included to ensure the pins break as this is essential to the proper functioning of the recovery system and the surrounding components were selected to be capable of withstanding this additional force.

Table 45: Pressurized Section Dimensions

Module	Black Powder Amount (g)
NED (Fore)	1.86
PED (Middle)	3.84
FED (Aft)	1.61

4.2.3 Ejection Module Housing

Previously, a 3D printed charge mount bolting scheme housed the PVC pipe that held the black powder charges. However, the PVC pipe on one of the charge housings cracked last year

due to contact with a quicklink from the shock cord assembly. Alternative methods were thus evaluated this year to evaluate whether the PVC pipe would be sufficient in durability to survive recovery events this year. Durability in Table 52 refers to the method's ability to withstand the force of the black powder charge or quicklink damage. The values in the chart for durability were derived from the material's ultimate tensile strength measured in psi. Density refers to the mass per unit volume of the material which provides an indication for how the mass of the components would vary for similar sized assemblies. Containability refers to how effectively the ejection charge stays in place during launch. Ease of assembly refers to the number of parts and the difficulty of assembly for each method. It is given the lowest weight because each part has a relatively similar design that has minimal changes and complexity. The density is weighted the heaviest as several ejection charges are used for each module making the total mass difference from the material differences significant. Containability and ease of assembly are ranked on a scale of 1 to 5.

Table 46: Ejection Charge Trade Study

		3D Cap with PVC (Friction)		3D Cap with PVC (Bolted)		Fully 3D Printed Tube (ABS)		Aluminum Pipe	
Criteria	**Weight**	**Value**	**WNV**	**Value**	**WNV**	**Value**	**WNV**	**Value**	**WNV**
Durability (ksi)	0.35	7.5	0.056	7.5	0.056	4.4	0.032	14.5	0.107
Density (in^3/lb)	0.35	20.1	.094	21.55	0.101	23	0.107	10.3	.048
Containability (1-5)	0.3	3	0.05	5	0.083	5	0.083	5	.083
Ease of Assembly (1-5)	0.1	4	0.025	4	0.025	5	.031	3	.019
Total WNV		**0.224**		**0.265**		**0.254**		**0.257**	

While the trade study suggests both Aluminum and the 3-D printed cap with PVC that is bolted from the side would have similar effectiveness, the Aluminum retains more heat which is potentially dangerous for the laundry and people handling the vehicle following recovery. Therefore, the 3D Cap with PVC that is bolted from the side was selected.

4.2.4 Ejection Charge Redundancy

The separation of each intended section is critical to ensuring a safe landing and mission success. There will be three separation events: one for the drogue parachute, one for the main parachute, and one to eject the nose cone. If the sections containing the parachutes were to not separate, this would lead to a catastrophic failure as they are critical to a successful landing. Additionally, the ejection of the nose cone is mission critical as the payload cannot deploy if the nose cone remains attached to the payload body tube. Since all of these separation events are vital to the team's success, each separation event will have three redundant charge detonations to guarantee the separation of the sections. Each of these detonations will be triggered by an independent altimeter that is not connected to the circuitry of the ACS or payload electronics.

4.3 Laundry

The vehicle will descend under two different parachutes during the recovery process. Details of these parachutes and their accompanying components will be considered in this section.

4.3.1 Parachute Selection and Sizing

The main parachute was selected first based on its ability to slow the vehicle to a velocity that would keep the kinetic energy of the section of the vehicle with the most mass under 65 ft-lb (NASA Req. 3.3). The projected masses for each section that were used for calculations can be viewed in Table 47, below.

Table 47: Vehicle Mass Section Estimates, Unseparated Post Burnout

Nosecone (oz)	Payload (oz)	ACS (oz)	Fin Can (oz)	Total (oz)
87.18	206.41	275.92	206.98	776.493

It is worth noting that some of these sections have less effective mass after recovery events occur. For example, once the vehicle is separated, the masses of the parachutes are no longer in the ACS section thus reducing its mass for the max kinetic energy calculation. Following this consideration, the section with the most mass upon landing is projected to be the Fin Can section at 206.98 oz (this section's mass reduces following the consumption of the propellant during ascent which is reflected in this mass value). Considering this, the equation

$$v_{max} = \sqrt{\frac{2KE_{max}}{m_{max}}} \tag{5}$$

was used to calculate the max velocity of the vehicle where v_{max} is the max velocity, KE_{max} is 65 ft-lb (NASA Req. 3.3), and m_{max} is the mass of the payload section. This equation was integrated into a custom MATLAB script, `main_parachute_selection.m`, which yielded a v_{max} of 17.98 ft/s. Next, a simple force balance equation could be set up to determine the parameters of the parachute needed for the vehicle. During the final descent of the vehicle, the drag produced by the parachute and the weight of the entire vehicle equal as the vehicle is in terminal velocity. Thus, the equation

$$\frac{1}{2}\rho v_{max}^2 C_d A = m_{tot} g \tag{6}$$

where ρ is the standard air density, v_{max} is the value calculated in Equation 5, $C_d A$ is the unknown value to be solved for and the right side of the equation is the weight of the full vehicle after burnout. Since everything is known except for $C_d A$, we can solve for that dimensionless value and obtain a minimum $C_d A$ value for the parachute if the vehicle is to abide by the kinetic energy requirement. This $C_d A$ was determined to be 126.28 using the `main_parachute_selection.m` script as well. Only parachutes that met this $C_d A$ value were considered with parachutes being especially close to this value deemed favorable as they would reduce drift and descent time while still fulfilling kinetic energy requirements. This would later allow the team to select a larger drogue parachute to keep that descent velocity more reasonable. Cost was also considered due to the squad's budget which eliminated several high-cost parachutes from consideration. Packing volume was considered as lower packing volumes result in less tightly packed body tubes which decreases the likelihood of failed parachute deployments. Large mass values were also considered as detrimental to a parachute. Finally, the presence of a spill hole was viewed as favorable due to the increased stability it provides to the vehicle's descent and increased likelihood of the main parachute actually deploying (a problem the team briefly experienced last year). With all of this considered, the Rocketman 9ft High Performance Parachute was selected largely due to its close $C_d A$ value and reasonable cost. The full analysis can be viewed in Table 48, below.

Table 48: Main Parachute Trade Study

		Rocketman 14ft Standard Parachute - C_d = .97		Rocketman 9ft High Performance Parachute - C_d = 2.2		Rocketman 10ft Ultra Light High Performance - C_d = 2.2		Fruity Chutes 10ft IRIS Ultra Parachute - C_d = 2.2	
Criteria	**Weight**	**Value**	**WNV**	**Value**	**WNV**	**Value**	**WNV**	**Value**	**WNV**
Cost (1/$)	0.25	0.01	0.10	0.00	0.05	0.00	0.02	0.00	0.03
Packing Volume ($1/in^3$)	0.2	0.01	0.02	0.01	0.04	0.03	0.11	0.01	0.03
Excess $C_d A (1/ft^2)$	0.25	0.04	0.05	0.11	0.13	0.02	0.03	0.02	0.03
Mass (1/oz)	0.2	0.04	0.03	0.05	0.04	0.10	0.09	0.05	0.04
Stability (Spill Hole) (0 or 1)	0.15	0	0	1	0.05	1	0.05	1	0.05
Total WNV		**0.20**		**0.27**		**0.25**		**0.13**	

The drogue parachute selection was subsequently conducted so that it would be compatible with the chosen main parachute. The primary considerations for the drogue parachute selection were descent time, drift distance, and acceleration at the main parachute deployment. The descent time and drift distance of the main parachute calculated using `main_descent_calc.m` were used to calculate max $C_d A$ values for the drogue parachute so that the vehicle would abide by NASA Reqs. 3.10 and 3.11. Similar to the force balance from Equation 6, the equation

$$C_d A = \frac{2 m_{tot} g}{\rho v_{droguemin}^2} \tag{7}$$

where

$$v_{droguemin} = \frac{h_{apo} - h_{main}}{t_{max} - t_{main}} \tag{8}$$

was used to determine the max $C_d A$ value based on the descent time. All of the variables found in Equation 7 are identical to those used in the main parachute equations except for $v_{droguemin}$. In Equation 8, there are several new variables including h_{apo} which is the projected apogee of 4600 ft, h_{main} which is the worst case main deployment altitude of 600 ft,

t_{max} which is 80 seconds per NASA Req. 3.10, and t_{main} which is the time the vehicle descends under the main parachute (34.58 s). This resulted in a $V_{droguemin}$ of 88.07 ft/s and, in conjunction with Equation 7, a C_dA value of 5.26. The other max C_dA value for the drift radius was calculated using the same Equation 7 but with $v_{droguemin}$ calculated differently using

$$v_{droguemin} = \frac{h_{apo} - h_{main}}{t_{droguemax}} \tag{9}$$

where

$$t_{droguemax} = \frac{r_{max} - d_{main}}{v_{wind}} \tag{10}$$

.

The $t_{droguemax}$ value is the max time the drogue can descend under worst case wind conditions, v_{wind} (20 mph), taking into account the max drift radius, r_{max} of 2500 ft (NASA Req. 3.10) and the drift under main, d_{main} (1014.4 ft). This value was then integrated with Equation 9 to calculate the second $v_{droguemin}$ to be used with Equation 7. The second $V_{droguemin}$ was calculated to be 78.98 ft/s which resulted in a C_dA of 6.55. Both maximum C_dA values were calculated using the script `drogue_parachute_selection.m` and resulted in the final C_dA values of 5.26 and 6.55 for the descent time and drift radius requirements, respectively. Only the smaller of the max C_dA values was considered for parachute selection as both must be fulfilled. Lastly, the minimum C_dA value was calculated to ensure the global acceleration on the vehicle is not unreasonable for load bearing components. A max acceptable acceleration, a, of 30gs was assumed given the mass of the vehicle and the loads this would exert on components at main deployment. Using this information, the force balance equation

$$\frac{1}{2}\rho v_{maxdrogue}^2 C_d A_{main} - m_{tot} g = m_{tot} a \tag{11}$$

was used to find the $v_{maxdrogue}$ (96.61 ft/s). This velocity was then used in tandem with Equation

$$C_dA = \frac{2m_{tot}g}{\rho v_{maxdrogue}^2} \tag{12}$$

to calculate a minimum C_dA value. The `drogue_parachute_selection.m` script determined this C_dA value to be 4.38. Given these calculations, the team knew the drogue C_dA value had to be between 4.38 and 5.26 so only parachutes with values in that range were considered. The

same criteria for choosing main parachutes was applied to the drogue parachute selection process except that $C_d A$ values near the middle of the desired range were seen as favorable. Values near the middle of this range ensure the drogue is as far away as possible from breaching either the acceleration $C_d A$ restriction or the drift time/radius restriction. The 2ft Rocketman Elliptical Parachute was selected for this application primarily due to its cost, mass, and stability. Additionally, the parachute is already in the team's inventory which is beneficial to the overall budget. The full trade study for the drogue parachute can be viewed in Table 49, below.

Table 49: Drogue Parachute Trade Study

		2ft Rocketman Elliptical Parachute - $C_d = 1.6$		2ft Fruity Chutes: Drogue Chute - $C_d = 1.5$		10in x 62ft Rocketman Extreme Streamer - $C_d = 0.093$	
Criteria	**Weight**	**Value**	**WNV**	**Value**	**WNV**	**Value**	**WNV**
Cost (1/$)	0.25	0.02	0.12	0.01	0.08	0.01	0.05
Packing Volume ($1/in^3$)	0.2	0.08	0.08	0.08	0.08	0.03	0.03
Proximity to Target $C_d A (1/ft^2)$	0.2	14.22	0.03	9.12	0.02	68.03	0.15
Mass (1/oz)	0.2	0.48	0.09	0.46	0.09	0.10	0.02
Stability (Spillhole) (0 or 1)	0.15	1	0.08	1	0.08	0	0
Total WNV		**0.33**		**0.27**		**0.25**	

4.3.2 Parachute Protection

The launch vehicle parachutes and black powder ejection charges will be housed in the same body tube sections. The black powder ejection charges will combust and emit gas, which has the potential to cause serious damage to the parachutes. Protection for the parachutes will be used to keep the parachutes unharmed from the heat of the ejection charges. Three parachute protectors were analyzed in a trade study to determine the optimal choice. Cost and weight were the two criteria used to evaluate each parachute protector. Size was not considered so long as each parachute protector had a minimum area of 144 in^2 as this was the minimum

area needed to ensure the full protection of the drogue parachute. All parachute protectors analyzed for this trade study had an area of 324 in^2 for standardization. The results from the trade study indicated that Rocketry Works was the optimal choice. However, the Rocketry Works parachute protector is currently out of stock. Apogee Rockets was determined to be the second best option, and the team is in possession of an Apogee Rockets parachute protector that meets the minimum area requirement and has no rips or tears. The team will be using the Apogee Rockets parachute protector, which has a weight of 1.94 oz. Table 50 below shows the parachute protectors trade study.

Table 50: Parachute Protector Trade Study

		Rocketman		Apogee Rockets		Rocketry Works	
Criteria	**Weight**	**Value**	**WNV**	**Value**	**WNV**	**Value**	**WNV**
Cost (1/$)	0.8	0.04	0.14	0.08	0.31	0.09	0.35
Mass (1/oz)	0.2	0.52	0.07	0.52	0.07	0.44	0.06
Total WNV		**0.214**		**0.378**		**0.408**	

4.3.3 Payload Protection

When the nose cone is ejected to allow the payload to deploy out the forward end of the payload tube, the payload camera and electronics must be protected from the black powder ejection gasses. A removable G10 fiberglass wall will be placed in the front end of the payload tube between the recovery module and the camera system. This wall will be slightly smaller in diameter than the inner diameter of the payload tube and will be restrained from moving aft in the payload tube by standoff blocks in the payload body tube. However, the wall will be free to move in the forward direction which will allow the wall to be pulled out of the payload tube with the nose cone via an additional shock cord. A flame resistant blanket will also be placed between this removable wall and the recovery module to stop any black powder ejection charge gas from moving past the wall and interfering with the camera system. The wall will be responsible for protecting the camera from the force of the blast. The blanket and bulkhead will both be pulled free from the launch vehicle once the nose cone has been ejected from the launch vehicle to allow the camera to deploy properly.

4.4 Avionics Design

Various electrical components including altimeters and a GPS will be required to properly recover the vehicle. Altimeters are essential to triggering the separation events based on the altitude of the vehicle while the GPS allows the team to track the vehicle's location. These

components will be powered by lithium ion batteries and were selected based on criteria detailed in this section.

4.4.1 Altimeter Selection

The design requires nine altimeters between the three recovery devices. Three altimeters per recovery device increases the redundancy of the recovery devices (NASA Req. 3.4.). The team considered barometric altimeters capable of triggering multiple recovery events with downloadable flight data (NASA Req. 3.4.). Each altimeter will have a dedicated power supply in the form of commercially available batteries (NASA Req. 3.5.). The altimeters considered in the trade study are as follows: the Featherweight Raven 4, the StratoLogger SL100, the StratoLogger CF, the RRC3 Sport, and the AIM USB. The team considered four criteria when selecting altimeters. The four criteria (cost, area, samples per second, and weight) determined the final altimeter selections. Altimeter area was determined to be the most important criteria because of the limited space within the recovery modules. The team wanted to minimize cost as much as possible so this was the next most important criteria. An ideal altimeter would also have a high sampling frequency so as to have additional data points and be lightweight.

Table 51: Altimeter Trade Study

		FR4		SLCF		SL100		RRC3		AIM	
Criteria	**Weight**	**Value**	**WNV**	**Value**	**WNV**	**Value**	**WNV**	**Value**	**WNV**	**Value**	**WNV**
Cost (1/$)	0.3	0.006	0.002	0.014	0.074	0.017	0.085	0.013	0.064	0.009	0.064
Mass (1/oz)	0.1	4.395	0.033	2.632	0.020	2.223	0.017	1.516	0.012	2.213	0.017
Area ($1/in^2$)	0.4	0.694	0.119	0.595	0.102	0.404	0.069	0.275	0.047	0.370	0.063
Sampling Freq. (1/s)	0.2	20	0.05	20	0.05	20	0.05	10	0.025	10	0.025
Total WNV		**0.204**		**0.246**		**0.222**		**0.128**		**0.150**	

The StratoLogger CF was ultimately chosen as the preferred altimeter due primarily to its low cost and high sampling frequency. In addition, the Featherweight Raven 4 and StratoLogger 100 were both chosen, since they both scored highly in the trade study and have been effectively used by the team in past years.

The team inventory contains six reliable altimeters: two Featherweight Raven4 altimeters, two StratoLogger CF altimeters, and two StratoLogger 100 altimeters. The quality of these altimeters is evidenced by past launches as well as the team's current trade study, and using the altimeters in inventory allows the team to stay within budget more easily. For these reasons, the team will use the six existing altimeters and buy three StratoLogger CF altimeters to satisfy the remaining needs, which is justified by Table 51.

Figure 45 shows the electrical schematics for the chosen altimeters.

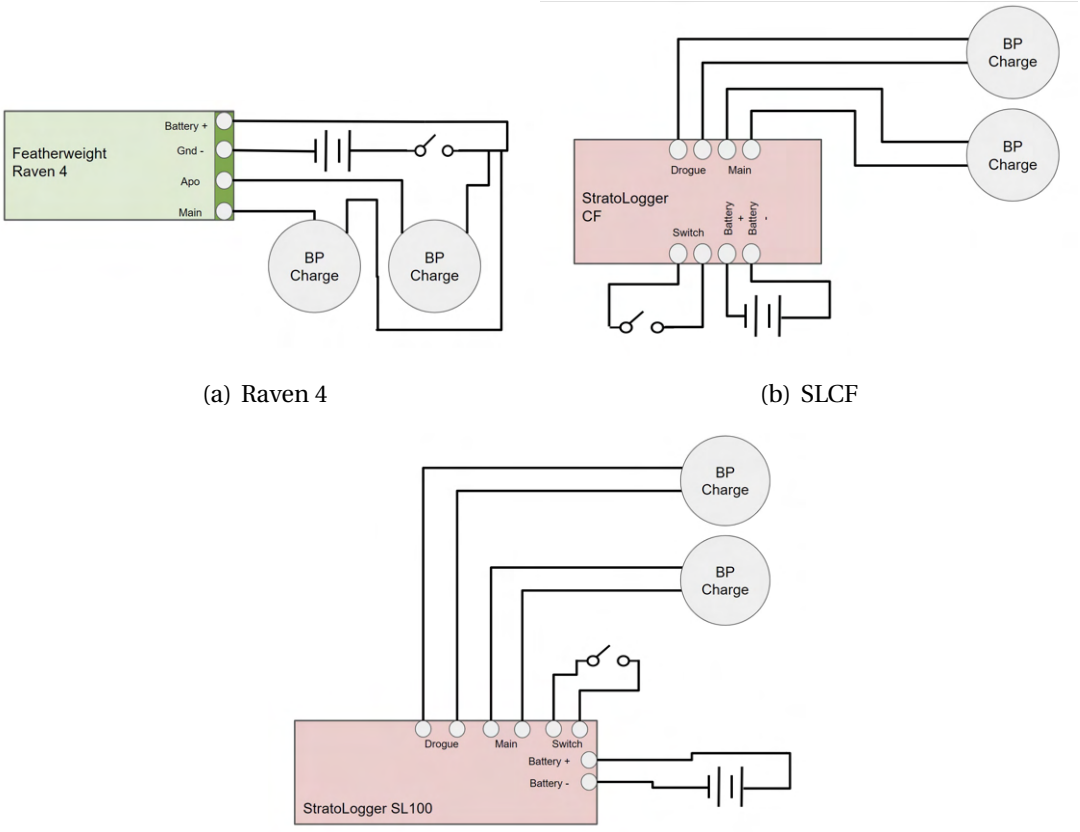

(a) Raven 4

(b) SLCF

(c) SL 100

Figure 45: Electrical Schematics

4.4.2 GPS Selection

After a thorough investigation of different GPS transmitters, the Featherweight GPS Tracker was selected due to its accuracy and reliability, along with other criteria provided in Table 52. Accuracy and reliability are of paramount importance as they are critical in locating the vehicle following landing. The selected GPS system was used in the previous launch vehicle and performed up to the team's standards. Furthermore, the selected GPS has a long range

that allows it to collect data up to 164,042 ft away. Even when the launch vehicle reaches high altitudes, this GPS still provides accurate data as supported by many reviews attesting to its accuracy and reliability. Additionally, the GPS is paired with an iPhone to obtain the data, which makes it convenient and easy to use. The reason for the lower score on ease of assembly can be attributed to the extended time it takes for the GPS to pair with the iPhone and calibrate. Comparing the Featherweight GPS Tracker to the two other devices, its accuracy and reliability were almost identical to the Apogee Components Simple GPS Tracker, but performed considerably better than the Missile Works T3 System. While the weighted values in the trade study of the Featherweight GPS Tracker and Apogee Tracker were nearly identical, the team's past success with the Featherweight GPS Tracker led to a confident selection of that system. Due to the radio transmission needs of the GPS, it cannot be housed in a carbon fiber body tube due to carbon fiber's RF blocking characteristic. Therefore, the GPS antenna will be mounted in the fiberglass nose cone of the vehicle in close proximity to the NED.

Table 52: GPS Selection Trade Study

		Featherweight GPS Tracker		Apogee Components Simple GPS Tracker		Missile Works T3 System	
Criteria	**Weight**	**Value**	**WNV**	**Value**	**WNV**	**Value**	**WNV**
Cost (1/$)	0.15	0.003	0.037	0.002	0.030	0.006	0.084
Mass (1/oz)	0.1	1.890	0.034	2.181	0.039	1.471	0.027
Area ($1/in^2$)	0.15	0.305	0.04	0.357	0.047	0.482	0.063
Accuracy (Scale of 1-5)	0.3	4	0.109	5	0.136	2	.055
Ease of Assembly (Scale of 1-5)	0.1	2	0.033	1	0.017	3	0.050
Reliability (Scale of 1-5)	0.2	5	.083	4	0.067	3	0.050
Total WNV		**0.337**		**0.335**		**0.328**	

4.4.3 Other Electrical Components

Switch selection evaluation was based on the following criteria: ease of use, ease of assembly, safety and reliability, area, and cost. The switches must be easy to access so they can be armed/disarmed on the pad (NASA Req. 3.6), integrate effectively with other electrical

components, have a low likelihood of arming/disarming unintentionally (NASA Req. hyperlink3.7.3.7), and be low in cost. Based on this evaluation criteria, the keyed switches were selected to activate the recovery system. This is supported by the trade study in Table 56, below, as the keyed switch has the highest overall score of all the potential switches considered. The exact switch of this type to be purchased will be the 3/4" Panel-Mount Key Switch from McMaster-Carr due to its positive reliability reviews, easy screw-terminal integration with other avionics components, and low cost.

Table 53: Switch Selection Trade Study

		Keyed Switch		Allen Key Switch		Screw Switch		Pull Pin Switch	
Criteria	**Weight**	**Value**	**WNV**	**Value**	**WNV**	**Value**	**WNV**	**Value**	**WNV**
Ease of Use (Scale of 1-5)	0.25	4	0.09	2	0.05	2	0.05	3	0.07
Ease of Assembly (Scale of 1-5)	0.25	3	0.06	3	0.06	2	0.04	4	0.08
Safety and Reliability (Scale of 1-5)	0.3	3	0.10	3	0.10	1	0.03	2	.07
Area ($1/in^2$)	0.05	0.68	0.01	0.62	0.01	0.20	0.00	1.46	0.02
Cost (1/$)	0.15	0.17	0.03	0.10	0.02	0.33	0.07	0.14	0.03
Total WNV		**0.30**		**0.24**		**0.19**		**0.27**	

Several auxiliary electrical components are necessary for the avionics to function properly and be easily accessible to the team. WAGO splicing connectors will be used on the recovery modules to allow for the easy connection of black powder charges to the circuitry of the altimeters at the launch field with minimal equipment. Stranded wire will be used to connect the components this year instead of solid wire due to a stranded wire's ability to withstand violent vibrations and flexing without breaking. This should reduce the likelihood of a wire failure which occurred on the team's last flight last year with solid wires. A new electrical component the team will consider including on the recovery modules is an indicator light for each altimeter circuit. The indicator lights would help indicate whether electrical components like altimeters are armed when the key switch is turned to the "on" position. Given the large number of altimeters this year, the lights would provide a visual form of confirmation that the altimeters are armed to supplement the beeping that is built in to the altimeters used on the vehicle. However, the power draw of the lights and the subsequent effect on battery life must

be further evaluated during CDR before the team is comfortable implementing this addition. The trade study for indicator lights can be viewed in Table 54, below.

Table 54: Indicator Light Selection Trade Study

		Kingbright WP711SURC/E		CreeLED XMLBWT-00-0000-000LT60E4	
Criteria	**Weight**	**Value**	**WNV**	**Value**	**WNV**
Ease of Installation (Scale of 1-5)	0.4	3	0.15	5	0.25
Cost (1/$)	0.35	1.64	0.30	0.26	0.05
Forward Voltage (V)	0.25	2.5	0.12	2.72	0.13
Total WNV		**0.57**		**0.43**	

4.5 Integration

All of the avionics discussed in the previous section will be integrated into all three recovery modules: the FED, NED, and PED. The FED and PED will be identical modules that each contain three independent altimeters and recovery charges. The NED will be nearly identical to the PED and FED except for the slight reduction in diameter of the bulkheads due to its location in the nose cone. While this reduction in bulkhead size is not anticipated to have a material impact on its ability to transmit the load of the eyebolt to the nose cone, further FEA analysis will be conducted to confirm this during CDR. The FED will be responsible for the drogue deployment at apogee while the PED will be responsible for the main parachute deployment and the NED will separate the nose cone so the payload can function properly. The PED/FED integrated design can be viewed in Figure 46, below while the NED can be seen in Figure 47. Two additional rendered views of the PED/FED and NED modules can be viewed in Figure 48.

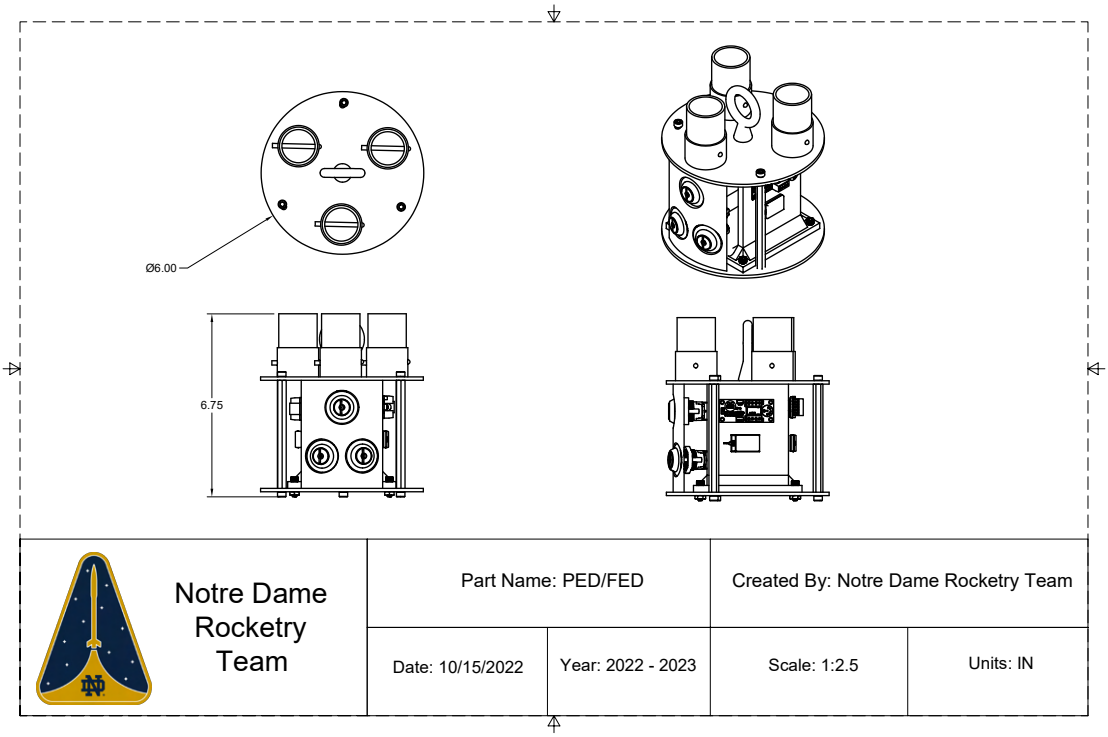

Figure 46: PED/FED CAD Drawing

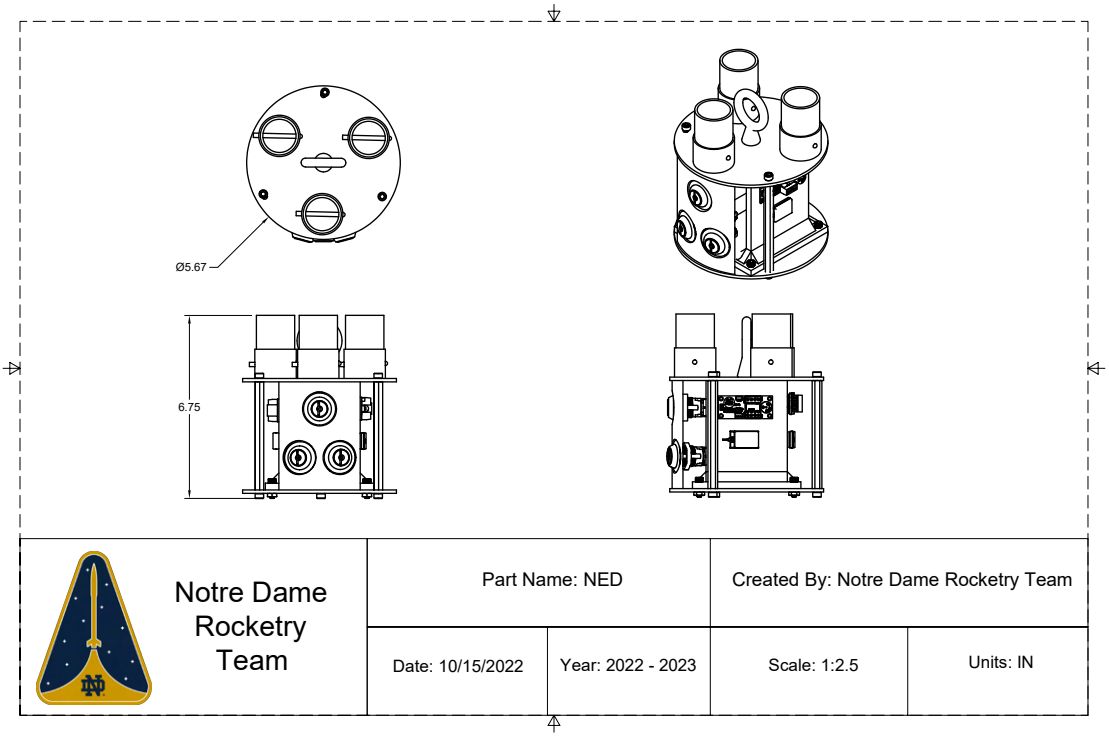

Figure 47: NED CAD Drawing

(a) PED/FED Rendered View (b) NED Rendered View

Figure 48: Additional PED, FED, and NED Rendered Views

The following section will discuss the material selections for the main structural components of the recovery modules.

4.5.1 Bulkhead Material Selection

The team evaluated the bulkhead material based on the following criteria: density, cost, tensile strength, tensile modulus, thermal resistance, and the material's ability to shield radio waves. The tensile strength of the material prevents the bulkhead from breaking in tension as it experiences a lot of stress while transferring the load from the shock cords to the vehicle body. A low density is important to reduce the mass of the bulkhead. Since the bulkheads are one of the main load-bearing structural components, a high tensile modulus rating is necessary to prevent deformation of the bulkhead within the body tube. NASA Req 3.13 also requires that recovery devices cannot be adversely affected by any other electronics during or after flight, which means that it is beneficial to have the bulkhead have the ability to block the transmission of radio waves. Otherwise, additional shielding is required. As seen in the trade study in Table 55 below, the fore and aft bulkheads of each recovery module will be made out of carbon fiber as it fulfills the criteria most effectively. FEA analysis will be conducted during the CDR phase to ensure the thickness and material selections are sufficient to prevent failure based on anticipated in-flight loads with a sufficient factor of safety.

Table 55: Bulkhead Material Trade Study

		Carbon Fiber		Fiberglass (S-glass)		Aluminum	
Criteria	**Weight**	**Value**	**WNV**	**Value**	**WNV**	**Value**	**WNV**
Density (in^3/lb)	0.15	15.63	0.06	11.12	0.05	10.24	0.042
Cost (1/$)	0.05	0.10	0.003	0.33	0.01	1.02	0.04
Tensile Strength (ksi)	0.35	784	0.18	667	0.16	44.9	0.011
Blocks Radio Waves (0 or 1)	0.1	1	0.05	0	0.00	1	0.05
Strength-to-weight Ratio ($ksi/lb/in^3$)	0.15	12253	0.09	7416	0.06	460	0.003
Tensile modulus (ksi)	0.15	42640	0.10	12760	0.03	9993	0.02
Thermal resistance (1-5)	0.05	5	0.03	4	0.02	1	0.01
Total WNV		**0.51**		**0.32**		**0.17**	

4.5.2 Altimeter Mounting Board Material Selection

The Altimeter Mounting Board will house the altimeters, battery, and necessary wiring for the avionics on each module and will be located in the center of each module. When selecting the Altimeter Mounting Board material, the density, cost, temperature resistance, ease of manufacturing, tensile strength, and the flexibility of the considered materials were analyzed. The three most important criteria were deemed to be the cost due to the squad's limited budget, the density to keep the mass of board minimized, and the tensile strength to ensure the board can withstand in-flight forces and vibrations. The trade study, listed below in Table 56, informed the team's decision to select acrylonitrile butadiene styrene (ABS) for the Altimeter Mounting Board material selection due to its low cost and ease of manufacturing, especially for complex designs. The relatively lower tensile strength is not of major concern to the team as the avionics board will not be made load bearing for the overall structure of each module. Instead, axial loads will be transmitted via a load path through the structural supports discussed subsequently in Section 4.5.3.1.

Table 56: Altimeter Mounting Board Material Trade Study

		Carbon Fiber		ABS		Carbon Kevlar Core Hybrid		Carbon Fiber Foam	
Criteria	**Weight**	**Value**	**WNV**	**Value**	**WNV**	**Value**	**WNV**	**Value**	**WNV**
Density (in^3/lb)	0.2	15.8	0.01	26.1	0.02	142.7	0.11	69.2	0.05
Cost (1/$)	0.25	0.05	0.02	0.59	0.22	0.00	0.00	0.03	0.01
Melting Point (F°)	0.05	5432	0.02	221.00	0.00	932	0.00	5432	0.02
Ease of Manufacturing (Scale of 1-5)	0.1	3.00	0.03	5.00	0.05	1.00	0.01	2.00	0.02
Tensile Strength (ksi)	0.3	500.00	0.10	4.10	0.00	500.00	0.10	500	0.10
Flexibility (Mpsi)	0.1	34.00	0.05	0.30	0.00	2.00	0.00	34.00	0.05
Total WNV		**0.23**		**0.29**		**0.23**		**0.26**	

4.5.3 Hardware Selections

Several of the structural hardware components deemed the most critical to the modules were tentatively selected for PDR to ensure they comply with the maximum global acceleration expected based on assumptions made in Section 4.3.1, above, and at least a factor of safety of 1.5. While 1.5 is typically assumed to be a reasonable factor of safety in the aerospace industry, a larger factor of safety will likely be targeted by the team during final component selection to avoid a critical in-flight failure (further safety considerations noted in Section 8). Smaller hardware components will be finalized by CDR and will be able to sustain this acceleration of 30gs as well.

4.5.3.1 Structural Support The team decided the material composition of the recovery module structural supports based on the density of the material, compression and shear strengths, torsion based on Poisson's ratio, cost of the material, and its machinability in a trade study shown in Table 57. Based on all of these factors, aluminum was selected for this structural application. Aluminum is a light metal with comparable compressive strength to hot rolled steel. In addition, it is much cheaper and easier to work with than steel. While

carbon fiber is a lot stronger, it's hard to work with and the strength it provides is significantly higher than anything the launch vehicle will experience. The ABS plastic is fairly cheap and very easy to work with, but would likely have a high chance of failure with its comparatively weak strength. For all of these reasons, aluminum is the best material for the supports.

Table 57: Structural Support Material Trade Study

		Aluminum		Hot Rolled Steel		Carbon Fiber		3D-Printed Plastic	
Criteria	**Weight**	**Value**	**WNV**	**Value**	**WNV**	**Value**	**WNV**	**Value**	**WNV**
Density (in^3/lb)	0.05	10.29	0.01	3.52	0.00	15.38	0.01	22.32	0.02
Compressive Strength (ksi)	0.25	40.0	0.03	34.81	0.02	275.57	0.20	2.60	0.00
Shear Strength (ksi)	0.05	0.50	0.03	0.20	0.01	13.05	0.01	4.79	0.00
Torsion (Poisson's Ratio)	0.05	0.34	0.01	0.29	0.01	0.77	0.02	0.36	0.01
Cost (1/$)	0.30	0.44	0.17	0.15	0.06	0.15	0.06	0.02	0.01
Machinability (1-5)	0.30	4.00	0.10	2.00	0.05	1.00	0.03	5.00	0.13
Total WNV		**0.35**		**0.16**		**0.33**		**0.17**	

4.5.3.2 Bulkhead Bolt Shock cords will attach to the bulkheads of the ejection devices by attaching a quicklink at the end of the shock cord to a bolt on each bulkhead. The team considered bolts with vertical load ratings of 1200 lbf or above, with higher vertical load ratings favorable as they increased the factor of safety. While this is an estimated load capacity the team anticipates needing based on preliminary mass estimates and parachute selections, more precise loads anticipated for the bolt component will be determined during the CDR phase. Recovery modules must be constrained to minimal lengths to keep the vehicle of a reasonable total length. Therefore, the team considered the protruding length of bolts above the bulkhead as a negative characteristic. The team considered cost due to the limited recovery system budget. Quicklinks should minimally contact charge wells during flight which requires that the bulkhead bolts limit the quicklink freedom of movement. Bolts that effectively limit quicklink movement were assigned a 1 and those that did not were assigned a score of 0. The team selected an eyebolt due to the high vertical load rating, small protruding length, relatively low cost, and limited quicklink freedom of movement. A summary of the bolt

considerations and results is shown in the trade study in Table 58, below.

Table 58: Bulkhead Bolt Trade Study

		Eyebolt (3014T956)		Rotating Eyebolt (3059T71)		U-Bolt (29605T44)		Square U-Bolt (3060T158)	
Criteria	**Weight**	**Value**	**WNV**	**Value**	**WNV**	**Value**	**WNV**	**Value**	**WNV**
Vertical Load Rating (lb)	0.3	1800	0.08	1650	0.07	1200	0.05	2000	0.09
Protruding Length (1/in)	0.2	0.32	0.06	0.35	0.06	0.27	0.05	0.22	0.04
Cost (1/$)	0.3	0.19	0.13	0.01	0.01	0.13	0.09	0.11	0.07
Quicklink Restriction of Movement (0 or 1)	0.2	1	0.1	1	0.1	0	0	0	0
Total WNV		**0.37**		**0.24**		**0.19**		**0.20**	

4.5.4 Module Integration Method

The team has traditionally manufactured the launch vehicle in such a way that the gap between the recovery modules and the inner body tubes is minimal which will continue to be the case this year. This will ensure that the recovery system does not have excessive freedom of movement during flight. However, this has the drawback that integrating the modules into the launch vehicle before flight will likely require immense force due to friction. In order to make it easier to integrate the different systems while preserving this tight fit with the body tubes, the team has decided to use a form of lubricant to apply to the bulkheads of the recovery modules and the inner walls of the body tubes. The team analyzed five lubricants in a trade study with three different criteria to determine the optimal choice. The most important criterion was the coefficient of friction which compares how well lubricants reduce friction. The team's research found Molybdenum Disulfide exceeded in this respect. The team also considered cost, although it was the least important factor due to the small amount of lubricant required. The last criterion was the ease of cleanup, with solid-based lubricants being favored over oil-based lubricants. Molybdenum Disulfide proved to be the ideal lubricant for this launch vehicle due to its low coefficient of friction and powder base. Table 59 below shows the applicable lubricant trade study.

Table 59: Lubricant Trade Study

		WD-40		Graphite		Tri-Flow		MoS_2	
Criteria	**Weight**	**Value**	**WNV**	**Value**	**WNV**	**Value**	**WNV**	**Value**	**WNV**
Coefficient of Friction ($1/\mu$)	0.6	9.09	0.08	10.00	0.09	12.5	0.12	33.33	0.31
Cost (1/$)	0.1	1.52	0.05	1	0.03	0.5	0.02	0.15	0.00
Ease of Cleanup (Scale of 1-5)	0.3	1	0.03	4	0.12	1	0.03	4	0.12
Total WNV		**0.16**		**0.24**		**0.16**		**0.43**	

4.6 Recovery Preliminary Testing Plan

Table 60 lists the preliminary testing plans for the recovery system. The list of tests is subject to change or expand in the future.

Table 60: Recovery Preliminary Testing Plan

Test Name	Description	Success Criteria
Ignition Interfacing Test	Altimeters and LED lights representing e-matches will be integrated in a circuit. Simulated flight data will be fed to the altimeter to verify it signals e-match ignition at the desired altitude	E-matches send ignition signals at the desired altitudes
Static Loading Test	Bulkhead, U-bolts, shock cords, and altimeter mounting boards will be subjected to static loading in an ATS load frame to simulate 1.5 times the loads these parts will experience during flight	The parts withstand the load and do not exhibit signs of failure including fracture or complete breakage

Table 60: Recovery Preliminary Testing Plan (continued)

Test Name	Description	Success Criteria
Arming Switch Vibrations Test	Arming switches will be subjected to vibrations of 1.5 times the amount experienced during flight	The switches maintain their armed status
GPS Vibrations Test	The GPS will be subjected to vibrations of 1.5 times the amount experienced during flight	The GPS remains operational and attached to the mounting board
Ground Ejection Test	Electronically initiated recovery events that detonate the black powder charges will be demonstrated	The charges are sized to generate an appropriate force during separation events
Electronics Shielding Test	Electronics from each system will be shielded and receive simulated flight data separately, then receive the same data while shielded and placed in the same configuration as within the launch vehicle	Data from all electronics are similar when placed separately and together

5 Vehicle Mission Performance

5.1 Simulation Methods

The team used multiple simulation methods for the same type of mission performance analysis as a method of redundancy and method of finding precise data. Future tests, including stress tests, subscale flights, and full-scale demonstration flights, will evaluate the accuracy of the simulation methods. The team has used the following simulation methods in past years and have found them both accurate and precise, given the proper inputs. Table 61 lists the type of mission performance analysis, respective simulation methods, methods for simulating the mission performance, and what stage the mission performance will be evaluated at.

Squad component masses (ACS, Payload, Recovery) were based off of basic masses (masses based off of what each squad predicted the respective component will weigh). The only exception to this was for Payload, where instead the allowable mass was used. Recovery derived their expected mass based on previous designs for the recovery modules, while accounting for expected design changes. ACS derived their expected mass based on similar past designs for ACS, while also accounting for expected design changes. Payload's allowable mass was derived based on the understanding that the design will continue to change, usually resulting in the addition, not reduction, of features.

Table 61: Mission Performance Method Overview

Mission Performance Method	Description	Methods of Analysis	Stage of Analysis
Simulated Flight Profiles	Analysis on launch vehicle altitude, velocity, and acceleration as a function of time	OpenRocket, RockSim, MATLAB	PDR, CDR, FRR, PLAR
Launch Target Apogee	After an analysis of the launch vehicle predicted apogee, the team sets a target apogee during PDR	OpenRocket, RockSim	PDR(target apogee set) CDR, FRR (how target apogee will be reached)
Stability	Analysis on launch vehicle CP, CG , and Stability margin, both for the static (on-rail stability) stability margin and the dynamic (during flight) stability margin	OpenRocket, RockSim	PDR, CDR, FRR, PLAR
CFD	Analysis on air flow around launch vehicle, due to camera shroud and any other protruding component of the launch vehicle	Ansys, Wind Tunnel Testing	CDR, FRR
Terminal Kinetic Energy	Analysis on launch vehicle kinetic energy at landing for each independent and. tethered section of the launch vehicle	OpenRocket, RockSim, MATLAB	PDR, CDR, FRR, PLAR
Descent Time	Analysis on launch vehicle expected descent time for the rocket and any. section that descends untethered from the rest of the vehicle	OpenRocket, RockSim, MATLAB	PDR, CDR, FRR, PLAR
Drift Radius	Analysis on launch vehicle expected drift for each independent section of the launch vehicle from the launch pad	OpenRocket, RockSim, MATLAB	PDR, CDR, FRR, PLAR
Structural Verification	Analysis of the structure of launch vehicle components at critical moments, including parachute deployment, peak thrust, and landing. At this critical moments, all launch vehicle components will be analyzed to ensure they can withstand all launch loads. The launch vehicle components' factor of safety will be calculated from this analysis	Ansys, SOLIDWORKS, hand calculation using finite element methods theory (weak formation, Ritz method, etc.)	CDR, FRR: parachute deployment, peak thrust, and landing

5.1.1 OpenRocket Versus RockSim

Two methods were used to simulate the altitude of the launch vehicle during flight: OpenRocket and RockSim. Both methods are flight simulators, but they offer different perspectives on the same data.

The following list are the benefits of OpenRocket:

- OpenRocket is free, so more team members can access the software (RockSim costs $20 per account)
- OpenRocket is supported on Linux
- OpenRocket software is very user-friendly
- OpenRocket offers 6 degrees of freedom for simulations
- OpenRocket offers photo-realistic 3D rendering

The following list are the benefits of RockSim:

- RockSim offers a greater variations to flight simulations
- RockSim can animate simulations
- RockSim offers a more detailed mass estimate and optimization breakdown
- RockSim can perform calculations to determine if weather-cocking will be an issue for the design

Both methods are viable for the team launch vehicle's conditions. Both methods were compared to each other to see the precision of the simulation data in the following sections. For more information on OpenRocket, one can go to their website. As well, for more information on RockSim, one can go to their website.

5.2 Simulated Flight Profiles

5.2.1 Flight Altitude

The team simulated various flight conditions to understand the projected altitude of the launch vehicle as a function of time. Per NASA's USLI PDR requirements, the simulated flight

conditions included varying launch rail angles and wind speeds. The simulations used launch rail angles of 5, 7, and 10 degrees, and for each launch rail angle, wind speeds of 0, 5 10, 15, and 20 miles per hour were used. All other launch conditions were held constant between iterations. The team simulated flights using both OpenRocket and RockSim. Section 5.2.1.1 lists the altitude results for the OpenRocket simulations and Section 5.2.1.2 lists the altitude results for the RockSim simulations.

5.2.1.1 OpenRocket Simulations

Figures 49, 50, and 51 list the OpenRocket simulations for the launch vehicle altitude for various launch rail angles and wind speeds.

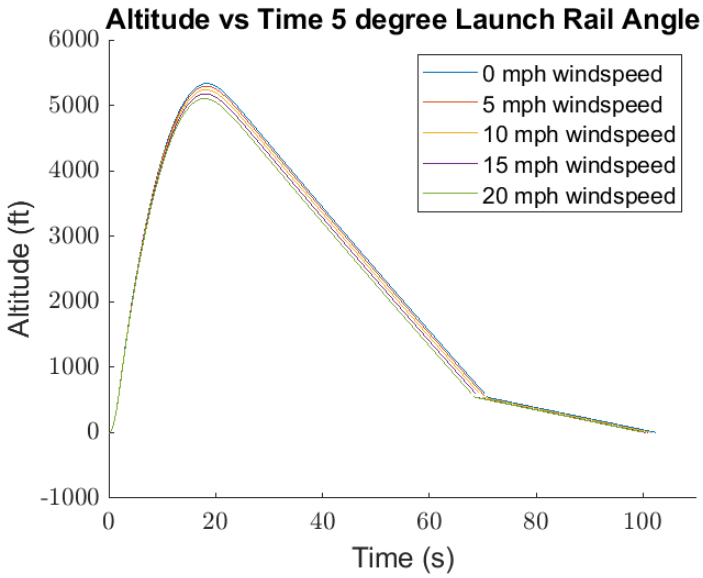

Figure 49: OpenRocket: Simulated Altitude vs Time for Various Wind Speeds, 5° Rail Angle

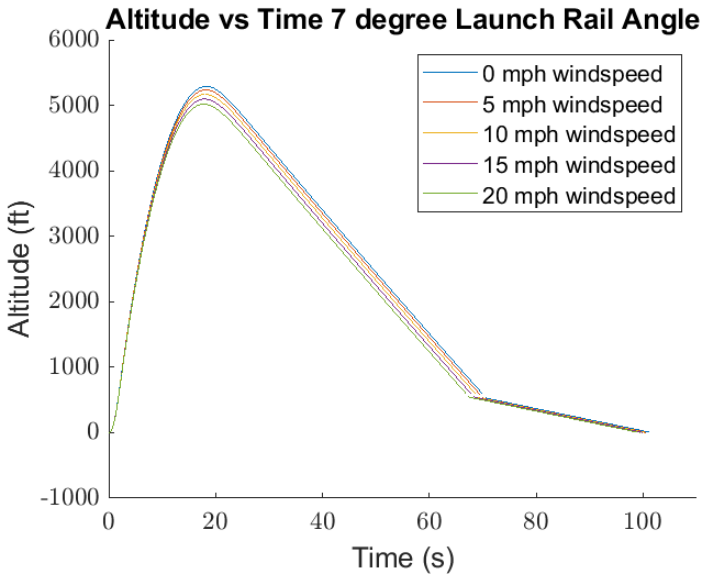

Figure 50: OpenRocket: Simulated Altitude vs Time for Various Wind Speeds, 7° Rail Angle

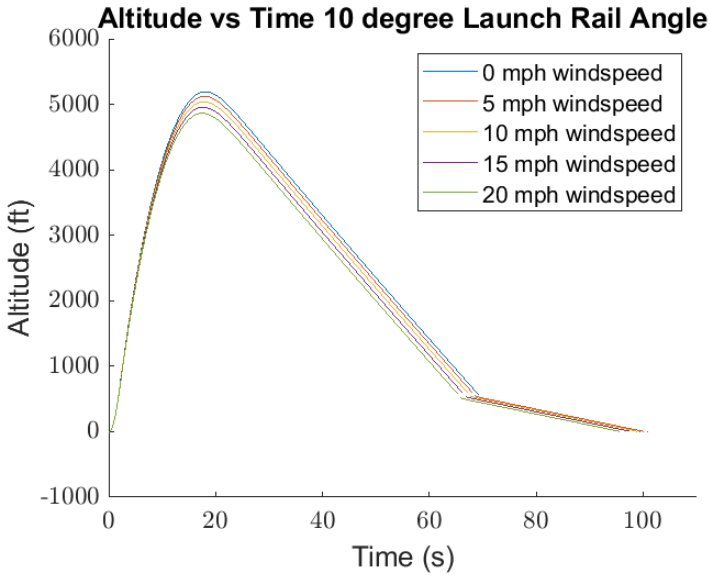

Figure 51: OpenRocket: Simulated Altitude vs Time for Various Wind Speeds, 10° Rail Angle

Table 62 summarizes the results of the OpenRocket altitude simulations. From the table, the highest predicted apogee is 5333.9 ft, and the lowest predicted apogee is 4863.5 ft. Understanding the range of apogees helps to determine the target apogee (See Section 5.2.1.3).

Table 62: OpenRocket Altitude Simulations

	Launch Rail 5° (ft)	Launch Rail 7° (ft)	Launch Rail 10° (ft)
0 MPH Wind	5333.9	5288.7	5193.4
5 MPH Wind	5292.4	5234.4	5121.6
10 MPH Wind	5238.3	5169.1	5041.0
15 MPH Wind	5175.1	5096.5	4955.2
20 MPH Wind	5105.0	5017.0	4863.5

5.2.1.2 RockSim Simulations Figures 52, 53, and 54 lists the RockSim simulations for the launch vehicle altitude for various launch rail angles and wind speeds.

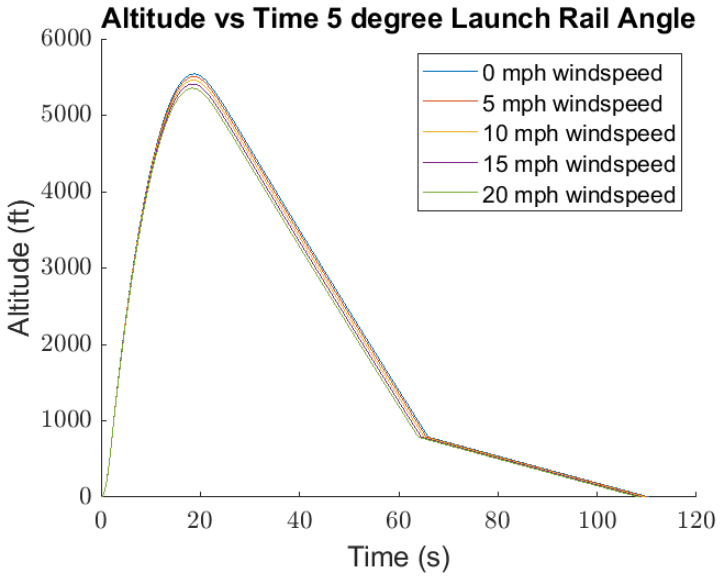

Figure 52: RockSim: Simulated Altitude vs Time for Various Wind Speeds, 5° Rail Angle

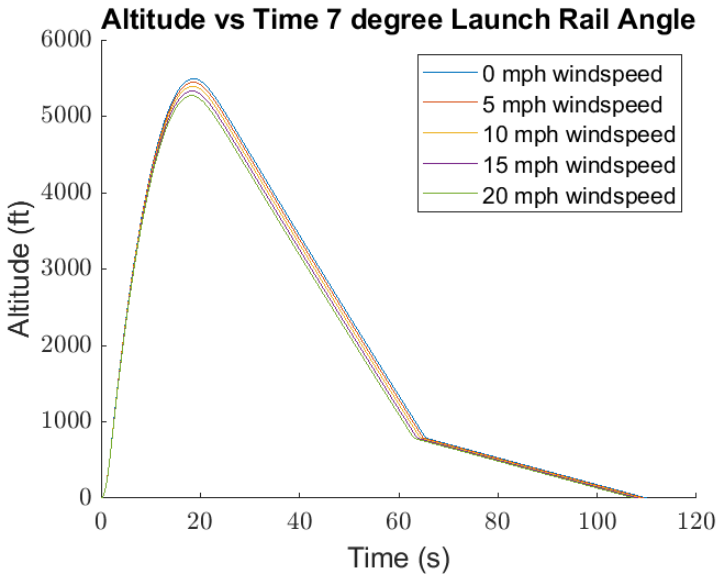

Figure 53: RockSim: Simulated Altitude vs Time for Various Wind Speeds, 7° Rail Angle

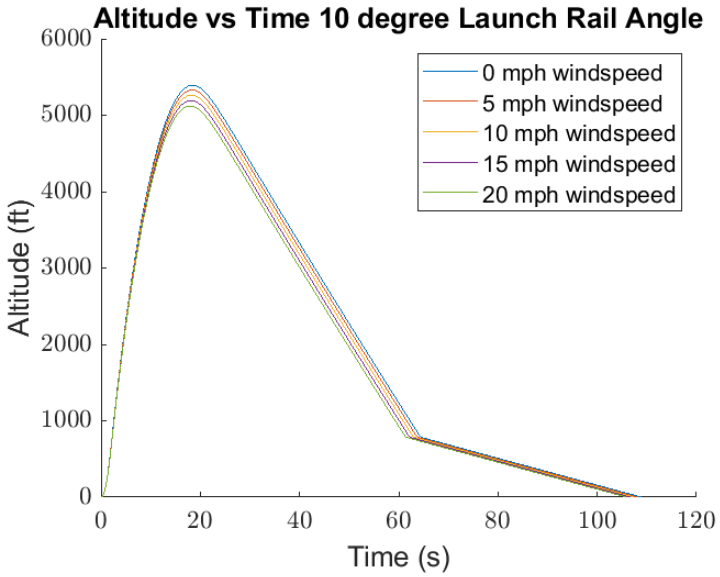

Figure 54: RockSim: Simulated Altitude vs Time for Various Wind Speeds, 10° Rail Angle

Table 63 summarizes the results of the RockSim altitude simulations. From the table, the highest predicted apogee is 5540.3 ft, and the lowest predicted apogee is 5120.6 ft. Understanding the range of apogees helps to determine the target apogee (See Section 5.2.1.3).

Table 63: RockSim Altitude Simulations

	Launch Rail 5° (ft)	Launch Rail 7° (ft)	Launch Rail 10° (ft)
0 MPH Wind	5540.3	5493.0	5393.9
5 MPH Wind	5504.5	5446.1	5331.6
10 MPH Wind	5460.1	5391.9	5264.0
15 MPH Wind	5409.2	5332.4	5193.1
20 MPH Wind	5353.8	5269.5	5120.6

5.2.1.2.1 OpenRocket vs RockSim Values & the Average Apogee The team found a significant difference between the predicted apogees between both flight simulation softwares. This section serves to explain the believed cause of the difference and list the average apogee for each flight condition between the two simulation softwares.

There were slight differences in the database's values for the L2200 motor; the RockSim model simulated the L2200 motor using a longer burntime (2.40 seconds) compared to the OpenRocket model (2.27 seconds). These settings could not be changed within either program. A proper understanding of the L2200 Vendor's motor specifications may assist the team in the future for determining the more accurate model. The subscale launch will demonstrate which model has better modeling.

Table 64 lists the average predicted apogee of the two simulation softwares for all flight conditions. The average between the two softwares provides the best method to determine the predicted apogee considering that the models have both demonstrated accuracy in previous years.

Table 64: Average Apogee Between OpenRocket and RockSim Simulations

	Launch Rail 5° (ft)	Launch Rail 7° (ft)	Launch Rail 10° (ft)
0 MPH Wind	5437.1	5390.9	5293.7
5 MPH Wind	5398.5	5340.3	5226.6
10 MPH Wind	5349.2	5280.5	4998.1
15 MPH Wind	5292.2	5214.5	5074.2
20 MPH Wind	5229.4	5143.3	4992.1

5.2.1.3 Launch Target Altitude An analysis of the launch vehicle's predicted apogee needed to be performed before determining the target apogee. This analysis is in Section 5.2.1.

The team's OpenRocket analysis found a maximum predicted apogee of 5333.9 ft, and a minimum predicted apogee of 4863.5 ft. The team's RockSim analysis found a maximum

predicted apogee of 5540.3 ft, and a minimum predicted apogee of 5120.6 ft. Averaging the two simulation methods out, the total predicted range of the launch vehicle apogee is 5437.1 ft - 4992.1 ft.

Recall that the objective is to overshoot the target apogee, and the ACS will induce drag to slow the launch vehicle down to the correct apogee. Thus, the team will select a lower target apogee than the predicted apogee range of 5437.1 ft - 4992.1 ft.

For the 2022-2023 season, the target apogee will be set to 4600 ft. The range at which ACS needs to reduce the apogee within 663.5 ft - 909.5 ft. Last year, the ACS flaps were the same dimensions as the proposed size for this year (2in by 6in), but now the ACS will actuate the flaps faster to the maximum drag angle. The ACS achieved over 600ft of drag last year with slower drag actuation mechanics, so the team predicts ACS will induce more drag this year. Therefore, the need to induce 663.5 - 909.5 ft of drag is within a realistic expectation. For more information on how the ACS will work, see Section 7.

5.2.2 Flight Velocity Simulations and Off-Rail Velocity Values

The team ran simulations for various flight conditions to understand the projected altitude of the launch vehicle as a function of time. Per NASA's USLI PDR requirements, the varied flight conditions included launch rail angles and wind speeds. The launch rail was angled at 5, 7, and 10 degrees, and for each launch rail angle, the wind speeds were placed at 0, 5 10, 15, and 20 miles per hour; all other launch conditions were held constant between iterations. The team ran launch simulations using both OpenRocket and RockSim. Section 5.2.2.1 outlines the velocity results for the OpenRocket simulations and Section 5.2.2.2 outlines the velocity results for the RockSim simulations.

5.2.2.1 OpenRocket Simulations

Figures 55, 56, and 57 lists the OpenRocket simulations for the launch vehicle velocity for various launch rail angles and wind speeds.

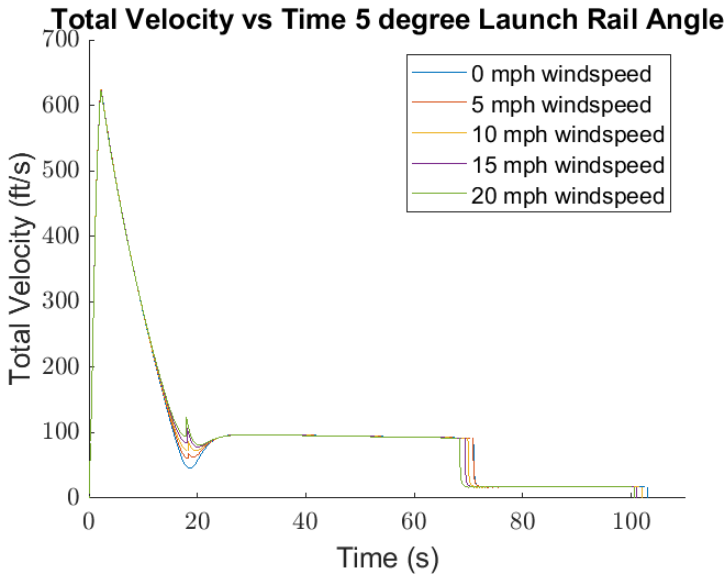

Figure 55: OpenRocket: Simulated Velocity vs Time for Various Wind Speeds, 5° Rail Angle

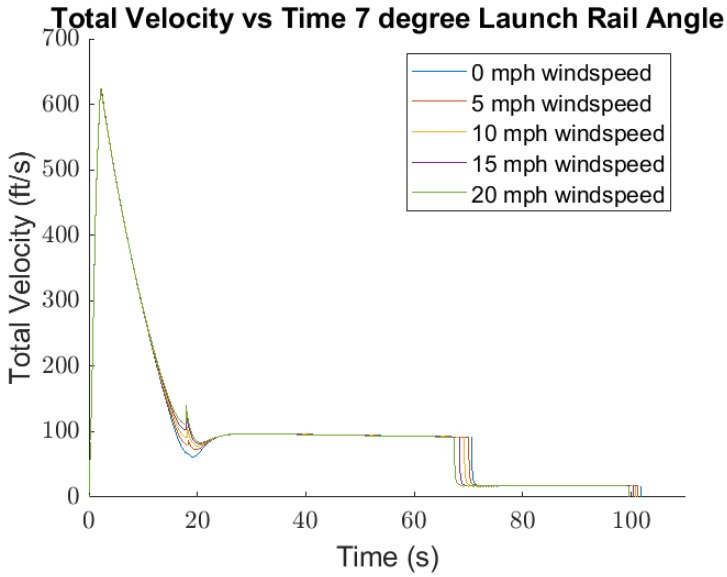

Figure 56: OpenRocket: Simulated Velocity vs Time for Various Wind Speeds, 7° Rail Angle

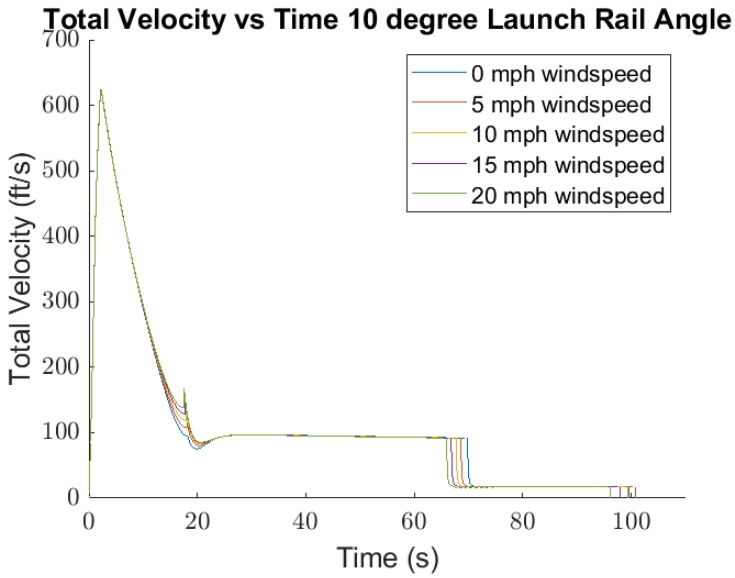

Figure 57: OpenRocket: Simulated Velocity vs Time for Various Wind Speeds, 10° Rail Angle

NASA Vehicles Req. 2.17. states that the launch vehicle must have an off-rail velocity of at least 52 fps. For all OpenRocket simulations the launch vehicle went off-rail at 0.3 seconds. Table 65 lists the off-rail velocity for the launch vehicle for all OpenRocket simulations. From the table, one can see that the launch vehicle is projected to abide by this NASA requirement within a safe margin.

Table 65: OpenRocket Simulations' Off-Rail Velocity of Launch Vehicle

	Launch Rail 5° (fps)	Launch Rail 7° (fps)	Launch Rail 10° (fps)
0 MPH Wind	87.761	87.796	87.870
5 MPH Wind	87.754	87.789	87.863
10 MPH Wind	87.745	87.779	87.852
15 MPH Wind	87.739	87.773	88.845
20 MPH Wind	87.737	87.769	87.840

5.2.2.2 RockSim Simulations Figures 58, 59, and 60 lists the RockSim simulations for the launch vehicle velocity for various launch rail angles and wind speeds.

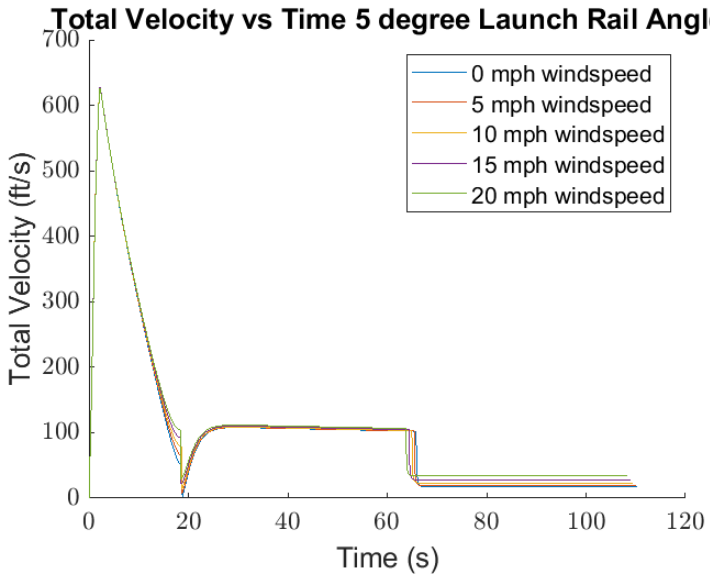

Figure 58: RockSim: Simulated Velocity vs Time for Various Wind Speeds, 5° Rail Angle

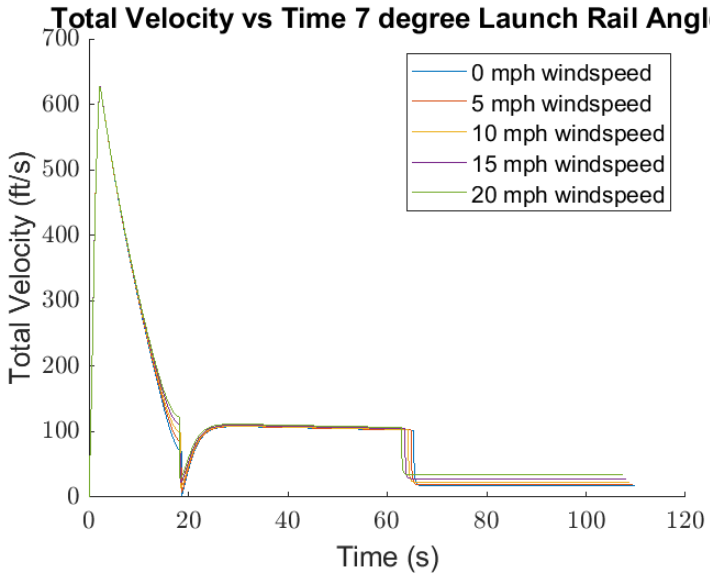

Figure 59: RockSim: Simulated Velocity vs Time for Various Wind Speeds, 7° Rail Angle

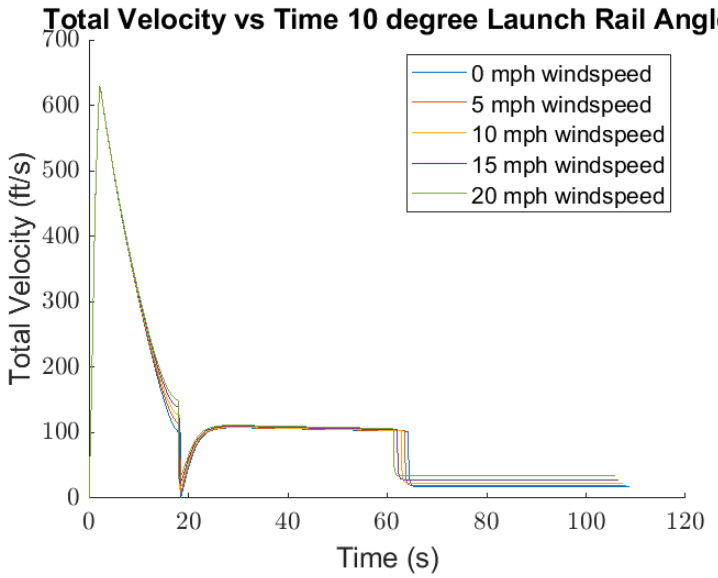

Figure 60: RockSim: Simulated Velocity vs Time for Various Wind Speeds, 10° Rail Angle

NASA Vehicles Req. 2.17. states that the launch vehicle must have an off-rail velocity of at least 52 fps. For all RockSim simulations the launch vehicle went off-rail at 0.294 seconds. Table 66 lists the off-rail velocity for the launch vehicle for all RockSim simulations. From the table, predicted values of the launch vehicle abide by this NASA requirement within a safe margin.

Table 66: RockSim Simulations' Off-Rail Velocity of Launch Vehicle

	Launch Rail 5° (fps)	Launch Rail 7° (fps)	Launch Rail 10° (fps)
0 MPH Wind	82.168	80.243	80.242
5 MPH Wind	82.168	80.243	80.242
10 MPH Wind	80.243	80.243	78.322
15 MPH Wind	80.243	80.243	78.322
20 MPH Wind	80.243	80.243	78.322

5.2.2.2.1 OpenRocket vs RockSim Values & the Average Velocity The off-rail velocities between both flight simulation softwares is comparable, with a difference of around 5 fps. The reasonable precision allows the team to compare the two versions. This section explains the believed cause of the small difference and list the average apogee for each flight condition between the two simulation softwares.

Slight differences exist within the database's values for the L2200 motor; the OpenRocket model gave the L2200 motor a more generous average thrust (2243 Newtons) compared to the RockSim model (2126.7 Newtons). A smaller average thrust would yield a smaller off-rail velocity, as reflected in the data. The team attempted to change the motor's specifications

without avail. A proper understanding of the L2200 Vendor's motor specifications may assist the team in the future for determining the more accurate model. The subscale launch will demonstrate which model has better modeling.

Table 70 lists the average value of the two simulation softwares for all flight conditions. The average between the two softwares provides the best method to determine the predicted apogee because the models demonstrate equal accuracy based on previous years. Every average off-rail velocity value exceeds 75 fps, so the launch vehicle abides by NASA Req.2.17..

Table 67: Average Off-Rail Velocity Between OpenRocket and RockSim Simulations

	Launch Rail 5° (fps)	Launch Rail 7° (fps)	Launch Rail 10° (fps)
0 MPH Wind	84.965	84.020	84.056
5 MPH Wind	84.961	84.016	84.053
10 MPH Wind	80.994	84.011	83.087
15 MPH Wind	83.991	84.008	83.584
20 MPH Wind	83.991	84.006	83.081

5.2.3 Flight Acceleration

The team ran simulations for various flight conditions to understand the projected acceleration of the launch vehicle as a function of time. Per NASA's USLI PDR requirements, the varied flight conditions included launch rail angles and wind speeds. The launch rail was angled at 5, 7, and 10 degrees, and for each launch rail angle, the wind speeds were placed at 0, 5 10, 15, and 20 miles per hour; all other launch conditions were held constant between iterations. The team ran launch simulations ran for both OpenRocket and RockSim. Section 5.2.3.1 lists the acceleration results for the OpenRocket simulations and Section 5.2.3.2 lists the acceleration results for the RockSim simulations. The team determined acceptable precision between the softwares based on the similarity between the two software's data.

5.2.3.1 OpenRocket Simulations Figures 61, 62, and 63 lists the OpenRocket simulations for the launch vehicle acceleration for various launch rail angles and wind speeds.

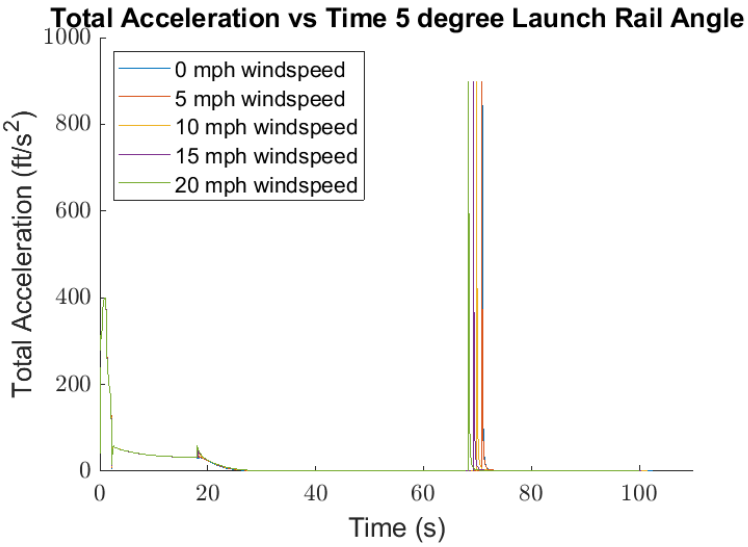

Figure 61: OpenRocket: Simulated Acceleration vs Time for Various Wind Speeds, 5° Rail Angle

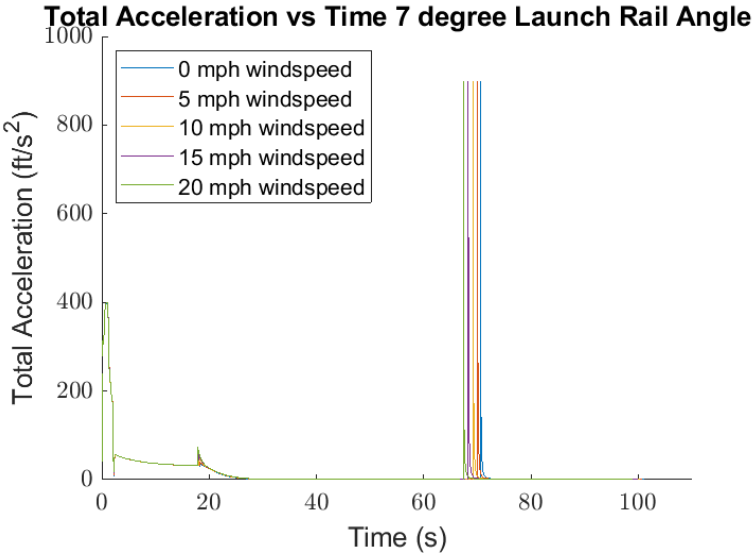

Figure 62: OpenRocket: Simulated Acceleration vs Time for Various Wind Speeds, 7° Rail Angle

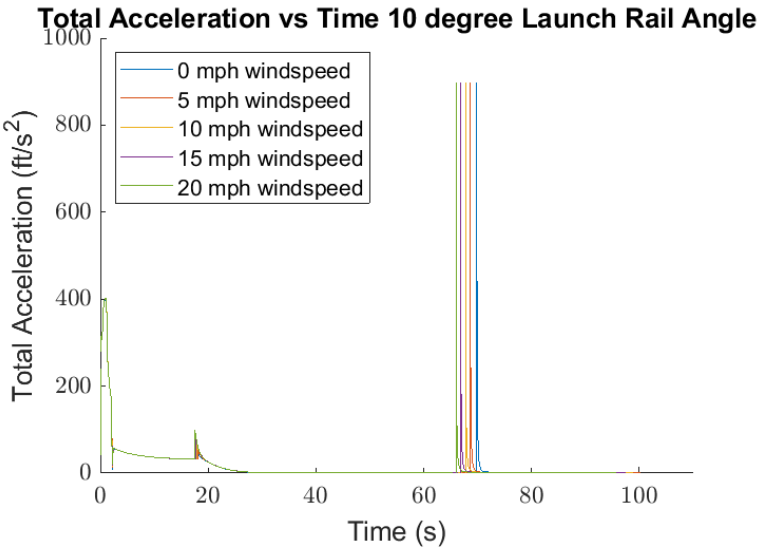

Figure 63: OpenRocket: Simulated Acceleration vs Time for Various Wind Speeds, 10° Rail Angle

5.2.3.2 RockSim Simulations Figures 64, 65, and 66 lists the RockSim simulations for the launch vehicle acceleration for various launch rail angles and wind speeds.

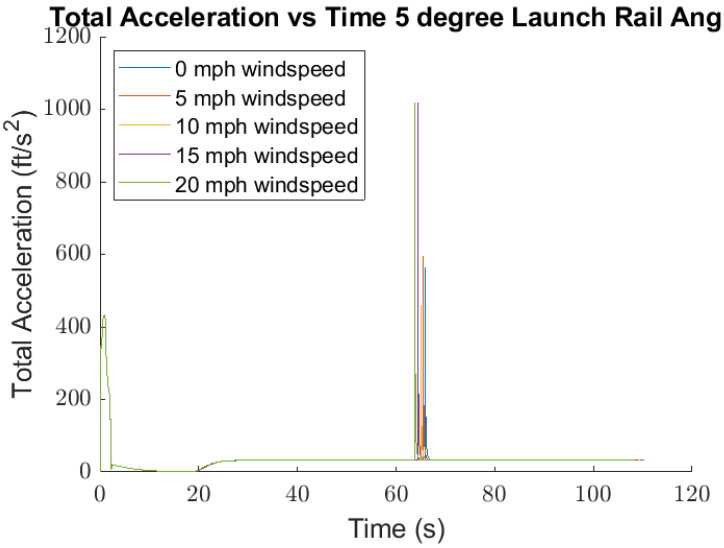

Figure 64: RockSim: Simulated Acceleration vs Time for Various Wind Speeds, 5° Rail Angle

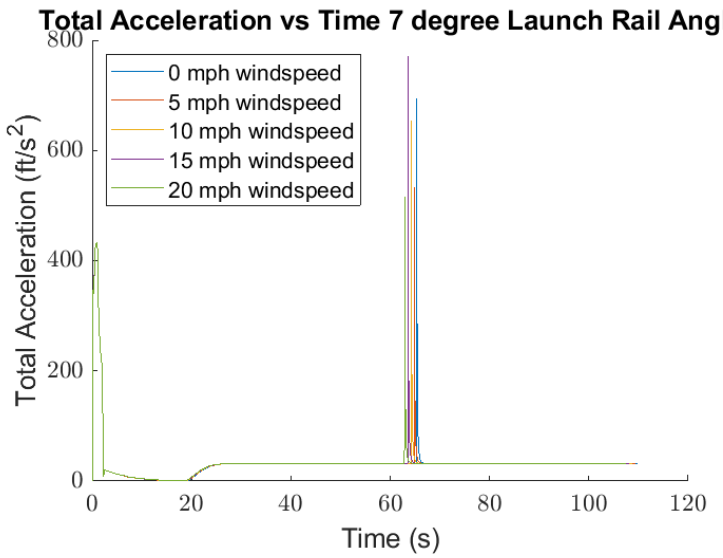

Figure 65: RockSim: Simulated Acceleration vs Time for Various Wind Speeds, 5° Rail Angle

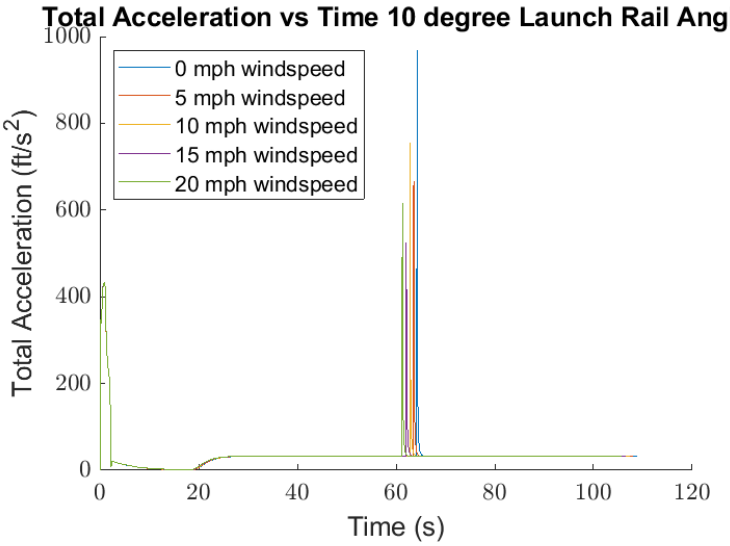

Figure 66: RockSim: Simulated Acceleration vs Time for Various Wind Speeds, 5° Rail Angle

5.2.4 Stability

5.2.4.1 Static Stability The following equation is used to find the static stability of the launch vehicle:

$$\text{Stability} = \frac{CP - CG}{d_{outer}} \tag{13}$$

where CP is the location of the center of pressure (in), CG is the location of the center of

gravity (in), and d_{outer} is the outer diameter of the body tubes (in). Note: the CG and CP origin is the nose cone tip.

Per NASA Req. 3.5., the launch vehicle must have a static stability margin of 2.00 cal at the point of launch rail exit.

5.2.4.1.1 OpenRocket Static Stability Margin The notable values of CP, CG, and the outer diameter from the OpenRocket model are:

- CG = 71.593 in
- CP = 91.335 in
- Outer Diameter 6.17 in

One can now plug the values into the equation:

$$\text{Stability} = \frac{CP - CG}{d_{outer}} = \frac{91.335 - 71.593}{6.17} = 3.20cal \tag{14}$$

The OpenRocket's predicted stability margin exceeds the NASA Requirement of 2.00 cal. A large static stability margin may cause concern for weather-cocking, but given the plan to overshoot the target apogee, weather-cocking will not lead to a failed target apogee. The team would need a significantly larger static stability margin for weather-cocking to become a major issue.

5.2.4.1.2 RockSim Static Stability Margin The notable values of CP, CG, and the outer diameter from the RockSim model are:

- CG = 71.631 in
- CP = 91.1245 in
- Outer Diameter 6.17 in

One can now plug the values into the equation:

$$\text{Stability} = \frac{CP - CG}{d_{outer}} = \frac{91.1245 - 71.631}{6.17} = 3.16cal \tag{15}$$

The stability margin predicted by Rocksim exceeds the NASA Requirement of 2.00 cal. A large static stability margin may cause concern for weather-cocking, but given the plan to overshoot the target apogee, weather-cocking will not lead to a failed target apogee. Furthermore, RockSim contains intensive calculations for weather-cocking, and the software deemed the model "safe" from weather-cocking affects.

5.2.4.1.3 OpenRocket versus RockSim Values There is around a 1.25% difference between the two different static stability values. This difference comes from the CP value, which is calculated slightly differently for the two softwares. The small difference between the stability values allows the team to determine acceptable precsion for the two softwares. As noted before, the software's accuracy cannot be confidently determined until a demonstration flight occurs during CDR.

5.2.4.2 Dynamic Stability Simulations and Off-Rail Stability Values Dynamic stability comes from analyzing changing forces on the launch vehicle. While this is not a specific NASA requirement, the team plans on having the dynamic stability margin as close to 2.00 cal as possible. The same equation, Equation 14, is used to calculate the dynamic stability, but with CP and CG values that change during flight.

The team ran simulations for various flight conditions to understand the projected dynamic stability of the launch vehicle as a function of time. Per NASA's USLI PDR requirements, the varied flight conditions included launch rail angles and wind speeds. The launch rail was angled at 5, 7, and 10 degrees, and for each launch rail angle, the wind speeds were placed at 0, 5 10, 15, and 20 miles per hour; all other launch conditions were held constant between iterations. Launch simulations were ran for both OpenRocket and RockSim. Section 5.2.4.2.1 lists the stability results for the OpenRocket simulations and Section 5.2.4.2.2 lists the altitude results for the RockSim simulations.

5.2.4.2.1 OpenRocket Simulations Figures 67, 68, and 69 lists the OpenRocket simulations for the launch vehicle stability for various launch rail angles and wind speeds.

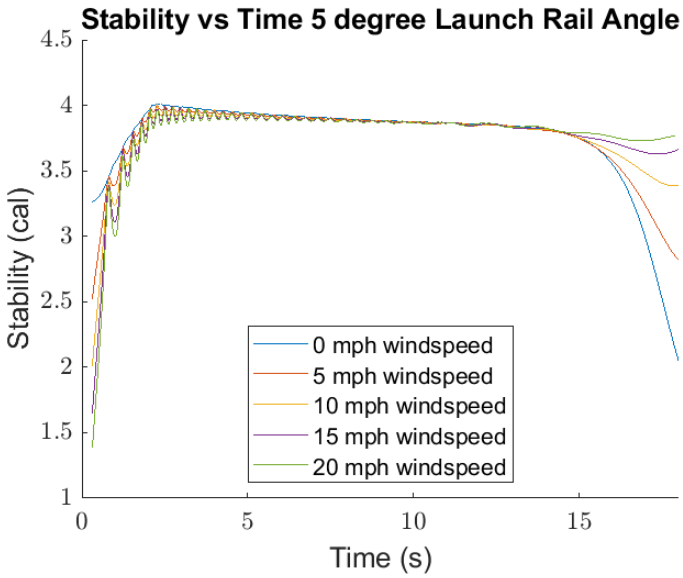

Figure 67: OpenRocket: Simulated Stability vs Time for Various Wind Speeds, 5° Rail Angle

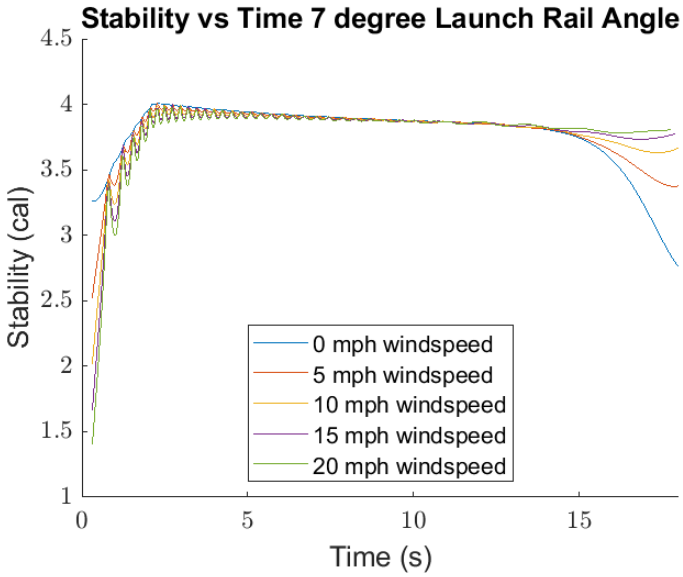

Figure 68: OpenRocket: Simulated Stability vs Time for Various Wind Speeds, 7° Rail Angle

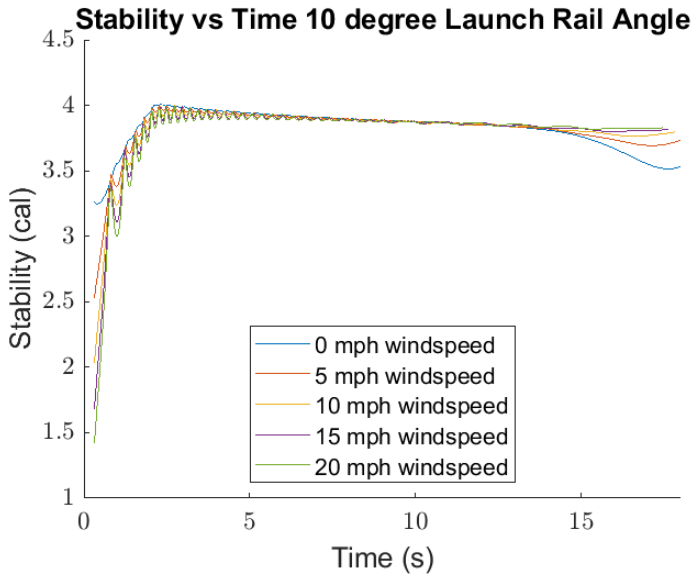

Figure 69: OpenRocket: Simulated Stability vs Time for Various Wind Speeds, 10° Rail Angle

As expected, the stability increases during flight as the CP shifts aftward (due to an increased velocity) and the CG shifts forward (due to motor burnout removing weight). For all OpenRocket simulations the launch vehicle went off-rail at 0.3 seconds. Table 68 lists the off-rail stabilities for the launch vehicle for all OpenRocket simulations. From the table, the launch vehicle abides by this NDRT requirement for winds 10MPH or less. A brief re-design during CDR may allow the launch vehicle to abide under all wind conditions, but there may be limitations due to the max velocity of the motor by burnout; CP is affected by the launch vehicle's velocity.

Table 68: OpenRocket Simulations' Off-Rail Dynamic Stability of Launch Vehicle

	Launch Rail 5°(cal)	Launch Rail 7°(cal)	Launch Rail 10°(cal)
0 MPH Wind	3.2651	3.2630	3.2599
5 MPH Wind	2.5222	2.5250	2.5306
10 MPH Wind	2.0142	2.0214	2.0342
15 MPH Wind	1.6532	1.6640	1.6822
20 MPH Wind	1.3897	1.4029	1.4250

5.2.4.2.2 RockSim Simulations Figures 70, 71, and 72 lists the RockSim simulations for the launch vehicle altitude for various launch rail angles and wind speeds.

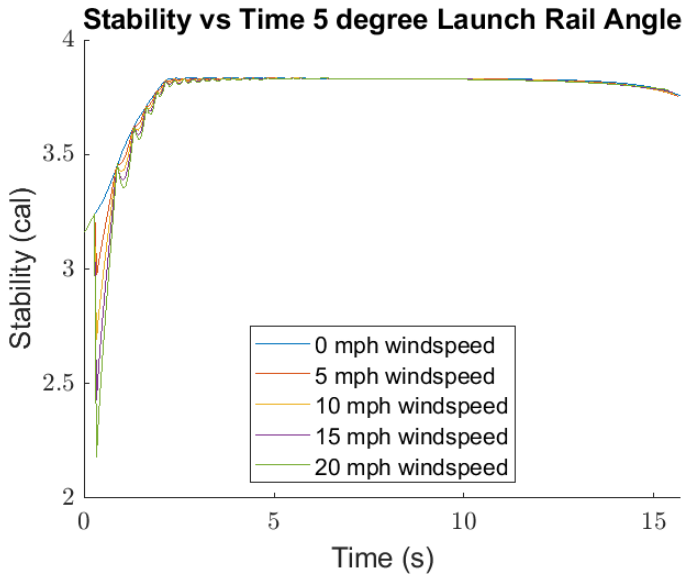

Figure 70: RockSim: Simulated Stability vs Time for Various Wind Speeds, 5° Rail Angle

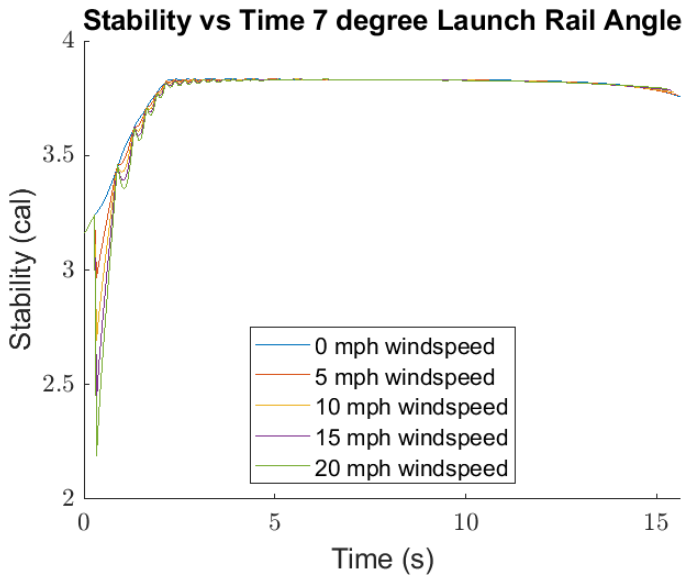

Figure 71: RockSim: Simulated Stability vs Time for Various Wind Speeds, 7° Rail Angle

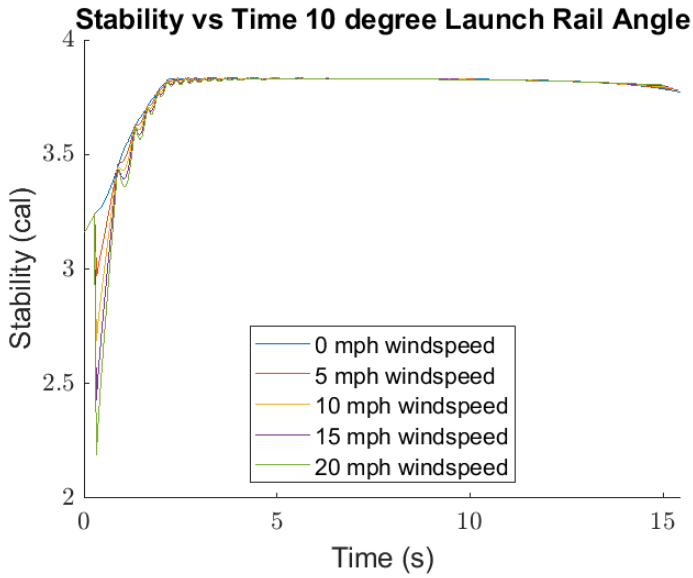

Figure 72: RockSim: Simulated Stability vs Time for Various Wind Speeds, 10° Rail Angle

As expected, the stability increases during flight as the CP increases (due to an increased velocity) and the CG decreases (due to motor burnout removing weight). The software also says that, for weathercocking, "with current settings, the rocket stays inside the 40 degree weathercocking cone before apogee which is considered safe."

Table 69 lists the off-rail stabilities for the launch vehicle for all RockSim simulations. All RockSim simulations went off-rail at 0.294 seconds, and the value in Table 69 is the stability at that time point. From the table, the RockSim model for calculating the stability does not differ as the launch angle or wind changes. For all situations, the CG would change the same. The CP should change but the altering flight conditions have no logical influence on the CP value. Therefore, it makes sense as to why the values appear the same. Given that all values are above the desired 2.00 cal, the launch vehicle is at a stable level of stability.

Table 69: RockSim Simulations' Off-Rail Dynamic Stability of Launch Vehicle

	Launch Rail 5°(cal)	Launch Rail 7°(cal)	Launch Rail 10°(cal)
0 MPH Wind	3.2404	3.2385	3.2385
5 MPH Wind	3.2404	3.2385	3.2385
10 MPH Wind	3.2385	3.2385	3.2366
15 MPH Wind	3.2385	3.2385	3.2366
20 MPH Wind	3.2385	3.2385	3.2366

5.2.4.2.3 OpenRocket versus RockSim Values and the Average Off-Rail Stability Between Versions The difference between the predicted stability margin of the simulation methods is

noticeable. This section serves to explain the believed cause of the small difference and list the average apogee for each flight condition between the two simulation softwares.

As previously mentioned, the CP does not change for the RockSim model, but it does for the OpenRocket model.

Table 70 lists the average value of the two simulation softwares for all flight conditions. The average between the two softwares provides the best method to determine the predicted apogee because both models have demonstrated accuracy in the past. Every average off-rail stability margin value exceeds the needed 2.00 cal, so the launch vehicle abides by NASA Req. 2.14.

Table 70: Average Off-Rail Stability Between OpenRocket and RockSim Simulations

	Launch Rail 5°(cal)	Launch Rail 7°(cal)	Launch Rail 10°(cal)
0 MPH Wind	3.33	3.33	3.41
5 MPH Wind	2.96	2.96	3.33
10 MPH Wind	2.71	2.71	2.97
15 MPH Wind	2.53	2.53	2.54
20 MPH Wind	2.40	2.40	2.41

5.3 Flight Descent Predictions

5.3.1 Terminal Kinetic Energy

The kinetic energy values for the various sections of the launch vehicle during descent were calculated using OpenRocket, Rocksim, and the MATLAB script full_vehicle_descent_calc.m. The kinetic energy of each section was calculated using the equation

$$KE = \frac{1}{2} m_{section} v^2 \tag{16}$$

where $m_{section}$ is the mass of the section of interest and v is the descent rate of the overall vehicle during the relevant phase of flight (under the drogue or main parachute). During majority of the drogue descent, the vehicle will be in two main sections: a forward section composed of the nosecone, Payload Bay, and ACS Bay and an aft section composed of the Fin Can. After main deployment, the vehicle will descend to touchdown as four separate tethered sections.

5.3.1.1 OpenRocket Simulations Tables 71, 72, 73, and 74 list the landing kinetic energy for all four independent launch vehicle sections with the OpenRocket simulations. From the tables, one can see that no independent section of the launch vehicle exceeds 75 ft-lbs. Thus, the OpenRocket model of the launch vehicle abides by NASA Requirement 3.3.

Table 71: OpenRocket Simulations' Landing Kinetic Energy for the Nose Cone

	Launch Rail 5° (ft-lb)	Launch Rail 7° (ft-lb)	Launch Rail 10° (ft-lb)
0 MPH Wind	21.287	21.289	21.292
5 MPH Wind	21.287	21.287	21.287
10 MPH Wind	21.287	21.292	21.292
15 MPH Wind	21.289	21.287	21.289
20 MPH Wind	21.274	21.287	21.284

Table 72: OpenRocket Simulations' Landing Kinetic Energy for the Payload Bay

	Launch Rail 5° (ft-lb)	Launch Rail 7° (ft-lb)	Launch Rail 10° (ft-lb)
0 MPH Wind	57.450	57.457	57.464
5 MPH Wind	57.450	57.450	57.450
10 MPH Wind	57.450	57.464	57.464
15 MPH Wind	57.457	57.450	57.457
20 MPH Wind	57.415	57.450	57.444

Table 73: OpenRocket Simulations' Landing Kinetic Energy for the ACS Body Tube

	Launch Rail 5° (ft-lb)	Launch Rail 7° (ft-lb)	Launch Rail 10° (ft-lb)
0 MPH Wind	52.972	52.978	52.984
5 MPH Wind	52.972	52.972	52.972
10 MPH Wind	52.972	52.984	52.984
15 MPH Wind	52.978	52.972	52.978
20 MPH Wind	52.939	52.972	52.965

Table 74: OpenRocket Simulations' Landing Kinetic Energy for the Fin Can

	Launch Rail 5° (ft-lb)	Launch Rail 7° (ft-lb)	Launch Rail 10° (ft-lb)
0 MPH Wind	57.608	57.615	57.622
5 MPH Wind	57.608	57.608	57.608
10 MPH Wind	57.608	57.622	57.622
15 MPH Wind	57.615	57.608	57.615
20 MPH Wind	57.573	57.608	57.601

5.3.1.2 RockSim Simulations

Tables 75, 76, 77, and 78 list the landing kinetic energy for all four independent launch vehicle sections with the RockSim simulations, using the vertical velocity only. From the tables, one can see that not all independent section of the launch vehicle are under 75 ft-lbs. However, at this moment the most reliable value of kinetic energy is the average value between OpenRocket, RockSim, and MATLAB. As well, RockSim has been notoriously higher in value for almost everything when compared to the other simulation methods, so one should keep that in mind. Still, the value of the kinetic energy that exceeds 75 ft-lbs is barely over the value; small design changes during CDR (it parachute changes) can allow that number to go lower.

Table 75: RockSim Simulations' Landing Kinetic Energy for the Nose Cone

	Launch Rail 5° (ft-lb)	Launch Rail 7° (ft-lb)	Launch Rail 10° (ft-lb)
0 MPH Wind	28.199	28.199	28.199
5 MPH Wind	28.199	28.199	28.199
10 MPH Wind	28.199	28.199	28.199
15 MPH Wind	28.199	28.199	28.199
20 MPH Wind	28.199	28.199	28.199

Table 76: RockSim Simulations' Landing Kinetic Energy for the Payload Bay

	Launch Rail 5° (ft-lb)	Launch Rail 7° (ft-lb)	Launch Rail 10° (ft-lb)
0 MPH Wind	76.105	76.105	76.105
5 MPH Wind	76.105	76.105	76.105
10 MPH Wind	76.105	76.105	76.105
15 MPH Wind	76.105	76.105	76.105
20 MPH Wind	76.105	76.105	76.105

Table 77: RockSim Simulations' Landing Kinetic Energy for the ACS Body Tube

	Launch Rail 5° (ft-lb)	Launch Rail 7° (ft-lb)	Launch Rail 10° (ft-lb)
0 MPH Wind	70.171	70.171	70.171
5 MPH Wind	70.171	70.171	70.171
10 MPH Wind	70.171	70.171	70.171
15 MPH Wind	70.171	70.171	70.171
20 MPH Wind	70.171	70.171	70.171

Table 78: RockSim Simulations' Landing Kinetic Energy for the Fin Can

	Launch Rail 5° (ft-lb)	Launch Rail 7° (ft-lb)	Launch Rail 10° (ft-lb)
0 MPH Wind	76.313	76.313	76.313
5 MPH Wind	76.313	76.313	76.313
10 MPH Wind	76.313	76.313	76.313
15 MPH Wind	76.313	76.313	76.313
20 MPH Wind	76.313	76.313	76.313

5.3.1.3 MATLAB Calculations The MATLAB kinetic energy calculations can be found in Table 79, below. As you can see, the energy at impact does not exceed the NASA limit of 75 ft-lbs. The kinetic energy values calculated using the MATLAB script full_vehicle_descent_calc.m.

Table 79: Kinetic Energy of Vehicle Sections at Impact

Section	MATLAB (ft-lb)
Nose Cone	22.36
Payload	60.36
ACS	55.65
Fin Can	60.52

5.3.1.3.1 OpenRocket versus RockSim versus MATLAB Values and the Average Landing Kinetic Energy Between Versions Table 80 lists the highest average landing kinetic energy for the launch vehicle against all flight conditions. It should be noted that the MATLAB values were applied for the three different launch rail values and wind conditions when calculating the average. As you can see, no landing kinetic energy value exceeds 75 ft-lbs; thus, the landing kinetic energy abides by the NASA Requirement 3.3.

Table 80: Highest Average Landing Kinetic Energy of the Launch Vehicle's Independent Sections, Relative to Apogee

Section	Landing Kinetic Energy °(ft-lb)
Nose Cone	23.950
Payload	64.643
ACS	59.602
Fin Can	64.818

5.3.2 Descent Time

The total vehicle descent time were calculated using OpenRocket, RockSim, and the MATLAB script full_vehicle_descent_calc.m.

5.3.2.1 OpenRocket Simulations Table 81 lists the final descent time for the launch vehicle for various launch conditions. While the descent time does not exceed the NASA requirement of 90 seconds, one should acknowledge that this simulation has the apogee without the implementation of ACS. Thus the apogee is far higher than the target apogee of 4600ft. Due to the higher apogee, the descent time for the OpenRocket model is far higher than the realistic descent time. If the OpenRocket model has the descent time under 90 seconds, and the actual apogee of the launch will be far lower, then the team can confidently state that the launch vehicle will be within the descent time and maybe under 80 seconds

Table 81: OpenRocket Simulations' Descent Time of the Launch Vehicle, Relative to Apogee

	Launch Rail 5°(s)	Launch Rail 7°(s)	Launch Rail 10°(s)
0 MPH Wind	84.637	83.407	81.410
5 MPH Wind	82.707	82.987	82.757
10 MPH Wind	83.839	82.800	81.597
15 MPH Wind	82.892	82.531	80.310
20 MPH Wind	83.605	81.769	78.654

5.3.2.2 RockSim Simulations Table 82 lists the final descent time for the launch vehicle for various launch conditions. While the descent time does exceed the NASA requirement of 90 seconds, one should acknowledge that this simulation has the apogee without the implementation of ACS. Thus the apogee is far higher than the target apogee of 4600ft. Due to the higher apogee, the descent time for the RockSim model is far higher than the realistic descent time. If the RockSim model has the descent time under 90 seconds, and the actual

apogee of the launch will be far lower, then the team can confidently state that the launch vehicle will be within the descent time and maybe under 80 seconds

Table 82: RockSim Simulations' Descent Time of the Launch Vehicle, Relative to Apogee

	Launch Rail 5°(s)	Launch Rail 7°(s)	Launch Rail 10°(s)
0 MPH Wind	91.463	91.080	90.145
5 MPH Wind	91.125	90.585	89.595
10 MPH Wind	90.750	90.090	89.010
15 MPH Wind	90.310	89.595	88.311
20 MPH Wind	89.760	88.990	87.613

5.3.2.3 MATLAB Calculations The MATLAB descent time calculation can be found in Table 83, below. The MATLAB script uses the descent velocities calculated for the main and drogue parachutes in addition to the the deployment altitudes for said parachutes to calculate the total descent time. As you can see, the descent time does not exceed the NASA limit of 90 seconds. As well, one should acknowledge that this simulation, unlike the OpenRocket and RockSim models, does account for the target apogee of 4600 ft. This is the main reason as to why the descent time is below most OpenRocket and RockSim values,

Table 83: MATLAB Calculation for Total Vehicle Descent Time

MATLAB (s)
78.36

5.3.2.3.1 OpenRocket versus RockSim versus MATLAB Values and the Average Descent Time Between Versions Table 84 lists the average drift radius for the launch vehicle for all flight conditions. It should be noted that the MATLAB value was applied for the three different launch rail values when calculating the average. As you can see, no average descent time exceeds 90 seconds; thus, the descent time abides by the NASA Requirement 3.11. Again, it should be noted that two of the three values in the average had apogee values that were above the expected apogee, so the realistic value of the average should be below 80 seconds.

Table 84: Average Descent Time of the Launch Vehicle, Relative to Apogee

	Launch Rail 5°(s)	Launch Rail 7°(s)	Launch Rail 10°(s)
0 MPH Wind	84.820	84.282	83.305
5 MPH Wind	84.064	83.977	83.571
10 MPH Wind	84.316	83.750	82.989
15 MPH Wind	83.854	83.495	82.756
20 MPH Wind	83.908	83.040	81.542

5.3.3 Drift Radius

The total vehicle descent drift were calculated using OpenRocket, RockSim, and the MATLAB script full_vehicle_descent_calc.m. The MATLAB script uses the descent time and the worst case scenario wind velocity of 20 mph to calculate the total drift.

5.3.3.1 OpenRocket Simulations Figures 73, 74, and 75 lists the OpenRocket simulations for the launch vehicle drift radius for various launch rail angles and wind speeds.

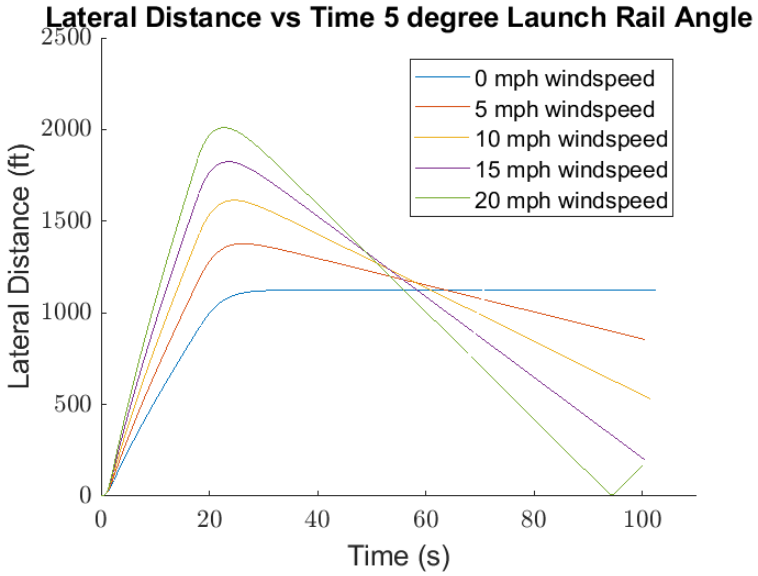

Figure 73: OpenRocket: Simulated Drift Radius vs Time for Various Wind Speeds, 5° Rail Angle

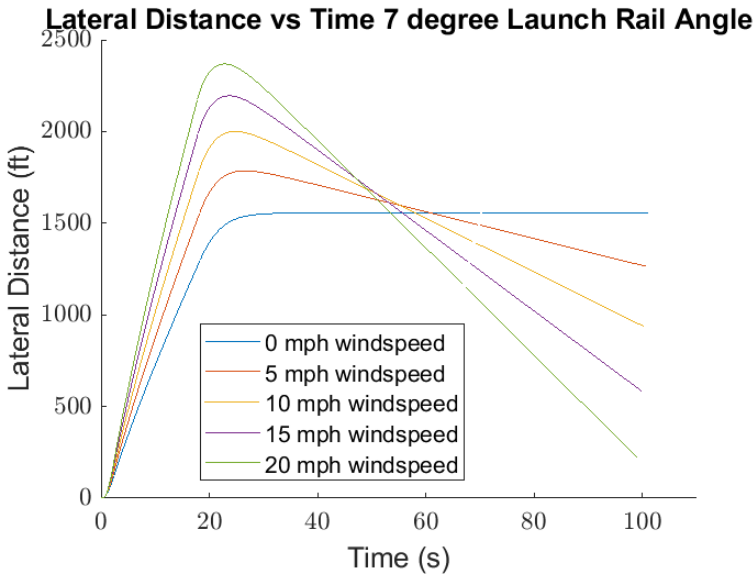

Figure 74: OpenRocket: Simulated Drift Radius vs Time for Various Wind Speeds, 7° Rail Angle

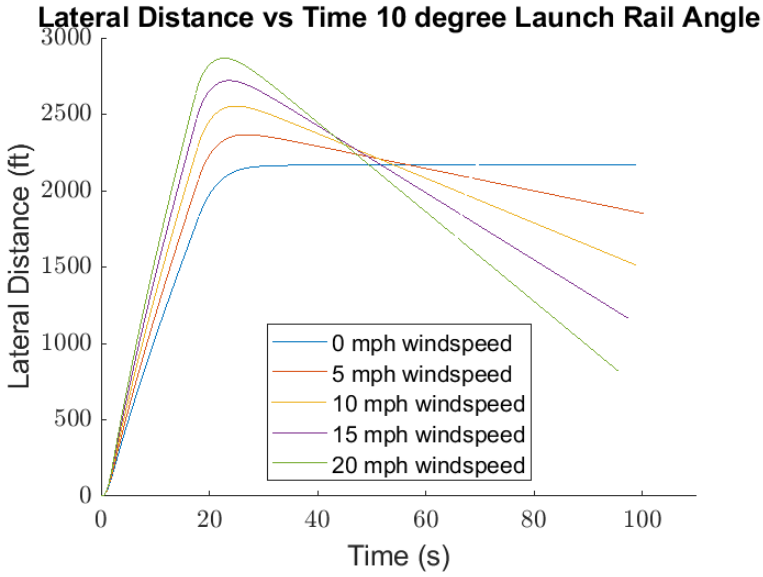

Figure 75: OpenRocket: Simulated Drift Radius vs Time for Various Wind Speeds, 10° Rail Angle

Table 85 lists the final drift radius for the launch vehicle for various launch conditions. The maximum OpenRocket drift does not exceed the NASA requirement of 2500ft. As well, one should acknowledge that this simulation has the apogee without the implementation of ACS. Thus the apogee is far higher than the target apogee of 4600ft. Due to the higher apogee, the drift radius for the OpenRocket model is far higher than the realistic drift radius. If the OpenRocket model has the drift radius under 2500 ft, and the actual apogee of the launch will be far lower, then the team can confidently state that the launch vehicles will be within the drift radius.

Table 85: OpenRocket Simulations' Absolute Drift Radius of the Launch Vehicle, Relative to Apogee

	Launch Rail 5° (ft)	Launch Rail 7° (ft)	Launch Rail 10° (ft)
0 MPH Wind	194.91	258.70	336.30
5 MPH Wind	343.36	293.10	226.70
10 MPH Wind	912.36	852.24	772.60
15 MPH Wind	1461.90	1415.50	1317.90
20 MPH Wind	1660.2	1959.50	1831.60

5.3.3.2 RockSim Simulations

Figures 76, 77, and 78 lists the RockSim simulations for the launch vehicle drift radius for various launch rail angles and wind speeds.

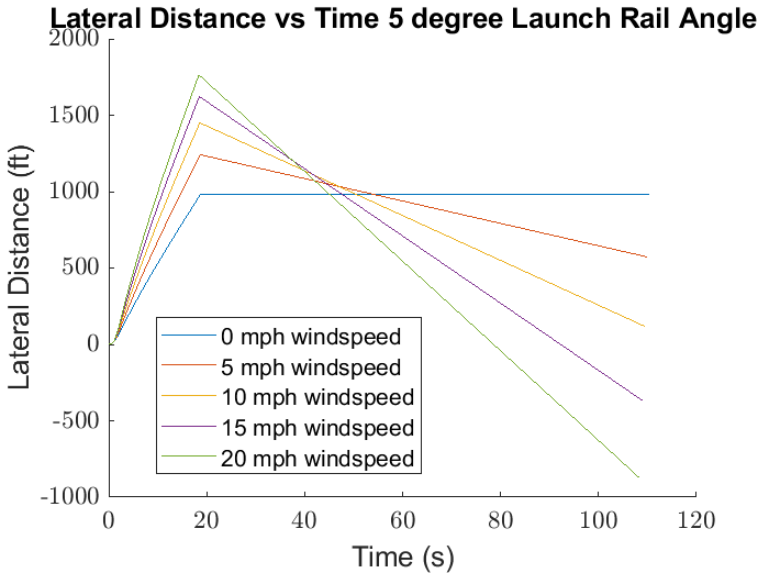

Figure 76: RockSim: Simulated Drift Radius vs Time for Various Wind Speeds, 5° Rail Angle

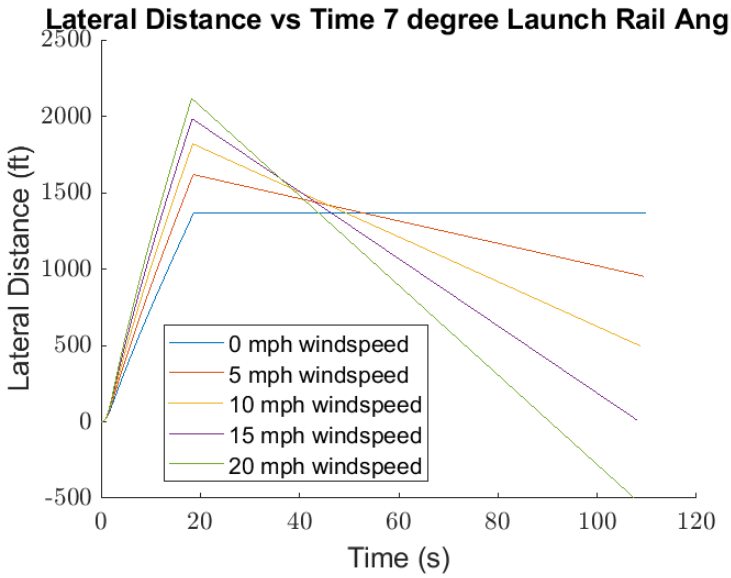

Figure 77: RockSim: Simulated Drift Radius vs Time for Various Wind Speeds, 7° Rail Angle

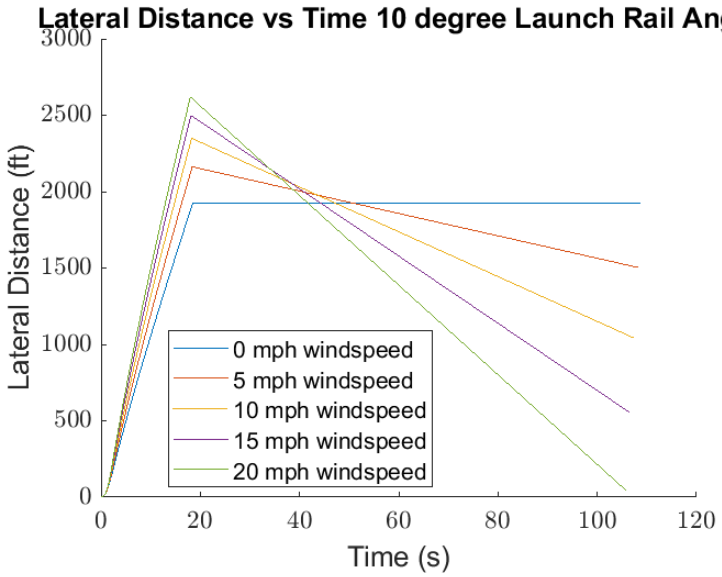

Figure 78: RockSim: Simulated Drift Radius vs Time for Various Wind Speeds, 10° Rail Angle

Table 86 lists the final drift radius for the launch vehicle for various launch conditions. While the drift does exceed the NASA requirement of 2500ft, one should acknowledge that this simulation has the apogee without the implementation of ACS. Thus the apogee is far higher than the target apogee of 4600ft. Due to the higher apogee, the drift radius for the RockSim model is far higher than the realistic drift radius. If the RockSim model has the drift radius barely over 2500 ft, and the actual apogee of the launch will be far lower, then the team can confidently state that the launch vehicles will be within the drift radius.

Table 86: RockSim Simulations' Drift Radius of the Launch Vehicle, Relative to Apogee

	Launch Rail 5° (ft)	Launch Rail 7° (ft)	Launch Rail 10° (ft)
0 MPH Wind	0.189	0.527	0.000
5 MPH Wind	669.90	665.90	658.643
10 MPH Wind	1333.90	1324.50	1304.9
15 MPH Wind	1989.10	1975.90	1946.10
20 MPH Wind	2639.40	2616.8	2576.30

5.3.3.3 MATLAB Calculations The MATLAB drift calculations can be found in Table 87, below. As you can see, the drift radius does not exceed the NASA limit of 2,500 ft. As well, one should acknowledge that this simulation has the apogee without the implementation of ACS. Thus the apogee is far higher than the target apogee of 4600ft. Due to the higher apogee, the drift radius for the MATLAB model is far higher than the realistic drift radius. If the MATLAB model has the drift radius under 2500 ft, and the actual apogee of the launch will be far lower, then the team can confidently state that the launch vehicles will be within the drift radius.

Table 87: Total Vehicle Descent Drift

	MATLAB (ft)
0 MPH Wind	0
5 MPH Wind	574.61
10 MPH Wind	1149.21
15 MPH Wind	1723.82
20 MPH Wind	2298.42

5.3.3.3.1 OpenRocket versus RockSim versus MATLAB Values and the Average Drift Radius Between Versions Table 88 lists the average drift radius for the launch vehicle for all flight conditions. It should be noted that the MATLAB values were applied for the three different launch rail values when calculating the average. As you can see, no average drift radius exceeds 2500 ft; thus, the drift radius abides by the NASA Requirement 3.10. Again, it should be noted that two of the three values in the average had apogee values that were above the expected apogee, so the realistic value of the average should be much lower.

Table 88: Average Drift Radius of the Launch Vehicle, Relative to Apogee

	Launch Rail 5° (ft)	Launch Rail 7° (ft)	Launch Rail 10° (ft)
0 MPH Wind	65.033	86.41	112.1
5 MPH Wind	529.29	511.20	486.65
10 MPH Wind	1131.82	1108.65	1075.57
15 MPH Wind	1724.94	1705.07	1662.61
20 MPH Wind	2199.34	2291.57	2235.44

6 Technical Design: 360° Rotating Optical Imager

6.1 System Objective and Mission Success Criteria

The Notre Dame Rocketry Team's payload for the 2022-2023 NASA Student Launch Initiative is the **3**60° **R**otating **O**ptical **I**mager (**TROI**). The payload will remain inside the launch vehicle for the duration of the flight. Once the launch vehicle is stationary on the ground, a camera assembly is actuated out of the launch vehicle along the axis of the payload tube using a lead screw. The camera assembly orients and raises above the payload tube for operation. The TROI receives radio signal commands and rotates the camera assembly on a stepper motor to capture the desired image as instructed. The TROI processes the images after they are taken per the radio command sequence and stores the images on the payload. In the following sections, the TROI layout and the design options currently under consideration are described. In order to satisfy all aspects of the payload mission, the TROI is composed of multiple subsystems. The TROI can be broken down into five main subsystems: deployment, retention, electrical, orientation, and radio communication. The structure of the payload and its subsystems are seen in Table 89.

Table 89: TROI Subsystems Overview

System	Description
Retention	Includes the physical structure of the payload retention system including bulkhead material selection, load calculations, and overall structure of the payload system.
Deployment	Includes the contents of the payload tube and their assembly including the lead screws, springs, stepper motors, and interfacing with the removable bulkhead from the recovery system.
Electrical	Includes the selection and integration of sensors and electronics into the overall TROI system. Includes microcontroller selection, battery selection, RF receiver selection, camera selection, stepper motor selection, sensor selection, and processor.
Imaging Orientation	Includes configuring the camera assembly to orient and operate properly for any sequence of given commands.
Radio Communication	Includes configuring the selected microcontroller and RF receiver to receive NASA's RF commands as well as processing the commands into operations for the imaging orientation subsystem.

6.1.1 Mission Success Criteria

The following criteria will be used to determine if the payload system fulfills the mission successfully:

- The payload system, TROI, shall be rigidly fixed inside the payload tube of the launch vehicle during flight, so that only the imaging orientation subsystem deploys quickly and accurately once the launch vehicle has landed.
- The TROI shall protect the electronics from potential water damage or residue from the flight recovery systems.
- The TROI shall deploy with the correct camera orientation and is orientated with the z-axis perpendicular to the ground plane.
- The TROI shall take a series of clear pictures without obstructions in any order when commands are received via RF instructions. The TROI shall modify those images if requested per the RF commands.

- The TROI shall successfully receive and execute set commands sent by NASA's ARPS protocol.
- The TROI shall be serviceable and have ease of access for changes during tests and the competition.

6.2 Functional System Designs

Design considerations for the TROI are a critical part of the team's goal to successfully complete the mission. They provide a foundation for the team to analyze the integration of different sub-systems within the TROI as well as compare alternative sub-system designs. In addition, they allow for the team to conduct trade studies based on their provided criteria to help determine the most operative design.

6.2.1 Design Considerations

The primary design considerations for the TROI are controlling the deployment and orientation of the camera in order to obtain clear images of the landing site. The success of the mission depends on the quality of the images obtained and their consistency with the provided RF commands through the ARPS protocol. The TROI can only obtain clear images if the camera lands, deploys, and orients correctly, regardless of visual obstructions. The design must accommodate the team derived requirements for the TROI in addition to given NASA requirements. These include a maximum diameter of 6 in. and a maximum tube length of 12 in. within the payload tube of the launch vehicle (NDRT Req. TROI.10). The TROI has an allotted mass of no greater than 90 oz. which is necessary to support the TROI system and the redundancies set in place to support mission success (NDRT Req. TROI.11). All the TROI components must be able to withstand maximum loads with a factor of safety of 1.5 (NDRT Req. TROI.7). To meet these design objectives, several potential designs for the payload were considered. These designs included a mechanism with robotic legs that extends to orient the payload tube upright upon landing, a rover that drives out of the payload tube with a camera, and a gimbal on a linear actuator that comes out of the payload tube. These designs focused on obtaining unobstructed images by moving the view of the camera either above or around possible obstructions, including the payload tube of the launch vehicle. These ideas will be further discussed in Section 6.2.2.

6.2.2 System Alternatives

The payload will receive RF command transmissions and capture 360° images about the z-axis oriented perpendicular to the ground. This task will be completed by a payload that is not ejected from the launch vehicle during flight, however the payload may leave the launch vehicle after landing. To meet these design objectives, the team first completed a trade study to compare three system level alternative designs. The first payload design operates out of the payload tube and is called an internal payload. The second payload design departs and separates from the launch vehicle after landing and is called an external payload. The third payload design orients the entire payload tube that it is retained in and is called a semi-external payload. The trade study comparing the three system level alternative designs is presented in Table 90.

Table 90: Payload System Level Design Alternatives Trade Study

		Internal Payload		External Payload		Semi-External Payload	
Criteria	**Weight**	**Value**	**WNV**	**Value**	**WNV**	**Value**	**WNV**
Mission Reliability	35%	5	0.13	5	0.13	4	0.10
Deployment Reliability	25%	4	0.11	3	0.083	2	0.056
Complexity of Design	15%	3	0.056	1	0.019	4	0.075
Machinability	10%	5	0.050	2	0.020	3	0.030
Cost	5%	3	0.015	2	0.010	5	0.025
Weight	10%	4	0.044	1	0.11	4	0.044
Total WNV		**0.374**		**0.317**		**0.309**	

The results of Table 90 demonstrate that an internal payload is the best option given the unpredictable terrain, conditions, and launch vehicle orientation after landing.

The team considered multiple mechanical designs for the payload. The top candidate designs included the use of a rover, using the payload tube itself to orient the camera to vertical by means of hinged legs interfacing with the airframe, and using a system that remains attached to the payload tube and internal bulkhead while extending out and upward as needed. Top factors of consideration for these designs were ease in manufacturing, simplicity in interfacing with other systems of the launch vehicle, and overall minimization of design and assembly complexity. Utilizing a payload that remains attached to the internal bulkhead but uses a lead

screw to extend out of the payload tube and a spring mechanism to extend the camera assembly upwards was chosen as the final design. This design minimizes mechanical complexity and allows for ease in interfacing with the electrical components.

The rover and payload tube orientation designs were also considered but were ultimately discarded after the team completed the system level trade study. The rover design introduced unnecessary design complexity due to the unknown orientation of the payload tube upon landing. Using the payload tube to orient the camera subassembly with flaps cut in the launch vehicle that would extend as legs further introduced unnecessary design complexity. The ACS uses a similar design for hinged flaps which made utilizing flaps as legs an attractive option, but due to the design, manufacturing, and assembly complexity of this option, the idea was ultimately discarded.

After completing the system level trade study and deciding to create an internal payload, the team next developed a suitable device that meets the necessary requirements. The team studied four ideas: A combination of a double servo motor design and gravity oriented design, a double lead screw design, a spring popout design, and a double linear actuator design. All of these design ideas originate within the body tube of the vehicle, however each has unique processes that both benefit and challenge the reliability and effectiveness of the design.

The double servo design consists of a step motor mounted at the back of the payload tube connected to a linear actuator that will extend a secondary system consisting of the camera and a second linear actuator. Upon extension beyond the payload tube, the secondary system will activate, extending the camera above the diameter of the payload tube, where the camera system could then operate. This design optimizes a successful deployment.

In contrast, the spring pop-out design is a passive deployment system that would employ a counterweight that would be released upon landing and deployment of the payload. The counterweight would allow the payload camera system to orient with the z-axis as required by NASA Req. 4.2.1.1. The counterweight would be locked in a certain position during the launch and recovery phase, and would be released when landing has been detected. This minimizes the complexity of the design.

The double lead screw design consists of a system of perpendicular lead screws and servo motors to move the camera out and above the payload tube to complete the RF commands. The first lead screw is along the axis of the payload tube, and the second lead screw is mounted to a stepper motor attached to the end of the first lead screw. The double linear actuator design is similar to the double lead screw design, except it consists of two linear actuators instead of lead screws. The two designs are different as linear actuators are heavier, more complicated, and more expensive than lead screws for these designs.

A trade study comparing the four preliminary designs is shown in Table 91, and the four designs were compared on deployment reliability, camera orientation reliability, retention reliability, image reliability, overall design simplicity, and complexity with other systems.

Table 91: Internal Payloads Trade Study

		Servo, Passive		Lead Screw		Spring Pop-Out		Linear Actuator	
Criteria	**Weight**	**Value**	**WNV**	**Value**	**WNV**	**Value**	**WNV**	**Value**	**WNV**
Deployment Reliability	30%	3	0.06	4	0.08	4	0.08	4	0.08
Camera Orientation Reliability	25%	2	0.036	5	0.089	2	0.036	5	0.089
Retention Reliability	15%	3	0.036	3	0.036	2.5	0.03	4	0.048
Image Quality	15%	4	0.043	4	0.02	2	0.021	4	0.043
Overall Design Simplicity	10%	3	0.038	3	0.038	5	0.063	1	0.013
Total WNV		**0.21**		**0.29**		**0.23**		**0.27**	

Due to its overall reliability and simplicity a lead screw based internal mechanism was selected as the optimal system configuration.

6.3 Current System Design

The TROI consists of the necessary mechanical and electrical parts to validate a safe and practical payload design. Decisions regarding the mechanical configuration of the TROI are informed through several trade studies to find the best method for retaining the payload and and actuating the TROI from the launch vehicle. The TROI's software and electrical configuration considers multiple trade studies on the myriad of necessary modules for the subsystems. The current payload in the deployed state is shown in Figure 79.

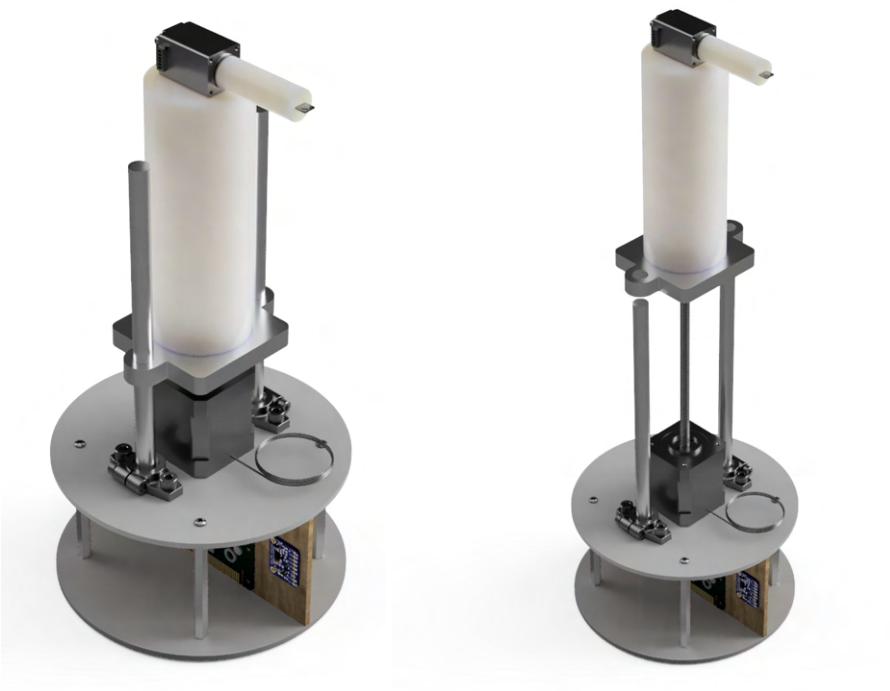

Figure 79: TROI Retained State (Left) and TROI Deployed State (Right)

A CAD drawing of the payload in the retained state is shown in Figure 80.

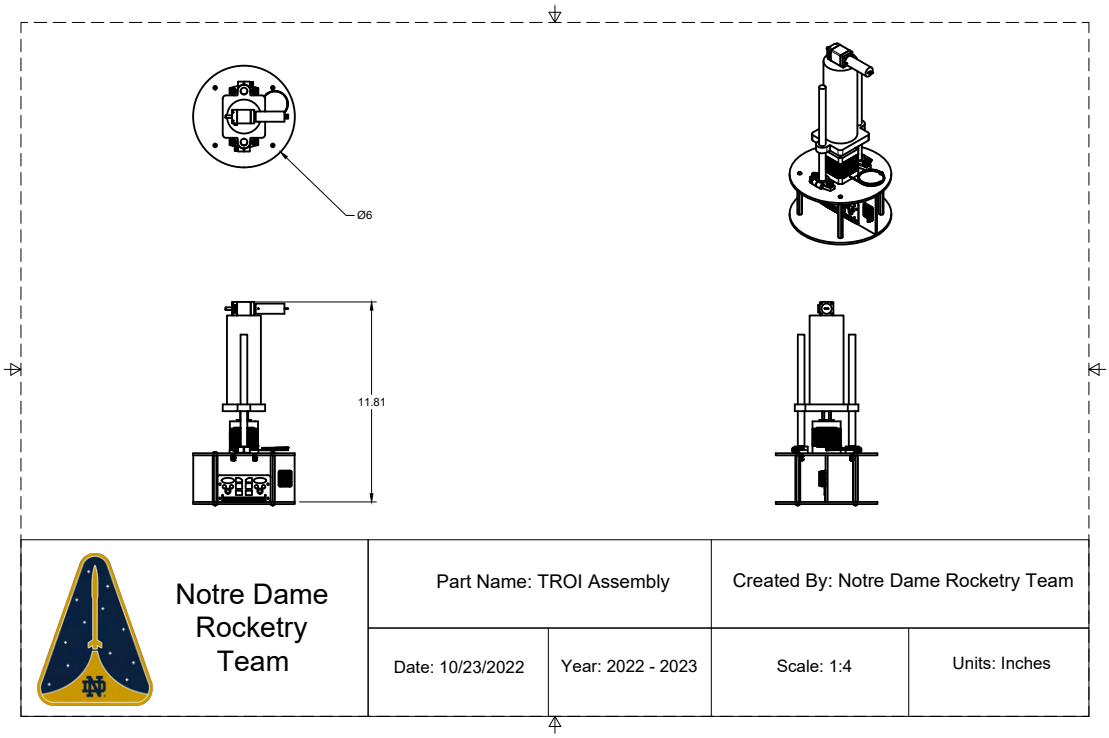

Figure 80: TROI Retained State CAD Drawing

6.3.1 Mechanical

The mechanical components of the TROI include the electronics retention, lead screw and camera subassemblies. These components must be retained within the payload bay of the launch vehicle and interface with the electrical components to complete the payload mission. Additionally, the payload and nose cone recovery system must work together to ensure that the nose cone is removed prior to landing for ease in payload deployment. The team designed the mechanical components of the system prioritizing simplicity, ease in manufacturing, and ease in interfacing with the electrical components of the system among other factors.

6.3.1.1 System Layout The mechanical elements of the payload system includes three subassemblies: the electronics retention, lead screw, and camera subassemblies. The electronics subassembly consists of two fiberglass bulkheads which enclose the electronics on a vertical mounting board. Four minimally load bearing aluminum standoffs connect the two bulkheads. Fiberglass was chosen as the bulkhead material based on the results of the trade study in Table 92. Fiberglass has a high tensile strength, is easily machinable, and is standardized with many of the bulkheads of other team systems. Carbon fiber was also considered but due to its RF blocking properties, it was discarded.

Table 92: Bulkhead Material Trade Study

		Plywood		Fiberglass		Aluminum 6061	
Criteria	**Weight**	**Value**	**WNV**	**Value**	**WNV**	**Value**	**WNV**
Ease of System Level Interfacing	15%	1	0.02	5	0.11	1	0.02
Tensile Strength (MPa)	35%	31.1	0.05	93	0.15	90	0.15
Machinability	20%	5	0.09	4	0.07	2	0.04
Cost ($)	10%	3.71	0.04	56	0.00	13	0.04
Density	20%	5	0.10	3	0.06	2	0.04
Total WNV		**0.308**		**0.392**		**0.282**	

The lead screw subassembly consists of a stepper motor, 6 in. lead screw, aluminum standoff rail tracks to mitigate rotational motion until desirable, and sleeve subassembly. Multiple lead screws and stepper motors were considered. The McMaster Carr Stepper Motor with linear actuation was selected due to its high torque capability, reliability, and minimized weight and volume as shown in Table 93.

Table 93: Lead Screw Trade Study

		McMaster-Carr Stepper Motor with Linear Actuation		Iverntech NEMA 17 Stepper Motor with Lead Screw		NEMA 23 Non-captive Linear Actuator	
Criteria	**Weight**	**Value**	**WNV**	**Value**	**WNV**	**Value**	**WNV**
Weight (lbs)	20%	0.71	0.14	1.1	0.06	1.43	0.00
Cost	10%	188.40	0.07	29.99	0.01	53.67	0.02
Reliability	10%	5	0.04	3	0.03	3	0.03
Ease of Integration	10%	5	0.04	3	0.03	4	0.03
Travel Length (in)	25%	6	0.06	9.45	0.10	7.87	0.08
Torque (lb· in)	10%	450	0.10	4.430	0.00	10.62	0.00
Volume of Motor (in^3)	15%	5.181	0.07	5.164	0.08	11.103	0.00
Total WNV		**0.45**		**0.23**		**0.17**	

The sleeve subassembly consists of a nut with a mounting board face and the sleeve itself. The nut and mounting board will travel linearly along the lead screw to extend the camera subassembly beyond the payload tube. The mounting board face will be machined from HDPE and interfaces with the two aluminum track rails which inhibit rotational motion until desirable. A cap machined from HDPE is attached to the end of the lead screw. This cap allows for rotational motion by allowing the nut and mounting board subassembly to rotate at the end of the lead screw where the mounting board is free of the aluminum rails. This allows for a single motor to be used to facilitate both linear motion out of the payload tube as well as rotational motion to orient the camera subassembly parallel with the z-axis. The camera subassembly interfaces with the lead screw subassembly by means of a cylindrical 3D printed sleeve. This sleeve is attached to the mounting board face and surrounds the lead screw.

The camera subassembly consists of a stepper motor, telescoping arm, arm actuation mechanism and camera and integrates with the lead screw subassembly. A stepper motor rotates the camera as needed based on RF communication.

The telescoping arm interfaces with the motor. Multiple methods for actuating the telescoping arm were considered including the use of a lead screw, linear actuator, and spring. The actuation method trade study can be found in Table 94. Based on the results, the telescoping arm will be actuated by a spring which will be triggered by the stepper motor after the camera

subassembly is completely beyond the payload tube. The spring mechanism will release a telescoping arm which will extend upward, moving the camera to a better vantage point. The camera will be attached to the telescoping arm and will take pictures as required based on the RF communication. This actuation method was chosen due to its low weight, simplicity, and reliability.

Table 94: Camera Arm Actuation Mechanism Trade Study

		Spring		Lead Screw		Linear Actuator	
Criteria	**Weight**	**Value**	**WNV**	**Value**	**WNV**	**Value**	**WNV**
Simplicity of Design	25%	5	0.104	3	0.063	4	0.083
Ease of Access	15%	4	0.055	2	0.027	5	0.068
Machinability	15%	4	0.050	3	0.038	5	0.063
Cost	5%	3	0.021	3	0.021	1	0.007
Weight	10%	4	0.044	4	0.044	1	0.011
Reliability	30%	4	0.109	3	0.082	4	0.109
Total WNV		**0.384**		**0.275**		**0.341**	

6.3.1.2 Mechanical Deployment The payload system deploys with multiple steps. The launch vehicle lands with the nose cone and recovery hardware fully removed from the payload tube. Upon landing, the stepper motor actuates the lead screw, moving the mounting board face, sleeve and camera subassembly forward linearly. The guide rails that interface with the mounting board face arrest any rotational motion while the components are in contact. When the motor has moved the camera subassembly past the end of the payload tube, the mounting board face moves beyond the end of the guide rails, allowing the camera subassembly to rotate with the lead screw to a vertical orientation as needed based on data from the electronics. A cap at the end ensures that the subassmebly remains in contact with the lead screw. Once the camera subassembly is oriented correctly with respect to the horizon, the camera subassembly stepper motor actuates the spring mechanism which deploys the telescoping arm. The telescoping arm extends upward, beyond the edge of the airframe. The camera subassembly motor then rotates the telescoping arm with the camera attached as needed based on RF communication.

6.3.2 Electrical

The electrical design of the payload system is of utmost importance to mission success. In order to carry out the mission set prescribed for the payload, it is necessary that the payload is capable of receiving commands using RF, deploying and orienting a camera system, and computationally altering the camera settings subject to these commands. Different sensors such as accelerometers and RF receivers will take in external inputs. This information will then be processed by the central microcontroller. The system will execute the respective physical and computational tasks according to these inputs and instructions using motors powered by a battery and software. The team will use a printed circuit board (PCB) in order to improve electrical efficiency and stability of the system, as well as reduce potential electromagnetic noise and interference. Figure 81 shows a preliminary wiring diagram.

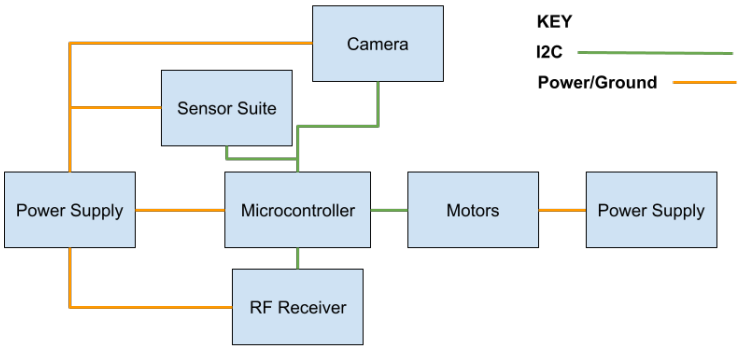

Figure 81: Preliminary Wiring Diagram

6.3.2.1 Sensors The TROI's electrical system will incorporate an accelerometer, which will be used for measuring acceleration in three directions in order to determine the state of motion of the launch vehicle. The accelerometer is crucial for detecting landing. Three options were examined: the Adafruit ADXL377, the DFRobot Gravity 12C H3LIS200DL, and the Adafruit ADXL375-EP. The following trade study, summarized in Table 95, was used to make a final selection. Evaluation criteria included cost, sampling rate, maximum acceleration, accuracy, and product availability. Accuracy and availability received the two highest weights, respectively, because they are most important to the accelerometer's purpose within the vehicle. Availability was relatively the same across all options so it received a lower weight. Maximum acceleration and cost were of lesser concern, and received the lowest weights.

Table 95: Accelerometer Trade Study

		Adafruit ADXL377		DFRobot Gravity 12C		Adafruit ADXL375-EP	
Criteria	**Weight**	**Value**	**WNV**	**Value**	**WNV**	**Value**	**WNV**
Accuracy	35%	3	0.105	4	0.140	3	0.105
Availability	20%	3	0.067	3	0.067	3	0.067
Sampling Rate	25%	3	0.068	3	0.068	3	0.068
Maximum Acceleration	10%	4	0.033	4	0.033	4	0.033
Cost	10%	2	0.022	5	0.056	2	0.022
Total WNV		**0.295**		**0.364**		**0.341**	

From this trade study, the DFRobot Gravity 12C H3LIS200DL, pictured in Figure 82, was selected. It provides a higher accuracy at a lower cost than the other two options, with comparable availability and maximum acceleration. Although the Adafruit ADXL375-EP offers the best sampling rate, this does not compensate for the higher cost and lower accuracy, leaving the DFRobot Gravity 12C H3LIS200DL as the preferred option.

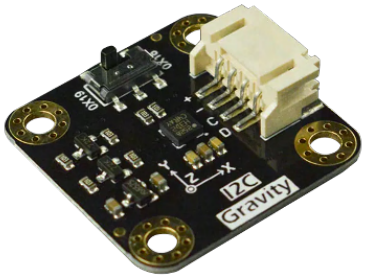

Figure 82: The DFRobot Gravity 12C H3LIS200DL

6.3.2.2 Camera The team conducted a trade study to compare and contrast three different camera options compatible with the selected ESP32 microcontroller. The options were selected from Arducam because they are highly recommended for use with MCUs. In order to get the best results, the camera selected for the payload system was chosen based on its cost, field of vision, physical size, reliability, simplicity, and image quality. Reliability was the foremost factor due to the fact that the camera must work consistently and without intervention, especially since the success of the payload mission is contingent on the camera's operation. Simplicity was also weighted heavily in order to reduce manpower expenditures in integrating the camera into the broader system.

Table 96: Camera Trade Study

		Arducam Mini 2MP Plus (OV2640)		Arducam Mini 5MP Plus (OV5642)		3MP Video Camera Module (OV3660)	
Criteria	**Weight**	**Value**	**WNV**	**Value**	**WNV**	**Value**	**WNV**
Cost	5%	5	0.018	4	0.014	5	0.018
Field of Vision	15%	3	0.056	3	0.056	2	0.038
Physical Dimensions	10%	5	0.033	5	0.033	5	0.033
Reliability	35%	4	0.117	4	0.117	4	0.117
Simple Integration	25%	4	0.083	4	0.083	4	0.083
Image Quality	10%	3	0.023	5	0.038	5	0.038
Total WNV		**0.331**		**0.342**		**0.327**	

The trade study determined that the best option is the Arducam OV5642 Camera. Although there were no many differences between the cameras, the 5MP option was chosen for its higher quality and ability to switch lenses to adjust FOV and focal length. The selected camera was a combination of the simplest to implement and the most customizable, making it overall the best choice. It is shown in Figure 83.

Figure 83: The Arducam OV5642 Camera

6.3.2.3 Microcontroller The microcontroller is primarily responsible for controlling the stepper motors to orient the camera in accordance with the commands sent through RF. The microcontroller must be compact enough to fit in the payload container, use minimal power to provide longer battery life, reasonably easy to use, adaptable or suited for our use, and be available for a reasonable cost. Raspberry Pi's are very difficult to acquire due to the chip

shortage and have a hefty markup making it easy to rule them out. Arduino's are less expensive and more available, but Arduino's also have extra features that are not needed for the operation of the TROI. A trade study determined the best microcontroller option and is shown in Figure 97.

Table 97: Microcontroller Trade Study

		ESP32 Custom PCB		Raspberry Pi (Zero W)		Arduino (MKR Zero)	
Criteria	**Weight**	**Value**	**WNV**	**Value**	**WNV**	**Value**	**WNV**
Adaptability	30%	5	0.136	3	0.082	3	0.082
Availability	20%	5	0.091	1	0.018	5	0.091
Voltage Input	10%	5	0.033	5	0.033	5	0.033
Cost	10%	5	0.056	1	0.011	4	0.033
Size	10%	5	0.038	4	0.031	4	0.031
Ease of Use	20%	4	0.073	2	0.036	5	0.091
Total WNV		**0.427**		**0.212**		**0.361**	

The option to best meet these requirements is an ESP32 with a custom PCB. By custom making the PCB, the team can reduce the cost of components. This also provides the smallest footprint possible for the microcontroller.

6.3.2.4 Battery The team will have one battery to supply power to the microcontroller, sensors, RF receiver, stepper motors, and camera. The battery will connect to a LDO (low-dropout) regulator in order to reduce the battery voltage to the required 3.3V. The LiPo chemistry was chosen for its ability to charge while the circuit is running. The battery must have ample capacity in order to power the circuit for the entire post-landing sequence. Lastly, the battery must meet requirements pertaining to physical attributes such as size and weight to fit the constraints of the payload. A trade study determined the best battery option and is shown in Table 98.

Table 98: Battery Trade Study

		MIKROE-4475		LP906090JH+PCM+2 WIRES 70MM		LP705176JS+PMC+2 WIRES 70MM	
Criteria	**Weight**	**Value**	**WNV**	**Value**	**WNV**	**Value**	**WNV**
Capacity	25%	5	0.096	5	0.096	3	0.058
Cost	20%	4	0.073	3	0.055	4	0.073
Size	10%	5	0.033	5	0.033	5	0.033
Reliability	20%	5	0.067	5	0.067	5	0.067
Simple Integration	15%	5	0.058	4	0.046	4	0.046
Availability	10%	3	0.027	5	0.045	3	0.027
Total WNV		**0.354**		**0.342**		**0.304**	

The battery that best meets our requirements is the MIKROE-4475 by MikroElektronika. This battery has a capacity of 6Ah supplying a voltage of 3.7V and current of 3A. This large capacity ensures sufficient lifespan and the low voltage reduces power consumed by the LDO.

6.3.2.5 Stepper Motor The camera will be actuated by a stepper motor. Multiple stepper motors were considered as seen in Table 99.

Table 99: Camera Stepper Motor Trade Study

		NEMA 8		NEMA 17		NEMA 17 Bipolar, Short Body	
Criteria	**Weight**	**Value**	**WNV**	**Value**	**WNV**	**Value**	**WNV**
Weight (lbs)	25%	0.073	0.16	0.628	0.00	0.309	0.09
Cost	15%	115.140	0.13	10.99	0.01	11.990	0.01
Reliability	15%	5	0.06	4	0.05	4	0.05
Ease of Integration	10%	5	0.04	3	0.02	5	0.04
Torque (lb· in)	15%	0.175	0.01	3.188	0.10	1.413	0.04
Volume of Motor (in^3)	20%	1.54	0.12	4.147	0.00	2.237	0.08
Total WNV		**0.39**		**0.18**		**0.23**	

After conducting a trade study, it was determined that a NEMA 8 (2.4" x 0.8" x 0.8") from McMaster-Carr would be the most successful stepper motor capable of rotating a camera 360°.

This was based off of the criteria of weight, cost, reliability, ease if integration, holding torque, and volume of the motor. Compared to the other stepper motor considerations, this stepper motor minimized weight and volume and had a high reliability and ease of integration, all top considerations for completing the payload mission. While the NEMA 8 does have the lowest holding torque, the torque was considered suitable for the job, causing the team to choose this motor for camera actuation.

6.3.2.6 RF Receiver The RF Receiving Module will receive transmissions from NASA. The transmissions will be sent via APRS (Automated Packet Reporting System) format and contain the sequence of commands for the camera, swivel, and filters. These APRS signals will be transmitted every 2 minutes, and the receiver will only start detecting these signals once the payload has landed. The signals will be sent via frequencies in the VHF (Very High Frequency) radio spectrum between 144.90 MHz and 145.10 MHz. The frequencies are within the 2-meter amateur radio band of the United States Frequency Allocations, allowing the opportunity to test the RF Receiving Module prior to launch. Communication engineers on the team have obtained Technician Level Amateur Ham radio licenses to simulate NASA's transmissions and test the RF receiver system. A licensed Ham Radio operator will transmit the APRS signal using the same format as NASA. The radio operator will use a Baofeng UV-5R Two Way Radio Dual Band 144-148/420-450Mhz Walkie Talkie to transmit the signal within the desired frequency range. The RF Receiving Module will receive this test signal and will aid in troubleshooting errors within the system.

A variety of receiving modules were considered as potential candidates. First, the Baofeng UV-5R Two Way Radio Dual Band 144-148/420-450Mhz Walkie Talkie can receive the signal without much modification. The radio can provide the correct frequency to the microcontroller via a custom programming cable. The programming cable can be made by modifying a stereo cable with 2.5mm to 3.5mm plugs. The cable is stripped to expose the Rx, Tx, and ground wire sections. The wires are then soldered onto the corresponding input ports of the microcontroller. The final option consists of the VHF Band HAM Amateur Radio Module DRA818V, a commonly used wireless voice transceiver. In fact, the transceiver is the same one used inside the Baofeng module. The transceiver is implemented into the system via the following circuit shown in Figure 84 to the microcontroller.

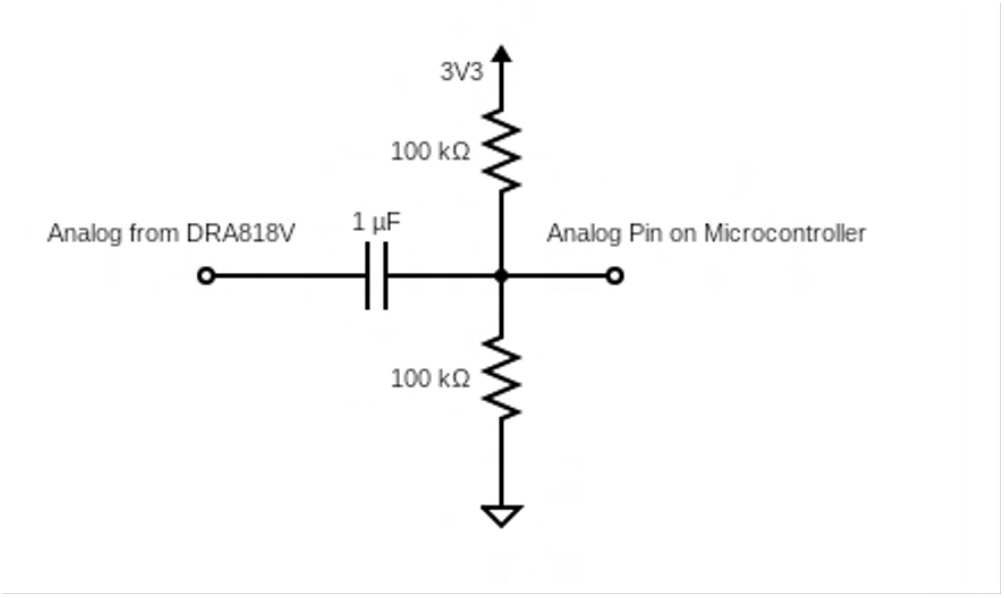

Figure 84: VHF Band HAM Amateur Radio Module DRA818V Circuit

The microcontroller communicates with the DRA818V using a modified version of libAPRS designed to work with the ESP32 microcontroller.

The following trade study was used to determine the receiver module for the payload.

Table 100: Receiver Module Trade Study

		DRA818V		Light APRS		Baofeng	
Criteria	**Weight**	**Value**	**WNV**	**Value**	**WNV**	**Value**	**WNV**
Operating Frequency	30%	5	0.1	5	0.1	5	0.1
Circuit Complexity	20%	4	0.073	3	0.055	4	0.073
Software Complexity	20%	3.5	0.074	2	0.042	4	0.084
Physical Dimensions	20%	4	0.089	3	0.067	2	0.044
Cost	5%	5	0.023	2	0.009	4	0.018
Simplicity of Integration	5%	5	0.018	3	0.014	4	0.018
Total WNV		**0.376**		**0.286**		**0.338**	

Based on this research, the DRA818V was determined to be the best option, with Baofeng as a

secondary. The decision is validated as the DRA818V serves as the internal transceiver of the Baofeng.

6.3.3 Software

6.3.3.1 Overall Control Flow Control flow is paramount to the effective operation of the payload in terms of data acquisition and processing. The microcontroller, once the launch vehicle has been launched and then lands, actuates to deploy the camera apparatus. The microcontroller takes in information from the different sensors (such as the electronic compass) in order to orient the camera in the desired direction. Once the camera is oriented properly, the RF receiver activates, awaiting commands. Upon receiving commands, the microcontroller reacts accordingly, actuating the camera orientation motors and calling functions in software to produce the desired effects. The TROI overall control flow is provided in Figure 85

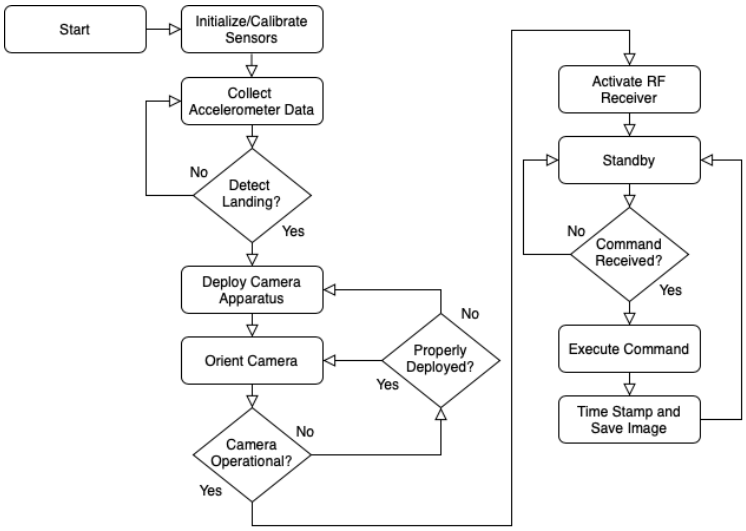

Figure 85: TROI Overall Control Flow

6.3.3.2 Software Testing In order to test and demonstrate the TROI's functions, rigorous software testing must be performed. Tests are planned for each component of the system to ensure that they operate individually and in the context of the software system. All sections of the code will be tested. In addition, each sensor will be tested both independently and within the system in controlled environments to validate every sensor's expected outputs and tolerances. Legacy data from previous years will be used to calibrate and validate certain data, such as position data. Upcoming test launches, both full-scale and subscale, will provide valuable data in informing next steps, and any and all problems that arise will be isolated and rectified in anticipation of successive launches.

6.4 Launch Vehicle Interfaces

The TROI interfaces with both the launch vehicle and the recovery system. The primary interface with the launch vehicle is the retention system. Securely retaining the payload within the launch vehicle during flight is important as it ensures that the payload will not withstand forces that could negatively impact the electronic and mechanical elements of the system. With the payload design including moving elements and a camera that has the potential to break with vibrations and forces from flight, the retention system is especially critical.

The sensor suite is contained between two bulkheads. The bulkheads are bolted into the airframe with airframe interface block to retain the system in place. This retention system was chosen based on the results of the trade study in Table 101. A twist-lock retention mechanism and a retention mechanism constraining the motion by using airframe interface blocks as stops above and below the bulkheads were traded against the bolting scheme. Bolting the bulkheads was ultimately chosen due to its simplicity and ease in machinability.

Table 101: Launch Vehicle Interface Trade Study

		Bolted into Airframe with Airframe Interface Blocks		Twist-Lock		Retained between Block Stops	
Criteria	**Weight**	**Value**	**WNV**	**Value**	**WNV**	**Value**	**WNV**
Simplicity of Design	25%	4	0.111	2	0.056	3	0.083
Ease of Access	15%	3	0.041	5	0.068	3	0.041
Machinability	15%	5	0.058	4	0.046	4	0.046
Cost	5%	4	0.015	5	0.019	4	0.015
Weight	10%	4	0.036	4	0.036	3	0.027
Reliability	30%	5	0.125	3	0.075	4	0.100
Total WNV		**0.386**		**0.300**		**0.313**	

The mounting board face and sleeve of the lead screw subassembly are retained with a tightly interfacing foam support around the elements to mitigate the impact of vibrations and movement on the flight camera during flight. Motorized and mechanically static retention systems were traded against the foam supports in Table 102. The permanent foam support was ultimately chosen due to its simplicity, ease of placement, and low cost. The lead screw system moves the mounting board face and sleeve forward, out of the foam retention system upon landing.

Table 102: Camera Subassembly Retention Trade Study

		Motorized Support		Mechanically Removed Support System		Permanent Foam Supports	
Criteria	**Weight**	**Value**	**WNV**	**Value**	**WNV**	**Value**	**WNV**
Simplicity of Design	25%	3	0.075	2	0.050	5	0.125
Ease of Placement	15%	2	0.030	3	0.045	5	0.075
Machinability	15%	3	0.045	3	0.045	4	0.060
Cost	5%	2	0.009	4	0.018	5	0.023
Weight	10%	2	0.020	4	0.040	4	0.040
Reliability	30%	5	0.136	3	0.082	3	0.082
Total WNV		**0.315**		**0.280**		**0.405**	

The payload interfaces with the recovery system as well to facilitate payload deployment. The recovery system in the payload bay ejects the nose cone during flight. Sensitive payload electronics including the camera will need to be shielded from the gas and debris from the black powder charges of the recovery system and the payload will need to extend beyond the initial placement of the recovery system to exit the payload tube. To mitigate the gas and debris experienced by the camera, a fiberglass bulkhead will be placed between the recovery system and the payload with standoffs keeping the bulkhead from pushing further into the payload tube. The bulkhead will interface with the payload tube and a fire retardant blanket will be placed between the bulkhead and the recovery system to further mitigate the movement of the debris beyond the bulkhead. Upon the ejection of the nose cone, the recovery system and the movable bulkhead will be pulled from of payload tube, allowing for the payload to move out of the payload tube upon landing.

Other designs were considered including adding trap doors to the recovery system bulkheads so that the recovery system stayed in place while the payload system pushed through the trap doors and out of the payload bay. This design was ultimately discarded due to its difficulty in manufacturing and assembly and a system that pulls the two recovery bulkheads free from the vehicle was ultimately chosen.

Figure 86 gives an overview of payload integration with the launch vehicle and recovery system.

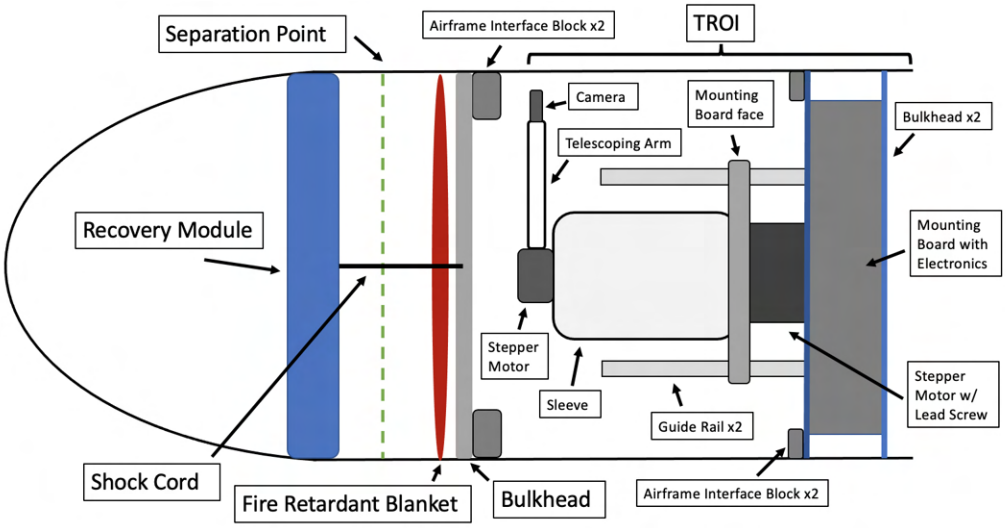

Figure 86: Launch Vehicle and Recovery System Integration with the TROI

Overall, the payload is retained in the payload tube by bolting the bulkheads of the electrical retention mechanism into the airframe. The camera is shielded from vibrations by a snugly interfacing foam retention system around the mounting board face and sleeve components during flight. The payload is shielded from the recovery system gas and debris by a movable bulkhead and fire retardant blanket which are pulled free of the vehicle with the recovery system upon the ejection of the nose cone during flight.

6.5 Preliminary Mass Statement

The precursory mass for the TROI payload system was determined after conducting thorough research into alternative methods for each subsystem of the payload. The MGA (mass growth allowance) was determined based on the type of components and the maturity of each design. It was determined that TROI should not exceed the total gross weight of 90 oz. (NDRT Req. TROI.11). Table 103 highlights the fundamental categories considered for each component: maturity, type, BME (basic mass estimate), MGA (mass growth allowance) percentage, the total basic mass, and the total predicted mass. These categories were used in determining the best key mass components in the TROI system.

Table 103: TROI Mass Breakdown

Component	Maturity	Type	Basic Mass (oz.)	MGA (%)	Predicted Mass (oz.)
Stepper Motor for Camera Z-Axis (NEMA 8)	3	MECH	1	10	1.1

Table 103: TROI Mass Breakdown

Component	Maturity	Type	Basic Mass (oz.)	MGA (%)	Predicted Mass (oz.)
Stepper Motor with Lead Screw	3	MECH	11.4	10	12.496
Aluminum Retention Blocks (8)	3	PRIM	4.3	6	4.56
Battery (MIKROE-4475) - 3.7V 6Ah	3	BAT	3.2	11	3.55
Printed Circuit Board (PCB)	3	ELEC	1.5	14	1.76
ESP32 Custom Integrated PCB Microcontroller	3	SENS	0.35	14	0.40
RF Receiver (DRA818V)	3	SENS	0.11	14	0.125
Wires	3	WIRE	2.9	17	3.39
Camera (Arducam Mini 5MP Plus (OV5642)	5	SENS	0.706	2	0.720
Retention Screws	5	PRIM	4	2	4.08
Fiberglass Retention Bulkheads	3	PRIM	9.76	6	10.3
Spring	3	MECH	0.01	10	0.011
Camera Retention Material (Aluminum 6061)	3	SEC	3.34	8	3.61
Guide Rails	3	SEC	1.06	8	1.14
Accelerometer (DFRobot Gravity 12C)	3	SENS	0.423	14	0.482
Aluminum Standoffs (4)	3	SEC	5	3	5.15
Power Board	3	ELEC	1.3	17	1.52
Antenna	3	SENS	0.37	14	0.422

Table 103: TROI Mass Breakdown

Component	Maturity	Type	Basic Mass (oz.)	MGA (%)	Predicted Mass (oz.)
Telescoping Arm Material	3	SEC	0.61	8	0.659
Foam Cushioning	3	SEC	1.1	8	1.12
Sleeve Material	3	SEC	11.7	8	12.6
Mounting Board Face	3	PRIM	1.18	6	1.25
Lead Screw Cap	3	SEC	0.34	8	0.367
Electronic Mounting Board	3	PRIM	0.714	6	0.757
Guide Rail Holders	3	MECH	2	10	2.2
Screws/nuts	3	MECH	2	10	2.2
Total	-	-	**70.3**	-	**76.1**

6.6 Payload Preliminary Testing Plan

NDRT has developed an initial testing plan for the TROI in order to properly verify its design, integration, and construction. NDRT's systems squad will utilize the initial tests listed in Table 104 to create a full, more detailed test plan for CDR.

Table 104: Payload Preliminary Testing Plan

Test Name	Description	Success Criteria
Electronics Unit Tests	Each sensor will be connected to a computer to print real time data from the sensor and evaluate the ability of each sensor to read physical input data	Each sensor accurately records physical input data within sensor specifications
Nose Cone Ejection Test	The nose cone will be ejected from the launch vehicle and the payload system will be represented by adhesive material in its location	No ejection particulate settles at the location of the payload section

Table 104: Payload Preliminary Testing Plan (continued)

Test Name	Description	Success Criteria
Camera Mobility Test	The mobility of the camera will be inspected with regards to swivel, z-axis rotation, and field of view range	Camera is able to perform a 360º swivel, have full z-axis rotation, and have a field of view of at least 100° and at most 180°
Camera Image Capturing Capability Test	The camera will be secured and the following performance metrics will be evaluated: quality of images produced, ability to store images, and accuracy of image time stamps	Images have satisfactory quality, are stored correctly, and have accurate time stamps
Camera RF Response Capability Test	The camera will be given varying radio commands; image quality and camera movement will be evaluated with each command	Camera appropriately responds to each command, image quality is still sufficient, and camera moves as intended with random radio commands
System Actuation Test	The launch vehicle's state will be changed to test the internal sensor's ability to recognize the vehicle state and communicate with deployment mechanisms	Sensor accurately reads the vehicle state and communicates with the deployment mechanisms
Static Load Test	Static loads representing 1.5 times the maximum load expected will be applied to each load-bearing component	Relevant components do not exhibit damage or failure
Deployment Conditions Test	The payload will be deployed at different angles on the ground relative to the z-axis	The payload is able to deploy at all ground angles in the range given by NDRT Req. TROI.5 and the camera's z-axis will not be impacted by the ground angle

Table 104: Payload Preliminary Testing Plan (continued)

Test Name	Description	Success Criteria
Battery Duration Test	The system will be activated in a cold environment in conjunction with other systems and a fully charged battery to simulate worst-case flight conditions and delays	System functions as intended for at least three hours, meeting the duration listed in NDRT Req. IN.2
Main Parachute Deployment Event Test	Deployment of the main parachute will be simulated to inspect the resulting condition of the payload module	Payload withstands the impulse caused by parachute deployment; the systems inside are undamaged and correctly perform to their requirements
Subscale Test Flight	The radio and camera modules will be integrated into the subscale launch vehicle to test the radio sequence interpretation capabilities of the module	Radio and camera modules accurately respond to all radio sequences transmitted on the test flight
Payload Demonstration Flight	The full system will be integrated into the launch vehicle for the Payload Demonstration Flight to analyze performance capabilities of the full payload system	System precisely demonstrates the correct operation of the payload deployment, radio receiving, and camera operation
Electronics Shielding Test	Electronics from each system will be shielded and receive simulated flight data separately, then receive the same data while shielded and placed in the same configuration as within the launch vehicle	Data from all electronics are similar when placed separately and together

6.7 Subscale

A prototype payload design will be included in the subscale mission. The objective of the prototype is to retain, hold, and test the operation of the electronics, RF communications equipment, and sensors needed for the full scale payload mission. The requirements of the

prototype are that it will have to fit in a 3 in. inner diameter payload tube and have a minimum length of 6 in. (NDRT Req. TROI.6). The prototype must be attached to the payload tube via airframe interface blocks, and the material for the structure must be transparent for radio signals.

7 Technical Design: Apogee Control System

7.1 System Overview

The Apogee Control System (ACS) is a subsystem on the launch vehicle that will autonomously adjust its apogee to within a narrow margin of the target apogee: 4,600ft, to meet the altitude requirement. The ACS mechanically actuates variable drag surfaces that continuously adjust the total drag force acting on the launch vehicle, and thus its net acceleration, between burnout and apogee. An electronics suite consisting of a microprocessor, several sensors, and a servo motor precisely controls how far the drag surfaces extend at any instant. Raw sensor data is first filtered and used to determine the state of the launch vehicle. If the launch vehicle is detected to be between burnout and apogee, a control algorithm commands the servo motor and attached drag surfaces to actuate to a calculated angle depending on the difference between the predicted apogee and target apogee. Once apogee has been reached, the drag surfaces retract and remain retracted for the rest of the flight.

7.1.1 Mission Success Criteria

The ACS must satisfy the requirements listed below for its mission to be considered successful:

- The system shall not actuate until after the launch vehicle reaches the burnout stage
- The system shall not adversely affect the stability of the launch vehicle
- The system will be located aft of the launch vehicle's burnout CG (NASA Req. 2.16)
- The system shall get the launch vehicle's apogee to within 25 ft. or less of the target
- The system shall be capable of fully actuating within 5 seconds, starting at burnout velocity
- The system shall filter raw data from sensors before evaluating launch vehicle trajectory
- The system shall retract and deactivate itself once apogee is detected
- The system shall perform a successful power-on self-test before it is armed

- The system shall be able to be integrated into the launch vehicle within 30 minutes and should remain fully armed for at least two hours before launch
- The system shall be mechanically prevented from actuating its variable drag surfaces asymmetrically

7.2 Aerodynamic Considerations

The aerodynamic effects of the ACS deployment on other systems and the launch vehicle's trajectory are considered here. Since the ACS actively manipulates the flow field around the launch vehicle, the ACS will not deploy above the launch vehicle's center of pressure so as to not impact the vehicle's stability. The drag surfaces will deploy aft of the burnout center of gravity, per NASA Req. 2.16. CFD analysis and wind tunnel testing will be conducted to understand how the ACS deployment impacts the flow field surrounding the launch vehicle. The ACS will only be deployed after burnout so as to not impact the launch vehicle's stability during ascent. After burnout, should the launch vehicle be predicted to overshoot the target apogee, the ACS will actuate the drag surfaces. The drag force, F_{drag}, is given by:

$$F_{drag} = \frac{1}{2}\rho C_d A v^2 \tag{17}$$

where is the density of air, C_d is the drag coefficient, A is the effective area, and v is the airspeed at the drag surface. The density of air is assumed to be constant and the effective area will be actively controlled by the ACS as the mechanism actuates. Since the velocity of the launch vehicle will be maximum at burnout, the drag force will also be maximum at burnout, which is when the ACS deploys. Therefore, when selecting the ACS servo motor, the team had to take into account the drag force acting at burnout to ensure that the servo motor torque was sufficient for successful flap actuation. The drag coefficient will be independently calculated for the launch vehicle and drag surface using CFD.

7.3 Mechanical Design

The Controlled Linearly-Actuating Mechanism (CLAM) will be used to radially extend and retract drag surfaces that will protrude from the ACS body tube between the burnout and apogee stages of flight. The mechanism will be designed to allow precise control of drag surface positioning as frequently as possible. This will minimize the error between the actual apogee and target apogee of 4600ft. Since the CLAM works by increasing the total area of the launch vehicle exposed to airflow, maximizing the size of the drag surfaces will yield the best performance. The physical dimensions of the ACS body tube and mass distribution

requirements constrain the maximum diameter of the CLAM to 6 inches and its maximum length to 12 inches. Additionally, the CLAM must be placed behind the burnout CG to avoid reducing launch vehicle stability and to comply with NASA requirements regarding the location of structural protuberances (NASA Req. 2.16). All components used in the CLAM will be chosen and tested to ensure that they can withstand the largest expected stresses during launch, burnout, and parachute deployment with a safety factor of 1.5.

7.3.1 Considered Mechanisms

During the ideation stage of the ACS design cycle, several possible mechanisms were considered that met both NASA and team-derived requirements. After comparing the mechanisms based on criteria such as drag efficiency, complexity, accuracy, and speed, the team shortlisted the three mechanisms below as strong candidates for this year's design.

7.3.1.1 Radially-Actuated Tab Design

The radially-actuated tab mechanism has proven reliable for the ACS in previous years. This design consists of a central shaft rotated by a standard servo. The servo's rotational motion is converted into translational motion on an axis perpendicular to the shaft axis through a set of four linkages. These linkages are attached to four tabs which can be extended or retracted by a specific amount based on the direction of servo rotation and the servo angle. A CAD design of the mechanism is shown in Figure 87.

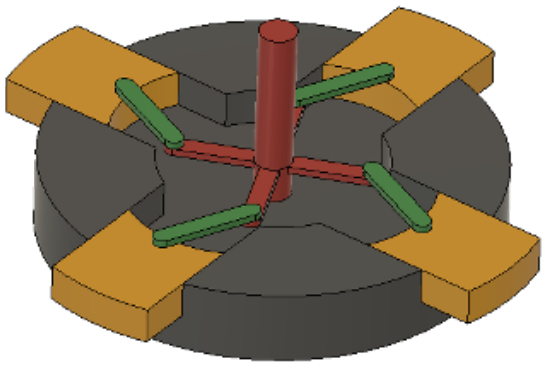

Figure 87: ACS Radially-Actuated Tab Mechanism

The mechanism's drag tabs protrude out of the launch vehicle's body tube and are angled perpendicular to oncoming airflow. They can increase or decrease the launch vehicle's cross-sectional area and thus modify the drag force acting on the launch vehicle.

A major advantage of this design is its actuation precision and speed. Using a standard servo, in contrast to a DC motor or continuous servo, allows the precise servo angle (and hence tab extension) to be controlled within the ACS control algorithm. Additionally, of all the mechanisms considered, the radially-actuated tab mechanism is the simplest to design and construct, and it minimizes the amount of material that needs to be cut out of the ACS body tube.

The most significant drawback of this design is its limited drag surface area. The size of the tabs and the extent to which they can extend out of the ACS body tube are limited by the diameter of the ACS body tube. This limits the maximum additional drag that the mechanism can induce and thus reduces the acceptable margin of apogee error that can be corrected by the ACS.

7.3.1.2 Leadscrew-Actuated Flap Design

The second ACS mechanism that was considered uses a leadscrew to actuate hinged flaps that induce drag by extending at an angle from the body of the launch vehicle. This mechanism was used in last year's Apogee Control System. The CAD design for the leadscrew-actuated flap design is shown in Figure 88.

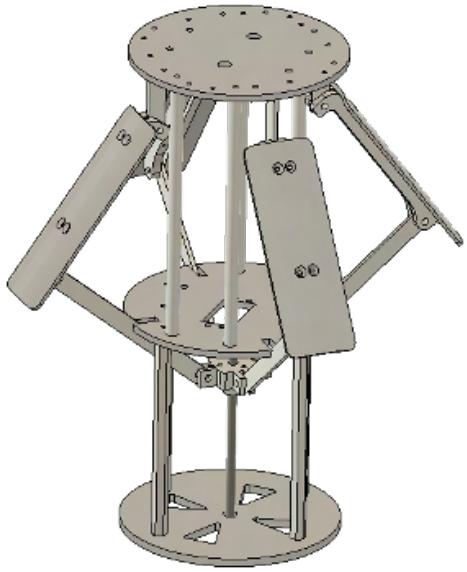

Figure 88: ACS Leadscrew-Actuated Flap Mechanism

The four drag flaps are actuated by a leadscrew that moves linearly along a central shaft. This moves the central hub vertically, which is hinged to pusher arms that actuate the drag flaps at

an angle. The drag flap hinges are fastened to the fore bulkhead, the motor is housed in the middle bulkhead, and the lead screw runs between the middle and aft bulkheads.

This design is advantageous due to its large effective surface area. The hinged flaps linked to pusher arms allow for the ACS to significantly increase the drag of the launch vehicle with a strong and robust mechanism. The pusher arms are designed such that they cannot be pushed back in once extended unless the leadscrew is rotated. Although this increases the stress on the leadscrew itself, it reduces the motor torque required to keep the flaps extended even at high velocities.

However, the use of a leadscrew coupled to the rotation of a continuous servo motor causes the leadscrew-actuated flaps to deploy slowly, which reduces the ACS effectiveness as there is a very short timespan between burnout and apogee in which the ACS must actuate to sufficiently reduce the launch vehicle's apogee. The continuous servo also introduces significant lag between the required flap angle being commanded by the control algorithm and the mechanism actually achieving that angle. Moreover, a continuous servo makes it difficult to precisely control flap actuation angle as it only allows control over rotation speed and direction, and not over the exact servo angle. Estimating the flap position by integrating servo velocity with respect to time proved to be a fairly unreliable technique when carried out on last year's system.

7.3.1.3 Linearly-Actuated Flap Design

The third mechanism considered was the Linearly-Actuated Flap Design. This design was inspired by both the radially-actuated tab mechanism and the leadscrew-actuated flap mechanism. It takes a hybrid approach by combining the two mechanisms, thus maximizing drag surface area and controllability. A CAD rendering of the Linearly-Actuated Flap Design is shown in Figure 89.

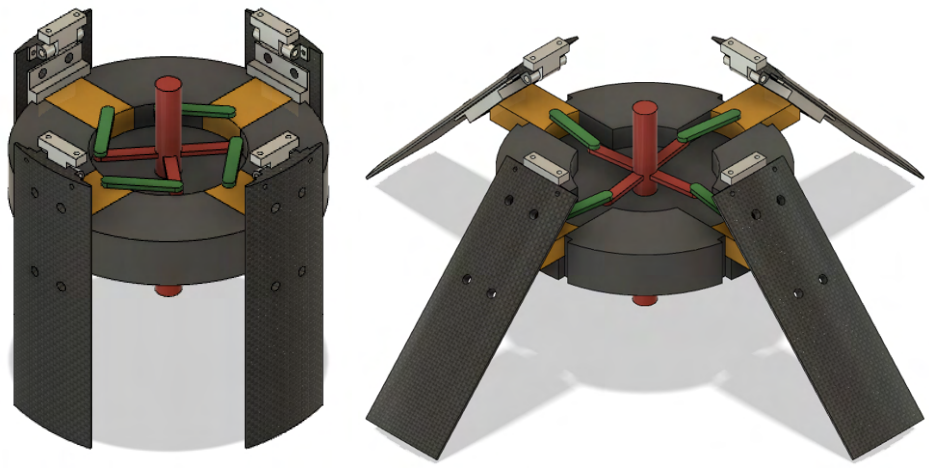

(a) Retracted Flaps (b) Extended Flaps

Figure 89: ACS Linearly-Actuated Flap Mechanism

This mechanism consists of a standard servo motor which rotates a central shaft. The rotation of the servo motor is linked to the extension of small tabs via a set of four linkages, similar to the radially-actuated tab mechanism. The radially-extending tabs then push outwards on flaps hinged on one end to the top bulkhead. This exerts a net torque on the flap about its pivot, which results in angular flap actuation. The tab size can be small because the flaps are the primary drag surfaces in this design. Although not included in the CAD rendering, the team has considered using a sliding drive retainer pin between the upper edge of the tab that slides through a slot in the flap bracket. This non-critical component will help secure the tab to the flap and prevent the flaps from opening independently of the tabs, especially after apogee, when drag may not always push down on the flaps.

This design combines many of the benefits associated with both the radially-extending tab mechanism and the leadscrew-actuated flap mechanism. Since a standard servo is used, flap actuation will be fast and precise. The relationship between servo angle and flap angle will be linear, making the system much easier to characterize and control accurately. Additionally, the placement of the drag tabs close to the flap hinge (pivot) will allow relatively small angles of servo actuation to produce a large flap angle. Since the flaps themselves can be made as large as those in the leadscrew-actuated flap mechanism, the same drag surface area can be maintained, which is significantly larger than that of the radially-actuated tabs alone.

Apart from the slightly added complexity of this design in comparison to the radially-actuated tabs alone, there are two potential drawbacks associated with the linearly-actuated flaps. Firstly, it requires the mechanism itself to withstand significant amounts of aerodynamic stress since aerodynamic forces will be transmitted along the flaps to the tabs and other structural components of the mechanism. The flaps and the other load-bearing components

used must be well reinforced in this design. Secondly, because tab actuation extent is limited by the diameter of the ACS body tube, pushing on the flaps close to the pivot will require a relatively high torque motor to overcome the aerodynamic forces.

7.3.1.4 Mechanism Trade Study and Selection

The mechanism designs were evaluated using a trade study with these criteria: drag surface area, precision, actuation speed, structural integrity, and simplicity. Because the function of the ACS is to accurately control the apogee of the launch vehicle by inducing drag, the highest weighted criteria in the trade study were the drag-inducing surface area at 30% and precision at 25%. The drag surface area was determined using the CAD model of each mechanism. Precision was determined by comparing standard servo characteristics with those of a continuous servo. The radially-actuated tab mechanism and linearly-actuated flap design use a standard servo, while the leadscrew-actuated flap design uses a continuous servo. The standard servo allows direct control over servo and hence flap actuation angle. The continuous servo only allows speed control, so flap position must be estimated by integrating over time (less precise). The next heavily weighted factor was the mechanism actuation speed at 20%, which is important because the mechanism must deploy in a short time frame between burnout and apogee. The actuation speed was determined by the time required to actuate the mechanism to its maximum extent. Structural integrity was given a weight of 15% because each mechanism involves legacy architecture that the team is confident it can design and manufacture to be reliably safe. The structural integrity was evaluated based on the amount of stress that would be placed on load-bearing components due to the drag force. Finally, simplicity was rated at 10% due to the team's experience with manufacturing similar mechanisms, and the score was determined based on the number of components and required tolerance between each component. The scores of each of these criteria for every mechanism are given in Table 105, which shows the complete trade study.

Table 105: ACS Mechanism Trade Study

		Radially-Actuated Tabs		Leadscrew-Actuated Flaps		Linearly-Actuated Flaps	
Criteria	**Weight**	**Value**	**WNV**	**Value**	**WNV**	**Value**	**WNV**
Drag Surface Area	30%	2	0.05	5	0.13	5	0.13
Precision	25%	5	0.10	3	0.06	5	0.10
Actuation Speed	20%	5	0.09	1	0.02	5	0.09
Structural Integrity	15%	4	0.06	3	0.05	3	0.05
Simplicity	10%	4	0.04	2	0.02	3	0.03
Total WNV		**0.34**		**0.27**		**0.39**	

The results of the trade study show that the linearly-actuated flap mechanism is the best overall mechanism due to its large surface area in addition to its high precision and actuation speed. This design combines the strengths of legacy NDRT ACS designs, and the team is confident that this mechanism is the best available option for the ACS. The team will conduct extensive analysis and testing to ensure the functionality of this mechanism and a minimum factor of safety of 1.5 for every component.

7.3.2 Material Selection

The team will use fiberglass in the form of disks for the middle and bottom ACS bulkheads because its rigid structure offers multiple electronics and mechanism mounting arrangements. While carbon fiber provides a significantly better strength to density ratio, it is too elastic and could amplify unwanted vibrations.

The Central shaft will be machined out of aluminum and will connect to radially extending tabs, which push out a set of flaps. These tabs will be under high aerodynamic loads during flight, so the team considered using a more durable material for them. The team compared Tungsten to Inconel and decided to use Inconel for the tabs to avoid exceeding the ACS mass budget as Tungsten is more than twice as dense as Inconel.

The structural supports between bulkheads will be made of Inconel tubes because a hollow tube is stronger than a rod of the same weight made of the same material. They are key components to the structural integrity of the whole construction and are some of the main load-bearing elements. The top bulkhead will be made of carbon fiber because of its strength and to shield the ACS from electromagnetic interference.

The flaps themselves will be made of carbon fiber with an aluminum bracket to prevent bending. Elasticity in the flaps is undesirable since the ACS apogee prediction calculations and drag calculations assume that all four flaps are rigid bodies. The region on the aluminum bracket where the tabs make contact with the flaps will have an Inconel plate attached to prevent the hard high-nickel steel tabs from cutting into the soft aluminum flap brackets.

7.3.3 Servo Motor Selection

The team has determined that a standard servo motor would be appropriate for this year's ACS mechanism. A standard servo allows for precise control over the servo angle. Standard servos usually have a limited range of rotation (180° or 270°) in contrast to continuous servos, but since the mechanism only requires about 50° of rotation to extend the flaps to about 45°, the team will use a standard servo for flap actuation. Most standard servos are fast and precise, which is important since the ACS will only be active between burnout and apogee phases of flight (about 10 seconds).

The servo motor trade study evaluated three servo motors based on five criteria. Of these, the stall torque at 7.4V criterion was given the highest weight at 40% because the motor's maximum torque is critical to the success of the ACS design. To achieve a large flap actuation angle with a small tab extension, the motor must be located close to the flap hinge (pivot), and hence needs to output a large torque to counteract the drag forces attempting to retract the flaps that act across their entire length. The second highest weight (30%) was given to stall current at 7.4V because high torque motors tend to draw very large currents. The team would like to minimize current draw to maximize servo motor battery life and to minimize the risk of electromagnetic interference to the ACS electronics. Physical dimensions and cost were given lower weights because only servo motors that would fit within the size constraints of the bulkhead were compared and all three were similar in that regard. Cost also did not differ too much between the motors, so it was given the lowest weight. The results of the trade study are shown in Table 106.

Table 106: ACS Servo Motor Trade Study

		TD-8160MG		Power HD 1235MG		ZOSKAY DS5180	
Criteria	**Weight**	**Value**	**WNV**	**Value**	**WNV**	**Value**	**WNV**
Stall Torque at 7.4V (Nm)	40%	5.88	0.12	3.92	0.08	9.61	0.20
Stall Current at 7.4V (A)	30%	10.4	0.18	9	0.20	6.5	0.22
Mass (g)	15%	158	0.10	178	0.1	162	0.10
Volume (in^3)	10%	5.71	0.07	5.89	0.07	5.69	0.07
Cost ($)	5%	35.89	0.04	43.25	0.03	49.99	0.03
Total WNV		**0.475**		**0.443**		**0.583**	

Based on the trade study, the team selected the ZOSKAY DS5180 standard servo motor for the ACS mechanism. This servo motor had the largest torque and lowest current draw at 7.4V, making it an ideal choice. The servo motor selected can operate at voltages between 6V and 8.4V. The team will be running the servo motor on a separate 7.4V battery to maximize its torque output during flap actuation.

7.3.4 Mechanical Test Plan

The mechanical system will be tested independently as well as when integrated with the ACS electrical and software components. The mechanical system will be tested separately by using the motor to actuate the tabs both inside and outside a wind tunnel. The test will have been passed when the mechanism fully deploys and retracts through its entire range of motion. The motor torque and mechanism strength will be tested by mounting weights on the flaps to simulate the maximum expected load during flight. Additionally, the mechanism's response to flight dynamics and loads will be analyzed prior to flight using FEA and CFD. Table 107 describes the mechanical component test plan, whereas the integrated system tests are specified in section 7.7.

Table 107: ACS Mechanical Test Plan

Test Name	Description	Success Criteria
Flap Mechanism Actuation Test	Actuate drag flaps through full range of motion using manual motor commands	The mechanism responds to motor commands as expected through full range of motion
Mechanism Torque Output Test	Attach weights to each flap equivalent to the maximum expected load, test motor torque by actuating flaps to maximum extension	The mechanism fully deploys the flaps without incurring structural damage
Finite Element Analysis (FEA)	Maximum expected loads will be modeled and stresses will be simulated for each load-bearing component to determine its factor of safety	Every part has a factor of safety of at least 1.5 when tested under maximum load (at burnout velocity)
Computational Fluid Dynamics (CFD)	Simulate drag forces acting on the ACS flaps at different angles from burnout to apogee	The simulated drag forces do not exceed the maximum force that the servo motor can exert on the flaps and the mechanism can induce sufficient additional drag to achieve the target apogee

7.4 Electrical Design

The Apogee Control System must detect and respond dynamically to changes in its environment. Therefore, its electrical design is key to its successful operation. A microprocessor, which operates based on input from several sensors that are connected to it, controls the standard servo motor that drives the mechanism. The entire electrical system must be powered by batteries. The team chose each of these components by carrying out trade studies. In general, sensor selection focused on maximizing the sampling rate because a higher sampling rate would yield more accurate flap actuation angles with minimal lag. Battery selection involved choosing a 3.7V battery boosted to 5V to drive the logic circuit (sensors and microprocessor) and a 7.4V battery to drive the servo motor. Both batteries were

chosen to have a high capacity so that the system can remain active on the launchpad for at least 2 hours.

The electrical connections between all components will be made via a Printed Circuit Board (PCB) to protect the connections between components from damage during flight. It would also reduce the number of loose wires required, reducing the number of solder connections, which reduces the number of possible points of failure in the ACS electrical subsystem. The logic circuit and the servo motor circuit will have a common ground at the microprocessor to avoid undefined behavior when polling the sensors and/or sending a signal to the microcontroller. The two circuits will otherwise be isolated from each other to avoid large currents in the servo motor circuit affecting the sensitive sensors in the logic circuit.

7.4.1 Battery Selection

The team will be using two batteries to power the ACS electronics suite. One battery will power the logic circuit and the other will power the servo motor. This decision was made for two reasons. Firstly, powering the logic circuit and servo motor on separate batteries would prevent one of the batteries from possibly exceeding their current rating. This design would also allow the system to remain powered for longer. Secondly, the logic circuit runs at a nominal voltage of 5V, whereas the servo motor provides maximum torque at 7.4V.

A 3.7V LiPo battery was chosen for the logic circuit and a 7.4V LiPo battery was chosen to power the servo motor. The logic circuit includes the Adafruit PowerBoost 1000C DC/DC boost converter module to step up the 3.7V from the logic circuit battery to 5V, the microprocessor's operating voltage. The servo motor will run directly from the 7.4V LiPo battery. The team had considered using two 7.4V LiPo batteries with a 5V DC/DC step-down (buck) converter on the logic circuit. However, it was decided that stepping up the voltage from the 3.7V battery would be a better option. 3.7V LiPo batteries are generally much smaller and lighter than their 7.4V counterparts with the same battery capacity.

The logic circuit consists of the Raspberry Pi microprocessor, three sensors (IMU, altimeter, accelerometer), and an Adafruit PCA 9685 PWM Servo Driver. Each of these components have varying current draws as some run on 5V and some run on 3.3V supplied by the microprocessor. The microprocessor draws the largest current in the logic circuit, which varies from around 540mA at idle to 1.28A at full CPU utilization on all four processor cores. The sensor/PWM driver current draw is minimal and does not exceed 5 mA in total. Therefore, the team ensured that all shortlisted logic circuit batteries had a maximum discharge current rating of at least 2A. The chosen digital servo motor will be powered by the 7.4V battery and has a maximum stall current draw of about 6.5 A. Hence, the team ensured that all shortlisted

servo motor circuit batteries have a maximum discharge current rating of at least 10A.

Several factors were considered when shortlisting battery choices. Two major factors were operating voltage and maximum current. LiPo batteries are sold as combinations of cells electrically connected in series (1S, 2S, etc.), where each cell supplies 3.7V. Therefore, one battery had to be 1S (3.7V) and the other 2S (7.4V). The maximum current rating depends on the battery's application within the system. The logic circuit will draw less current than the servo motor during flap actuation. All batteries shortlisted meet the voltage and current requirements. Another important factor considered was battery capacity, which is listed on the battery manufacturer's datasheet in milliamp-hours (mAh). Since a higher capacity would allow the system to remain armed on the ground for longer periods, that criterion was given the most weight in the trade studies (45%). Lastly, physical dimensions and cost of the batteries were also taken into account as the batteries selected should not be too large, heavy, or expensive. The trade studies used to select logic circuit and servo motor batteries are included in Table 108 and Table 109 respectively.

Table 108: ACS 3.7V LiPo Battery Trade Study

		AKZYTUE		YDL		EEMB		PKCELL	
Criteria	**Weight**	**Value**	**WNV**	**Value**	**WNV**	**Value**	**WNV**	**Value**	**WNV**
Capacity (mAh)	45%	10000	0.21	5000	0.11	3700	0.08	2500	0.05
Mass (g)	30%	163	0.16	74	0.24	74	0.24	50	0.26
Volume (in^3)	20%	4.14	0.11	2.12	0.16	2.00	0.16	1.27	0.17
Cost ($)	5%	15.99	0.04	25.99	0.03	19.99	0.04	14.95	0.04
Total WNV		**0.530**		**0.533**		**0.512**		**0.525**	

Based on the trade study of four battery models shown in Table 108, the team has determined that YDL 115659 5000mAh 3.7V LiPo battery would be the best choice for the logic circuit power source. Although the AKZYTUE battery also has a very similar trade study score because of its 10000mAh capacity, the team selected the YDL battery because of it takes up about half as much space and weighs about half as much as the AKZYTUE battery. Moreover, assuming an average logic circuit current draw of 1.5A, the 5000mAh capacity would allow the battery to last over three hours, which is significantly longer than the system is expected to be on the launchpad. The extra capacity of the 10000mAh battery is not worth the extra weight, size, and cost.

Table 109: ACS 7.4V LiPo Battery Trade Study

		Ovonic		Youme		Zeee	
Criteria	**Weight**	**Value**	**WNV**	**Value**	**WNV**	**Value**	**WNV**
Capacity (mAh)	45%	5000	0.15	5200	0.15	5200	0.15
Mass (g)	30%	197	0.22	289	0.18	250	0.20
Volume (in^3)	20%	8.97	0.14	9.92	0.13	9.85	0.13
Cost ($)	5%	17.39	0.04	25.00	0.03	19.50	0.03
Total WNV		**0.539**		**0.495**		**0.516**	

Using the trade study in Table 109, the team selected the Ovonic 2S 5000mAh 7.4V Lipo battery to power the servo motor. The three batteries compared had very similar capacities, so the team's selection was finalized based on physical dimensions of the batteries. A capacity of 5000mAh is sufficient to power the servo motor continuously for around 45 minutes at its stall current (6.5A), which is more than enough for the duration of the flight. The servo motor's stall current also does not exceed the battery's maximum discharge current of 250A, as is desired.

7.4.2 Accelerometer Selection

The ACS includes a 3-axis accelerometer for redundancy in the event of IMU failure, as linear acceleration data is required for the system to detect the different stages of flight and deploy the drag surfaces appropriately as part of the ACS control algorithm.

The most important criterion included in the trade study is resolution, which measures how accurately the sensor outputs the launch vehicle's acceleration. This affects how accurately the flaps detect burnout and begin deployment, so it is given a weight of 40%. The second criterion of comparison is the maximum output data rate in Hz, which refers to how frequently the sensor will send acceleration data to the microprocessor. This is important because it affects how quickly the microprocessor completes every iteration of the control loop. The higher the sample rate, the less lag there will be between the system issuing commands and the servo motor physically responding to them. However, it is less important than sensor resolution because all sensors compared have a reasonably high output data rate. The final two criteria of comparison were mass and cost. Mass was given a low weight because all the compared sensors have a relatively minimal impact on the overall mass the ACS. Cost was given a higher weight because the sensor is meant to be a backup and should not be too expensive. The trade study used to compare the four shortlisted accelerometers is included in Table 110.

Table 110: ACS Accelerometer Trade Study

		ADXL343		ADXL345		ADXL326		MMA8451	
Criteria	**Weight**	**Value**	**WNV**	**Value**	**WNV**	**Value**	**WNV**	**Value**	**WNV**
Resolution (*g*)	40%	16	0.11	16	0.11	16	0.11	8	0.06
Output Data Rate (Hz)	25%	3200	0.09	3200	0.09	1600	0.05	800	0.02
Cost ($)	25%	5.95	0.22	17.50	0.16	17.95	0.16	7.95	0.21
Mass (g)	10%	0.30	0.09	0.30	0.09	1.29	0.06	1.30	0.06
Total WNV		**0.52**		**0.46**		**0.38**		**0.35**	

Based on the results of the trade study, the team selected the Adafruit ADXL343 as the ACS accelerometer because it meets all the ACS requirements while also being cheaper than most other sensors of its kind. After all, the accelerometer is only a backup sensor in case the IMU fails, so it does not need to be very advanced or expensive.

7.4.3 Altimeter Selection

The altimeter is a sensor that measures the barometric pressure of its environment and uses that information to calculate its current altitude. This sensor is required for ACS in order to accurately determine the altitude of the launch vehicle so that the ACS can activate at burnout and deactivate at apogee. Moreover, accurately knowing the current altitude of the launch vehicle is key to accurately predicting its apogee based on its current trajectory and to detect if the launch vehicle overshoots its target apogee.

The most important criterion in the altimeter trade study is altitude resolution. This refers to how accurately the sensor determines the exact altitude of the launch vehicle. The lower the resolution, the higher the precision of the sensor. Altitude resolution is given almost half of the total weight, because accurately determining the launch vehicle's altitude is the altimeter's primary function. The second criterion weighted is the maximum data output rate in Hz, which refers to how frequently the sensor will send altitude data to the microprocessor. This is important because the system needs to detect a series of events that occur over a very short timespan and minimize output lag in the ACS control algorithm. The final two criteria were mass and price. These were weighted equally low because although they differ, they both have a relatively minimal impact on the overall mass/cost of the ACS as a whole. The trade study used to compare the three shortlisted altimeters is included in Table 111.

Table 111: ACS Altimeter Trade Study

		MPL3115A2		BMP280		BMP390	
Criteria	**Weight**	**Value**	**WNV**	**Value**	**WNV**	**Value**	**WNV**
Altitude Resolution (m)	45%	0.30	0.36	1.00	0.16	0.25	0.38
Output Data Rate (Hz)	35%	166	0.16	100	0.10	100	0.10
Mass (g)	10%	1.20	0.07	1.30	0.07	1.30	0.07
Cost ($)	10%	9.95	0.07	9.95	0.07	10.95	0.06
Total WNV		**0.66**		**0.39**		**0.60**	

The team selected the Adafruit MPL3115A2 as the ACS altimeter since it received the highest score on the trade study that was performed. The MPL3115A2 accurately measures the launch vehicle's altitude while yielding a high output data rate and maintaining a low power consumption. The team will also consider having a secondary altimeter on the ACS for redundancy in case the primary altimeter fails.

7.4.4 IMU Selection

A 9-axis IMU (Inertial Measurement Unit) is a sensor that uses an accelerometer, gyroscope, and magnetometer (compass) to measure the linear acceleration, angular velocity, and absolute heading respectively of an object. The ACS needs a 9-axis IMU in order to precisely measure the angular and linear acceleration, as well as heading in order to determine precisely the launch vehicle's trajectory based on the previous data points. Some IMUs also combine the angular acceleration and angular velocity data to continuously output their current absolute orientation as Euler angles relative to the x, y, and z axes.

The most heavily weighted criterion is degrees of freedom, which refers to whether the sensor is a 3, 6, or 9 axis IMU. The number of degrees of freedom was weighted heavily because it was important for the sensor to be able to provide more orientation data. This makes the apogee prediction algorithm more accurate as it will take into account the orientation of the launch vehicle to more precisely determine the trajectory of the launch vehicle at every instant, and hence its projected apogee. The second-heaviest weighted criterion was the maximum output data rate. This is important especially for the IMU, because both the acceleration and orientation data will be used to calculate the velocity of the launch vehicle to accurately determine when apogee has been reached so that the flaps can be retracted on time, before body tube separation and parachute deployment occurs. The next criterion weighted was the

accelerometer range, which determines the maximum acceleration (in g) that the IMU's accelerometer can record. While this is less important than other criteria, it is still useful to have a sensor that can record large accelerations at launch and burnout without raising errors or outputting null data. Finally, cost and mass were given the lowest weight as all of the sensors compared are lightweight and well within the ACS budget. The trade study used to compare the four shortlisted IMUs is included with the comparison criteria in Table 112.

Table 112: ACS IMU Trade Study

		BNO055		BNO085		ICM-20948		ISM330DHCX	
Criteria	**Weight**	**Value**	**WNV**	**Value**	**WNV**	**Value**	**WNV**	**Value**	**WNV**
Degrees of Freedom	35%	9	0.10	9	0.10	9	0.10	6	0.06
Output Data Rate (Hz)	30%	1000	0.12	500	0.06	100	0.01	833	0.10
Accelerometer Range (g)	15%	16	0.04	16	0.04	16	0.04	16	0.04
Mass (g)	15%	3.00	0.10	2.50	0.11	1.50	0.13	2.00	0.12
Cost ($)	5%	34.95	0.03	24.95	0.04	14.95	0.04	14.95	0.04
Total WNV		**0.39**		**0.34**		**0.31**		**0.36**	

Using the results of the trade study, the team selected the Adafruit BNO055 IMU, because it received the highest score and can directly output absolute orientation data as Euler angles, which makes it easier for the microprocessor to make accurate apogee predictions and send the appropriate signal to the ACS servo motor.

7.4.5 Microprocessor Selection

The team has chosen the Raspberry Pi 4 Model B to serve as the Apogee Control System's logic circuit microprocessor. The unit features 2 USB 2.0 ports, 2 USB 3.0 ports, 1 Micro-SD card slot, and a 40 pin GPIO header. This makes it a suitable choice for the ACS as it will need to interface with multiple sensors and other electronics. The GPIO header also supports the I^2C interface, which offers high data rates and makes it easy for sensors to communicate with the microcontroller. The presence of many peripherals and a built-in WiFi module would make it easier to prototype and debug any software issues that may arise during development.

The Raspberry Pi 4 has an operating temperature of 0°C-50°C, which will be sufficient for launch conditions. Additionally, the whole unit is 85x56mm which is small enough to fit

within the ACS body tube. The team has chosen the variant of the Raspberry Pi 4 with 4GB of RAM and a 1.5GHz Quad-Core CPU, which should be more than enough to run its Raspbian operating system and the team's ACS Python code without causing any bottlenecks in terms of computing power. The team chose a microprocessor (embedded single-board computer) over a microcontroller (such as the Arduino UNO) because the microprocessor can run an operating system and perform more computationally expensive tasks such as data filtering more efficiently due to its larger memory and faster CPU. An image of the selected microprocessor with labeled ports and headers has been included in Figure 90.

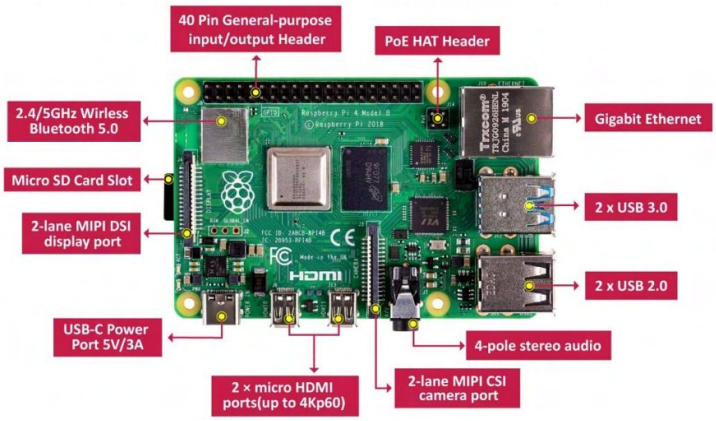

Figure 90: ACS Microprocessor: Raspberry Pi 4 Model B

7.4.6 Electrical Test Plan

All electrical components of the ACS system will be rigorously tested to minimize the chance of failure. Since the ACS cannot function correctly without accurate sensor data, each sensor will be tested to ensure that it outputs accurate data within the tolerances specified in its manufacturer's datasheet. This test will also help establish sensor calibration parameters if required. The other electrical components that will be tested are the two LiPo batteries (3.7V and 5V), the PCB/wiring, and the servo motor. These tests will minimize the risk of electrical failure on board the Apogee Control System. Details of the testing procedure and success criteria for each electrical test are included in Table 113.

Table 113: ACS Electrical Test Plan

Test Name	Description	Success Criteria
Battery Duration Test	The batteries will be fully charged and connected to the logic circuit and servo motor with the system active and the servo motor occasionally actuating. The system will be tested in both hot and cold environments. Voltage readings will be taken at the end of the test	The system remains functional and can actuate after three hours of being active. The 3.7V battery remains above 3.2V when tested with a voltmeter and the 7.4V battery remains above 6.4V after three hours
PCB Electrical Continuity Test	A multimeter with continuity test will be used to check for electrical continuity between PCB-mounted components at their solder joints	The system passes the continuity test (multimeter beeps) with each trace on the PCB connecting the correct pair of pins on both components
Solder Joint Reliability Test	Solder joints will be tested by physically pulling on soldered components and wires with moderate force. Solder joints will be visually inspected for quality	The solder joints remain intact and none of the wires come loose; no cold solder joints or poor solder joints are found during visual inspection

Table 113: ACS Electrical Test Plan

Test Name	Description	Success Criteria
Sensor Unit Tests	Each sensor will be physically moved around or rotated and its data output analyzed. These tests will be done on a breadboard to verify sensor functionality before soldering to a PCB	When not moving, the accelerometer and IMU should read approximately 0. When dropped from a low height, their acceleration should read around -9.8 m/s^2 (-g). The IMU orientation sensor should closely reflect its actual orientation angle. Altimeter readings closely reflect actual elevation data
Standalone Servo Motor Test	The servo motor will be tested outside of the mechanism using a simple servo controller board and powered by a 7.4V battery	The servo motor actuates from 0° to 180° within 1 second at no load and is precise to within ±3 degrees of the commanded servo angle
Redundant Sensor Test	The ACS batteries will be fully charged and one set of sensors measuring the same parameters will be disabled for each iteration of the test; remaining active sensors will be fed simulated flight data	The system remains functional in every iteration of the test and all sensors report similar data

7.5 Software and Control Structure Overview

The Apogee Control System will use a closed software control loop written in Python and run by a Raspberry Pi 4 microprocessor to precisely actuate its mechanical design. The ACS software loop begins by initializing and calibrating all sensors the first time it is started. After a successful power-on self test, the system will consider the launch vehicle as being in an 'On Ground' state and the control loop will start reading and filtering data, and logging the output consistently. The ACS will be inactive as it is not required before burnout. When the ACS

accelerometer and IMU detect a large instantaneous acceleration and the altimeter detects a significant change in altitude, the system will consider the launch vehicle as being in a 'Powered Ascent' state and the ACS will prepare for deployment at burnout, but the control tabs (and attached flaps) will remain retracted. At burnout, the ACS will be activated and will use control algorithm to dynamically adjust the flap actuation angle based on the apogee error. The rapid deceleration that occurs at burnout will be detected and will activate the ACS. Flight data will also be used to continuously predict the final apogee when the ACS is active so that the flaps can be adjusted accordingly. If the system detects that it has overshot the target apogee, it will fully extend the flaps to minimize the apogee error. Finally, when the system records a velocity close to 0, it will retract the flaps and deactivate itself. The ACS control structure is outlined in Figure 91.

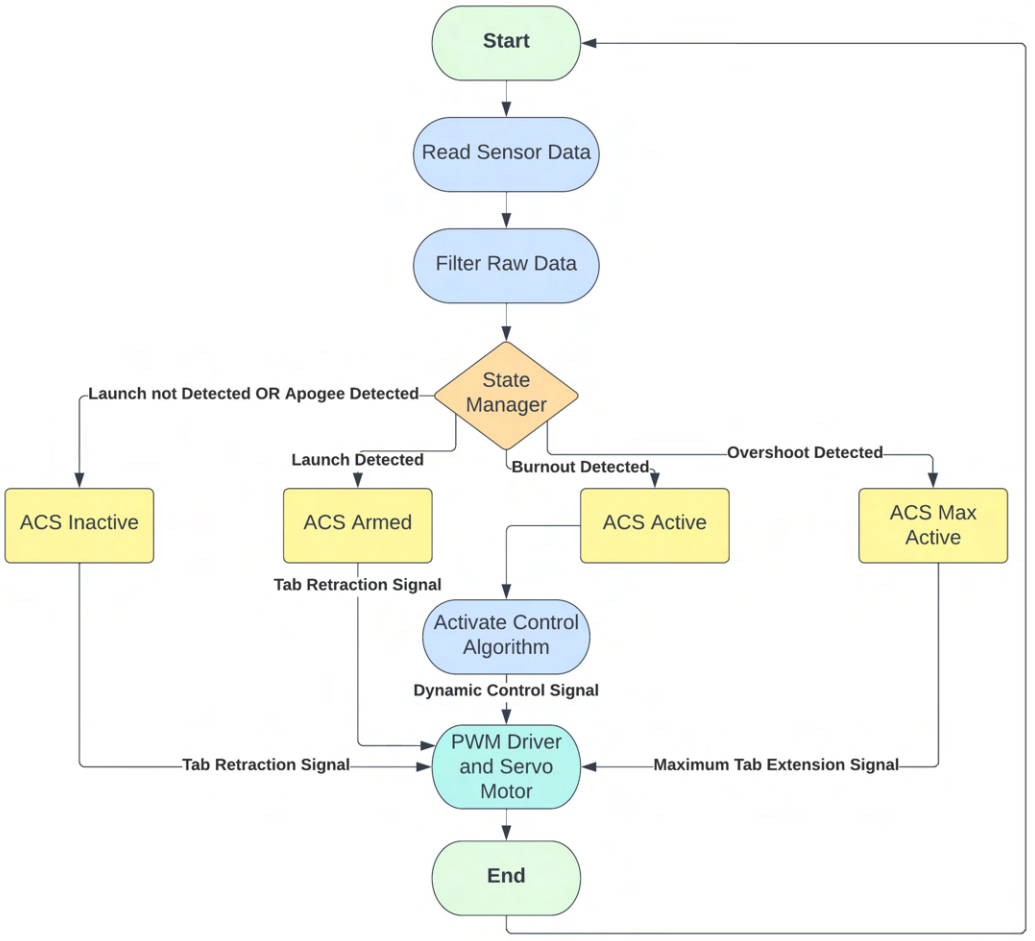

Figure 91: ACS Control Structure Flowchart

7.5.1 Data Filtering

As the launch vehicle ascends, the ACS sensors that continuously log data (the accelerometer, altimeter, and inertial measurement unit) will experience noticeable fluctuations in data output signals as a result of the randomness of open environments. Additionally, no sensor is 100% accurate and small amounts of electrical noise may persist even when using a PCB, so the raw sensor data cannot be trusted completely. To minimize the effects of random noise spikes and electromagnetic interference, the ACS will use sensor data together with a physical data model of the launch vehicle in its data filtering algorithm to accurately determine the current state of the launch vehicle and to feed more accurate data to the ACS actuation control algorithm.

The team will consider several factors when choosing an appropriate data filtering algorithm. The most important of these is the effectiveness of the algorithm. More specifically, how well the algorithm minimizes noise spikes while also not significantly modifying true sensor data. The algorithm should also not be too computationally expensive or introduce too much lag between time steps as this could cause a delayed response and could reduce the entire control loop's frequency. Two categories of filters were considered for the ACS software loop: single-stream filters and fusion filters. The fusion filters include the Kalman filter and Central Limit Theorem filter. Single-stream filters involve moving windows operations and include the averaging filter and the median filter.

Single-stream filters are filters that take in one stream of data and manipulate them to remove clean and noise from the data. They take the average of multiple previous inputs and produce a less noisy output. The window size needs to be calibrated in order to ensure that extra noise from the sensors is filtered out while retaining the rest of the data points. If the moving window is too small, the filtered data may not accurately reflect the true flight parameters of the launch vehicle due to the small sample size, and if the window is too large, rapid changes in flight parameters (such as during launch and burnout) will only be detected after significant delay. The median filter is similar to the averaging filter except that it takes the median of the window of inputs as the final output rather than the mean. In comparison with the averaging filter, the median filter is not affected heavily by unexpected input outliers since the median of a data set is not affected by outliers or extreme values. The window size again needs to be calibrated as data with higher expected spikes in values tend to have larger window sizes. An example of median-filtered legacy data with a moving window size of 29 data points in comparison to raw sensor data is shown in Figure 92.

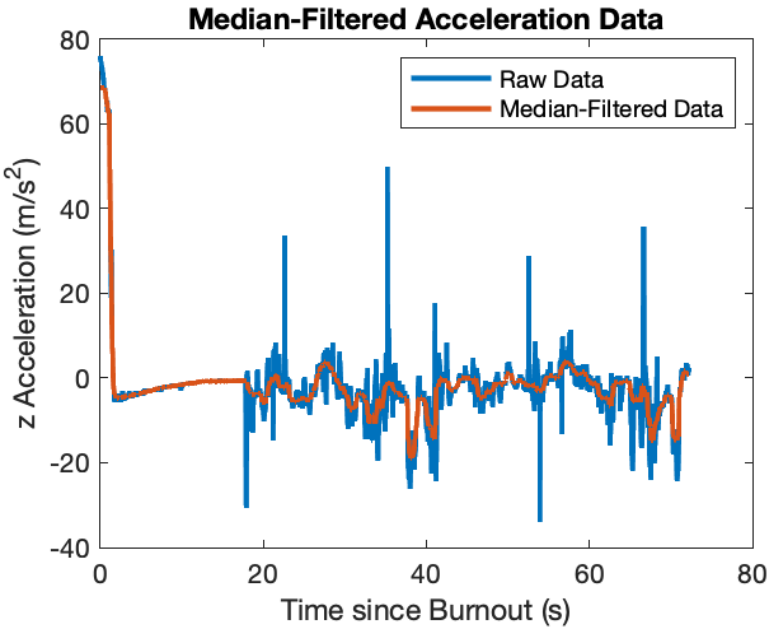

Figure 92: Raw and Median-Filtered z-axis Acceleration Data from a previous subscale launch

Fusion algorithms take in past and present data points from multiple sources and fuse them together to produce a high accuracy prediction. These sources can also include physical models of the system that calculate the expected data output from each sensor at every instant. These algorithms tend to predict the future pattern of data without being significantly affected by sensor noise and they allow control over which data sources is trusted more in comparison to all available data sources on the system. The Kalman filter is a predictive algorithm that takes in uncertain data (noise) and determines a more accurate value for each data point at every instant. As more data is input, the filter approaches a better estimation of the data, especially if the algorithm is tuned well (appropriate levels of trust are given to each data source). The Kalman filter can also use data points up to the current time to estimate time-dependent parameters. For example, the filter can use acceleration and angular velocity data to output the velocity vector of the launch vehicle at every instant, assuming that the system is at rest when initialized.

The Central Limit Theorem filter is a fusion algorithm that relies on the statistical concept of a bell curve. The more data input data a sensor collects, the more likely it is to represent a bell curve distribution where the more accurate data points are towards the middle of the curve and the less accurate noise falls on the tail ends. These bell curve models show the “true value” of the data, and these Central Limit Theorem filters use these curves to give out a consistent output value.

Since the team will be using multiple sensors to keep track of the launch vehicle’s trajectory

and changes in its environment, fusion filters would be the best choice as they combine data from multiple sources. Single-stream filters are very simple and effective (in terms of noise cancellation) only for single streams of data, and cannot effectively combine data from multiple sources to create an accurate flight model. Because the Kalman filter can combine data obtained from multiple sources with a mathematical model of how the system will evolve over time, errors in the mathematical model and erroneous sensor data spikes are both accounted for and diminished by the Kalman filter. This reduces the overall error in the filtered data, allowing the system to more accurately determine its trajectory.

The two limitations associated with the Kalman filter are its ability to handle a system that evolves non-linearly over time as the drag force acting on the system changes continuously in a non-linear fashion. Moreover, the Kalman filter is more computationally expensive than single-stream data filtering alternatives. However, when considering the advantages of fusion filters over single-stream data filters the team is confident that either a Central Theorem Limit Filter or the Kalman Filter would be a suitable choice as the ACS data filtering algorithm. Further testing will be carried out with both algorithms on a number of legacy data sets to determine which of the two data filters is more efficient.

7.5.2 Apogee Prediction and Actuation Control Algorithms

The launch vehicle's drag-inducing control surfaces will be controlled by an actuation control algorithm. At every instant between burnout and apogee, the drag force acting on the launch vehicle will vary, and hence the projected apogee will also vary due to the change in trajectory. As a result, the amount of flap actuation required to eliminate the apogee error (difference between changing projected apogee and fixed target apogee) will also change continuously. This necessitates the use of a precise software control algorithm to dynamically adjust the extent of servo actuation. Assuming that gravity and drag are the only two forces acting on the launch vehicle, the magnitude of the resultant force acting on the launch vehicle at any instant will be the sum of the drag force and the launch vehicle weight, as expressed in the equation:

$$F_r = F_g + F_d = mg + F_d \tag{18}$$

where F_r is the net force acting on the launch vehicle, F_g is the gravitational force, F_d is the total drag force, and m is the mass of the launch vehicle at burnout. The total drag force is split into two components: F_{dl} and F_{da}, where F_{dl} is the drag force acting on the launch vehicle (with no flap extension) and F_{da} is the drag force acting on the ACS flaps alone. Assuming that drag only acts along the negative z-axis yields the following first order differential drag equation:

$$F_d = F_{dl} + F_{da} = -\frac{1}{2}\rho C_{dl} A_l \dot{z}^2 - \frac{1}{2}\rho C_{da} A_a \dot{z}^2 \tag{19}$$

where C_{dl} is the drag coefficient of the launch vehicle, C_{da} is the drag coefficient of the ACS tabs, A_l is the cross-sectional area of the launch vehicle, and A_a is the cross-sectional area of the ACS flaps. Combining Equations 18 and 19 with Newton's second law yields the following second order differential equation:

$$m\ddot{z} = -mg - \frac{1}{2}\rho C_{dl} A_l \dot{z}^2 - \frac{1}{2}\rho C_{da} A_a \dot{z}^2 \tag{20}$$

This equation will be solved at every instance of the ACS software control loop using a Fourth Order Runge-Kutta numerical approximation method with a discrete time-step calculated as the difference between the current system time and the previous time. Real-time filtered sensor data will be fed to the actuation control algorithm as the initial conditions and the calculated solution will be used to find the projected apogee (maximum z value). This will be compared with the fixed target apogee and the required flap actuation will be determined based on the apogee error. CFD and wind-tunnel system testing will be used to determine drag coefficient values and to characterize the relationship between servo motor angle and the corresponding drag force induced as a function of servo angle or as a constant of proportionality between the two quantities.

The team compared two possible software actuation control algorithms: the Model Predictive Control algorithm and the PID (Proportional-Integral-Derivative) control algorithm. The Model Predictive Control algorithm is used for both complex and simple systems. The algorithm predicts the system's future behavior based on statistics provided by the input variables and is capable of handling multiple inputs, outputs, and the numerous interactions between each. It uses an optimization model, a cost function, and an internal dynamic model to predict the future behavior of the system. Operation constraints and prediction of outside disturbances are also taken into consideration along with the inputs of the system. The PID Control algorithm is an automatic, input based adjustment system that acts directly on the actuation system. It accounts for the error between the target value of actuation and the actual value of actuation and actuates the servo motor accordingly. This algorithm is more commonly used for simple systems as it takes into account a smaller number of input variables.

Since the team will be using a mechanism that only requires a single output: the angle of the servo motor which adjusts the angle of the flaps, the PID control algorithm is preferable over Model Predictive Control. The precision of the servo can be thrown off by many uncontrolled

external variables so the ACS needs to account for errors. Although Model Predictive Control algorithms do well in predicting the future behavior of the actuation system, the PID's error adjustments are sufficient and the PID system is much simpler to implement and debug, without too much overhead in terms of computing power or software complexity.

7.5.3 Software Test Plan

The team will conduct rigorous tests of each function within the control software of the Apogee Control System to ensure that all software algorithms function as expected, without raising any errors. The data acquisition test will ensure that sensor data output can be logged reliably. The data filtering algorithm will be tested to verify that erroneous data spikes are minimized. The state transition manager test will ensure that the ACS quickly and correctly determines the current state of the launch vehicle during the different phases of flight. The apogee prediction and control algorithms will also be tested to ensure that the microprocessor correctly predicts apogee based on current flight data and sends the appropriate signal to the servo motor as a part of the control algorithm. Finally, all software components will be tested in an on-ground software loop test to confirm that all algorithms can function together without throwing any errors over an extended period of time. A detailed description of the testing procedure and the success criteria for each software test are included in Table 114.

Table 114: ACS Software Test Plan

Test Name	Description	Success Criteria
Data Acquisition Test	Python data logging code will be written and tested. Sample rate will also be determined	The logged data is analyzed while physically moving the sensors and must reflect the changes in real time. Sample rate is greater than 10Hz
Data Filtering Algorithm Test	Data filtering algorithm will be fed noisy raw data and its output will be evaluated	Filtered data is smooth but remains accurate. Only erroneous spikes are diminished while true data is not significantly affected

Table 114: ACS Software Test Plan

Test Name	Description	Success Criteria
State Transition Manager Test	Various configurations of simulated flight data will be fed to the state transition function to analyze state transitions performed	The system transitions to the correct state based on the set parameters for launch and apogee acceleration and altitude without any exceptions raised
Apogee Prediction Algorithm Test	Different sets of altitude, acceleration, orientation, and flap angle data will be fed to the algorithm and its apogee prediction will be examined	The apogee prediction and test result do not differ significantly
Control Algorithm Test	Different sets of projected apogees will be fed to the control algorithm and its output servo angle will be checked against hand calculations	The servo and flap angles output by the control algorithm are proportional to the apogee error and approximately match hand calculations
On-Ground Software Loop Test	The entire ACS software loop will be run independently of the mechanism with legacy data and real data while on the ground	For all tested legacy datasets, the system performs as expected. When tested with real data, the system runs for a minimum of three hours without any unhandled exceptions

7.6 Integration of System Components

Design for manufacturability and design for assembly will be prioritized when designing the electrical and mechanical parts of the ACS. The ACS electronics will be mounted onto a PCB that is itself secured to a plate which spans the distance between middle bulkhead and bottom bulkhead and oriented perpendicular to the plane of the bulkheads. This will maximize the available space for the PCB and servo motor. The servo motor will be placed above the PCB

and will connect to the central shaft of the ACS mechanism. The servo motor will be appropriately shielded to minimize the electromagnetic interference with the electronics on the PCB. The radial tab portion of the ACS mechanism will be housed in between the top and middle bulkhead of the ACS as shown in Figure 89. Structural supports in between the three bulkheads will reinforce the design and reduce the stress on the mechanism. The flaps themselves will be housed within appropriately sized cutouts in the ACS body tube positioned to be flush with the airframe and attached to the ACS mechanism via hinges secured to the top bulkhead. Finally, the top bulkhead will serve as the attachment point for the main recovery parachute.

7.7 Integrated System Test Plan

The ACS electrical and software subsystems will be integrated during the subscale test to verify sensor data acquisition and the functionality of the data filtering algorithm. Subscale flight data will also be useful in future software tests for the full-scale ACS. The mechanical, electrical, and software components will be fully integrated and tested in flight during the launch vehicle demonstration flight and payload demonstration flight. This will test the mechanism and control algorithm's response to in-flight conditions and will be used to fine-tune the PID algorithm. The ACS will have passed this test when it demonstrates that it is capable of actuating according to the signal from the sensors, accurately controlling the apogee of the launch vehicle, and sustaining no damage during flight. The preliminary ACS integrated system test plan is described in Table 115 along with the success criteria for each test.

Table 115: ACS Preliminary Integrated System Test Plan

Test Name	Description	Success Criteria
Subscale Flight Test	All sensors, the microprocessor, and 3.7V logic circuit battery will be on-board the subscale launch vehicle. The data acquisition and data filtering algorithms will also be tested on this flight	The software initializes sensors, reads data, filters it, and logs the output to a csv file successfully. Sensor data is accurate when compared to other sensors on the launch vehicle

Table 115: ACS Preliminary Integrated System Test Plan

Test Name	Description	Success Criteria
Launch Vehicle Demonstration Flight Test	The fully assembled and integrated ACS will be in the launch vehicle. Pre-programmed actuation instructions will be followed without the dynamic control algorithm	The flaps actuate according to programmed instructions as recorded by the onboard camera. Logged apogee predictions are similar to the actual apogee
Payload Demonstration Flight Test	The fully assembled and integrated ACS will be in the launch vehicle. The complete software loop, including the control algorithm, will be programmed onto the microprocessor	Dynamic flap actuation is recorded on the onboard camera and actual apogee is within 25 feet of the target apogee. The flaps retract after apogee and all data is logged successfully
Electronics Shielding Test	Electronics from each system will be shielded and receive simulated flight data separately, then receive the same data while shielded and placed in the same configuration as within the launch vehicle	Data from all electronics are similar when placed separately and together

8 Safety

8.1 Safety Officer Role

The NDRT Safety Officer for the 2022-2023 season is Christopher Fountain. The Safety Officer is primarily responsible for defining, evaluating, and mitigating the various failure modes that can occur throughout the design process of the team throughout the competition. The general responsibilities and duties carried out to analyze these failure modes are, but not limited to, the following:

- Update the Safety Handbook to reflect the most current information for the 2022-2023

season.

- Enforcing general practices throughout the design process.
- Teaching and assessing safe fabrication methods.
- Updating and creating Standard Workshop Operating Procedures so that team members have a proper understanding of fabrication methods during launch vehicle construction.
- Assessing various failure modes and possible mitigations with FMEA tables.
- Developing a detailed Standard Launch Operating Procedures prior to the first full-scale launch to ensure safe launches
- Being a point of reference for any team member to refer to with safety-related questions.
- Attending all launches to ensure procedures are followed correctly.
- Contributing to the Safety portion of all NASA deliverables
- Promoting a culture that promotes safety and proper design over deadlines and other time constraints.
- Developing and following a plan for disposing of hazardous waste materials.
- Developing and following a plan for handling broken launch vehicle items.
- Ensuring all team members follow all NAR, NASA, and University safety regulations.
- Ensuring all team members follow all state, county, and local safety regulations.

8.2 Risk Assessment Method

All FMEA tables feature the hazard that the team may face, its cause and outcome, mitigations to reduce the hazard's risk, and verifications that ensure such mitigations are followed. All failure modes are also defined a pre-mitigation risk value, which is the product of its probability of occurrence and severity should it occur. After mitigations and verifications, the hazard is given a secondary risk value. This value is again the product of the hazard's probability of occurrence and severity from its occurrence, but these values are chosen with the assumption that the listed mitigations have been taken. Ideally, after effective mitigations, all hazard risk levels will decrease. Table 116 defines the criteria for assigning a certain probability to a hazard.

Table 116: Probability Assessment Criteria

Definition	Value	Probability of Occurrence
Improbable	1	Less than 1%
Sparse	2	Between 1% and 10%
Occasional	3	Between 10% and 25%
Unlikely	4	Between 25% and 50%
Probable	5	Above 50%

Table 117 defines the criteria for assigning a severity value to a specific hazard based on the different facets it may impact.

Table 117: Hazard Severity Criteria

Description	Value	Physical Environment	Team Personnel	Launch Vehicle	Overall Mission Success
Negligible	1	No damage	Minor or no injuries	Insignificant	Complete mission success
Minimal	2	Minor and reversible damage	Minor injuries	Minimal damage	Near complete mission success
Dangerous	3	Moderate reversible damage or minor irreversible damage	Moderate injuries	Major damage	Partial mission failure
Catastrophic	4	Major irreversible damage	Life-threatening injuries	Complete loss	Complete failure

After determining a hazard's probability and severity levels, the two are multiplied together to net an overall risk assessment value. Table 118 displays the possible combinations that a hazard can have. The colored cells correspond to the different levels of risk the team has identified, which is defined in Table 119.

Table 118: Risk Value Criteria

Probability	**Severity**			
	Negligible (1)	Minimal (2)	Dangerous (3)	Catastrophic (4)
Improbable (1)	1	2	3	4
Sparse (2)	2	4	6	8
Unlikely (3)	3	6	9	12
Occasional (4)	4	8	12	16
Probable (5)	5	10	15	20

Table 119 identifies how different risk values correspond to different risk identifications.

Table 119: Risk Level Categories

Risk Identification	**Range**	**Color**
Desired	Less than 5	Green
Acceptable	5 to 9	Yellow
Unacceptable	Greater than 10	Red

All identified hazards are given an appropriate label according to their name. The convention takes the form of AAA.N, where A is any letter up to three letters, and N is the nth hazard identified for that category. Table 120 defines the different labels the team has identified as having significant failure modes.

Table 120: Label Definitions for FMEA Tables

Label	Definition
C	Construction FMEA
LO	Launch Operations FMEA
VS	Vehicle Structures FMEA
VFM	Vehicle Flight Mechanics FMEA
R	Recovery FMEA
ACS	Apogee Control Systems FMEA
TROI	Payload FMEA
TROII	Payload Integration & Deployment FMEA
LE	Launch Equipment FMEA
VE	Vehicle Risks to Environment
EV	Environment Risks to Vehicle
PR	Project Risks

8.3 Overall Risk Reduction

After an analysis of all systems of the launch vehicle and the design process, the team has identified 124 total hazards that could occur. Following mitigations, the distribution of failure modes greatly improved, with a significant number of hazards moving from the unacceptable and acceptable risk categories to the acceptable and desired risk categories. The team will continue to monitor the design process and construction activities and will add failure modes or modify mitigations and verifications as more accurate data emerges.

Table 121 identifies the distribution of all risks before are implemented with Table 122 summing the risks into the three identified risk categories. Table 123 describes the risk distribution following mitigations with Table 124 summing these risks into the aforementioned categories.

Table 121: Risk Categories Pre-Mitigation

Probability	Severity			
	Negligible (1)	Minimal (2)	Dangerous (3)	Catastrophic (4)
Improbable (1)	0.00%	0.00%	2.32%	4.03%
Sparse (2)	0.00%	1.61%	10.48%	21.8%
Occasional (3)	0.00%	3.23%	16.13%	24.19%
Unlikely (4)	0.00%	4.03%	0.81%	5.65%
Probable (5)	1.61%	4.03%	0.00%	0.00%

Table 122: Risk Categories Pre-Mitigation Summary

Level	Quantity	Percentage
Desired	10	7.96%
Acceptable	71	57.28%
Unacceptable	43	34.68%

Table 123: Risk Categories Post-Mitigation

Probability	Severity			
	Negligible (1)	Minimal (2)	Dangerous (3)	Catastrophic (4)
Improbable (1)	2.42%	3.23%	26.61%	42.74%
Sparse (2)	0.81%	7.26%	6.45%	5.65%
Occasional (3)	0.00%	0.00%	0.81%	0.00%
Unlikely (4)	0.81%	0.81%	0.00%	0.00%
Probable (5)	2.42%	0.00%	0.00%	0.00%

Table 124: Risk Categories Post-Mitigation Summary

Level	Quantity	Percentage
Desired	104	83.88%
Acceptable	20	16.14%
Unacceptable	0	0.00%

8.4 Personnel Hazard Analysis

Table 125: Construction Failure Modes and Effects Analysis

Label	Hazard	Cause	Outcome	Probability	Severity	Before	Mitigation	Verification	Probability	Severity	After
C.1	Team member is punctur- ed by a tool	1. Inattentiveness to task at hand 2. Improper workshop training 3. Lack of knowledge about tool 4. Insufficient PPE	1. Minor or serious physical injury to team member 2. Infection if injury results in open wound 3. Damage to workshop tools	4	4	16	1. Team members will be knowledgeable about the construction and fabrication methods 2. Team members will be trained in proper PPE usage 3. First-Aid and emergency resources will be readily available	1. All team members must complete basic EIH certification in order to participate in any construction or attend launches 2. The First-Aid/burn kit in the workshop is fully stocked and the Notre Dame police number is posted inside the workshop 3. The Safety Handbook and Standard Workshop Operating Procedures will be available for all team members	2	4	8
C.2	Team member ingests toxin	1. Inattentiveness to task at hand 2. Improper workshop training 3. Insufficient PPE	1. Serious potential injury to team member 2. Possibility of death depending on the inhaled toxins severity	2	4	8	1. Team members will be knowledgeable about the construction and fabrication methods 2. Team members will be trained in proper PPE usage 3. First-Aid and emergency resources will be readily available	1. All team members are required to sign a safety contract affirming their commitment to safe workshop practices and wearing proper PPE 2. All team members must complete basic EIH certification in order to participate in any construction or attend launches 3. The First-Aid/burn kit in the workshop is fully stocked and emergency contacts are posted clearly inside the workshop 4. The Safety Handbook and Standard Workshop Operating Procedures will be available for all team members	1	4	4

C.3	Team member is burned	1. Inattentiveness to task at hand 2. Improper workshop training 3. Lack of knowledge about tool, 4. Insufficient PPE	1. Serious injury or death to team member 2. Spreading of fire to other members or workshop itself 3. Damage to workshop equipment	2	4	8	1. Team members will be knowledgeable about the construction and fabrication methods 2. Team members will be trained in proper PPE usage 3. First-Aid and emergency resources will be readily available	1. All team members are required to sign a safety contract affirming their commitment to safe workshop practices and wearing proper PPE 2. All team members must complete basic EIH certification in order to participate in any construction or attend launches 3. The First-Aid/burn kit in the workshop is fully stocked and emergency contacts are clearly posted in the workshop 4. The Safety Handbook and Standard Workshop Operating Procedures will be available for all team members	1	4	4
C.4	Fire in workshop	1. Inattentive team members 2. Improper workshop training 3. Lack of knowledge of method or tool	1. Serious injury or death for team members and any other occupants of the building 2. Loss of property and equipment	2	4	8	1. Knowledge of fire exits 2. Understanding of safe construction methods	1. All team members are required to sign a safety contract affirming their commitment to safe workshop practices and wearing proper PPE 2. All team members must complete basic EIH certification in order to participate in any construction or attend launches 3. The First-Aid/burn kit in the workshop is fully stocked and emergency contacts are clearly posted in the workshop 4. The Safety Handbook and Standard Workshop Operating Procedures will be available for all team members	1	4	4
C.5	Launch vehicle breaks during assembly	1. Inattentiveness during integration 2. Faulty construction	1. Partial or complete loss of launch vehicle 2. Project timeline setback	3	4	12	1. Base knowledge of construction methods 2. Close attention and care while construction and integration	1. All team members are required to sign a safety contract affirming their commitment to safe workshop practices and wearing proper PPE 2. All team members must complete basic EIH certification in order to participate in any construction or attend launches 3. The First-Aid/burn kit in the workshop is fully stocked and emergency contacts are clearly posted in the workshop 4. The Safety Handbook and Standard Workshop Operating Procedures will be available for all team members	2	3	6

C.6	Team member comes into physical contact with toxic substan- ce	1. Improper following of workshop procedures 2. Lack of appropriate PPE	1. Minor serious damage to skin, internal organs, or other body parts 2. Team member is potentially poisoned	2	4	8	1. Knowledge of proper workshop procedures 2. Appropriate PPE during fabrication or construction 3. Appropriate leadership supervision 4. Readily available resources to help in the event a team member is in contact with toxic substances	1. All team members are required to sign a safety contract affirming their commitment to safe workshop practices and wearing proper PPE 2. All team members must complete basic EIH certification in order to participate in any construction or attend launches 3. The First-Aid/burn kit in the workshop is fully stocked and emergency contacts are clearly posted in the workshop 4. The Safety Handbook and Standard Workshop Operating Procedures will be available for all team members 5. Safety glasses will be worn for all construction	1	3	3
C.7	Horsepl- ay in the worksh- op	1. Inattentive team members 2. Improper following of workshop procedures	1. Potential for serious injury 2. Damage to launch vehicle 3. Potential to damage or break a workshop machine	3	3	9	1. Prohibition and enforcement of horseplay in the workshop 2. Knowledge of general safe workshop practices among team members 3. Squad leads will be present in workshop	1. All team members are required to sign a safety contract affirming their commitment to safe workshop practices and wearing proper PPE 2. All team members must complete basic EIH certification in order to participate in any construction or attend launches 3. The First-Aid/burn kit in the workshop is fully stocked and emergency contacts are clearly posted in the workshop 4. The Safety Handbook and Workshop Operating Procedures will be available for all team members 5. Any official NDRT function in any construction space will include at least one member of the leadership team	1	3	3

C.8	Explosion in the workshop	1. Improper following of workshop procedures 2. Failure of a workshop tool	1. Major injury or death to team members or others in the building 2. Fire 3. Loss to property and launch vehicle	2	4	8	1. Knowledge of fire exits 2. Understanding of safe construction methods	1. All team members are required to sign a safety contract affirming their commitment to safe workshop practices and wearing proper PPE 2. All team members must complete basic EIH certification in order to participate in any construction or attend launches 3. The First-Aid/burn kit in the workshop is fully stocked and emergency contacts are clearly posted in the workshop 4. The Safety Handbook and Workshop Operating Procedures will be available for all team members	1	4	4
C.9	Injury to eyes during constr-ucting	1. Improper following of workshop procedures 2. Lack of eye protection during construction	1. Damage to eyes, temporary or permanent blindness	3	4	12	1. Knowledge of proper workshop procedures 2. Appropriate eyewear during construction 3. Appropriate supervision	1. All team members are required to sign a safety contract affirming their commitment to safe workshop practices and wearing proper PPE 2. All team members must complete basic EIH certification in order to participate in any construction or attend launches 3. The First-Aid/burn kit in the workshop is fully stocked and emergency contacts are clearly posted in the workshop 4. The Safety Handbook and Workshop Operating Procedures will be available for all team members 5. All team members will wear safety glasses for any construction procedures	1	3	3

C.10	Exposure to epoxy	1. Improper following of workshop procedures 2. Lack of appropriate PPE	Irritation for contact area	3	2	6	1. Knowledge of proper workshop procedures 2. Appropriate PPE 3. Presence of team leadership of other supervision during epoxy application	1. All team members are required to sign a safety contract affirming their commitment to safe workshop practices and wearing proper PPE 2. All team members must complete basic EIH certification in order to participate in any construction or attend launches 3. The First-Aid/burn kit in the workshop is fully stocked and emergency contacts are clearly posted in the workshop 4. The Safety Handbook and Workshop Operating Procedures will be available for all team members	1	2	2
C.11	High noise levels	1. Inherent noise levels of construction methods 2. Lack of appropriate PPE	Temporary or permanent ear damage	2	3	6	1. Knowledge of proper workshop procedures 2. Earphones for necessary machines and environments 3. Presence of team leadership or other supervision	1. All team members are required to sign a safety contract affirming their commitment to safe workshop practices and wearing proper PPE 2. All team members must complete basic EIH certification in order to participate in any construction or attend launches 3. The First-Aid/burn kit in the workshop is fully stocked and emergency contacts are clearly posted in the workshop 4. The Safety Handbook and Workshop Operating Procedures will be available for all team members 5. Appropriate ear protection will be provided when in necessary noise environments	1	3	3
C.12	Improper disposal of chemical- ly hazardo- us materials	Improper knowledge of disposing of chemical waste	1. Physical or chemical harm to individuals disposing of chemical waste 2. Potential harm to environment that waste is transported to	3	3	9	All team members will be knowledgeable of and how to dispose of the materials that need to be disposed of differently than general waste due to their chemical nature before construction	Procedures for disposing of chemically dangerous materials will be published by the Safety Officer and readily available for all team members	1	3	3

Table 126: Launch Operations Failure Modes and Effects Analysis

Label	Hazard	Cause	Outcome	Probability	Severity	Before	Mitigation	Verification	Probability	Severity	After
LO.1	Recovery of launch vehicle	1. Team members touch the launch vehicle without proper authorization 2. Motor is still hot 3. Sharp pieces are extruding from launch vehicle	Burns or penetration during recovery	3	3	9	1. Team members will exercise extreme caution when approaching the launch vehicle after launch 2. Team members will be knowledgeable about the risks associated with touching a launch vehicle post-launch	The Vehicles Squad Lead and Safety Officer will be responsible for inspecting the launch vehicle and ensuring that all charges are dead before permitting anyone to touch the launch vehicle, 2. Team members will be reminded of this procedure the night prior to the launch during the Launch Rehearsal	1	3	3
LO.2	Incorrect motor installati- on	Improper motor handling from lack of knowledge or certification	1. Uncontrollable flight path 2. Motor failure or explosion upon launch 3. Serious injury to team members 4. Serious damage to launch vehicle	4	4	16	The team will ensure that the personnel installing the motor is properly NAR certified to handle that specific motor	1. NAR/TRA Level 3 certified NDT Team Mentor Dave Brunsting will be responsible for any and all motor operations and is appropriately certified to do so 2. Team members will be reminded of the above procedure at the launch rehearsal the night before the launch	1	4	4
LO.3	Improper black powder charge handling before launch	Team members are not cautious with the energetics during integration	1. Separation charges are not correctly installed and thus do not properly function during launch 2. Launch vehicle fails to separate and recovery system fails to operate	3	4	12	The team will ensure that the personnel installing black powder charges is properly NAR certified to handle such energetics	1. NAR/TRA Level 3 certified NDT Team Mentor Dave Brunsting will be responsible for any and all black powder charge operations 2. Team members will be reminded of the above procedure at the launch rehearsal the night before the launch	1	4	4

LO.4	Distract- ed team members	Reckless behavior or general inattention	Team members miss important instructions and jeopardize safety of other team members and/or bystanders	3	3	9	Team members will be reminded of the danger that high-powered rocketry poses to the individual and will be reminded to take extra caution for themselves and their teammates	1. All team members are required to sign a team contract affirming that they will be attentive and obey all launch orders from the Safety Officer and RSO 2. A reminder about being alert and attentive will be emphasized at the launch rehearsal the night before the launch	1	2	2
LO.5	Team members come too close to the launch vehicle before launch	Disregard of the safety precautions set in place by the local launch site	1. Possible burns from motor ignition 2. Serious potential injury or death in the event of motor explosion	2	4	8	1. All team members will be located a distance no less than 300 feet from the launch vehicle per NAR guidelines 2. The Safety Officer will aid in ensuring that all team members abide by this minimum safety distance	The RSO will have the final verdict over whether or not a launch is safe to initiate given team member's proximity to the launch vehicle	1	4	4
LO.6	Sun exposure	Lack of sunscreen	Sunburn and an increased risk of skin diseases	4	2	8	1. Team members will be reminded of the dangers UV exposure poses to the body 2. Team members will be reminded to consider the weather and bring sunscreen to the launch site 3. Team members will be required to wear sunscreen if heavy UV exposure is present on launch day	1. The Safety Officer will bring a spare bottle of sunscreen to ensure members are adequately protected should the sun pose harmful UV radiation the day of the launch 2. Announcements and reminders concerning the weather will be sent out to the team before launch day	2	2	4
LO.7	Launch vehicle is lost	1. High drift radius from parachute 2. Uncontrollable flight pattern 3. Poor visibility	1. Complete loss of launch vehicle 2. Large project budget setback	2	4	8	The launch vehicle will not be launched under high winds (speeds above 20 miles per hour) or considerably poor visibility (i.e., fog)	The Safety Officer and Project Manager will continually check the weather to assess wind speeds and cloud cover and determine if launch conditions are appropriate	1	2	2

LO.8	Dehydra- tion during launch	1. Inadequate amounts of water present at launch	Dizziness, lightheadedness, and more serious symptoms of dehydration	1	3	3	The Safety Officer will inform all team members that they must bring water to ensure that they are properly hydrated during the launch	1. Announcements and reminders will be sent out to the team regarding bringing water 2. Bottles of water will be provided as part of launch equipment	1	1	1
LO.9	Heat exhausti- on or stroke during launch	1. Lack of hydration 2. Heavy physical exertion during launch day	Loss of consciousness, fatigue, and other serious potential harm to team members	1	4	4	1. The Safety Officer will inform all team members about the dangers of heat exhaustion and will require all members to be properly hydrated and be mindful of how much they exert themselves during the launch 2 If excessive heat is forecasted the launch will be postponed	1. Announcements and reminders will be sent out to the team regarding bringing water 2. Bottles of water will be provided as part of brought launch equipment 3. The Safety Officer and Project Manager will continually assess the weather and determine if projected launch day temperatures are safe to operate in	1	1	1
LO.10	Cold tempera- tures	Inadequate clothing for cold temperatures	Hypothermia, frostnip, frostbite, dizziness, loss of consciousness, loss of appendages	4	4	16	The Safety Officer will inform all team members about the dangers of cold temperatures and will require all members to be properly clothed for the weather	1. Team members that arrive to the launch not properly clothed for the cold temperatures will be sent home 2. Extra hand warmers will be brought to the launch site as part of launch equipment 3. The Project Manager and Safety Officer will continually assess the weather and determine if the temperatures are safe to launch in 4. The team will send announcements further reminding the entire team about the cold temperatures	2	4	8

8.5 Failure Modes and Effects Analysis

Table 127: Vehicle Structures Failure Modes and Effects Analysis

Label	Hazard	Cause	Outcome	Probability	Severity	Before	Mitigation	Verification	Probability	Severity	After
VS.1	Motor ignition failure	1. Incorrect installation of motor 2. Motor is misaligned 3. Faulty motor purchased	1. Launch vehicle fails to launch 2. Complete mission failure	4	4	16	1. Motor installation will be carefully monitored by a team member with proper certification and experience 2. Motor purchased will be of high quality	1. Team Mentor (NAR/TRA Level 3 Certified) Dave Brunsting will be responsible for handling and installing all energetics and will abide by NAR regulations while doing so 2. Motor purchased will be from a trusted and respected brand	1	4	4
VS.2	Bulkhead failure	1. Improper analysis of static loading for faulty material, material imperfections 2. Improper sizing of bulkhead	1. Bulkhead may fracture during flight 2. Internal components damaged by flying bulkhead debris 3. Internal components are not contained, jeopardizing stability	3	4	12	1. Bulkhead material will be tested and/or analyzed to verify it can withstand maximum static loading 2. Construction of bulkheads will be intentional and thorough	1. Standard Workshop Operating Procedures that would include fabrication methods for constructing the bulkheads will be readily available for all team members 2. Bulkhead material and design will be tested to verify it can withstand maximum static loading during launch with a factor of safety of 1.5	1	4	4
VS.3	Nose cone failure	1. Material imperfections 2. Nose cone fails to withstand maximum static loading during flight 3. Blunt force to nose cone	1. Nose cone fractures and fails to distribute drag force to the launch vehicle 2. Stability is jeopardized due to non-uniform air flow	2	4	8	1. Bulkhead material will be tested and/or analyzed to verify it can withstand maximum static loading 2. Construction of nose cones will be intentional and thorough 3. Weather will be inspected to avoid the presence of blunt force during launch (i.e., hail)	1. Standard Workshop Operating Procedures that would include fabrication methods for constructing nose cones will be readily available for all team members 2. Nose cones material and design will be tested to verify it can withstand maximum static loading during launch with a factor of safety of 1.5 3. The Safety Officer will continually inspect launch weather forecasts to ensure no blunt force in the air (i.e., hail) will be present during launch that may harm the nose cone	1	4	4

VS.4	Body tube failure during launch	1. Blunt force to body tube during launch (i.e., hail) 2. Blunt force to the body tube upon landing (i.e., high descent velocity) 3. Imperfections in material 4. Separation charges damage body tube	1. Minor to major damage to launch vehicle 2. Potential harm to internal components	1	3	3	1. Body tube material will be of high quality and tested to ensure that separation charges do not damage it 2. Successful recovery system 3. Material for the body tube will be of high quality 4. Weather will be consistently inspected to avoid the presence of blunt force during launch (i.e., hail)	1. The Safety Officer will continually inspect launch weather forecasts to ensure no blunt force in the air will be present during launch that may harm the nose cone 2. Material for the body tube will be from a trusted vendor and approved by the Project Manager and Vehicles Squad Lead prior to purchase 3. The body tube will be tested with the black powder charges to ensure, upon inspection, that the combustion reaction does not damage the body tubes 4. The procedures for conducting the separation charges will be made available for all teammates once written 5. The recovery system will be verified through a subscale launch before a full-scale launch	1	3	3
VS.5	Launch vehicle is damaged at landing	1. Blunt force to launch vehicle at landing 2. Unacceptable descent velocity at landing 3. Failure for parachutes to deploy	Minor to major damage to launch vehicle	3	3	9	1. Body tube material will be of high quality and strength material 2. The recovery system will be tested to be functional prior to launch	1. The material for the body tube will be of high quality and/or from a trusted and respected vendor 2. Recovery system will be verified through a subscale launch before a full-scale launch	2	3	6
VS.6	Shear pin failure	1. Separation charges are not sized or installed properly 2. Faulty shear pins	1. Launch vehicle fails to separate when necessary 2. Launch vehicle separates unpredictably 3. Recovery system fails to function 4. Flying debris during launch	3	4	12	1. Shear pins purchased will be of high quality 2. Separation charges will be installed properly 3. Selection of shear pins will be verified through testing and/or simulation of black powder charges to analyze the appropriate force of separation range	1. The shear pins will be purchased from a respected and trusted vendor and will be approved by the Project Manager and Vehicles Squad Lead prior to purchase 2. All energetics will be handled and installed by Team Mentor (NAR/TRA Level 3 Certified) Dave Brunsting 3. Shear pins will be selected based on simulations of black powder charges and the results of these simulations only	1	4	4

VS.7	Coupler failure	1. Material imperfections 2. Damage from separation charges to couplers	1. Launch vehicle may not separate upon separation charge ignition 2. Coupler does not properly hold in place separation points	2	3	6	1. Material for couplers will be of high quality and durability 2. Coupler material will be verified to be able to withstand the force and combustion experienced from the separation charges	1. Coupler material will be purchased from a respected and trusted vendor and selection will be approved by the Project Manager and Vehicles Squad Lead prior to purchase 2. Coupler material will be analyzed or tested to withstand the maximum combustion force with a factor of safety of 1.5	1	3	3
VS.8	Motor explosion	1. Improper motor installation 2. Motor is misaligned 3. Faulty motor purchased	1. Major damage to launch vehicle 2. Potential fire 3. Potential injury to bystanders	3	4	12	1. Motor installation will be carefully monitored by a team member with proper certification and experience 2. Motor purchased will be of high quality	1. Team Mentor (NAR/TRA Level 3 Certified) Dave Brunsting will be responsible for handling and installing all energetics and will abide by NAR regulations while doing so 2. Motor purchased will be from a trusted and respected vendor and approved by the Project Manager and the Vehicles Squad Lead prior the purchase	1	4	4
VS.9	Centering ring failure	1. Imperfections in material used 2. Misalignment or improper installation	1. Motor is misaligned 2. Launch vehicle flight pattern is not controlled 3. Unsuspecting objects are in new flight path that would have otherwise been safe	3	4	12	1. Centering rings will be installed carefully and will be verified by a third party 2. Material used for centering rings will be of high quality	1. Centering rings will be purchased from a trusted and respected vendor and approved by the Project Manager and Vehicles Squad Lead prior to purchase 2. The Vehicles Squad Lead and the Safety Officer will both sign off on the Standard Launch Operating Procedures that the centering rings were installed properly 3. Procedures for installing centering rings will be made available for all team members	1	4	4

VS.10	Epoxy breaks from landing	1. High impact upon launch 2. Faulty recovery deployment leading to high descent velocity 3. Stiff ground 4. Disadvantageous landing position putting excess stress on the epoxy	1. Minor damage to launch vehicle 2. Additional time and resources spent rebuilding repairing broken components	2	3	6	Epoxy will be installed carefully and thoroughly to ensure a strong bond between launch vehicle components	1. Standard Workshop Operating Procedures for installing epoxy will be readily available for all team members 2. A design lead will be present whenever epoxy is being applied to ensure proper installation	1	3	3
VS.11	Epoxy melts near the fin	Heat generated by motor ignition	Weakened bonds leading to fractures before landing or during launch	2	3	6	1. Epoxy will be installed carefully and thoroughly to ensure a strong bond between launch vehicle components 2. A high quality epoxy will be selected with a consideration for its heat resistance	1. Standard Workshop Operating Procedures for installing epoxy will be readily available for all team members 2. A design lead will be present whenever epoxy is being applied to ensure proper installation 3. The epoxy selected will be from a respected and quality vendor and will be approved by the Project Manager and Vehicles Squad Lead before purchase	1	3	3
VS.12	Vehicle is dropped	1. Launch vehicle is not carefully carried 2. Reckless behavior	Minor to major damage of the launch vehicle	2	3	6	Team members will exercise extreme caution when handling the launch vehicle during integration and launch setup	Three members will be required to have both hands (one hand above the launch vehicle and one below) in contact with the launch vehicle whenever it is being moved	1	3	3
VS.13	Vehicle compone- nts vibrate inside vehicle during flight	Components are not secured properly during integration	Components may come lose and both cause and sustain substantial damage to vehicle during flight	3	4	12	All vehicle components will be securely fastened during integration and verified by the Safety Officer and Vehicles Squad Lead	The Safety Officer will include a section on the Standard Launch Operation Procedures ensuring that the Vehicles Design Lead oversees the fastening of all launch components during integration and verifies that they are properly fastened	1	4	4

Table 128: Vehicle Flight Mechanics Failure Modes and Effects Analysis

Label	Hazard	Cause	Outcome	Probability	Severity	Before	Mitigation	Verification	Probability	Severity	After
VFM.1	Launch vehicle is overstab- le	1. Improper placement of internal components in launch vehicle 2. Incorrect mass estimates 3. Center of gravity or center of pressure is not correctly estimated	Launch vehicle trajectory gradually turns towards the wind	3	4	12	1. Mass estimates will be closely monitored during construction 2. The center of pressure and center of gravity will be verified before launch 3. The center of pressure and gravity will be calculated after integration but before launch and compared to the experimental values	1. Mass of materials will be recorded on a shared spreadsheet readily available to all team members and continually updated as construction proceeds 2. The Safety Officer and Vehicle Squad Lead will sign off on this procedure agreeing that the center of pressure and center of gravity estimates match with the experimental values before proceeding with the Standard Launch Operating Procedures	1	4	4
VFM.2	Launch vehicle is overweig- ht	1. Incorrect mass estimates 2. Improper budgeting of material	1. Launch vehicle falls short of apogee 2. Shock cords experience more force when deployed, possibly leading to a fracture and sending the launch vehicle into free fall	2	3	6	1. Mass estimates will be closely monitored during construction 2. Material used will be recorded	1. Mass of materials will be recorded on a shared spreadsheet and readily available to all team members 2. Spreadsheet will be continually updated to keep up with design changes and the construction process	1	3	3
VFM.3	Launch vehicle is underwei- ght	1. Incorrect mass estimates 2. Improper budgeting of material	Launch vehicle reaches above predicted apogee and possibly violates NASA Req. 2.1.	2	3	6	1. Mass estimates will be closely monitored during construction 2. Material used will be recorded	1. Mass of materials will be recorded on a shared spreadsheet and readily available to all team members 2. Spreadsheet will be continually updated to follow design changes and the construction process	1	3	3

VFM.4	Fins fails to keep launch vehicle in a stable configur-ation	1. Improper sizing of fins 2. Fin material fails to withstand static loading of flight	Launch vehicle fails to maintain stability and gradually directs its trajectory into the wind, leading to weathercocking	2	4	8	1. Fin sizing will be carefully calculated to induce the necessary stability 2. Fins will be tested to ensure they can withstand maximum static loading	1. The Project Manager and Vehicles Squad Lead must agree to the shape and size of the fins before proceeding in their construction 2. Fin material will be purchased from a trusted and respected vendor and will be approved by the Project Manager and Vehicles Squad Lead prior to purchase 3. Fin material will be tested or analyzed to verify it can withstand the maximum static loading with a factor of safety of 1.5	1	4	4
VFM.5	Launch vehicle exits the launch rail with too low of an exit velocity	1. Faulty motor performance 2. Partial motor failure 3. Centering ring failure	Launch vehicle flight pattern is unpredictable	3	4	12	1. Motor will be properly and safety installed 2. Centering rings will be properly centered during integration 3. Motor selection will provide proper combustion to initiate successful launch	1. Team Mentor (NAR/TRA Level 3 Certified) Dave Brunsting will be the sole individual responsible for handling and installing all motor functions and will abide by NAR guidelines while doing so 2. Standard Launch Operating Procedures for installing the centering rings properly will be clearly listed and made available to all team members 3. Motor selection will provide the appropriate thrust needed for the launch vehicle's expected weight 4. Motor will be bought from a respected and trusted vendor and will be approved by the Project Manager and Vehicles Squad Lead prior to purchase	1	4	4

VFM.6	Launch vehicle fails to leave launch rail	1. Motor failure 2. Centering ring failure	1. Active motor remains inside launch vehicle 2. Team members are unable to confidently determine if the launch vehicle is safe to remove from launch rail 3. Complete mission failure	2	4	8	1. Motor will be properly and safety installed 2. Centering rings will be properly centered during integration 3. Motor selection will provide proper combustion to initiate successful launch	1. Team Mentor (NAR/TRA Level 3 Certified) Dave Brunsting will be the sole individual responsible for handling and installing all motor functions and will abide by NAR guidelines while doing so 2. Standard Launch Operating Procedures for installing the centering rings properly will be clearly listed and made available to all team members 3. Motor selection will provide the appropriate thrust needed for the launch vehicle's expected weight 4. Motor will be bought from a respected and trusted vendor and will be approved by the Project Manager and Vehicles Squad Lead prior to purchase	1	4	4
VFM.7	Incorrect launch angle	1. Incorrect calculation of vehicle flight path 2. Incorrect flight simulations	1. Unpredictable flight pattern 2. Potential for the vehicle to impact objects or persons that are not under proper precautions of the launch area if vehicle launches closer to the ground	1	4	4	1. Launch angle will be chosen based on careful calculation and analysis of the project flight patterns given the launch vehicle characteristics 2. Safe launch angle guidelines will be followed	Launch angle will be chosen on a quantitative basis based on the results from multiple rocket software simulations 3. All NAR and NASA guidelines will be observed when selecting a launch angle	1	4	4
VFM.8	Fin flutter	Incorrect calculation of forcing frequency of launch	Fins experience resonance possibly leading to fracture and a loss of stability	3	4	12	The team will calculate the velocity necessary for fin flutter to occur and ensure, via launch simulations, that it is not reached during launch	The calculated velocity and launch simulations will be approved or done by the Vehicles Squad Lead	1	4	4

Table 129: Recovery Failure Modes and Effects Analysis

Label	Hazard	Cause	Outcome	Probability	Severity	Before	Mitigation	Verification	Probability	Severity	After
R.1	Main parachute does not deploy	1. Parachute was installed incorrectly 2. Black powder charges failed to ignite 3. Shear pins held launch vehicle together through the detonation of black powder charges 4. Altimeter failed to send data to the separation charges	1. Launch vehicle lands with unacceptable descent velocity 2. Launch vehicle may sustain considerable damage 3. Launch vehicle landing creates unsafe landing area	3	4	12	1. Parachute installation will be closely monitored by the Recovery Squad Lead and Safety Officer 2. Procedures for installing the main parachute will be clearly defined 3. The recovery system will feature altimeter redundancy with proper shielding	1. Both the Recovery Squad Lead and Safety Officer will monitor the main parachute installation and sign off on the Standard Launch Operating Procedures that it was installed correctly 2. The system will feature altimeter redundancy with appropriate electromagnetic shielding material (i.e., electric tape) shielding any altimeter present from electromagnetic interference 3. Procedures for installing the main parachute will be clearly written out in the Standard Launch Operating Procedures and reviewed during the launch rehearsal the day before the launch 4. Parachute installation procedures will be readily available for all team members once written	2	4	8

R.2	Drogue parachut- e does not deploy	1. Parachute was installed incorrectly 2. Black powder charges failed to ignite 3. Shear pins held launch vehicle together 4. Altimeter failed	1. Launch vehicle likely lands with unacceptable descent velocity 2. Main parachute may not be able to sustain high shock of deployment 3. Launch vehicle landing may create an unsafe landing area 4. Shock cords must sustain a higher impulse when main parachute deploys due to higher descent velocity	3	3	9	1. Parachute installation will be closely monitored by the Recovery Squad Lead and Safety Officer 2. Procedures for installing the drogue parachute will be clearly defined 3. Shock cords will be reinforced in the event that the drogue parachute does not deploy 4. The recovery system will feature altimeter redundancy with proper shielding	1. Both the Recovery Squad Lead and Safety Officer will monitor the main parachute installation and sign off on the Standard Launch Operating Procedures that it was installed correctly 2. The system will feature altimeter redundancy with appropriate electromagnetic shielding material (i.e., electric tape) encapsulating any altimeter present which will be verified with inspection of the launch vehicle 3. Installing the main parachute will be clearly written out in the Standard Launch Operating Procedures and reviewed during the launch rehearsal the day before the launch 4. Shock cords will be capable of handling the maximum impulse of descent with a factor of safety of 1.5 5. Parachute installation procedures will be readily available for all team members once written	2	3	6
R.3	Launch vehicle fails to separate after apogee	1. Improper installation of black powder charges 2. Shear pins provide too much force for the charges to separate the launch vehicle	1. Main nor drogue parachute deploys, launch vehicle becomes ballistic 2. Launch vehicle sustains considerable damage upon landing	3	4	12	1. Black powder charges will be installed carefully and properly 2. Black powder charges will be tested before launch to ensure separation will occur	1. Team Mentor (NAR/TRA Level 3 Certified) Dave Brunsting will be responsible for handling and installing all energetics, and will abide by NAR regulations while doing so 2. The black powder charges will be tested and capable of separating launch vehicle components with the procedures available to all team members	2	4	8

R.4	Altimeter fails to ignite black powder charge	1. Altimeter fails to send data to separation charges for detonation 2. Faulty circuit wiring/soldering 3. Electrical interference 4. Loss of power 5. Dead battery	1. Launch vehicle does not separate 2. Parachute does not deploy and launch vehicle becomes ballistic	4	4	16	1. The recovery system will feature altimeter redundancy 2. Soldering activities will be closely reviewed to ensure quality electronic connections 3. Altimeters shall have proper electromagnetic shielding	1. Each recovery device will feature at least two altimeters which will be verified by inspection 2. Any altimeter present in the system will be properly shielded by an appropriate shielding material (i.e., electric tape) with will be verified by inspection of the launch vehicle 3. Soldering procedures will be approved by the ACS Squad and made easily accessible and available for all team members Lead	2	4	8
R.5	Main parachute deploys prematur- ely	1. Improper altimeter performance 2. Shear pins do not provide enough strength to hold launch vehicle together	Launch vehicle drifts outside acceptable radius from launch site, violating NASA Req. 3.10.	3	3	9	1. The recovery system will feature altimeter redundancy with proper shielding 2. Shear pins will be analyzed via simulations to ensure they will separate with a predetermined amount of black powder charge	1. Each recovery device will feature at least two altimeters with appropriate shielding material encapsulating it (i.e., electric tape) which will be verified by inspection of the launch vehicle 2. Test procedures for verifying shear pin and black powder charge strength will be available for all team members	2	3	6
R.6	Drogue parachut- e shroud lines tangle	Improper packing of drogue parachute	1. Drogue parachute will not adequately slow the launch vehicle's descent 2. Main parachute sustains considerably more shock during its deployment 3. Launch vehicle's descent may exceed the maximum descent velocity	3	3	9	Drogue parachute installation will be closely monitored by the Recovery Squad Lead and Safety Officer	1. Both the Recovery Squad Lead and Safety Officer will monitor the drogue parachute installation and sign off on the Standard Launch Operating Procedures that it was installed correctly 2. Parachute installation procedures will be readily available for all team members once written	1	3	3

R.7	Main parachut- e shroud lines tangle	Improper installation of main parachute	1. Main parachute will not adequately slow the launch vehicle's descent 2. Launch vehicle's descent may fall outside the maximum descent velocity, violating NASA Req. 3.3. 3. Landing area becomes unsafe	4	4	16	Main parachute installation will be closely monitored by the Recovery Squad Lead and Safety Officer	1. Both the Recovery Squad Lead and Safety Officer will monitor the drogue parachute installation and sign off on the Standard Launch Operating Procedures that it was installed correctly 2. Parachute installation procedures will be readily available for all team members once written	1	4	4
R.8	Parachut- e deploys below the minimu- m deploym- ent height	1. Improper parachute installation 2. Failure for altimeter to send calculations (or correct calculations) to separation charges	1. Launch vehicle descent velocity exceeds the maximum limit per NASA Req. 3.3. 2. Violation of NASA Req. 3.1.1. 3. Landing area becomes unsafe	3	4	12	1. Main and drogue parachute installations will be closely monitored by the Recovery Squad Lead and Safety Officer 2. The system will feature altimeter redundancy with appropriate electromagnetic shielding	1. Both the Recovery Squad Lead and Safety Officer will monitor the main and drogue parachute installation and sign off on the Standard Launch Operating Procedures that it was installed correctly 2. Parachute installation procedures will be readily available for all team members once written 3. The system will feature altimeter redundancy with appropriate electromagnetic shielding material (i.e., electric tape) which will be verified by inspection of the launch vehicle	2	4	8

R.9	Parachut- e deploys but fails to slow the launch vehicle below maximu- m descent velocity	1. Improper parachute installation 2. Improper parachute sizing 3. Altimeter fails to send correct data to separation charges	Launch vehicle descent velocity is above the maximum limit, violating NASA Req. 3.3.	3	3	9	1. Parachute sizing calculations will be closely reviewed 2. Main and drogue parachute installations will be closely monitored by the Recovery Squad Lead and Safety Officer	1. Both the Recovery Squad Lead and Safety Officer will monitor the main and drogue parachute installation and sign off on the Standard Launch Operating Procedures that it was installed correctly 2. The parachute will be bought from a trusted and respected vendor and approved by the Project Manager and Recovery Squad Lead prior to purchase 3. The system will feature altimeter redundancy with appropriate electromagnetic shielding material (i.e., electric tape) which will be verified by inspection of the launch vehicle	1	3	3
R.10	Drogue parachut- e does not leave the parachut- e bag	Improper drogue parachute installation	1. Drogue parachute fails to or only partially deploys 2. Main parachute shock cords must endure more force, possibly causing them to break 3. Descent velocity is uncontrolled and launch vehicle may become ballistic	3	4	12	Drogue parachute installation will be closely monitored by the Recovery Squad Lead and Safety Officer	1. A section on proper parachute installation procedures will be included on the Standard Launch Operating Procedures 2. Both the Recovery Squad Lead and Safety Officer will monitor the drogue parachute installation and sign off on the Standard Launch Operating Procedures that it was installed correctly 3. Parachute installation procedures will be readily available for all team members once written 4. Shock cords will be capable of handling the maximum impulse of descent with a factor of safety of 1.5	1	3	3

R.11	Frayed shock cords	Failure to examine shock cords before launch	1. Shock cords may not be able to handle parachute deployment force and may break upon separation, causing a ballistic descent	3	4	12	1. Shock cords will be calculated to withstand the expected loads during launch 2. Shock cords will be examined before launch	1. A section on checking the status of the shock cords will be included on the Standard Launch Operating Procedures 2. The Safety Officer and Recovery Squad Lead will sign off on the Standard Launch Operating Procedures to ensure shock cords are not frayed during integrating on launch day 3. Shock cords will be tested or analyzed to be able to withstand the maximum expected force during launch with a factor of safety of 1.5	1	4	4
R.12	E-match position cannot be verified	Inability to see inside the launch vehicle once fully integrated	1. Lack of confidence in altimeter and charge detonation statuses 2. Significant time spent verifying switch position because launch vehicle must be taken apart in order to see the E-match	5	1	5	Multiple team members will verify the E-match position before recovery is in the correct position	1. The Safety Officer will include a section verifying the completion of this integration step on the Standard Launch Operating Procedures 2. The Safety Officer, Recovery Lead, and at least three other members must verify that the E-match switches are in the correct setting before integrating it into the launch vehicle	1	1	1

R.13	Launch vehicle exceeds drift radius	1. Main and/or drogue parachute is installed incorrectly 2. Incorrect altimeter data 3. Software error	1. Launch vehicle becomes hazard for those not in the drift radius defined by NASA Req. 3.10. 2. Partial mission failure due to violation of NASA Req. 3.10.	3	3	9	1. The system will feature altimeter redundancy with proper shielding, parachute installation will be closely monitored 2. Software will be tested with test data to ensure its functionality	1. The system will feature altimeter redundancy with appropriate electromagnetic shielding material (i.e., electric tape) encapsulating any altimeter present and will be verified by inspection of the launch vehicle 2. Procedures for testing software with simulated data will be available for all team members once written 3. Procedures for installing the main and/or drogue parachute will be readily available for all team members once written and will be included on the Standard Launch Operating Procedures 4. The Recovery Squad Lead and Safety Officer will oversee the installation of the parachute and sign off on the Standard Launch Operating Procedures that its correct installation occurred	2	3	6
R.14	Main parachut- e is not pulled from parachute bag during flight	Improper main parachute installation	Launch vehicle is not sufficiently slowed, leading to an unsafe descent velocity and/or one that is unacceptable per NASA Req. 3.3.	3	4	12	Main parachute installation will be closely monitored by the Recovery Squad Lead and Safety Officer	1. Procedures for installing the main and/or drogue parachute will be readily available for all team members once written and will be included on the Standard Launch Operating Procedures 2. Both the Recovery Squad Lead and Safety Officer will monitor the main parachute installation and sign off on the Standard Launch Operating Procedures that it was installed correctly	1	4	4
R.15	Shock cords break	1. Failure to examine shock cords before launch 2. Incorrect calculations when sizing shock cords	Launch vehicle begins ballistic descent	3	4	12	Shock cords will be calculated to withstand the expected loads during launch	Shock cords will be tested or analyzed to be able to withstand the maximum expected force during launch with a factor of safety of 1.5	1	4	4

R.16	Nose cone fails to separate from launch vehicle	1. Altimeter fails to ignite black powder charges 2. Shear pins hold nose cone in place	1. Drogue parachute does not deploy, causing the launch vehicle a high descent velocity that may violate NASA Req. 3.3. 2. Payload is not able to deploy 3. Complete mission failure	3	4	12	1. There will be at least two altimeters with appropriate electromagnetic shielding present in each recovery bay to ensure redundancy 2. Shear pin selection will be based on calculations of expected force from the black powder charges and reviewed and approved before selection	1. The Recovery Lead will verify the calculations of the sheer pin selection 2. The system will feature altimeter redundancy with appropriate electromagnetic shielding material (i.e., electric tape) which will be verified by inspection of the launch vehicle	1	4	4

Table 130: Apogee Control System Failure Modes and Effects Analysis

Label	Hazard	Cause	Outcome	Probability	Severity	Before	Mitigation	Verification	Probability	Severity	After
ACS.1	ACS battery dies while the launch vehicle is on the launch pad	1. Battery is not charged sufficiently 2. Calculation for necessary battery is incorrect	Complete system failure	3	3	9	The ACS battery shall be capable of being operational for the maximum time (two hours) on the launch pad at the NASA SLI National Competition	The ACS battery will be capable of being operational for three hours starting from a full charge	1	3	3
ACS.2	ACS placeme-nt within the launch vehicle decreases stability during flight	1. Improper calculation of launch vehicle stability 2. Inaccurate mass estimates	Launch vehicle is unstable during flight	3	4	12	1. The ACS will be as close to the center of pressure as possible 2. The ACS will to be aft of the center of gravity location after burnout, per NASA Requirement 2.16.	The placement of ACS into the launch vehicle will be verified by the Vehicles Lead before construction to ensure it is at the correct location in relation to the vehicle's center of pressure and center of gravity	1	4	4

ACS.3	ACS fails to perform accurate actuation compar- ed to predicted estimates	1. Improper calculation for system performance during launch 2. Software errors 3. Insufficient servo motor	Improper actuation	4	2	8	1. The servo motor will be capable of performing accurate actuation under predicted maximum static loading 2. The software will be continually reviewed to ensure it is accurate to flight conditions	1. The ACS shall be tested to perform accurate actuation under the maximum static loading with a factor of safety of 1.5 2. The software will be tested by using simulated data to perform the various required functions of the system	2	1	2
ACS.4	Actuation tabs are not securely fastened before launch	Improper fastening during integration	1. Actuation tabs fracture during launch creating debris 2. System does not function properly	3	3	9	The ACS Squad Lead will ensure that, during integration, actuation tabs are securely fastening to the launch vehicle before completing ACS integration	The Safety Officer and ACS Squad Lead will inspect the fastening of the actuation tabs and sign off on the Standard Launch Operating Procedures that it was done correctly	1	3	3
ACS.5	Frayed electrical wires	1. Poor wire organization 2. Failure to inspect wire condition 3. High usage of electrical wires	Short circuiting	2	4	8	1. The ACS will minimize the number of physical wires used and maximize the distance between those that remain 2. Wires will be neatly organized to avoid frayed electrical wires 3. Wires will be continually inspected to identify fraying	1. The ACS will use a printed circuit board (PCB) to avoid short circuits and promote wire management 2. Heat shrink will be used to cover any frayed wires 3. The only physical wires present will be those connecting to the servo motor and battery	1	3	3
ACS.6	Servo motor interfer- ence	Heavy current draw from the motor and continuous change in current, creating a magnetic field	Motor experiences partial or complete failure	1	3	3	1. Shielding will be put over the servo motor to prevent interference 2. Continuous changes in current draw will be minimized	1. The servo motor will only turn on and off once during flight, minimizing current change 2. Electrical tape will be put over the servo motor to prevent a magnetic field becoming present	1	2	2
ACS.7	Insuffici- ent voltage provided to batteries	Current draw from servo motor takes away from that of batteries	Microcontroller may behave erratically	2	3	6	Stall current of servo motor and other components will be limited	Servo motor and other components requiring current draw shall not exceed a combined current of three amps	1	3	3

ACS.8	Servo motor current is too strong	Stall current of motor is too high	System may overheat or explode	3	4	12	Stall current of servo motor will be limited	Servo motor will be chosen and purchased that is reliable and does not exceed a stall current draw of three amps	1	4	4
ACS.9	Altimeter fails to send data to servo motor	1. Failure of batteries 2. Errors in software	Complete system failure	3	3	9	The ACS will implement redundancy to account for the failure of an altimeter	1. Two altimeters will be present with appropriate electromagnetic shielding in the ACS to ensure redundancy 2. Redudancy of ACS will be verified with inspection of the launch vehicle	2	3	6
ACS.10	Noisy signal data from servo motor	Software composition	Vibration of drag flaps when extended and suboptimal performance	3	2	6	The signal to the servo motor will be streamlined	A pulse-width modulation (PWM) controller will be present in the ACS to prevent noisy signal to the servo motor	1	2	2
ACS.11	PWM to servo motor is ripped or disconne- cted	Mismanaged wires	1. Other wires may be ripped or disconnected 2. System or individual component failure 3. Fire may occur inside ACS bay from ripped wires	3	4	12	1. The ACS will minimize the number of physical wires used and maximize the distance between those that remain 2. Wires will be neatly organized to avoid frayed electrical wires 3. Wires will be continually inspected to identify fraying	1. The ACS will use a PCB to avoid short circuits and promote wire management 2. The only physical wires present will be those connecting to the servo motor and battery	1	4	4

Table 131: Payload Failure Modes and Effects Analysis

Label	Hazard	Cause	Outcome	Probability	Severity	Before	Mitigation	Verification	Probability	Severity	After
TROI.1	Interfer- ence from other sensors and other electron- ics	Improper shielding of sensors and electronics may interrupt transmission to or from the payload system	Launch vehicle status is not properly assessed, causing the system to fail to extend from body tube and complete mission	2	4	8	Proper shielding will be installed on all applicable payload components	The shielding for the electronics will be tested and verified prior to use by the electronics subteam and the Payload Lead	1	4	4

TROI.2	Other systems physical- ly or mechanic- ally interfere with payload system	Improper organization and placement of various systems	Payload is damaged and may not be able to function as intended	3	3	9	The payload system will be placed to not interfere with the recovery system	The Payload Lead will verify with the other design leads that the placement of the system does not harm the functionality of other launch vehicle systems	1	3	3
TROI.3	Camera fails to capture images of objects other than vehicle body tube	1. Improper orientation of payload camera 2. Improper sizing of extension arm 3. Incorrect calculation in software 4. Motor failure	Partial mission failure as payload fails to take all necessary photos, violating NASA Req. 4.2.1.	3	3	9	The payload will raise the camera system above the vehicle tube to provide for clear images	The payload will be tested at different landing angles and configurations	2	3	6
TROI.4	Payload battery dies during launch	1. Improper selection of battery 2. Insufficient consideration of temperature's impact on battery health	Payload fails to function	3	4	12	The payload battery shall be capable of being operational for the maximum time (two hours) on the launch pad at the NASA SLI National Competition	1. The payload battery will be capable of being operational for three hours starting from a full charge which will be verified with a battery test 2. The procedures for testing the payload battery will be made available to all team members once written	1	4	4
TROI.5	Payload system is set to the wrong radio frequen- cy	Improper selection of radio frequency prior to launch	Payload fails to receive any commands from ground station and thus is a complete mission failure	2	4	8	The payload system shall be tested to confirm it receives sample radio commands on the correct frequency prior to launch in accordance with NASA Req. 4.2.3.1.	The Safety Officer will include a section on the Standard Launch Operating Procedures to ensure that the radio frequency is at the correct setting prior to integration before launch	1	4	4

TROI.6	Camera breaks or is damaged during or upon landing	Camera system was not properly retained or securely fastened	Camera fails to take images demanded	3	4	12	1. Camera system is tested to verify it can handle maximum descent kinetic energy 2. The camera system will be securely fastened to the payload and approved by the Safety Officer and Payload Squad Lead prior to launch	1. Test procedures to conduct the camera durability test will be readily available for all team members 2. Procedures for fastening the camera system to the payload will be included on the Standard Launch Operating Procedures	1	4	4
TROI.7	Low quality image	1. Quality of camera is insufficient Camera is in motion when picture is taken 3. Debris falls onto the camera	1. Images related to ground station are not acceptable 2. Partial mission failure	2	3	6	1. The payload system will utilize a high quality camera 2. The payload system will be tested at different configurations to verify that the camera is stationary before taking a picture	1. The camera selected will be from a trusted and respectable vendor which will be approved by the Payload Squad Lead and Project Manager 2. Test procedures for verifying the camera's motion will be readily available for all team members	1	3	3
TROI.8	Images are not stored after being taken	1. Improper software structure 2. SD card runs out of space	Complete mission failure	3	4	12	The payload digital storage space will be verified prior to every launch and/or payload test	The Safety Officer will include a section on the Standard Launch Operating Procedures that the digital storage space will be verified prior to launch and the completion of this test will be verified by the Payload Lead	1	4	4
TROI.9	Time stamps for resultant images are inaccura- te	1. Incorrect software structure 2. Improper syncing of clock	1. Images sent to ground station are of the incorrect time 2. Partial mission failure 3. Failure of NASA Req. 4.2.1.3.	2	3	6	The payload system will pass a basic functionality test prior to being used, which includes verification of proper timestamps on images	Test procedures to conduct this test will be readily available for all team members	1	3	3

Table 132: Payload Integration and Deployment Failure Modes and Effects Analysis

Label	Hazard	Cause	Outcome	Probability	Severity	Before	Mitigation	Verification	Probability	Severity	After
TROII.1	Water damage	1. Launch vehicle lands in water which seeps into the payload bay 2. Precipitation during launch leads to water presence inside payload bay	1. System experiences partial or complete failure from water damage 2. Possibility of short circuiting and other electrical damage from water exposure to payload electronics	2	4	8	1. All electronics will be tested before integration into launch vehicle 2. A bulkhead will be installed within the payload bay just above the electronics to prevent water presence in the electronics bay	1. The Safety Officer will include a section in the Standard Launch Operating Procedures concerning the electronics test prior to integration 2. The bulkhead's presence in the launch vehicle will be verified via inspection of the launch vehicle	1	3	3
TROII.2	Payload deploym- ent is limited by an obstruct- ion	1. Disadvantag- eous landing orientation 2. Large debris in ground where launch vehicle lands	1. Payload fails to fully deploy 2. Partial or complete mission failure	1	4	4	The payload system will feature an emergency stopping software component that automatically halts deployment (and takes pictures from that point) if the system senses an obstruction. Its functionality verified through testing	The procedures for conducting the functionality test for the emergency stopping system will be readily available for all team members	1	3	3
TROII.3	Sensors fail to accurate- ly assess launch vehicle status	Software composition of system was done incorrectly	Payload fails to leave the launch vehicle and complete its mission	4	4	16	All sensors will have verified functionality prior to launch	The Safety Officer will include a section on the Standard Launch Operating Procedures to ensure that sensors are tested prior to launch to verify the system can assess the launch vehicle status	1	4	4
TROII.4	Payload retention system is damaged or complete-ly fails	Retention system strength and durability were unable to withstand forces associated with launch and landing	Camera system fails to extend outwards and capture required images	3	4	12	Retention system will be made of a material that is durable and capable of withstanding reasonable landing forces	Retention system will be tested with differing forces with simulation software to verify that no damage occurs upon landing	2	4	8

TROII.5	Motors lack enough torque to meet system demands	Trade studies and evaluation of components were done incorrectly	Payload fails to operate in any capacity	2	4	8	Trade studies and calculations associated with system demands will be done twice to ensure redundancy	Selected motors will be checked and approved by the Payload Lead	1	4	4

Table 133: Launch Equipment Failure Modes and Effects Analysis

Label	Hazard	Cause	Outcome	Probability	Severity	Before	Mitigation	Verification	Probability	Severity	After
LE.1	Insufficie- nt launch material is brought to the launch site	Inadequate planning during launch rehearsal and morning of launch	1. Insufficient material to complete integration 2. Unnecessary time is spent retrieving additional material 3. Launch window may be missed	4	2	8	1. A packing list will be developed to ensure that all necessary items are brought to the launch site 2. Team members will work together before the launch to complete this packing list	1. The Safety Officer will be responsible for creating Standard Launch Operating Procedures which will include a comprehensive packing list 2. The team will conduct a launch rehearsal the night before the launch to pack all necessary items on the listitems will be checked the morning of the launch before departure by the Safety Officer for additional redundancy	2	2	4
LE.2	Launch rail is at an incorrect angle	1. Incorrect calculation of predicted flight path 2. Inattentiveness during launch setup	1. Uncontrollable flight path 2. Potential for launch vehicle to impact objects or persons that have taken proper precautions	2	4	8	1. Launch angle will be closely monitored during flight setup 2. The Range Safety Officer (RSO) will monitor the launch setup 3. The team will use NAR guidance and regulations to determine the appropriate launch angle	1. The Safety Officer and the Vehicles Squad Lead will be responsible for ensuring the launch vehicle is set to the proper angle 2. NDRT Mentor Dave Brunsting will be responsible for setting the launch vehicle to the proper angle 3. The RSO will verify that the launch vehicle is set to a proper angle that is within 30 degrees of the vertical, per NAR regulations	1	4	4

LE.3	Launch wires do not function	1. Improper wiring 2. Wires are in need of replacement	Launch vehicle fails to initiate motor burn and flight does not occur	2	4	8	1. The team will only launch at official NAR/TRA launch sites 2. The team will verify that the wires are functional before launch	1. The team will primarily launch at the Michiana Rocketry Club's launch field on official launch days. Alternative sites will also be assured to be NAR/TRA certified before traveling to them 2. The RSO will verify that all components are functional before launch	1	4	4
LE.4	Launch wires are live during vehicle setup	Failure to check wire status before vehicle setup	Launch vehicle may initiate launch prematurely before team members have had time to leave the launch rail	2	4	8	The team will verify that the launch wires are not live before bringing the launch vehicle to the launch rail	1. The team will verify with the RSO that the launch wires are not live 2. The Safety Officer will include the step to verify launch wires are not live on the Standard Launch Operating Procedures	1	4	4

8.6 Environmental Risks

Table 134: Vehicle Risks to Environment

Label	Hazard	Cause	Outcome	Probability	Severity	Before	Mitigation	Verification	Probability	Severity	After
VE.1	Motor explosion expels gases into atmosph-ere	Low-quality motor purchase	1. Emitted gases from explosion may harm local wildlife 2. Emitted gases contribute to global warming by acting as greenhouse gases	5	2	10	1. The purchased motor will be of high quality and expel minimal emissions into the atmosphere 2. Minimal black powder charges will be used 3. Distance from those that an explosion would impact will be maximized	1. The launch vehicle will be launched in an open field, void of most wildlife 2. The motor will be selected by a reputable vendor and reviewed by the Vehicles Squad Lead and the Project Manager to ensure that is it an environmentally conscious purchase 3. The team will analyze, determine, and use the minimum amount of black charges needed to safely initiate a successful recovery sequence 4. All team members and bystanders will be required to stay a minimum of 300 feet away from the launch rail, per NAR guidelines	5	1	5
VE.2	Launch vehicle hits tree	1. Uncontrollable flight path 2. High winds 3. Improper motor installation	1. Minor to major damage to launch vehicle 2. Possible harm to tree and thus local environment	2	3	6	The launch vehicle will launch in area that is void of trees and other wildlife	1. The team will primarily launch at the Michiana Rocketry Club launch site which is in a farming area with minimal trees present 2. The Safety Officer and other design leads will inspect the site upon arrival (if not the Michiana Rocketry Club launch site) to ensure that minimal trees are present	1	3	3
VE.3	Launch vehicle hits a power line	1. Uncontrollable flight path 2. High winds 3. Improper motor installation	1. Electrical fire or explosion 2. Partial or complete loss of launch vehicle 3. Loss of power for local residents 4. Property damage from fire 5. Loss of funds from property repairs	2	4	8	The launch vehicle will launch in area that is void of power lines	1. The team will primarily launch at the Michiana Rocketry Club launch site which is in a farming area with minimal power lines present 2. The Safety Officer and other design leads will inspect the site upon arrival (if not the Michiana Rocketry Club launch site) to ensure that minimal power lines are present	1	4	4

VE.4	Launch vehicle hits spectato- rs, the crowd, or a team member	1. Uncontrollable flight path upon launch 2. Poor visibility 3. Drogue or main parachutes fail to deploy 4. Inattentive spectators/team members 5. Unacceptable drift radius	Serious injury or death to personnel hit by launch vehicle	2	4	8	1. All team members and bystanders will be required to remain at least 300 feet, the NAR-derived Minimum Safe Distance, away from the launch vehicle before launch 2. All team members will be knowledgeable in safe operating procedures in watching the launch vehicle descend	1. The RSO and Safety Officer will ensure that all team members and bystanders abide by the Minimum Safe Distance measurement before launch 2. All team members will be reminded of the safe operating procedures should the launch vehicle be descending in their vicinity	1	4	4
VE.5	Launch vehicle hits a car	1. Uncontrollable flight path 2. Unacceptable drift radius 3. Parachutes fail to deploy	1. Minor or major damage to car 2. Sustained damage to launch vehicle 3. Possibility of fire or explosion if launch vehicle hits the car at a critical point 4. Potential legal action from the victim	3	3	9	1. Launch attendees will be reminded of the danger that they put their vehicles in by parking near the launch site 2. The team will use minimal transport to attend the launch	1. The Safety Officer will remind the team of the dangers that owner's cars face by attending the launch during the Launch Rehearsal the day before the launch 2. Carpooling will be utilized in order to minimize cars at the launch site	3	3	9

VE.6	Launch vehicle lands on a major road	1. Unacceptable drift radius 2. Uncontrollable flight path	1. Potential for complete loss of launch vehicle if hit by oncoming traffic 2. Presence of launch vehicle becomes major road hazard and causes traffic 3. An oncoming car that hits the launch vehicle will sustain major damage and possibly become involved in an accident 4. Motor may explode from being run over by traffic	2	4	8	The launch vehicle will launch in area that is void of major roads or highways	1. The team primarily launches at the Michiana Rocketry Club launch site, a site where no major roads are present within the maximum allowable drift radius, per NASA Req. 3.10. 2. The Safety Officer and other design leads will inspect the launch site (if different than the Michiana Rocketry Club launch site) upon arrival to ensure that no major roads are present within the maximum allowable drift radius from NASA Req. 3.10.	1	4	4
VE.7	Launch vehicle expels carbon dioxide into air	Natural byproduct of combustion reactions	1. Contribution to greenhouse gas emissions into atmosphere 2. Decrease in air quality for local residents	5	2	10	The purchased motor will be of high quality and expel minimal emissions into the atmosphere	The motor will be selected by a reputable vendor and reviewed by the Vehicles Squad Lead and the Project Manager to ensure that it is an environmentally sound purchase	5	1	5
VE.8	Launch vehicle hits a house	1. Uncontrollable flight path 2. Unacceptable drift radius 3. Parachutes fail to deploy	Minor or major damage to house 4. Potential to injury and inhabitants that were present when the launch vehicle impacted the building 5. Potential legal action from inhabitants of house that is hit	2	4	8	The launch vehicle will launch in area that is void of houses	1. The team will primarily launch at the Michiana Rocketry Club launch site which is in a farming area with minimal houses present 2. The Safety Officer and other design leads will inspect the site upon arrival (if not the Michiana Rocketry Club launch site) to ensure that minimal houses are present	1	4	4

VE.9	General waste	Team members do not clean up general waste (i.e., food wrappers, water bottles) before departing the launch site	1. Immediate launch site environment health is harmed 2. Nearby water sources may be harmed from any debris that spills over into it 3. Wildlife may attempt to eat general waste and become physically injured	4	2	8	1. Team members will be responsible for ensuring all waste is cleaned up before departing the launch site 2. The Safety Officer will ensure that waste cleanup occurs	1. The Safety Officer will include a step on the Standard Launch Operating Procedures to clean up all general waste 2. All team members will be required to inspect the team's setup area to confirm no waste is left behind	2	2	4
VE.10	Launch vehicle equipme- nt waste	General operating of launch vehicle may leave behind trace waste materials (i.e., chipped paint, string from parachutes)	1. Immediate launch site environment health is harmed 2. Nearby water sources may be harmed from any debris that spills over into it 3. Wildlife may attempt to eat general waste and become injured	5	2	10	1. Team members that assist in any stage of launch will be responsible for ensuring all launch vehicle waste is cleaned up in the area of their respective stage 2. The Safety Officer will ensure that waste cleanup occurs	1. The Safety Officer will include a step to inspect the area where the launch vehicle is integrated, launched from, and recovered to find any launch vehicle waste and dispose of it properly 2. All team members that assist in any stage of the launch will be required to analyze their immediate area for any launch vehicle waste before moving onto the next stage of the launch	2	2	4
VE.11	Improper disposal of chemical- ly hazardo- us materials during launch	1. Improper knowledge of chemical waste	1. Potential contamination of soil and water sources 2. Harm to wildlife	2	3	6	All team members will be knowledgeable of and how to dispose of the materials that need to be disposed of differently than general waste due to their chemical nature before the launch	Procedures for disposing of chemically dangerous materials will be published by the Safety Officer and readily available for all team members	1	3	3

VE.12	Fire	Motor combustion may set fire to the landscape upon launch	1. Immediate damage to the launch site soil 2. Land is temporarily unable to be used for agriculture or any other purpose 3. Serious physical harm or death to any wildlife in that area	2	3	6	1. Fire extinguishers will be available in the event of a fire during launch 2. The launch rail will be located in an area void of flammable objects 3. The motor selected will be of high quality	1. The Safety Officer will confirm that the launch rail is in an area void of flammable objects before launch 2. The motor purchased will from a trusted and respectable vendor and approved by the Project Manager and Vehicles Lead prior to purchase	1	3	3
VE.13	High noise levels during launch	Launch generates loud sound source to the surrounding area	1. Possible hearing damage to nearby wildlife and/or bystanders 2. Startling of local wildlife can lead to unsafe conditions for bystanders nearby	4	2	8	1. The launch vehicle will be launched in an area void of most wildlife and bystanders 2. Appropriate ear protection will be provided as needed	The team will launch their launch vehicle in an open farm, far from most houses and wildlife	1	2	2
VE.14	Battery acid leakage	Failure for the battery components to remain closed	Acidity leaks out of the battery and contaminates the soil and/or water sources	3	3	9	1. All team members will be knowledgeable of the disposal of faulty batteries 2. The battery used will be of high quality	1. All batteries will be inspected prior to launch and will be a step on the Standard Launch Operating Procedures 2. Team members will be able to access procedures for how to dispose of faulty batteries 3. Batteries purchased will be from a trusted vendor and approved by the Project Manager prior to launch	1	3	3
VE.15	High-velocity impact upon landing	Partial or complete failure of recovery system	Damage to the soil in contact with the launch vehicle that would be used for agriculture	2	2	4	The recovery system will be thoroughly and carefully integrated into the launch system to ensure a soft landing	1. The recovery integration will follow the Standard Launch Operating Procedures written by the Safety Officer	1	2	2

Table 135: Environment Risks to Vehicle

Label	Hazard	Cause	Outcome	Probability	Severity	Before	Mitigation	Verification	Probability	Severity	After
EV.1	Vehicle experien- ces high drift radius during recovery stages	High winds	1. Launch vehicle is potentially lost 2. Launch vehicle may land in a congested area of people, wildlife, or structures 3. Launch vehicle lands outside of acceptable drift radius, violating NASA Req. 3.10.	3	3	9	The team will not launch in wind speeds of higher than 20 mph	The Safety Officer will continually monitor the weather forecast in the week preceding the launch to ensure that winds stay within acceptable ranges. If forecasted or actual wind speeds exceed 20 mph during launch day, the launch will be postponed	1	3	3
EV.2	Failure of batteries or other electrical compone- nts	Cold temperatures decrease battery and electronics performance	1. Individual systems fail to perform basic functions 2. Complete or partial mission failure	3	4	12	1. The team will not launch in temperatures lower than 15 degrees Fahrenheit 2. Batteries will not be stored in cold temperatures 3. All electronics will be tested to ensure that they are capable of performing at temperatures ranging from 0 to 100 degrees Fahrenheit, per NDRT Requirement IN.1	1. Procedures for conducting an electronics/battery test for verifying functionality in cold temperatures will be made available for all team members once written 2. The Safety Officer will continually monitor the weather forecast in the week preceding the launch to ensure that temperatures remain in acceptable conditions. If expected (or observed if on the day of the launch) temperatures fall below 15 degrees Fahrenheit, the launch will be postponed 3. Batteries and other electronics will be stored at room temperature whenever possible while setting up for launch	1	4	4

EV.3	Water leaks into launch vehicle	1. Rain, snow, sleet, or high humidity brings high moisture presence around launch vehicle 2. Insufficient fastening and tightening of launch vehicle subcomponents	1. Electrical fires or explosions due to water coming into contact with electronics 2. Partial or complete mission failure	3	4	12	1. The team will not launch in an area with any form of precipitation 2. Batteries/electronics and the launch vehicle will be kept dry whenever possible	The Safety Officer will continually monitor the weather forecast in the week preceding the launch to ensure that precipitation chances remain minimal. If expected (or observed if on the day of the launch) precipitation is apparent launch will be postponed, batteries/electronics and the launch vehicle will be stored inside the workshop and in a dry area until it is necessary to launch	1	4	4
EV.4	Physical damage to launch vehicle or electroni- cs	Hail	1. Hail may hit critical launch components, causing partial or complete mission failure 2. Fire or explosion if hail hits motor	1	4	4	The team will not launch in hail	The Safety Officer will continually monitor the weather forecast in the week preceding a launch. If it is apparent (or observed on launch day) that there is hail present, the launch will be postponed	1	4	4
EV.5	Electrical discharge during launch	Rain, snow, thunderstorms	1. Electrical fires or explosions 2. Electrical components fail to function during launch	2	4	8	The team will not launch with any form of precipitation	The Safety Officer will continually monitor the weather forecast in the week preceding a launch. If it is apparent (or observed on launch day) that there is precipitation, the launch will be postponed	1	4	4
EV.6	Inability to track launch vehicle moveme- nt	Fog	1. Loss of launch vehicle 2. Inability to notify spectators or team members if returning vehicle is inbound towards them	3	3	9	The team will not launch in an area with considerable fog or generally low visibility	The Safety Officer will continually monitor the weather forecast in the week preceding a launch. If it is apparent (or observed on launch day) that there is low visibility and/or fog, the launch will be postponed	1	3	3

EV.7	Unstable launchi- ng ground	The ground on which the launch pad is located is too wet to provide stable ground	Launch vehicle launches at an unacceptable or unpredictable launch angle	3	4	12	1. If considerable precipitation has occurred in the days and weeks leading up to the launch that would give reason to believe the launch pad would not be on stable ground, the launch will be postponed 2. The team and RSO will ensure that the ground the launch pad is located on is firm and suitable for using as a base for the launch pad and launch vehicle	1. The Safety Officer will inspect the ground where the launch pad is located and ensure it is stable to provide appropriate support for the launch 2. The RSO will provide further confirmation that the ground is firm enough to launch a launch vehicle from 3. The Safety Officer will continually monitor the weather forecast in the week preceding a launch. If it is apparent (or observed on launch day) that there is considerable precipitation that would cause the launch pad to not be on stable ground, the launch will be postponed until this condition is met	1	4	4
EV.8	Thermal expansi- on of launch vehicle compon- ents	High temperatures	1. Launch vehicle fails to integrate properly 2. Increased pressure on joints possibly leading to fractures	2	2	4	1. Launch vehicle components will be kept in room temperature for as long as possible 2. The team will not launch in considerably high temperature	1. The team will not launch in temperatures higher than 90 degrees Fahrenheit The Safety Officer will continually monitor the weather forecast in the week preceding the launch to ensure that temperatures remain in acceptable conditions. If expected (or observed if on the day of the launch) temperatures cross above 90 degrees Fahrenheit, the launch will be postponed 3. Launch vehicle components will be kept in the workshop or another temperature-controlled environment and only brought outside when needed for integration and launch 4. When the launch vehicle is at the launch site, it will be left in a car or another moderate temperature environment until needed	1	2	2

EV.9	Thermal contract- ion of launch vehicle compon- ents	Cold temperatures	1. Launch vehicle fails to integrate properly 2. Increased pressure on joints possibly leading to fractures	3	2	6	1. Launch vehicle components will be kept in room temperature for as long as possible 2. The team will not launch in considerably high temperature	1. The team will not launch in temperatures lower than 15 degrees Fahrenheit 2. The Safety Officer will continually monitor the weather forecast in the week preceding the launch to ensure that temperatures remain in acceptable conditions. If expected (or observed if on the day of the launch) temperatures fall below 15 degrees Fahrenheit, the launch will be postponed 3. Launch vehicle components will be kept in the workshop or another temperature-controlled environment and only brought outside when needed for integration and launch 4. When the launch vehicle is at the launch site, it will be left in a car or another moderate environment until needed	1	2	2
EV.10	High voltage	1. Increased temperatures increase resistance of wires	1. Overheating 2. Possible electrical fires or explosions 2. Failure of critical system components	2	4	8	1. High quality electrical components will be used 2. The team will not launch in temperatures above 90 degrees	1. Electrical components will be from a trusted vendor and approved by the Project Manager before purchase 2. The Safety Officer will continually monitor the weather forecast in the week preceding a launch. If it is apparent (or observed on launch day) that there are temperatures exceeding 90 degrees Fahrenheit or a lightning storm, the launch will be postponed	1	4	4
EV.11	Uncontr- ollable launch vehicle trajectory	1. High winds 1. Lightning	1. Launch vehicle flies in unpredictable trajectory 2. Possibility to land in areas of high population or wildlife density	2	4	8	The team will not launch in winds exceeding 20 mph or in a lightning event	The Safety Officer will continually monitor the weather forecast in the week preceding a launch. If it is apparent (or observed on launch day) that there is winds exceeding 20 mph or a lightning storm, the launch will be postponed	1	4	4

EV.12	Launch vehicle is struck by lightning	Presence of thunderstorm	1. Electrical fires or explosions 2. Complete or partial launch vehicle 3. Debris being released from the launch vehicle with possibility of hitting persons or team members	2	4	8	The team will not launch in a lightning storm	The Safety Officer will continually monitor the weather forecast in the week preceding a launch. If it is apparent (or observed on launch day) that there is a lightning storm, the launch will be postponed	1	4	4

8.7 Project Risks Analysis

Table 136: Project Risks

Label	Hazard	Cause	Outcome	Probability	Severity	Before	Mitigation	Verification	Probability	Severity	After
PR.1	Team depletes all available funds	1. Reckless spending 2. Lack of organized budget	1. Team no longer has funds to continue the competition 2. Complete mission failure	1	4	4	1. The team will limit purchases to only those necessary for project success	1. The Project Manager will meet with each squad to determine a reasonable budget for each squad 2. The Project Manager will be responsible for creating a budget spreadsheet that tracks all purchases 3. The Project Manager will set up a form to allow for necessary team purchase requests which can be approved or rejected at the Project Manager's discretion	1	4	4
PR.2	Team misses a major delivera- ble report to NASA Student Launch Initiative	Inadequate project management planning	1. Disqualification from competition 2. Complete mission failure	2	4	8	The team will set internal deadlines in addition to NASA derived deadlines to ensure the team meets deliverable requirements	The Project Manager will meet with each squad at the beginning of the academic year to set reasonable internal deadlines, which will be visualized through the use of Gantt Charts	1	4	4
PR.3	Team member becomes sick	1. Seasonal illnesses 2. General spreading of illness in high population density areas such as college campuses	1. Member is unable to fully participate in team mission 2. Potential for illness to progress to a more serious affliction	5	1	5	Team members will be encouraged to monitor their own health and refrain from engaging in team activities and meetings if they feel ill	All team members are required to sign a team contract to participate in any construction or attend any launches, which includes a clause on refraining from attending meetings and/or launches if one feels ill	5	1	5

PR.4	Team member is infected with COVID-19	Prevalence of COVID-19 in the United States	1. Member is unable to fully participate in team mission for duration of their sickness 2. Possibility of the virus progressing to a more serious affliction 3. COVID-19 may pass onto other team members resulting in depleted productiveness	3	3	9	1. Team members will be encouraged to monitor their own health and test if they suspect they have COVID-19 2. Team members will take appropriate precautions to prevent infection and spreading of COVID-19	1. All team members are required to sign a team contract to participate in any construction or attend any launches, which includes a clause on refraining from attending meetings and/or launches if they test positive for COVID-19 2. All team members will abide by the University requirements on COVID-19 testing, contact tracing, masking, and isolation/quarantine	2	3	6
PR.5	Noncom- pliance with regulati- ons set forth by FAA, NAR, or TRA	Inattention or lack of knowledge of regulations	Potential legal action and unsafe launch conditions	3	4	12	Team members will be informed of relevant regulations as they pertain to the design process and launch	1. The Safety Officer and Project Manager will be responsible for informing team members about relevant FAA, NAR, and TRA regulations 2. FAA, NAR, and TRA regulations will be readily accessible for team members	1	4	4
PR.6	Loss of team members	1. Lack of interest or participation as the school year progresses 2. Schoolwork becomes increasingly demanding on team members' schedules	1. Lack of personnel to complete necessary tasks 2. Increased strain on remaining team members	5	2	10	1. Understanding of the natural decrease of members in a voluntary club 2. Respect for those that must leave the design team 3. Improved understanding of an individual's responsibility on the team	1. Design Leads and other involved members are aware of assuming added responsibilities from any team member that may choose to leave the club 2. The team will make team meetings engaging and enjoyable 3. Team members will work on tasks that are appropriate for their knowledge level 4. The team will promote a culture that is accepting of any team member that chooses to leave	4	1	4

PR.7	Shipping and manufa- cturing delays	1. Global supply chain issues 2. General logistics of shipping goods	1. Lack of material to perform tests or aid in construction 2. Elevated time constraint to complete major deliverables by deadlines	5	2	10	1. Parts will be ordered well in advance of their intended use timeline 2. An organized system for ordering parts with the team's budget will be implemented	1. A purchase request form is currently open for any lead that wishes to purchase a piece for construction 2. Leaders are consistently reminded to order parts as early as they can	4	2	8
PR.8	Insuffic- ient testing material	1. Lack of available testing equipment on campus 2. Certain testing equipment is restricted for undergraduate students	1. Inability to verify the functionality of certain system 2. Confidence in launch vehicle safety is compromised due to lack of understanding of how systems function	3	3	9	1. Appropriate staff with access to requested testing equipment are reached out to well in advance of deliverable deadlines 2. Appropriate research is done on design functionality 3. Different systems that can be appropriately tested are explored	1. Appropriate staff are contacted at least two months ahead of the deliverable or testing deadline for the particular system 2. If a system cannot be tested, appropriate research and analysis will be done in place of the test and will be approved by the appropriate design lead, Safety Officer, and Project Manager before it is proceeded with 3. The team will explore at least one different concept that can be appropriately tested and verify that it is not more efficient or effective than the original design before proceeding with the concept that cannot be appropriately tested (which would be analyzed and researched in place of being tested)	1	3	3
PR.9	Missing PPE	Necessary PPE is used and not refilled in a timely manner	Team members are not able to safely participate in construction, halting the assembly process	4	3	12	1. The Safety Officer will be responsible for inspecting and purchasing additional PPE 2. Team members will be encouraged to report missing PPE to the Safety Officer	1. The Safety Officer shall conduct an inspection of the workshop to identify missing PPE every two weeks. Missing PPE will promptly be reported to the Project Manager to purchase additional equipment 2. Team members will be encouraged to reach out to the Safety Officer with reports of any missed PPE	1	3	3

8.8 Workshop Safety

Being knowledgeable of the inherent risks construction poses to team members and what mitigations have proven to be successful, the Notre Dame Rocketry Team will be continuing construction safety mitigations from the 2021-2022 season. These practices primarily include the Workshop Safety Agreement, otherwise known as the Safety Contract. All members are required to sign this contract to participate in any construction of the launch vehicle and attend any launches. The Safety Contract outlines basic safety practices and agreements to follow directions of the RSO and Safety Officer at all times. To date, 38 team members have signed the Workshop Safety Agreement. The Safety Agreement can be located in Appendix A.

The Engineering Innovation Hub (EIH) in the Fitzpatrick Hall of Engineering and the AIAA Workshop in the Stinson-Remick Hall of Engineering feature most of the tools the team will need for construction. All team members must complete basic fabrication certification, formally called EIH certification, in order to participate in any physical design of the launch vehicle and use any of these tools or machines. The certification involves team members reading about proper usage of fabrication tools and then passing a short quiz on proper workshop practices. To date, 38 team members have completed the EIH certification. This certification must be renewed every subsequent year, so returning members must complete it as well. The site where team members earn their certification can be found here.

The team has also made readily available Safety Data Sheets (SDS) for any material or substance used in fabrication. These sheets feature basic information about the substance, effects from different forms of ingestion or exposure to the body, proper PPE, and other important information. Copies of these sheets are readily available in print in the workshop and on the team's website. The NDRT Safety Handbook is also readily available in the aforementioned formats, and outlines safety practices for the workshop and basic fabrication tools.

The Safety Officer will be responsible for updating the Standard Workshop Operating Procedures to provide team members with an understanding of how to use certain construction equipment. These procedures will be readily available in the workshop and online for team members to easily access. Standard Launch Operating Procedures will also be written. Such procedures will guide the team through packing, integration, setup, launch, and recovery of the launch vehicle in a manner that is clear and safe for the team to follow.

The team website, where SDSs, Standard Launch and Workshop Operating Procedures, and the Safety Handbook can be found, is linked here.

9 Project Plan

9.1 Requirements Verification

9.1.1 NASA Requirements

The 2023 NASA Student Launch Requirements for the College/University Student Launch Initiative Launch Division are listed in Tables 137, 138, 139, 140, 141, and 142.

Table 137: NASA General Requirements

Req. ID	Description
1.1.	Students on the team will do 100% of the project, including design, construction, written reports, presentations, and flight preparation with the exception of assembling the motors and handling black powder or any variant of ejection charges, or preparing and installing electric matches (to be done by the team's mentor). Teams will submit new work. Excessive use of past work will merit penalties.
1.2.	The team will provide and maintain a project plan to include, but not limited to the following items: project milestones, budget and community support, checklists, personnel assignments, STEM engagement events, and risks and mitigations.
1.3.	The team shall identify all team members who plan to attend Launch Week activities by the Critical Design Review (CDR). Team members will include:
1.3.1.	Students actively engaged in the project throughout the entire year.
1.3.2.	One mentor (see requirement 1.13)
1.3.3.	No more than two adult educators
1.4.	Teams shall engage a minimum of 250 participants in Educational Direct Engagement STEM activities in order to be eligible for STEM Engagement scoring and awards. These activities can be conducted inperson or virtually. To satisfy this requirement, all events shall occur between project acceptance and the FRR due date. A template of the STEM Engagement Activity Report can be found on pages 39–42.
1.5.	The team will establish and maintain a social media presence to inform the public about team activities.

Table 137: NASA General Requirements (continued)

Req. ID	Description
1.6.	Teams will email all deliverables to the NASA project management team by the deadline specified in the handbook for each milestone. In the event that a deliverable is too large to attach to an email, inclusion of a link to download the file will be sufficient. Late submissions of PDR, CDR, FRR milestone documents shall be accepted up to 72 hours after the submission deadline. Late submissions shall incur an overall penalty. No PDR, CDR, FRR milestone documents shall be accepted beyond the 72-hour window. Teams that fail to submit the PDR, CDR, FRR milestone documents shall be eliminated from the project.
1.7.	Teams who do not satisfactorily complete each milestone review (PDR, CDR, FRR) shall be provided action items needed to be completed following their review and shall be required to address action items in a delta review session. After the delta session the NASA management panel shall meet to determine the teams' status in the program and the team shall be notified shortly thereafter.
1.8.	All deliverables shall be in PDF format.
1.9.	In every report, teams will provide a table of contents including major sections and their respective sub-sections.
1.10.	In every report, the team will include the page number at the bottom of the page.
1.11.	The team will provide any computer equipment necessary to perform a video teleconference with the review panel. This includes, but is not limited to, a computer system, video camera, speaker telephone, and a sufficient Internet connection. Cellular phones should be used for speakerphone capability only as a last resort.
1.12.	All teams attending Launch Week will be required to use the launch pads provided by Student Launch's launch services provider. No custom pads will be permitted at the NASA Launch Complex. At launch, 8-foot 1010 rails and 12-foot 1515 rails will be provided. The launch rails will be canted 5 to 10 degrees away from the crowd on Launch Day. The exact cant will depend on Launch Day wind conditions.

Table 137: NASA General Requirements (continued)

Req. ID	Description
1.13.	Each team shall identify a "mentor." A mentor is defined as an adult who is included as a team member, who will be supporting the team (or multiple teams) throughout the project year, and may or may not be affiliated with the school, institution, or organization. The mentor shall maintain a current certification, and be in good standing, through the National Association of Rocketry (NAR) or Tripoli Rocketry Association (TRA) for the motor impulse of the launch vehicle and must have flown and successfully recovered (using electronic, staged recovery) a minimum of 2 flights in this or a higher impulse class, prior to PDR. The mentor is designated as the individual owner of the rocket for liability purposes and must travel with the team to Launch Week. One travel stipend will be provided per mentor regardless of the number of teams he or she supports. The stipend will only be provided if the team passes FRR and the team and mentor attend Launch Week in April.
1.14.	Teams will track and report the number of hours spent working on each milestone.

Table 138: NASA Launch Vehicle Requirements

Req. ID	Description
2.1.	The vehicle will deliver the payload to an apogee altitude between 4,000 and 6,000 feet above ground level (AGL). Teams flying below 3,500 feet or above 6,500 feet on their competition launch will receive zero altitude points towards their overall project score and will not be eligible for the Altitude Award.
2.2.	Teams shall declare their target altitude goal at the PDR milestone. The declared target altitude will be used to determine the team's altitude score.
2.3.	The launch vehicle will be designed to be recoverable and reusable. Reusable is defined as being able to launch again on the same day without repairs or modifications.
2.4.	The launch vehicle will have a maximum of four (4) independent sections. An independent section is defined as a section that is either tethered to the main vehicle or is recovered separately from the main vehicle using its own parachute.
2.4.1.	Coupler/airframe shoulders which are located at in-flight separation points will be at least 2 airframe diameters in length. (One body diameter of surface contact with each airframe section).
2.4.2.	Nosecone shoulders which are located at in-flight separation points will be at least ½ body diameter in length.

Table 138: NASA Launch Vehicle Requirements (continued)

Req. ID	Description
2.5.	The launch vehicle will be capable of being prepared for flight at the launch site within 2 hours of the time the Federal Aviation Administration flight waiver opens.
2.6.	The launch vehicle and payload will be capable of remaining in launch-ready configuration on the pad for a minimum of 2 hours without losing the functionality of any critical on-board components, although the capability to withstand longer delays is highly encouraged.
2.7.	The launch vehicle will be capable of being launched by a standard 12-volt direct current firing system. The firing system will be provided by the NASA-designated launch services provider.
2.8.	The launch vehicle will require no external circuitry or special ground support equipment to initiate launch (other than what is provided by the launch services provider).
2.9.	Each team shall use commercially available ematches or igniters. Hand-dipped igniters shall not be permitted.
2.10.	The launch vehicle will use a commercially available solid motor propulsion system using ammonium perchlorate composite propellant (APCP) which is approved and certified by the National Association of Rocketry (NAR), Tripoli Rocketry Association (TRA), and/or the Canadian Association of Rocketry (CAR).
2.10.1.	Final motor choices will be declared by the Critical Design Review (CDR) milestone.
2.10.2.	Any motor change after CDR shall be approved by the NASA Range Safety Officer (RSO). Changes for the sole purpose of altitude adjustment will not be approved. A penalty against the team's overall score will be incurred when a motor change is made after the CDR milestone, regardless of the reason.
2.11.	The launch vehicle will be limited to a single motor propulsion system.
2.12.	The total impulse provided by a College or University launch vehicle will not exceed 5,120 Newton-seconds (L-class).
2.13.	Pressure vessels on the vehicle will be approved by the RSO and will meet the following criteria:
2.13.1.	The minimum factor of safety (Burst or Ultimate pressure versus Max Expected Operating Pressure) will be 4:1 with supporting design documentation included in all milestone reviews.

Table 138: NASA Launch Vehicle Requirements (continued)

Req. ID	Description
2.13.2.	Each pressure vessel will include a pressure relief valve that sees the full pressure of the tank and is capable of withstanding the maximum pressure and flow rate of the tank.
2.13.3.	The full pedigree of the tank will be described, including the application for which the tank was designed and the history of the tank. This will include the number of pressure cycles put on the tank, the dates of pressurization/depressurization, and the name of the person or entity administering each pressure event.
2.14.	The launch vehicle will have a minimum static stability margin of 2.0 at the point of rail exit. Rail exit is defined at the point where the forward rail button loses contact with the rail.
2.15.	The launch vehicle will have a minimum thrust to weight ratio of 5.0 : 1.0.
2.16.	Any structural protuberance on the rocket will be located aft of the burnout center of gravity. Camera housings will be exempted, provided the team can show that the housing(s) causes minimal aerodynamic effect on the rocket's stability.
2.17.	The launch vehicle will accelerate to a minimum velocity of 52 fps at rail exit.
2.18.	All teams will successfully launch and recover a subscale model of their rocket prior to CDR. Success of the subscale is at the sole discretion of the NASA review panel. The subscale flight may be conducted at any time between proposal award and the CDR submission deadline. Subscale flight data shall be reported in the CDR report and presentation at the CDR milestone. Subscales are required to use a minimum motor impulse class of E (Mid Power motor).
2.18.1.	The subscale model should resemble and perform as similarly as possible to the full-scale model; however, the full-scale will not be used as the subscale model.
2.18.2.	The subscale model will carry an altimeter capable of recording the model's apogee altitude.
2.18.3.	The subscale rocket shall be a newly constructed rocket, designed and built specifically for this year's project.
2.18.4.	Proof of a successful flight shall be supplied in the CDR report.
2.18.4.1.	Altimeter flight profile graph(s) OR a quality video showing successful launch, recovery events, and landing as deemed by the NASA management panel are acceptable methods of proof. Altimeter flight profile graph(s) that are not complete (liftoff through landing) shall not be accepted.

Table 138: NASA Launch Vehicle Requirements (continued)

Req. ID	Description
2.18.4.2.	Quality pictures of the as landed configuration of all sections of the launch vehicle shall be included in the CDR report. This includes but not limited to nosecone, recovery system, airframe, and booster.
2.18.5.	The subscale rocket shall not exceed 75% of the dimensions (length and diameter) of your designed full-scale rocket. For example, if your full-scale rocket is a 4" diameter 100" length rocket your subscale shall not exceed 3" diameter and 75" in length.
2.19.	All teams will complete demonstration flights as outlined below.
2.19.1.	Vehicle Demonstration Flight—All teams will successfully launch and recover their full-scale rocket prior to FRR in its final flight configuration. The rocket flown shall be the same rocket to be flown for their competition launch. The purpose of the Vehicle Demonstration Flight is to validate the launch vehicle's stability, structural integrity, recovery systems, and the team's ability to prepare the launch vehicle for flight. A successful flight is defined as a launch in which all hardware is functioning properly (i.e. drogue chute at apogee, main chute at the intended lower altitude, functioning tracking devices, etc.). The following criteria shall be met during the full-scale demonstration flight:
2.19.1.1.	The vehicle and recovery system will have functioned as designed.
2.19.1.2.	The full-scale rocket shall be a newly constructed rocket, designed and built specifically for this year's project.
2.19.1.3.	The payload does not have to be flown during the full-scale Vehicle Demonstration Flight. The following requirements still apply:
2.19.1.3.1.	If the payload is not flown, mass simulators will be used to simulate the payload mass.
2.19.1.3.2.	The mass simulators will be located in the same approximate location on the rocket as the missing payload mass.
2.19.1.4.	If the payload changes the external surfaces of the rocket (such as camera housings or external probes) or manages the total energy of the vehicle, those systems will be active during the full-scale Vehicle Demonstration Flight.
2.19.1.5.	Teams shall fly the competition launch motor for the Vehicle Demonstration Flight. The team may request a waiver for the use of an alternative motor in advance if the home launch field cannot support the full impulse of the competition launch motor or in other extenuating circumstances.

Table 138: NASA Launch Vehicle Requirements (continued)

Req. ID	Description
2.19.1.6.	The vehicle shall be flown in its fully ballasted configuration during the full-scale test flight. Fully ballasted refers to the maximum amount of ballast that will be flown during the competition launch flight. Additional ballast may not be added without a re-flight of the full-scale launch vehicle.
2.19.1.7.	After successfully completing the full-scale demonstration flight, the launch vehicle or any of its components will not be modified without the concurrence of the NASA Range Safety Officer (RSO).
2.19.1.8.	Proof of a successful flight shall be supplied in the FRR report.
2.19.1.8.1.	Altimeter flight profile data output with accompanying altitude and velocity versus time plots is required to meet this requirement. Altimeter flight profile graph(s) that are not complete (liftoff through landing) shall not be accepted.
2.19.1.8.2.	Quality pictures of the as landed configuration of all sections of the launch vehicle shall be included in the FRR report. This includes but not limited to nosecone, recovery system, airframe, and booster.
2.19.1.9.	Vehicle Demonstration flights shall be completed by the FRR submission deadline. No exceptions will be made. If the Student Launch office determines that a Vehicle Demonstration Re-flight is necessary, then an extension may be granted. THIS EXTENSION IS ONLY VALID FOR RE-FLIGHTS, NOT FIRST TIME FLIGHTS. Teams completing a required re-flight shall submit an FRR Addendum by the FRR Addendum deadline.
2.19.2.	Payload Demonstration Flight—All teams will successfully launch and recover their full-scale rocket containing the completed payload prior to the Payload Demonstration Flight deadline. The rocket flown shall be the same rocket to be flown as their competition launch. The purpose of the Payload Demonstration Flight is to prove the launch vehicle's ability to safely retain the constructed payload during flight and to show that all aspects of the payload perform as designed. A successful flight is defined as a launch in which the rocket experiences stable ascent and the payload is fully retained until it is deployed (if applicable) as designed. The following criteria shall be met during the Payload Demonstration Flight:
2.19.2.1.	The payload shall be fully retained until the intended point of deployment (if applicable), all retention mechanisms shall function as designed, and the retention mechanism shall not sustain damage requiring repair.
2.19.2.2.	The payload flown shall be the final, active version.

Table 138: NASA Launch Vehicle Requirements (continued)

Req. ID	Description
2.19.2.3.	If the above criteria are met during the original Vehicle Demonstration Flight, occurring prior to the FRR deadline and the information is included in the FRR package, the additional flight and FRR Addendum are not required.
2.19.2.4.	Payload Demonstration Flights shall be completed by the FRR Addendum deadline. NO EXTENSIONS WILL BE GRANTED.
2.20.	An FRR Addendum will be required for any team completing a Payload Demonstration Flight or NASArequired Vehicle Demonstration Re-flight after the submission of the FRR Report.
2.20.1.	Teams required to complete a Vehicle Demonstration Re-Flight and failing to submit the FRR Addendum by the deadline will not be permitted to fly a final competition launch.
2.20.2.	Teams who successfully complete a Vehicle Demonstration Flight but fail to qualify the payload by satisfactorily completing the Payload Demonstration Flight requirement will not be permitted to fly a final competition launch.
2.20.3.	Teams who complete a Payload Demonstration Flight which is not fully successful may petition the NASA RSO for permission to fly the payload at launch week. Permission will not be granted if the RSO or the Review Panel have any safety concerns.
2.21.	The team's name and Launch Day contact information shall be in or on the rocket airframe as well as in or on any section of the vehicle that separates during flight and is not tethered to the main airframe. This information shall be included in a manner that allows the information to be retrieved without the need to open or separate the vehicle.
2.22.	All Lithium Polymer batteries will be sufficiently protected from impact with the ground and will be brightly colored, clearly marked as a fire hazard, and easily distinguishable from other payload hardware.
2.23.	Vehicle Prohibitions
2.23.1.	The launch vehicle will not utilize forward firing motors.
2.23.2.	The launch vehicle will not utilize motors that expel titanium sponges (Sparky, Skidmark, MetalStorm, etc.)
2.23.3.	The launch vehicle will not utilize hybrid motors.
2.23.4	The launch vehicle will not utilize a cluster of motors.
2.23.5.	The launch vehicle will not utilize friction fitting for motors.
2.23.6	The launch vehicle will not exceed Mach 1 at any point during flight.

Table 138: NASA Launch Vehicle Requirements (continued)

Req. ID	Description
2.23.7	Vehicle ballast will not exceed 10% of the total unballasted weight of the rocket as it would sit on the pad (i.e. a rocket with an unballasted weight of 40 lbs. on the pad may contain a maximum of 4 lbs. of ballast).
2.23.8.	Transmissions from onboard transmitters, which are active at any point prior to landing, will not exceed 250 mW of power (per transmitter).
2.23.9.	Transmitters will not create excessive interference. Teams will utilize unique frequencies, handshake/passcode systems, or other means to mitigate interference caused to or received from other teams.
2.23.10.	Excessive and/or dense metal will not be utilized in the construction of the vehicle. Use of lightweight metal will be permitted but limited to the amount necessary to ensure structural integrity of the airframe under the expected operating stresses.

Table 139: NASA Recovery Requirements

Req. ID	Description
3.1.	The full scale launch vehicle will stage the deployment of its recovery devices, where a drogue parachute is deployed at apogee, and a main parachute is deployed at a lower altitude. Tumble or streamer recovery from apogee to main parachute deployment is also permissible, provided that kinetic energy during drogue stage descent is reasonable, as deemed by the RSO.
3.1.1.	The main parachute shall be deployed no lower than 500 feet.
3.1.2.	The apogee event may contain a delay of no more than 2 seconds.
3.1.3.	Motor ejection is not a permissible form of primary or secondary deployment.
3.2.	Each team will perform a successful ground ejection test for all electronically initiated recovery events prior to the initial flights of the subscale and full scale vehicles.
3.3.	Each independent section of the launch vehicle will have a maximum kinetic energy of 75 ft-lbf at landing. Teams whose heaviest section of their launch vehicle, as verified by vehicle demonstration flight data, stays under 65 ft-lbf will be awarded bonus points.
3.4.	The recovery system will contain redundant, commercially available barometric altimeters that are specifically designed for initiation of rocketry recovery events. The term “altimeters” includes both simple altimeters and more sophisticated flight computers.

Table 139: NASA Recovery Requirements (continued)

Req. ID	Description
3.5.	Each altimeter will have a dedicated power supply, and all recovery electronics will be powered by commercially available batteries.
3.6.	Each altimeter will be armed by a dedicated mechanical arming switch that is accessible from the exterior of the rocket airframe when the rocket is in the launch configuration on the launch pad.
3.7.	Each arming switch will be capable of being locked in the ON position for launch (i.e. cannot be disarmed due to flight forces).
3.8.	The recovery system, GPS and altimeters, electrical circuits will be completely independent of any payload electrical circuits.
3.9.	Removable shear pins will be used for both the main parachute compartment and the drogue parachute compartment.
3.10.	The recovery area will be limited to a 2,500 ft. radius from the launch pads.
3.11.	Descent time of the launch vehicle will be limited to 90 seconds (apogee to touch down). Teams whose launch vehicle descent, as verified by vehicle demonstration flight data, stays under 80 seconds will be awarded bonus points.
3.12.	An electronic GPS tracking device will be installed in the launch vehicle and will transmit the position of the tethered vehicle or any independent section to a ground receiver.
3.12.1.	Any rocket section or payload component, which lands untethered to the launch vehicle, will contain an active electronic GPS tracking device.
3.12.2.	The electronic GPS tracking device(s) will be fully functional during the official competition launch.
3.13.	The recovery system electronics will not be adversely affected by any other on-board electronic devices during flight (from launch until landing).
3.13.1.	The recovery system altimeters will be physically located in a separate compartment within the vehicle from any other radio frequency transmitting device and/or magnetic wave producing device.
3.13.2.	The recovery system electronics will be shielded from all onboard transmitting devices to avoid inadvertent excitation of the recovery system electronics.
3.13.3.	The recovery system electronics will be shielded from all onboard devices which may generate magnetic waves (such as generators, solenoid valves, and Tesla coils) to avoid inadvertent excitation of the recovery system.
3.14.4.	The recovery system electronics will be shielded from any other onboard devices which may adversely affect the proper operation of the recovery system electronics.

Table 140: NASA Payload Experiment Requirements

Req. ID	Description
4.1.	College/University Division—Teams shall design a payload capable upon landing of autonomously receiving RF commands and performing a series of tasks with an on-board camera system. The method(s)/design(s) utilized to complete the payload mission shall be at the team's discretion and shall be permitted so long as the designs are deemed safe, obey FAA and legal requirements, and adhere to the intent of the challenge. An additional experiment (limit of 1) is allowed, and may be flown, but will not contribute to scoring. If the team chooses to fly an additional experiment, they will provide the appropriate documentation in all design reports so the experiment may be reviewed for flight safety.
4.2.	Radio Frequency Command (RAFCO) Mission Requirements
4.2.1.	Launch Vehicle shall contain an automated camera system capable of swiveling 360º to take images of the entire surrounding area of the launch vehicle.
4.2.1.1.	The camera shall have the capability of rotating about the z axis. The z axis is perpendicular to the ground plane with the sky oriented up and the planetary surface oriented down.
4.2.1.2.	The camera shall have a FOV of at least 100º and a maximum FOV of 180º
4.2.1.3.	The camera shall time stamp each photo taken. The time stamp shall be visible on all photos submitted to NASA in the PLAR.
4.2.1.4.	The camera system shall execute the string of transmitted commands quickly, with a maximum of 30 seconds between photos taken.
4.2.2.	NASA Student Launch Management Team shall transmit a RF sequence that shall contain a radio call sign followed by a sequence of tasks to be completed. The list of potential commands to be given on launch day along with their radio transcriptions which shall be sent in a RF message using APRS transmission in no particular order are: A1—Turn camera 60º to the right B2—Turn camera 60º to the left C3—Take picture D4—Change camera mode from color to grayscale E5—Change camera mode back from grayscale to color F6—Rotate image 180º (upside down). G7—Special effects filter (Apply any filter or image distortion you want and state what filter or distortion was used). H8—Remove all filters.
4.2.2.1.	An example transmission sequence could look something like, "XX4XXX C3 A1 D4 C3 F6 C3 F6 B2 B2 C3." Note the call sign that NASA will use shall be distributed to teams at a later time.
4.2.3.	The NASA Student Launch Management Panel shall transmit the RAFCO using APRS.

Table 140: NASA Payload Experiment Requirements (continued)

Req. ID	Description
4.2.3.1.	NASA will use dedicated frequencies to transmit the message. NASA will operate on the 2-Meter amateur radio band between the frequencies of 144.90 MHz and 145.10 MHz. No team shall be permitted to transmit on any frequency in this range. The specific frequency used will be shared with teams during Launch Week. NASA reserves the right to modify the transmission frequency as deemed necessary.
4.2.3.2.	The NASA Management Team shall transmit the RAFCO every 2 minutes.
4.2.3.3.	The payload system shall not initiate and begin accepting RAFCO until AFTER the launch vehicle has landed on the planetary surface.
4.2.4.	The payload shall not be jettisoned.
4.2.5.	The sequence of time-stamped photos taken need not be transmitted back to ground station and shall be presented in the correct order in your PLAR.
4.3.	General Payload Requirements
4.3.1.	Black Powder and/or similar energetics are only permitted for deployment of in-flight recovery systems. Energetics shall not be permitted for any surface operations.
4.3.2.	Teams shall abide by all FAA and NAR rules and regulations.
4.3.3.	Any secondary payload experiment element that is jettisoned during the recovery phase will receive real-time RSO permission prior to initiating the jettison event, unless exempted from the requirement the CDR milestone by NASA.
4.3.4.	Unmanned aircraft system (UAS) payloads, if designed to be deployed during descent, will be tethered to the vehicle with a remotely controlled release mechanism until the RSO has given permission to release the UAS.
4.3.5.	Teams flying UASs will abide by all applicable FAA regulations, including the FAA's Special Rule for Model Aircraft (Public Law 112–95 Section 336; see https://www.faa.gov/uas/faqs)
4.3.6.	Any UAS weighing more than .55 lbs. shall be registered with the FAA and the registration number marked on the vehicle.

Table 141: NASA Safety Requirements

Req. ID	Description
5.1.	Each team will use a launch and safety checklist. The final checklists will be included in the FRR report and used during the Launch Readiness Review (LRR) and any Launch Day operations.

Table 141: NASA Safety Requirements (continued)

Req. ID	Description
5.2.	Each team shall identify a student safety officer who will be responsible for all items in section 5.3.
5.3.	The role and responsibilities of the safety officer will include, but are not limited to:
5.3.1.	Monitor team activities with an emphasis on safety during:
5.3.1.1	Design of vehicle and payload
5.3.1.2	Construction of vehicle and payload components
5.3.1.3.	Assembly of vehicle and payload
5.3.1.4.	Ground testing of vehicle and payload
5.3.1.5	Subscale launch test(s)
5.3.1.6	Full-scale launch test(s)
5.3.1.7.	Competition Launch
5.3.1.8.	Recovery activities
5.3.1.9.	STEM Engagement Activities
5.3.2.	Implement procedures developed by the team for construction, assembly, launch, and recovery activities.
5.3.3.	Manage and maintain current revisions of the team's hazard analyses, failure modes analyses, procedures, and MSDS/chemical inventory data.
5.3.4.	Assist in the writing and development of the team's hazard analyses, failure modes analyses, and procedures.
5.4.	During test flights, teams will abide by the rules and guidance of the local rocketry club's RSO. The allowance of certain vehicle configurations and/or payloads at the NASA Student Launch does not give explicit or implicit authority for teams to fly those vehicle configurations and/or payloads at other club launches. Teams should communicate their intentions to the local club's President or Prefect and RSO before attending any NAR or TRA launch.
5.5.	Teams will abide by all rules set forth by the FAA.

Table 142: NASA Final Flight Requirements

Req. ID	Description
6.1.	NASA Launch Complex
6.1.1.	Teams are not permitted to show up at the NASA Launch Complex without permission from the NASA management team.

Table 142: NASA Final Flight Requirements (continued)

Req. ID	Description
6.1.2.	Teams shall complete and pass the Launch Readiness Review conducted during Launch Week.
6.1.3.	The team mentor shall be present and oversee rocket preparation and launch activities.
6.1.4.	The scoring altimeter shall be presented to the NASA scoring official upon recovery.
6.1.5.	Teams may launch only once. Any launch attempt resulting in the rocket exiting the launch pad, regardless of the success of the flight, will be considered a launch. Additional flights beyond the initial launch, will not be scored and will not be considered for awards.
6.2.	Commercial Spaceport Launch Site
6.2.1.	The launch shall occur at a NAR or TRA sanctioned and insured club launch. Exceptions may be approved for launch clubs who are not affiliated with NAR or TRA but provide their own insurance, such as the Friends of Amateur Rocketry. Approval for such exceptions shall be granted by NASA prior to the launch.
6.2.2.	Teams shall submit their rocket and payload to the launch site Range Safety Officer (RSO) prior to flying the rocket. The RSO will inspect the rocket and payload for flightworthiness and determine if the project is approved for flight. The local RSO will have final authority on whether the team's rocket and payload may be flown.
6.2.3.	The team mentor shall be present and oversee rocket preparation and launch activities.
6.2.4.	BOTH the team mentor and the Launch Control Officer shall observe the flight and report any off-nominal events during ascent or recovery on the Launch Certification and Observations Report.
6.2.5.	The scoring altimeter shall be presented to BOTH the team's mentor and the Range Safety Officer
6.2.6.	The mentor, the Range Safety Officer, and the Launch Control Officer must be three separate individuals who must ALL complete the applicable sections of the Launch Certification and Observations Report. The Launch Certification and Observations Report document will be provided by NASA upon completion of the FRR milestone and shall be returned to NASA by the team mentor upon completion of the launch.
6.2.7.	The Range Safety Officer and Launch Control Officer certifying the team's flight shall be impartial observers and shall not be affiliated with the team, individual team members, or the team's academic institution.

Table 142: NASA Final Flight Requirements (continued)

Req. ID	Description
6.2.8.	Teams may launch only once. Any launch attempt resulting in the rocket exiting the launch pad, regardless of the success of the flight, will be considered a launch. Additional flights beyond the initial launch will not be scored and will not be considered for awards.

9.1.2 NDRT Derived Requirements

The NDRT Derived Requirements are listed in Tables 143, 144, 145, 146, and 147.
Team-derived requirements set design standards that optimize performance and functionality of all launch vehicle components, modules, and systems. Internal NDRT guidelines for requirement derivation focused on mitigating failure modes and uncertainties surrounding loads enacted during various stages and events during flight, flight conditions, and system integration.

The NDRT Integration Requirements in Table 147 were newly introduced for the 2023 competition. These requirements are universally applicable for launch vehicle modules and systems and encourage collaboration across different design systems. Further justification for the inclusion of this category of requirements include a decrease in repetitive team-derived requirements and streamlined testing further into launch vehicle design and development.

Table 143: NDRT Launch Vehicle Requirements

Req. ID	Description	Justification
LV.1	The distance between the ACS and the CP of the launch vehicle shall be minimized by design.	The ACS must be located near the CP in order to reduce the impact it will have on launch vehicle stability when actuating its flaps during flight.
LV.2	The launch vehicle must be able to overshoot the NDRT-determined target apogee.	The launch vehicle must be capable of reaching an apogee higher than the target in order for the ACS to influence its flight path and guide it towards the target.
LV.3	No body tube shall include more than two squads' components.	Limiting the amount of components in a single body tube reduces physical and transmission-based interference between them.

Table 143: NDRT Launch Vehicle Requirements (continued)

Req. ID	Description	Justification
LV.4	The launch vehicle design shall accomodate vehicle speeds that avoid fin flutter.	Designing to avoid fin flutter during flight will avoid resonance conditions for the fins and increase the stability of the launch vehicle.
LV.5	Payload and recovery system components shall not come in physical contact with each other during any point of the mission.	Modules must be properly secured and retained within the body tube to reduce damage during flight.
LV.6	All launch vehicle airframe components shall be designed with a factor of safety of 1.5 above predicted forces inflicted.	A factor of safety of 1.5 prevents failure and accounts for unanticipated forces during flight and landing. Additionally, it contributes to the reusability of the launch vehicle.
LV.7	All body tubes containing electronic components used for communication shall be constructed using material that does not obstruct RF transmission.	Sensor communication is critical to mission success and must not be obstructed by airframe material that blocks RF transmissions to or from sensors.
LV.8	All launch vehicle airframe components shall be designed to withstand cyclical loading and additional causes of fatigue.	The launch vehicle must be able to withstand loading associated with multiple flight demonstrations that occur throughout the competition season.

Table 144: NDRT Recovery Requirements

Req. ID	Description	Justification
R.1	Heat-sensitive laundry items such as parachutes and shock cords shall have sufficient thermal protection.	Parachutes and shock cords are critical flight components and also prevent each independent section of the launch vehicle from exceeding 75 ft-lbf of kinetic energy per NASA Requirement 3.3. They must be protected from damage during black powder charge detonation.

Table 144: NDRT Recovery Requirements (continued)

Req. ID	Description	Justification
R.2	Shock cords and structural components necessary to in-flight separation shall have a factor of safety of 1.5 beyond projected loads.	The recovery system must be able to withstand loads of greater magnitude than expected to increase the reliability of the system and chances of reusability per NASA Req. 2.3.
R.3	There shall be three non-identical altimeters included in each separate recovery module.	Redundancy contributes to a fail safe system should one or more altimeter fail during flight. Functional altimeters enable successful separation events, which are critical to preventing each independent section of the launch vehicle from exceeding 75 ft-lbf per NASA Req. 3.3.

Table 145: NDRT Payload Experiment Requirements

Req. ID	Description	Justification
TROI.1	The tolerance of the camera system's defined z-axis shall be no more than 10 degrees from the NASA-defined z-axis.	Including tolerance limits will enable the NDRT camera z-axis to achieve higher accuracy against the defined z-axis in NASA Req. 4.2.1.1.
TROI.2	Motor torque shall be rated with a factor of safety of 1.5 in relation to the calculated torque required for the system actuation.	Having a motor that can exceed the predicted torque required for camera system actuation and deployment will increase the likelihood of a successful mission.
TROI.3	All load-bearing payload system components shall have a factor of safety of 1.5 with regards to calculated forces exerted upon them during the mission.	Designing load-bearing components to withstand additional forces reduces the likelihood of failure, accomodates for unpredicted forces, and improves reusability.
TROI.4	The camera shall be capable of capturing images with a minimum resolution of five megapixels.	Cameras with a resolution of approximately five megapixels will take clear images and fit within the body tube.

Table 145: NDRT Payload Experiment Requirements (continued)

Req. ID	Description	Justification
TROI.5	The payload deployment mechanism shall function properly for launch vehicle landing positions from -15 to +45 degrees relative to the horizontal axis.	The deployment mechanism must be functional for all probable angles the launch vehicle will come to rest at, of which a reasonable range is -15 to +45 degrees.
TROI.6	The payload will have an alloted tube length of 12 in. and an inner diameter of 6 in.	The payload system must fit within the body tube dimensions and accomoate for additional systems retained.
TROI.7	The payload system shall be able to extend out of the body tube of the launch vehicle.	NDRT is designing a payload system that requires the camera to extend out of the body tube to take images.

Table 146: NDRT Non-Scoring Payload (ACS) Requirements

Req. ID	Description	Justification
ACS.1	The system shall be capable of performing maximum actuation within 3 seconds of the team's predicted time duration.	Accurate actuation ensures that estimates made by software components are accurate and effective during launch.
ACS.2	The ACS shall be capable of actuating solid drag flaps to induce additional drag to aid in achieving the team's apogee estimates.	Basic functionality of the system ensures it can aid in slowing the launch vehicle below any apogee above the team's predicted, necessitated by NDRT Req. LV.2.
ACS.3	The ACS drag taps shall be capable of withstanding the maximum projected static loading force with a factor of safety of 1.5.	Basic functionality of the system ensures that the flaps can remain actuated during flight.
ACS.4	Sensors shall sample at a minimum rate of 10 Hz.	Provides basic functionality and timely responsiveness for the system during flight.
ACS.5	The ACS shall be capable of actuating solid drag flaps that are under a load of X lbs.	The ACS will be actuated while launch vehicle has significant vertical velocity and as such, drag forces will be working against actuation.

Table 146: NDRT Non-Scoring Payload (ACS) Requirements (continued)

Req. ID	Description	Justification
ACS.6	The ACS shall log each sampled data point and state changes in a CSV formatted file for analysis.	The ACS functionality must be able to be verified upon returning to base station.
ACS.7	The ACS shall be capable of determining the launch vehicle's current stage of flight using the flight parameters of altitude, linear acceleration, angular accleeration, and magnetic field.	Basic functionality of the system is confirmed by this requirement.
ACS.8	The stall current of the servo motor shall be no more than 10 Amps.	Currents that exceed the stall current lead to insufficient voltage allocated to batteries and risk overheading of the system.

Table 147: NDRT Integration Requirements

Req. ID	Description	Justification
IN.1	Batteries for all launch vehicle systems must be sized for three hours of operation in temperatures ranging from 0F to 100F.	Three hours of operation is a factor of safety of 1.5 above the two hours of function listed by NASA Req. 2.6. This sizing accommodates for systems (ie. ACS, Payload) that continue to function mid- or post-flight. The batteries must also function across all probable flight conditions, of which a reasonable temperature range is 0F to 100F.
IN.2	All electronic components involved in transmission or reception of data and/or magnetic activities shall be properly shielded.	Shielding will prevent interference with sensors located across separate systems and within each system of the launch vehicle. This ensures accurate reading and storage of data.
IN.3	Electronics that are critical to flight and/or the mission shall have redundancy in their respective systems.	Redundancy creates systems that are more reliable and can function with component failure. This increases the likelihood of mission success.

Table 147: NDRT Integration Requirements (continued)

Req. ID	Description	Justification
IN.4	Electronic components and systems shall be rated to function in temperatures ranging from 0F to 100F.	Components in the launch vehicle must be capable of operation in probable flight conditions, of which a reasonable temperature range is 0F to 100F.
IN.5	Each system and/or module retained within the launch vehicle shall not exceed their mass as allocated by the mass budget.	Accurate mass and weight values are necessary to determine launch vehicle components and meet the 5.0 : 1.0 thrust to weight ratio listed in NASA Req. 2.15.
IN.6	Sensitive components (ie. camera) in any system shall be protected from black powder charges.	Sensitive components require protection from particulate matter or forces caused by black powder charge detonation.
IN.7	Epoxy used near high-heat components (ie. motors and black powder charges) shall be rated to withstand the maximum temperature of those components.	Epoxy used in joints and connections must be heat-resistant to maintain strong bonds to reduce the risk of bond failure and loose components during flight.

9.2 Educational Outreach Update

NDRT has had a successful start to the year in terms of STEM Engagement events. The team has led events with South Bend's Place to Be Me and the Mishawaka High School Robotics Team catering activities to the age groups of the students of the respective organizations. With the two events combined, 17 NDRT members have been able to serve over 25 participants.

NDRT will continue to run educational outreach events throughout the South Bend community for the remainder of the fall semester. These events are being designed with a primary focus on rocketry but will also include the engineering design process, astronomy, space, and structural geometry. Upcoming events are planned with the Saint Joseph County Public Library, Cub Scout Pack 364, the Society of Women Engineers, and the Girl Scouts of Northern Indiania-Michiana.

9.3 Budget

Table 148 gives an overview of NDRT's budget for the 2023 project. Funding comes primarily from last year's rollover, donations from corporate sponsors including The Boeing Company and Blue Origin, and team fundraising events such as merchandise sales and alumni outreach. The team has appointed a student business operator to focus on securing new corporate sponsorship to ensure sufficient funding for this and future projects. Only small portions of each squad's budget have been expended thus far due to focusing on procurements of components for subscale construction and full-scale prototyping; purchases for the full-scale vehicle will begin in December. The team is expected to remain within budget through project completion.

Table 148: NDRT Overall Budget 2022-23

Category	Allocation	Spent	Margins
Launch Vehicle	$4,200.00	$458.09	10.91%
Recovery System	$1,500.00	$0.00	0.00%
Apogee Control System	$1,200.00	$170.88	14.24%
360° Rotating Optical Imager	$1,700.00	$66.82	3.93%
Vehicle Subtotal	***$8,600.00***	***$695.79***	***8.09%***
Safety	$200.00	$28.87	14.44%
Educational Outreach	$200.00	$0.00	0.00%
Travel	$10,500.00	$0.00	0.00%
Miscellaneous	$1,000.00	$108.21	10.82%
Total	**$20,500.00**	**$832.87**	**4.06%**
Total Available	$36,505.00	$36,505.00	
Remaining Funds	$16,005.00	$35,672.13	

Tables 150 through 153 provide line-item breakdowns of team expenses by squad and/or category. Recovery and STEM Engagement have not yet made purchases due to reuse of materials remaining from previous years.

The parts listed have been sourced from vendors historically determined as reliable by the team and team mentor. NDRT will continue to work with these and other dependable vendors when ordering materials for the full-scale vehicle.

Table 149: TROI Expenses

Item	Vendor	Qty	Cost/Item	Total Cost
HAM Amateur Radio Module DRA818V	Tindie	2	$9.98	$19.96
Baofeng UV-5R Two Way Radio	Amazon	2	$21.90	$43.80
			Shipping and Tax	$3.06
			Total	$66.82

Table 150: Launch Vehicle Expenses

Item	Vendor	Qty	Cost/Item	Total Cost
RockSim Licenses	Apogee Components	4	$20.00	$80.00
G5000 RocketPoxy, 8 oz package	Apogee Components	1	$26.99	$26.99
3 in. G12 Fiberglass Tube, 5 ft	Composite Warehouse	1	$98.00	$98.00
3 in. G12 Fiberglass Coupler Tube, 12 in.	Composite Warehouse	1	$30.00	$30.00
Fiberglass Sheet 12×48×3/32 in.	Composite Warehouse	1	$68.00	$68.00
38 mm Fiberglass Motor Mount Tube	Composite Warehouse	1	$12.00	$12.00
38 mm Motor Retainer	Composite Warehouse	1	$29.17	$29.17
J-B Weld Professional Size, 10 oz	J-B Weld	1	$19.99	$19.99
1010 Rail Buttons, 2 pack	Chris' Rocket Supplies	1	$2.50	$2.50
			Shipping and Tax	$97.04
			Total	$458.09

Table 151: ACS Expenses

Item	Vendor	Qty	Cost/Item	Total Cost
YDL 3.7V 5000mAh LiPo	Amazon	2	$15.99	$31.98
PowerBoost 1000 Basic	Amazon	1	$14.59	$14.59
Ovonic 7.4V LiPo	Amazon	1	$17.39	$17.39
BNO055 IMU	Adafruit	1	$29.95	$29.95
ADXL343 Accelerometer	Adafruit	2	$5.95	$11.90
MPL3115A2 Altimeter	Adafruit	2	$9.95	$19.90
PWM Servo Driver	Adafruit	1	$14.95	$14.95
Piezo Buzzer	Adafruit	1	$1.50	$1.50
RGB LED	Adafruit	1	$2.00	$2.00
Power Switch	Adafruit	2	$0.95	$1.90
			Shipping and Tax	$24.82
			Total	$170.88

Table 152: Safety Expenses

Item	Vendor	Qty	Cost/Item	Total Cost
N95 Mask, 20 pack	Amazon	1	$16.99	$16.99
Nitrile-Vinyl Blend Exam Gloves, 100 Pack	Amazon	1	$9.99	$9.99
			Shipping and Tax	$1.89
			Total	$28.87

Table 153: Miscellaneous Expenses

Item	Vendor	Qty	Cost/Item	Total Cost
Pizza - PDR Writing Workshop	Domino's	1	$73.14	$73.14
Snacks - PDR Writing Workshop	Martin's Super Market	1	$29.75	$29.75
			Shipping and Tax	$5.32
			Total	$108.21

9.4 Timeline

NDRT completed all PDR deliverables on time and remains on track to finish future milestones by each due date. Subscale construction and work for CDR is set to commence upon completion of PDR. The first subscale vehicle launch is scheduled for November 6 with

backup flights planned for November 12 and December 3 in the event of inclement weather or unprecedented launch issues. Figures 93 through 99 show current progress and give updated schedules for the whole team and individual squads.

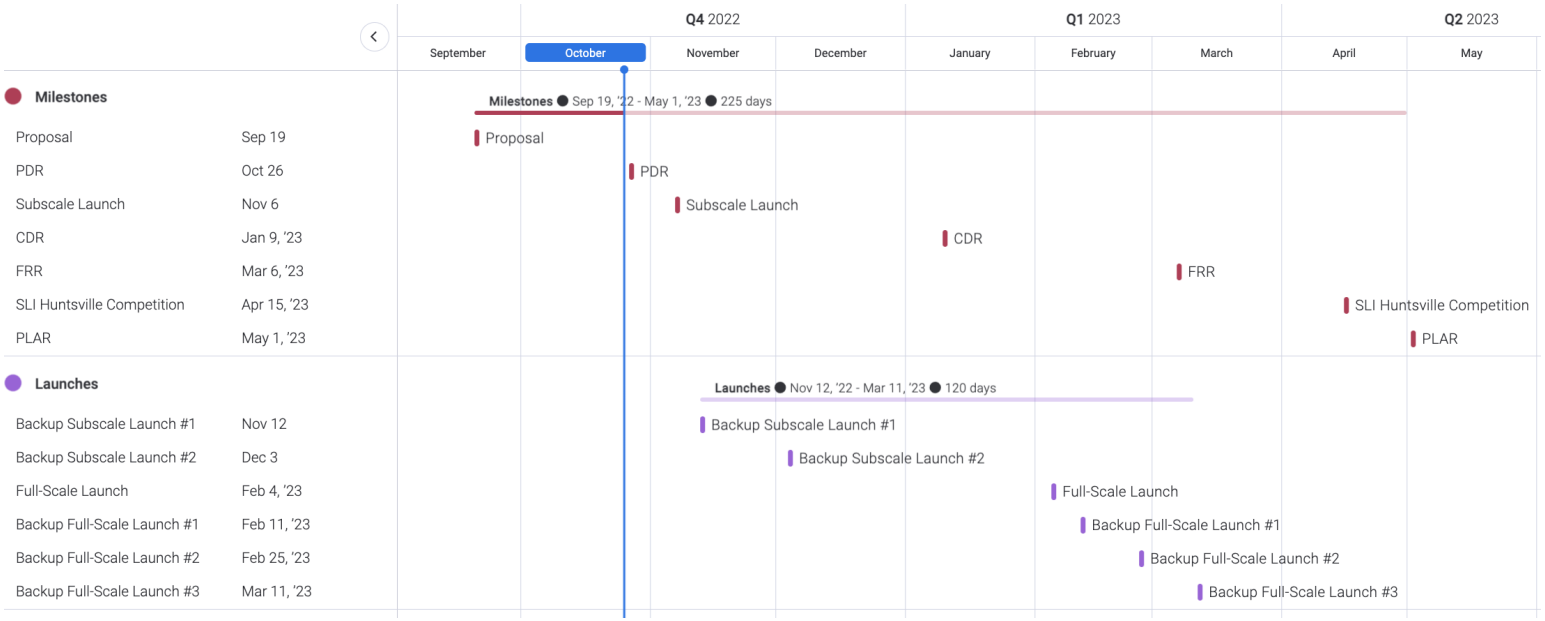

Figure 93: Gantt chart schedule for major project milestones.

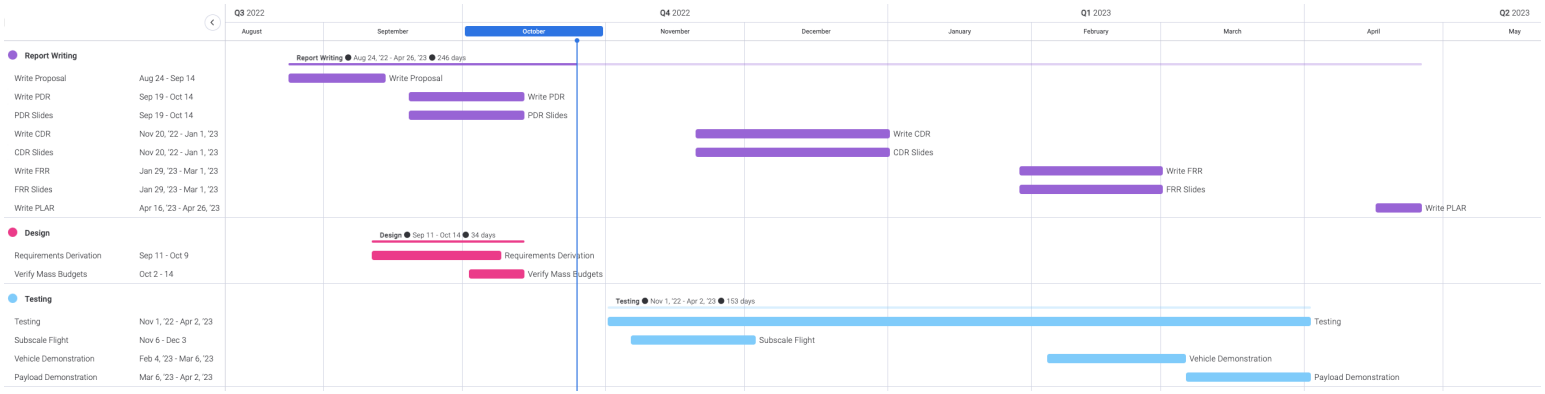

Figure 94: Gantt chart schedule for the Systems Squad.

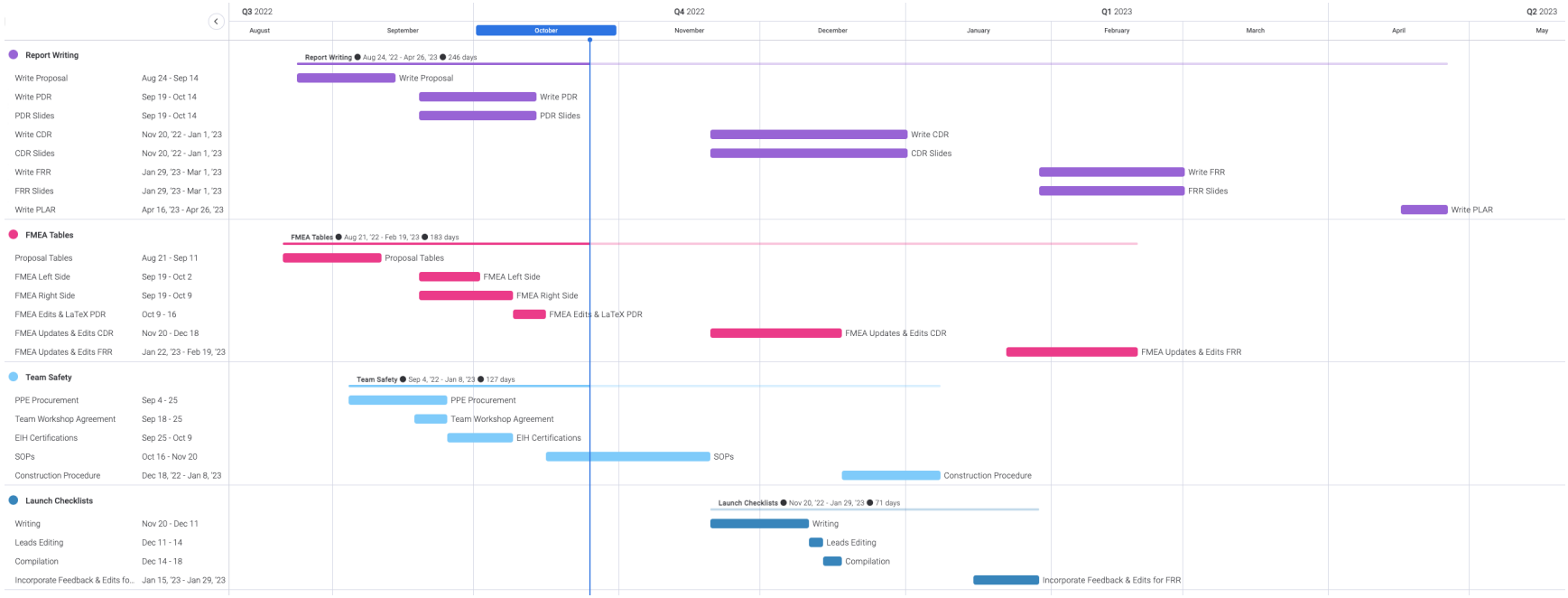

Figure 95: Gantt chart schedule for the Safety Squad.

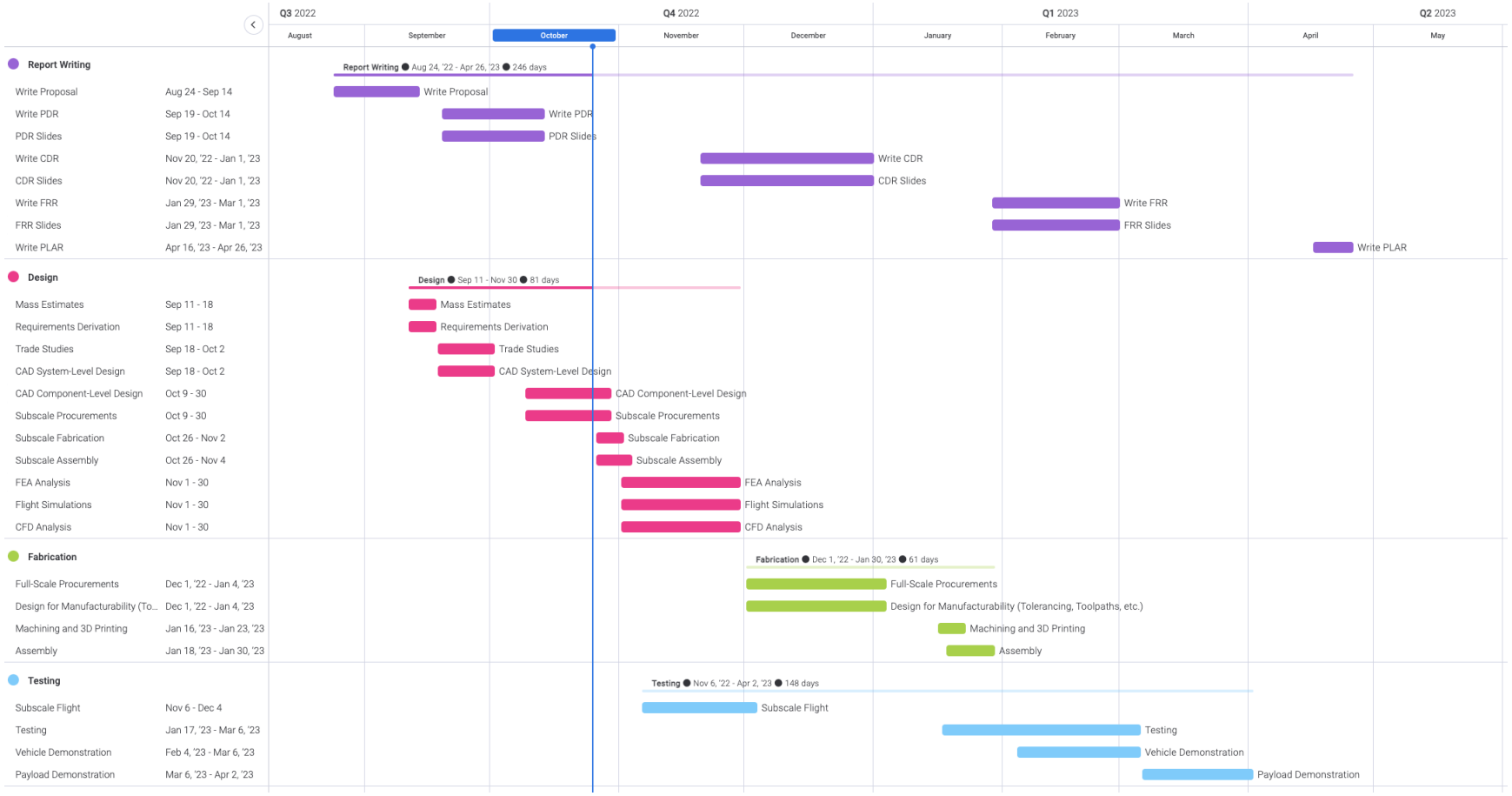

Figure 96: Gantt chart schedule for development of the launch vehicle.

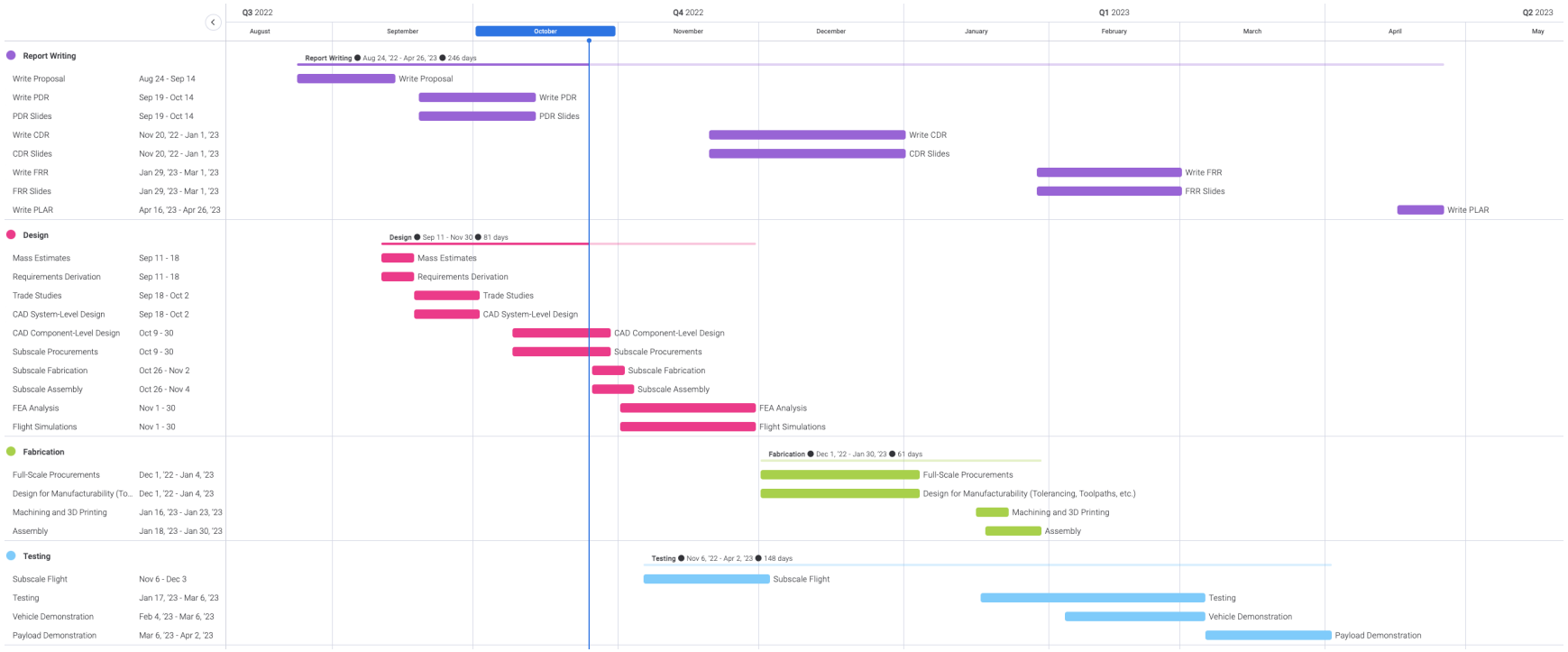

Figure 97: Gantt chart schedule for development of the recovery system.

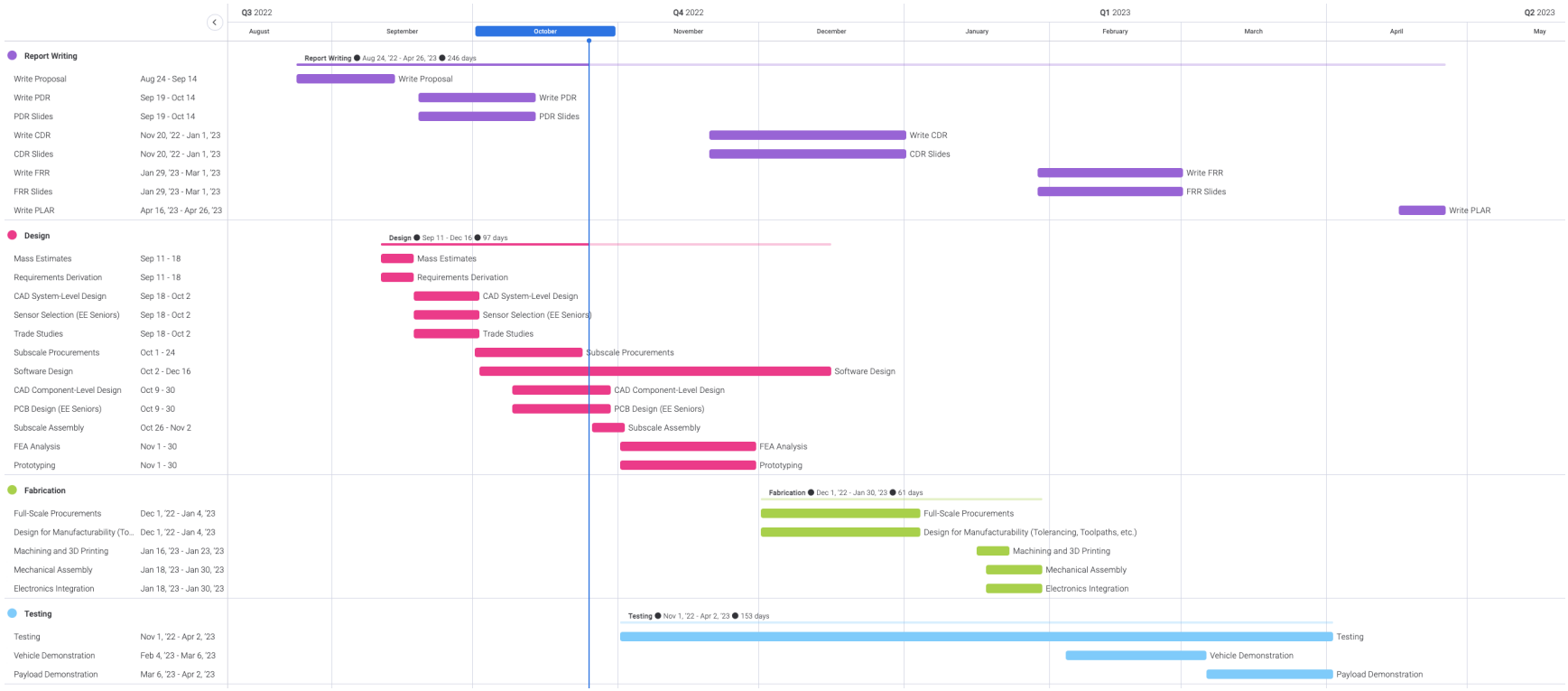

Figure 98: Gantt chart schedule for development of the TROI Payload.

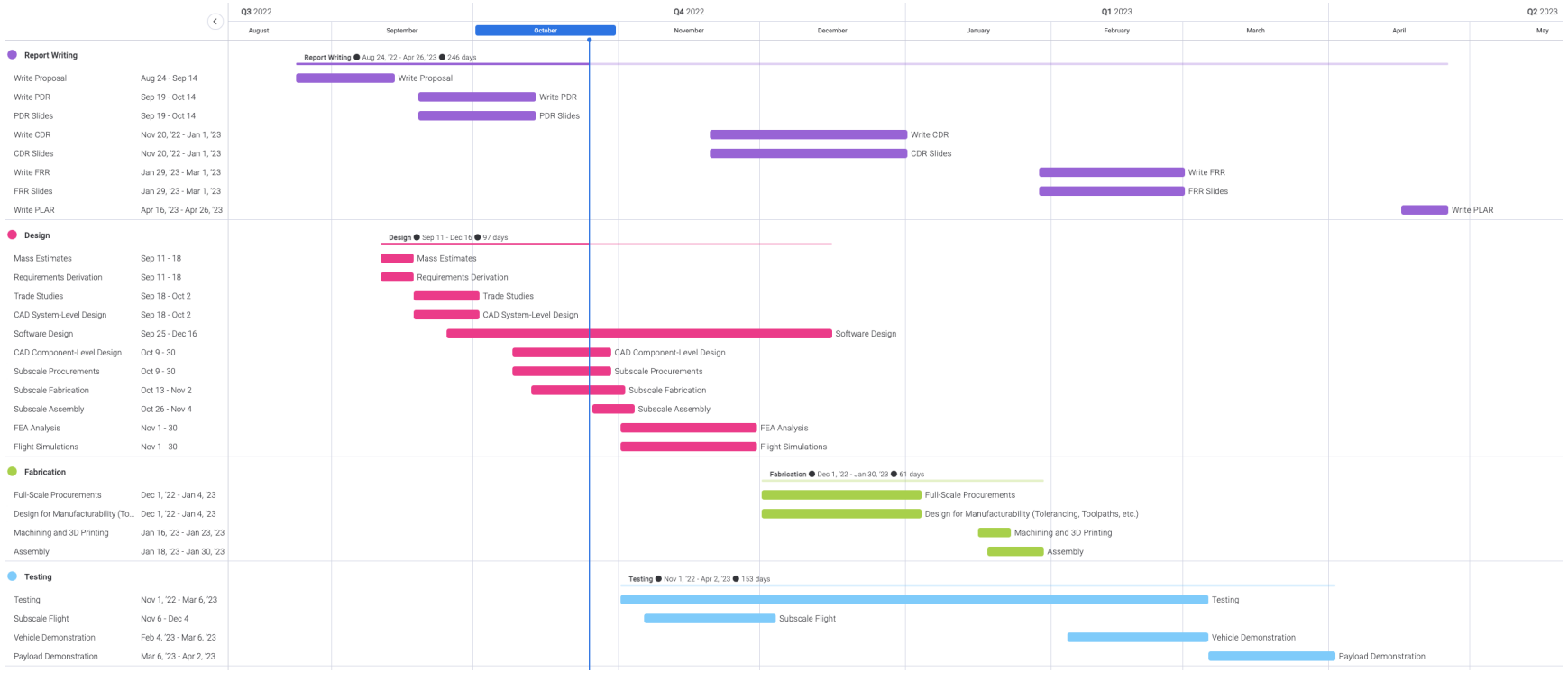

Figure 99: Gantt chart schedule for development of the apogee control system (ACS).

A Team Workshop Safety Agreement

Being a member of the Notre Dame Rocketry Team (NDRT) presents inherent risks and dangers as they relate to high-powered rocketry. Thus, in order to mitigate these risks, all team members must sign and abide by the 2022-2023 NDRT Safety Contract and its principles in order to participate in any capacity on the team.

1. All members will obtain the basic Engineering Innovation Hub (EIH) certification and sign this Safety Contract before participating in any fabrication and/or construction of the launch vehicle.
2. All members will wear the appropriate Personal Protective Equipment (PPE) during all fabrication and/or construction.
3. All members will only participate in fabrication and/or construction of the launch vehicle at official NDRT functions where at least one squad lead (or Project Manager) is present.
4. All members will only use equipment and machines that they are certified and confident in using.
5. All members will confront the Safety Officer, the Project Manager, a squad lead, or consult the Standard Workshop Operating Procedures if they are unsure of how to use any fabrication method.
6. All members will only use fabrication and/or construction equipment for their intended purpose.
7. No member will bring food into the workshop.
8. All members will abide by the instructions given by their squad leader when participating in construction and/or fabrication of the launch vehicle.
9. All members will abide by all Standard Workshop Operating Procedures and Standard Launch Operating Procedures.
10. All members will inform other team member(s) of correct workshop and/or launch procedures if they witness any unsafe behavior by such person(s).
11. All members will refrain from attending official NDRT functions if they feel unwell.
12. All members will abide by all University, state, and national COVID-19 precautions and will quarantine themselves accordingly.

13. If an emergency situation arises, all members will call NDPD (574-631-5555) or 911 immediately.
14. No member will handle or touch the launch vehicle's motor or other live energetics. NAR/TAR Level 3 and Team Mentor Dave Brunsting will be responsible for these components.
15. All members will listen to and abide by all orders of the Safety Officer and Range Safety Officer on launch days.
16. All members will abide by all NASA, NAR, Notre Dame, local, state, and national safety regulations as they relate to launch vehicles and rocketry.
17. All members will do my best to be a responsible and safe NDRT member for the sake of themselves, their teammates, and the community.

By signing this document, I agree to follow all components of this document.

Name:

Date:

B MATLAB Scripts

The following scripts were made by the team to automate the hand calculations necessary for the purposes of parachute selection and preliminary descent calculations. The `Input_Mass.m` function is used by all of the scripts to import the vehicle mass information in an organized manner. All of the scripts used for parachute selection can be viewed below.

```
function [M, M_KE, M_mainchute, M_droguechute, M_noseshockcord, ...
M_prop, M_heaviest] = Input_Mass()
% Imports Vehicle Masses in standard english units (slugs, lbf, etc)
%% Weight Inputs
% Total Masses (no laundry or prop)
M(1) = 76.481; % Nosecone Mass (oz)
M(2) = 206.412; % Payload Tube Mass (oz)
M(3) = 190.320; % Recovery Tube Mass (oz)
M(4) = 206.980; % Fin Can Mass (oz)
% Additional Mass Info
```

```
% mainchute_only = 25;
% mainchute_harnessql = 25; % Harness, bag, 2 QLs and Swivel
M_mainchute = 53.5; % oz
% droguechute_only = 2.1;
% droguechute_harnessql = 28.9; % Harness, blanket, 2 QLs and Swivel
M_droguechute = 32.1;% oz
M_noseshockcord = 10.7; % oz
M_prop = 90.984; % oz
% Total Masses (with laundry & prop)
M(1) = M(1) + M_noseshockcord; % Nosecone Mass (oz)
M(2) = M(2); % Payload Tube Mass (oz)
M(3) = M(3) + M_mainchute + M_droguechute; % Recovery Tube Mass (oz)
M(4) = M(4) + M_prop; % Fin Can Mass (oz)
Max_KE = 65; % ft-lb (Set by Competition)
%% Unit Conversions
oz2slug = 0.00194256; % Conversion
g = 32.17; % ft/s^2
rho = 0.0023769; % slug/ft^3
M = M.*oz2slug; % slugs
M_mainchute = M_mainchute*oz2slug; % slugs
M_droguechute = M_droguechute*oz2slug;% slugs
M_noseshockcord = M_noseshockcord*oz2slug; % slugs
M_prop = M_prop*oz2slug; % slugs
%% Calc Section for Max KE
M_KE = M;
M_KE(1) = M_KE(1) - M_noseshockcord;
M_KE(2) = M_KE(2);
M_KE(3) = M_KE(3) - M_mainchute - M_droguechute;
M_KE(4) = M_KE(4) - M_prop;
M_heaviest = max(M_KE);
end
```

The rest of the scripts that use the `Input_Mass.m` are available below.

```
%% main_parachute_selection.m
% This script helps find the CdA value needed for a parachute based on
% vehicle total mass and most massive section
% Author: Paul du Vair
```

```
clear
clc
[M, M_KE, M_mainchute, M_droguechute, M_shockcords, M_prop, ...
M_heaviest] = Input_Mass();
Max_KE = 65; % ft-lb (Set by Competition)
%% Unit Conversions
oz2slug = 0.00194256; % Conversion
g = 32.17; % ft/s^2
rho = 0.0023769; % slug/ft^3
%% V_Max Calc
v_max = sqrt(2*Max_KE/M_heaviest) % ft/s
disp('ft/s')
%% CdA Calc
M_tot_final_desc = sum(M) - M_prop;
CdA = (2*(M_tot_final_desc)*g)/(rho*v_max^2)
disp('dimless')
```

```
%% drogue_parachute_selection.m
% This script helps find the CdA value needed for a parachute based on
% vehicle total mass and most massive section
% Author: Paul du Vair
clear
clc
[M, M_KE, M_mainchute, M_droguechute, M_shockcords, M_prop, ...
M_heaviest] = Input_Mass();
Max_KE = 65; % ft-lb (Set by Competition)
t_max = 80; % seconds (Set by Competition)
M_tot_final_desc = sum(M) - M_prop;
%% Unit Conversions
oz2slug = 0.00194256; % Conversion
g = 32.17; % ft/s^2
rho = 0.0023769; % slug/ft^3
%% Inputs
CdA_main = 135.626;
t_main = 34.5805; % s
d_main = 1.0144e+03; % ft
h_apo = 4600; % ft
```

```
h_main = 600; % ft
v_wind = 29.333; % ft/s
max_r = 2500; % ft
a = 30*32.17; % Max Acceleration
%% Descent Calcs
t_dmax1 = t_max-t_main;
v_dmin1 = (h_apo-h_main)/(t_dmax1);
CdA_max1 = (2*M_tot_final_desc*g)/(rho*(v_dmin1)^2); % Time Restraint
t_dmax2 = (max_r - v_wind*t_main)/(v_wind);
v_dmin2 = (h_apo-h_main)/(t_dmax2);
CdA_max2 = (2*M_tot_final_desc*g)/(rho*(v_dmin2)^2); % Radius Restraint
if v_dmin1 > v_dmin2
   disp(['Min Descent Velocity: ', num2str(v_dmin1), ' ft(s) (Time Restraint)'])
   disp(['Max Drogue CdA: ', num2str(CdA_max1)])
else
   disp(['Min Descent Velocity: ', num2str(v_dmin2), ' ft(s) (Radius Restraint)'])
   disp(['Max Drogue CdA: ', num2str(CdA_max2)])
end
v_max_d = sqrt((2*(M_tot_final_desc)*(a+g))/(rho*CdA_main)); % ft/s
CdA_min = (2*M_tot_final_desc*g)/(rho*(v_max_d)^2); % Acceleration Constraint
disp(['Max Descent Velocity: ', num2str(v_max_d), ' ft(s) (Acceleration Restraint)'])
disp(['Min Drogue CdA: ', num2str(CdA_min)])
```

```
%% main_descent_calc.m
% Calcs descent time from main to ground
% Author: Paul du Vair
clear
clc
%% Inputs
% Total Mass Inputs
[M, M_KE, M_mainchute, M_droguechute, M_shockcords, M_prop, ...
M_heaviest] = Input_Mass();
Max_KE = 65; % ft-lb (Set by Competition)
v_wind = 29.3333; % ft/s (Set by Competition)
%% Unit Conversions
oz2slug = 0.00194256; % Conversion
g = 32.17; % ft/s^2
```

```
rho = 0.0023769; % slug/ft^3
h_main_dep = 600;
CdA_main = 135.626; % Dimensionless
%% Calculations
M_tot_final_desc = sum(M) - M_prop;
v_descent = sqrt((2*M_tot_final_desc*g)/(rho*CdA_main)) % ft/s
t_descent_main = h_main_dep/v_descent
drift_main = t_descent_main*v_wind
```

```
%% full_vehicle_descent_calc.m
% Calcs descent time from apogee to main deployment
% Author: Paul du Vair
clear
clc
%% Inputs
% Total Mass Inputs
[M, M_KE, M_mainchute, M_droguechute, M_shockcords, M_prop, ...
M_heaviest] = Input_Mass();
Max_KE = 65; % ft-lb (Set by Competition)
v_wind = 20; % mph (Set by Competition)
%% Unit Conversions
oz2slug = 0.00194256; % Conversion
g = 32.17; % ft/s^2
rho = 0.0023769; % slug/ft^3
h_apo = 4600; % ft
h_main_dep = 600; % ft
v_wind = 1.46666667*v_wind; % ft/s
CdA_drogue = 4.89; % Dimensionless
CdA_main = 135.626; % Dimensionless
%% Calculations
M_tot_final_desc = sum(M) - M_prop;
v_descent_drogue = sqrt((2*M_tot_final_desc*g)/(rho*CdA_drogue)); % ft/s
t_descent_drogue = (h_apo-h_main_dep)/v_descent_drogue; % seconds
drift_drogue = t_descent_drogue*v_wind;
v_descent_main = sqrt((2*M_tot_final_desc*g)/(rho*CdA_main)); % ft/s
t_descent_main = h_main_dep/v_descent_main;
drift_main = t_descent_main*v_wind;
```

```
%% Final Calcs
t_total = t_descent_drogue + t_descent_main;
drift_total = drift_drogue + drift_main;
%% KE Calcs
KE1d = .5.*(M_KE(1)).*v_descent_drogue.^2;
KE2d = .5.*(M_KE(2)).*v_descent_drogue.^2;
KE3d = .5.*(M_KE(3)).*v_descent_drogue.^2;
KE4d = .5.*(M_KE(4)).*v_descent_drogue.^2;
KE1m = .5.*(M_KE(1)).*v_descent_main.^2;
KE2m = .5.*(M_KE(2)).*v_descent_main.^2;
KE3m = .5.*(M_KE(3)).*v_descent_main.^2;
KE4m = .5.*(M_KE(4)).*v_descent_main.^2;
%% Displays
disp(['Drogue Descent Velocity: ', num2str(v_descent_drogue), ' ft/s'])
disp(['Drogue Descent Time: ', num2str(t_descent_drogue), ' s'])
disp(['Drogue Drift: ', num2str(drift_drogue), ' ft'])
disp(['Main Descent Velocity: ', num2str(v_descent_main), ' ft/s'])
disp(['Main Descent Time: ', num2str(t_descent_main), ' s'])
disp(['Main Drift: ', num2str(drift_main), ' ft'])
disp('Overall Time and Drift')
disp(['Total Descent Time: ', num2str(t_total), ' ft/s'])
disp(['Total Drift: ', num2str(drift_total), ' ft/s'])
disp(['KE Calculations'])
disp(['Fore Section KE during Drogue Descent: ', num2str(KE1d+KE2d+KE3d), ' ft-lb'])
disp(['Aft Section KE during Drogue Descent: ', num2str(KE4d), ' ft-lb'])
disp(['Nose Cone KE at Landing: ', num2str(KE1m), ' ft-lb'])
disp(['Payload KE at Landing: ', num2str(KE2m), ' ft-lb'])
disp(['ACS KE at Landing: ', num2str(KE3m), ' ft-lb'])
disp(['Fin Can KE at Landing: ', num2str(KE4m), ' ft-lb'])
```